Evidence-Based Complementary and Alternative Medicine

Complementary and Alternative Medicine for Liver Fibrosis 2021

Lead Guest Editor: Chan#Yen Kuo
Guest Editors: Chih-Yuan Ko and Chih-Wei Chou

Complementary and Alternative Medicine for Liver Fibrosis 2021

Evidence-Based Complementary and Alternative Medicine

Complementary and Alternative Medicine for Liver Fibrosis 2021

Lead Guest Editor: Chan#Yen Kuo
Guest Editors: Chih-Yuan Ko and Chih-Wei Chou

Contents

Hindawi
Evidence-Based Complementary and Alternative Medicine
Volume 2023, Article ID 4197955, 10 pages
https://doi.org/10.1155/2023/4197955

Research Article

Effects of Different Vegetable Oils on the Nonalcoholic Fatty Liver Disease in C57/BL Mice

Camila Sanches Manca,[1] **Lívia Maria Cordeiro Simões-Ambrosio**,[1] **Paula Payão Ovídio**,[1] **Leandra Zambelli Ramalho**,[2] **and Alceu Afonso Jordao**[1,3]

[1]*Department of Internal Medicine, Faculty of Medicine of Ribeirão Preto, University of São Paulo, Av. Bandeirantes 3900, Ribeirão Preto, SP 14049-900, Brazil*
[2]*Department of Pathology, Faculty of Medicine of Ribeirão Preto, University of São Paulo, Ribeirão Preto, São Paulo, Brazil*
[3]*Department of Health Sciences at Ribeirão Preto Medical School, University of Sao Paulo, Ribeirão Preto-SP 14049-900, Brazil*

Correspondence should be addressed to Alceu Afonso Jordao; aajordao@gmail.com

Received 8 May 2022; Revised 5 July 2022; Accepted 8 July 2022; Published 14 January 2023

Academic Editor: Chan-Yen Kuo

Background. Nonalcoholic fatty liver disease (NAFLD) is the most common hepatic disorder, affecting 22–28% of the adult population and more than 50% of obese people all over the world. Modulation of the fatty acids in diet as a means of prevention against nonalcoholic fatty liver disease in animal models (NAFLD) remains unclear. The treatment of NAFLD has not been described in specific guidelines so far. Thus, the justification for the study is to check modifications in macronutrients composition, fatty acids, in particular, play a significant role in the treatment of NAFLD regardless of weight loss. *Aim*. To investigate different vegetable oils in prevention and progression of NAFLD in animal models. *Methods*. For the experiment were used fifty C57BL/6J mice male fed with high fat and fructose diet (HFD) to induce the NAFLD status and they received different commercial vegetable oils for 16 weeks to prevent steatosis. Liver steatosis and oxidative stress parameters were analyzed using biochemical and histological methods. Fatty acids profile in the oils and in the liver samples was obtained. *Results*. The high fat and fructose diet led to obesity and the vegetable oils offered were effective in maintaining body weight similar to the control group. At the end of the experiment (16 weeks), the HFHFr group had a greater body weight compared to control and treated groups (HFHFr: 44.20 ± 2.34 g/animal vs. control: 34.80 ± 3.45 g/animal; $p < 0.001$; HFHFr/OL: 35.40 ± 4.19 g/animal; HFHFr/C: 36.10 ± 3.92 g/animal; HFHFr/S: 36.25 ± 5.70 g/animal; $p < 0.01$). Furthermore, the HFD diet has caused an increase in total liver fat compared to control ($p < 0.01$). Among the treated groups, the animals receiving canola oil showed a reduction of hepatic and retroperitoneal fat ($p < 0.05$). These biochemical levels were positively correlated with the hepatic histology findings. Hepatic levels of omega-3 decreased in the olive oil and high fat diet groups compared to the control group, whereas these levels increased in the groups receiving canola and soybean oil compared to control and the high fat groups. *Conclusion*. In conclusion, the commercial vegetable oils either contributed to the prevention or reduction of induced nonalcoholic fatty liver with high fat and fructose diet, especially canola oil.

1. Introduction

Nonalcoholic fatty liver disease (NAFLD) is the most common hepatic disorder, affecting 22–28% of the adult population and more than 50% of obese people all over the world [1, 2]. NAFLD is characterized by abnormal fat accumulation in the liver (simple steatosis), which can be reversed by changes in lifestyle. The progression of NAFLD to nonalcoholic steatohepatitis (NASH) covers a broad spectrum ranging from NAFLD with development of inflammatory changes to possible cirrhosis and cellular hepatocarcinoma. NAFLD/NASH is strongly associated with metabolic abnormalities such as obesity, insulin resistance, and dyslipidemia [3–7]. The mechanisms leading to disease progression and the treatment required have not been fully clarified.

Recent studies have focused on primary physiopathology of NAFLD and on mechanisms leading to NASH, fibrosis, and hepatocyte injury that have not been fully clarified

although it may be stated that the cause of these conditions is polygenic and multifactorial. There is an association between genes and the participation of the environment, alongside the diet and sedentarism, whose importance has been demonstrated [8, 9].

The currently most accepted mechanism is the classical two-hit theory. The first hit is characterized by steatosis resulting from an imbalance in the formation and turnover of triacylglycerides, and it is believed to be affected by insulin resistance. The second hit involves oxidative stress and inflammatory cytokines production leading to hepatic injury [5, 10]. The role of diet in physiopathology and in the progression of NAFLD is not clear. A high-calorie diet, excess of fatty acids (especially saturated ones), and high simple sugars intake, with greater importance on fructose and saccharose, have seemed to be implicated in the disease development. Fructose is used as a food preservative, mainly present in sugar-sweetened beverages, and it is known for stimulating *de novo* lipogenesis and increasing liver oxidation/inflammation [11–13]. In addition to fructose/saccharose, the consumption of saturated fatty acids is implicated in the pathogenesis of NAFLD [13, 14]. Despite obtaining contradictory results, specific fatty acids have been proposed to be involved in hepatic lipogenesis, possibly acting on the induction or reversal of the signs and symptoms of NAFLD [15–18].

The treatment of NAFLD has not been described in specific guidelines so far. Lifestyle changes are the primary disease treatment option and weight loss is strongly recommended for NAFLD patients. However, recent studies have demonstrated that modifications in macronutrient composition and fatty acids, in particular, play a significant role in the treatment of NAFLD regardless of weight loss [15–18]. An increase in saturated fat intake is usually associated with increased insulin resistance, which may induce the progression of NAFLD, whereas monounsaturated (MUFA) and polyunsaturated (PUFA) fatty acids may prevent it by inhibiting genes involved in the mechanisms of *de novo* lipogenesis [13]. Using different n-3, n-7, n-6, and n-9-rich lipid formulations, Siddiqui et al. [13] demonstrated NAFLD reduction.

The aim of this present study was settled in order to investigate the effect of different vegetable oils on the prevention of NAFLD.

2. Materials and Methods

2.1. Animals and Diet. Male C57/B6J mice weighing 20 g at the beginning of the experiment were obtained from the Central Animal House of the Faculty of Medicine of Ribeirão Preto (FMRP), University of São Paulo, and maintained under controlled conditions of temperature ($22 \pm 2^{\circ}$C) and of humidity and on a light (7:00 am–7:00 pm)/dark (7:00 pm–7:00 am) cycle. Water and food were supplied *ad libitum*. Animals were handled according to Brazilian College of Animal Experimentation recommendations and all procedures were approved by the Ethics Committee of FMRP (protocol no. 017/2015, March 30, 2015). Animals were randomly assigned to five experimental groups. The control group (CONT) received the AIN-93 diet for growth containing 20% protein (casein), 63% carbohydrates (53% cornstarch and 10% saccharose), 7% fat (soybean oil), 5% fiber, 3.5% AIN-93G mineral mix, 1% vitamin mix, 0.3% L-cysteine, 0.25% choline, and 0.002% di-terc-butyl methyl phenol [19]. Treated groups received a modified AIN-95 diet for growth in which lipid sources were elevated and all carbohydrate sources were replaced by fructose. The high-lipid + fructose group received western type diet containing 50% fat (lard) +20% fructose, 20% protein (casein), 5% fiber, 3.5% AIN-93G mineral mix, 1% vitamin mix, 0.3% L-cysteine, 0.25% choline, and 0.002% di-terc-butyl methyl phenol (HFHFr). The remaining treated groups received same composition diet except for the modulation of lipids, with 25% lard and 25% of the respective vegetable oils (olive oil, canola oil, and soybean oil), i.e., HFHFr/OL, HFHFr/CN, and HFHFr/S (Table 1).

The vegetable oils, extravirgin olive oil (®Gallo), soybean oil, and canola oil (®*Liza*) were purchased at the local market. The fatty acid profiles of lard and of respective oils are listed in Table 1, as well as peroxidability index [20]. Vitamin, mineral mix, choline, and L-cystine were purchased from Rhoster (Araçoiaba da Serra, Brazil).

Food intake and weight were determined per cage (2 animals/cage) over a period of 16 weeks, and are reported as mean food intake and weight in g/day. At the end of experiment, animals were starved for 12 hours and then anesthetized with ketamine and xylazine diluted in saline at the proportion of 1 : 1:2 ml. It was administrated dose applications of 10 μl/g weight each. Blood was immediately collected by cardiac puncture, left to rest at room temperature for 30 minutes, and centrifuged at 3500 rpm at 4°C for serum separation afterward. Serum was stored at −80°C for later analysis. Liver, epididymal adipose tissue, and retroperitoneal adipose tissue were weighed and frozen in aluminum parts for further analysis.

2.2. Hepatic Histology. Liver fragments were fixed in 10% buffered formalin for 24 hours and embedded in paraffin. Histological preparations containing 5 μm thick sections were stained with hematoxylin and eosin (H&E) for semiquantitative assessment of steatosis and/or steatohepatitis on 10 representative microscope fields at 40× magnification by a pathologist, who was blind to the samples. All divergent results were analyzed and discussed using a system of co-observer microscopic analysis [21].

2.3. Biochemical and Hepatic Analyses. Serum triacylglycerols (TAG), total cholesterol (TC), and cholesterol present in high-density lipoprotein (HDL) were determined using commercial kits (Labtest Diagnóstica S.A., Vista Alegre, Brazil), and very low-density lipoprotein (VLDL) cholesterol was then calculated. The same kits were used for the hepatic determinations as well. Total hepatic fat was extracted by adapted Bligh and Dyer method [22], and total TAG and total hepatic cholesterol levels were determined using commercial kits.

A direct transesterification method was applied to determine the hepatic fatty acid profile [23]. Fatty acid methylated esters were separated by gas chromatography

Table 1: Fatty acid composition of the lard and oils used in the diets.

Fatty acids	Lard	Olive oil	Canola oil	Soybean oil
Saturated fatty acids				
C16 : 0	23.86	9.53	4.50	0.01
C18 : 0	10.89	2.85	2.29	0.36
Monounsaturated fatty acids				
C16 : 1	1.96	0.75	0.29	11.57
C18 : 1 n-9	36.92	69.82	60.01	23.15
Polyunsaturated fatty acids				
C18 : 2 n-6	20.69	6.56	19.73	57.52
C18 : 3 n-3	1.04	1.14	8.02	5.20
C20 : 4 n-3	0.07	0.09	0.05	0.01
C20 : 5 n-3	0.02	0.10	0.33	0.42
C22 : 6 n-3	0.10	0.08	0.03	0.01
Total type of fats				
∑SFA	37.16	13.08	7.91	1.10
∑MUFAs	39.59	72.72	61.92	37.07
∑PUFAs	24.29	14.18	30.15	63.81
∑n-6	20.95	10.14	20.62	57.55
∑n-3	2.15	4.03	9.49	6.22
n-6/n-3 ratio	9.74	2.52	2.17	9.25
SFA/PUFA ratio	1.53	0.92	0.26	0.02
PI of the diets	64.52	77.00	79.60	89.00

SFA, saturated fatty acids; MUFAs, monounsaturated fatty acids; PUFAs, polyunsaturated fatty acids; PI, peroxidation index. Values are reported as mean mol percent of the total fatty acid methyl esters.

(Shimadzu Europe, Duisburg, Germany) using an instrument equipped with an AOC-20i self-injector (Shimadzu Europe, Duisburg, Germany) and a SP-2560 fused silica column (100 m, 0.25 mm I.D, film thickness 0.20 μm). Helium was used as the carrier gas. Synthetic air was used as the flame ionization detector at 250°C. Injections were performed in split mode and the time of fatty acid retention was determined by comparison with an external standard (Supelco 37 component FAME Mix).

2.4. Analysis of Glycemia and Insulin Resistance. Animals glycemia was determined at the end of experiment using obtained samples from animal's tail and the freestyle lite Abbot®A glucometer. The triglyceride/HDL-cholesterol ratio was calculated as a predictor of insulin resistance [24].

2.5. Analysis of Lipid Peroxidation and Antioxidant Parameters. Hepatic malondialdehyde MDA was determined by Gerard-Monnier et al. method [25] with some modifications, as it is thoroughly described in S1 text section.

Hepatic reduced glutathione (GSH) was determined from hepatic tissue by Sedlak and Lindsay method [26] with adaptations, and vitamin A (α-tocopherol) was determined by adapted Arnaud et al. method [27]. Complete methodology is detailed and described in S1 text section.

2.6. Statistical Analysis. One-way analysis of variance (ANOVA) was applied to the data of the various groups, followed by the Tukey post-test, using the GraphPad Prism software, version 5.00 for Windows (GraphPad Software, San Diego, CA, USA), with the level of significance set up at $p < 0.05$. Data are reported as mean ± standard deviation.

3. Results

3.1. Effects of MUFAs and PUFAs on Body Weight Gain, Food Intake, and Energy Intake. HFHFr animals' body weight started to increase significantly compared to control from 5th week on ($p < 0.05$). From 9th week, HFHFr animals' body weight increased significantly compared to control (35.00 ± 4.30 g/animal vs. 29.80 ± 2.48 g/animal, $p < 0.01$) and to treated groups (HFHFr/OL: 30.00 ± 1.89 g/animal; HFHFr/CN: 31.20 ± 2.34 g/animal; HFHFr/S: 30.63 ± 2.66 g/animal; $p < 0.05$). At the end of the experiment (16 weeks), HFHFr group had a greater body weight compared to control and treated groups (HFHFr: 44.20 ± 2.34 g/animal vs. Control: 34.80 ± 3.45 g/animal; $p < 0.001$; HFHFr/OL: 35.40 ± 4.19 g/animal; HFHFr/C: 36.10 ± 3.92 g/animal; HFHFr/S: 36.25 ± 5.70 g/animal; $p < 0.01$), suggesting that the oils were effective in maintaining body weight. There was some variation in mean food intake throughout the experimental period due to control animals ingesting more food and HFHFr animals ingesting less food. Among the treated groups, HFHFr/OL group ingested more food than any of them. Energy intake data were positively correlated with food intake data, whereas control and HFHFr groups showed lower energy intake throughout the experiment, the experimental groups, particularly HFHFr/OL group, showed greater energy intake. However, these variations were not expressed by the efficacy of diet in favoring weight gain as determined by the feed efficiency rate (FER), which only differed between control and HFHFr animals. The results are shown in Table 2.

3.2. Liver Weight and Epididymal and Retroperitoneal Adipose Tissue Weight and Their Relationship with Body Weight. Hepatic tissue weight was increased in the HFHFr group compared to control. Among treated groups, the PUFA-rich group (soybean oil) showed a significant reduction of hepatic tissue compared to the HFHFr group ($p < 0.05$), even though no significant reduction was observed in relation to body weight throughout the experiment. The HFHFr/CN group showed a reduction of retroperitoneal adipose tissue compared to the HFHFr group ($p < 0.05$), although there was no difference in relation to body weight. The sum of epididymal + retroperitoneal weight was higher for the HFHFr group compared to control ($p < 0.05$), but it did not differ from that of treated groups. No difference in epididymal adipose tissue or its relation to body weight was observed over 16 weeks of the experiment. The results are shown in Table 3.

3.3. Effects of Vegetable Oils on Triacylglycerol, Cholesterol, VLDL, HDL-C, Glycemia, and Triacylglycerol/HDL-Cholesterol Ratio. Serum triacylglycerol levels of the HFHFr/OL

Table 2: Final body weight, body weight gain, food intake, energy intake, and feed efficiency rate.

	Control	HFHFr	HFHFr/OL	HFHFr/CN	HFHFr/S
Final body weight (g)	34.7 ± 3.43	44.10 ± 5.66*	35.2 ± 4.54#	35.8 ± 4.11#	36.75 ± 36.29#
Δ body weight gain (g)	14.40 ± 3.20	23.50 ± 5.48	14.20 ± 4.02	16.30 ± 3.59	18.00 ± 6.92
Food intake (g/week)	24.44 ± 1.36	18.29 ± 1.36*	22.30 ± 2.14#	19.97 ± 0.976	20.28 ± 1.40
Energy intake (kcal/week)	96.55 ± 5.39	111.8 ± 8.34*	136.2 ± 13.11#	122.0 ± 5.97	123.9 ± 8.55
Feed efficiency rate (D)	025 ± 0.007	0.045 ± 0.038	0.033 ± 0.012	0.039 ± 0.018	0.054 ± 0.017

Data are reported as mean ± standard deviation. * $p \leq 0.05$ vs. control; # $p \leq 0.05$ vs. HFHFr. Groups: control; HFHFr, high fat and high fructose; HFHFr/OL, high fat and high fructose and 25% lard and 25% olive oil; HFHFr/CN, high fat and high fructose and 25% lard and 25% canola oil; HFHFr/S, high fat and high fructose and 25% lard and 25% soy oil.

Table 3: Phenotypic comparison of C57/BL mice fed the chow, HFHFr, HFHFr/OL, HFHFr/CN, and HFHFr/S diet for 16 weeks.

Parameters	Control	HFHFr	HFHFr/OL	HFHFr/CN	HFHFr/S
Liver weight (g)	1.25 ± 0.20	1.73 ± 0.51*	1.35 ± 0.22	1.38 ± 0.23	1.28 ± 0.35 #
Liver weight (%BW)	3.50 ± 0.38	3.8 ± 0.73	3.80 ± 0.62	3.80 ± 0.32	3.4 ± 0.44
Epididymal adipose tissue (g)	1.39 ± 0.47	2.15 ± 0.41	1.63 ± 0.71	1.57 ± 0.51	1.84 ± 0.86
Epididymal adipose tissue (%BW)	3.99 ± 1.17	4.92 ± 1.07	4.49 ± 1.75	4.29 ± 1.08	4.89 ± 1.77
Retroperitoneal adipose tissue (g)	0.35 ± 0.09	0.56 ± 0.13*	0.41 ± 0.20	0.36 ± 0.12 #	0.43 ± 0.18
Retroperitoneal (%BW)	1.00 ± 0.19	1.27 ± 0.30	1.16 ± 0.53	1.00 ± 0.27	1.15 ± 0.40
Adipose tissue sum (g)	1.75 ± 0.54	2.71 ± 0.52*	2.04 ± 0.89	1.94 ± 0.62	2.27 ± 1.07
Adipose tissue sum (%BW)	4.99 ± 1.31	6.19 ± 1.31	5.65 ± 2.21	5.30 ± 1.32	6.05 ± 2.14

Values are reported as mean ± standard deviation ($n = 10$ per group). Control; HFHFr; HFHFr/OL; HFHFr/CN; HFHFr/S. * $p \leq 0.05$ vs. control; # $p \leq 0.05$ vs. HFHFr. Groups: control; HFHFr, high fat and high fructose; HFHFr/OL, high fat and high fructose and 25% lard and 25% olive oil; HFHFr/CN, high fat and high fructose and 25% lard and 25% canola oil; HFHFr/S, high fat and high fructose and 25% lard and 25% soy oil.

group were significantly higher than those of HFHFr group (0.291 ± 0.049 vs.0.126 ± 0.027), whereas those of HFHFr/S group were lower than control (0.168 ± 0.037 vs. 0.258 ± 0.060) (Figure 1(a)). The same results were observed for VLDL values (Figure 1(b)). HFHFr/S group showed a higher total cholesterol level than control (4.208 ± 1.102 vs. 2.818 ± 0.599) (Figure 1(c)). HDL-C levels were higher for HFHFr/OL and HFHFr groups compared to control (2,175 ± 0.624 vs. 2.175 ± 0.420 vs. 1.457 ± 0.321), while they were lower in soybean oil group compared to HFHFr group (Figure 1(d)). Glycemia and the marker of insulin resistance (triacylglycerol/HDL-C ratio) did not differ among groups (Figures 1(e) and 1(f)). About treated groups, the HFHFr/CN group was the only one that did not show changes in serum parameters.

3.4. The MUFAs and PUFAs of Vegetable Oils Reduced the Accumulation of Hepatic Fat. As expected, the western diet (HFHFr) increased the accumulation of total hepatic fat compared to control ($p < 0.01$). Among treated groups, the group receiving canola oil, mainly rich in MUFAs and PUFAs, showed a reduction in total hepatic fat accumulation compared to HFHFr group ($p < 0.01$) (Figure 2(a)). Therefore, these data were positively correlated with the hepatic histology findings. HFHFr group exhibited moderate and severe diffuse microvesicular hepatic steatosis (Figure 2(b)). Groups that received a diet rich in MUFAs and PUFAs showed reduced steatosis compared to HFHFr group. Whereas HFHFr/OL group exhibited mild to moderate macro and microvesicular steatosis, HFHFr/CN and HFHFr/S groups exhibited mild steatosis. No group showed fibrosis or inflammation (Figure 2(b)), as it can be seen in Figure 3(c) based on the NAFLD score. Hepatic triacylglycerol levels were higher in the groups receiving a western diet compared to control (38.48 ± 16.86 vs. 17.28 ± 5.4, $p < 0.01$). Although the groups receiving diets rich in MUFAs and PUFAs showed reduced triacylglycerols, the difference was nonsignificant (Figure 2(d)). Hepatic cholesterol did not show changes among groups.

3.5. Effects of Vegetable Oils on Oxidative Stress Parameters. Oxidative stress, final resulted product of lipid peroxidation, was assessed on the basis of the levels of MDA. Hepatic MDA was increased in all treated groups compared to control (control: 0.772 ± 0.377 vs. HFHFr: 2.212 ± 0.962 vs. HFHFr/OL: 2,805 ± 0.364 vs. HFHFr/CN: 3.613 ± 1.794 vs. HFHFr/S: 3.122 ± 1.188). In comparison with HFHFr group, only the one receiving diet rich in canola oil showed increased hepatic MDA levels ($p < 0.05$) (Figure 3(a)). Antioxidant protection was assessed on the basis of hepatic GSH levels, which were found to be higher in groups HFHFr/CN and HFHFr/S, preventing oxidative stress compared to control and to the group receiving western diet (control: 0.856 ± 0.340 vs. HFHFr: 1.121 ± 0.275; vs. HFHFr/CN: 3.808 ± 1.984 vs. HFHFr/S: 4.254 ± 1.623) (Figure 3(b)). Vitamin E levels were significantly reduced in all treated groups compared to control ($p < 0.05$) (Figure 3).

3.6. Effect of the Diets on the Composition of Hepatic Fatty Acids. The diet rich in omega-9 (olive oil group) and the diet rich in omega-6 (soybean oil group) increased the levels of palmitic acid (C16 : 0) compared to the group receiving western diet (HFHFr) ($p < 0.05$), with no changes in C18 : 0 levels or in the total SFA sum. C16 : 1 levels were higher in

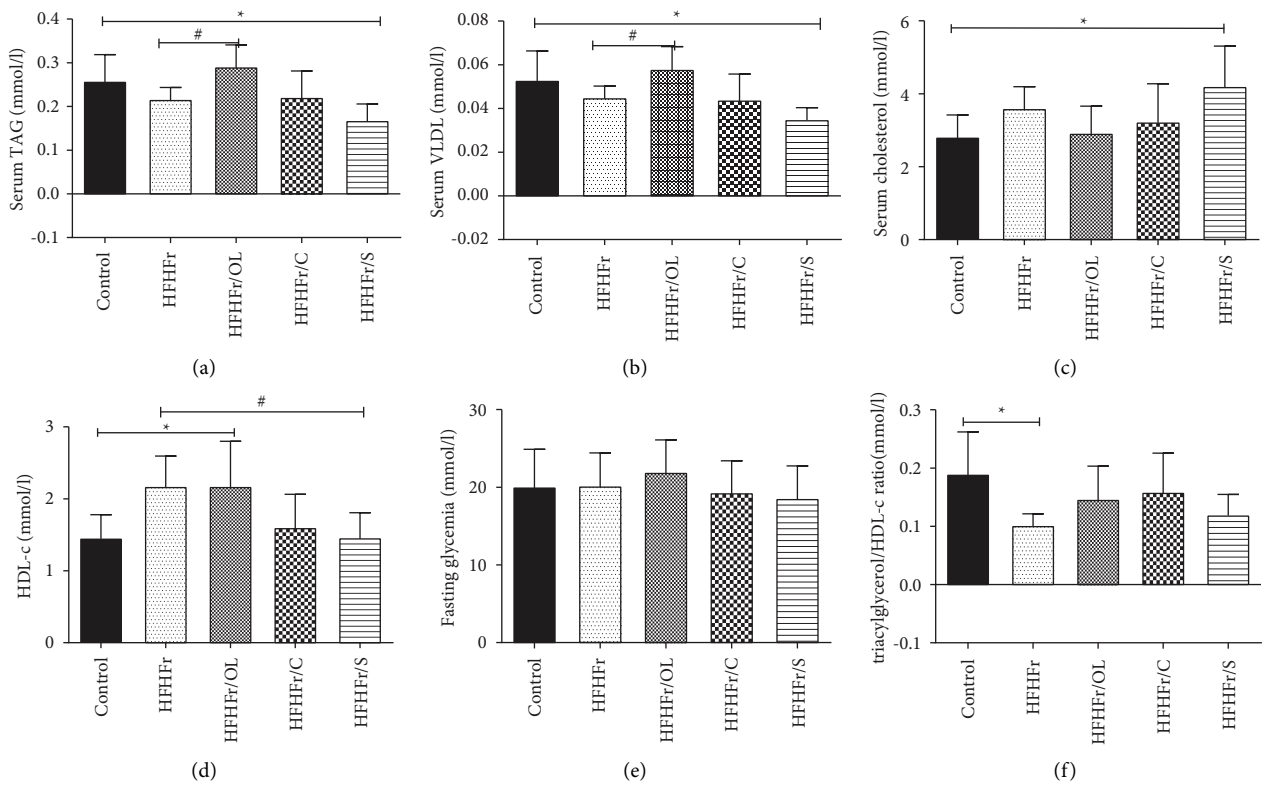

Figure 1: Analysis of lipid profile. Triacylglycerol (a). VLDL (b). Total cholesterol (c). HDL-C (d). Fasting glycemia (e). Triacylglycerol/HDL-C ratio (f). Data are reported as mean ± standard deviation for a period of 16 weeks. $^{*}p \leq 0.05$ vs. control; $^{\#}p \leq 0.05$ vs. HFHFr.

the control group than in any other group ($p < 0.001$), while there was no difference with regard to C18 : 1 or oleic acid (omega-9) levels or the total sum of fatty acids among all groups. Whereas an olive oil-rich diet reduced the hepatic levels of omega-6 (C18 : 1 n-6) compared to control (14.41 ± 1.43 vs. 21.90 ± 3.92), soybean oil-rich diet resulted in increased hepatic levels of C18 : 1 n-6 compared to control and to HFHFr group (HFHFr/S: 29.63 ± 1.44 vs. HFHFr: 18.19 ± 1.55 vs. control: 21.90 ± 3.92, $p < 0.05$). Omega-3 hepatic incorporation was reduced in both HFHFr/OL and HFHFr groups compared to control ($p < 0.05$), whereas it was increased in groups receiving canola oil (HFHFr/CN) and soybean oil (HFHFr/S) compared to control and to the HFHFr group ($p < 0.05$). Arachidonic acid levels were lower in the treated groups than in control ($p < 0.05$). Despite EPA (C20 : 5 n-3) was significantly increased in the groups receiving the canola oil and soybean oil diets compared to control ($p < 0.05$), it was only increased in the canola oil group compared to the HFHFr group ($p < 0.001$). Although DHA (C22 : 6 n-3) levels were higher in canola oil group, they did not differ significantly. The group receiving soybean oil had higher amounts of PUFAs compared to control ($p < 0.05$). The results are shown in Table 4.

4. Discussion

Even though it is well known that the MUFAS and PUFAS, in special long chain *n*-3 PUFAs (EPA and DHA), can affect hepatic metabolic processes, their precise effects across different physiological situations are not fully understood. Thus, not only is the quantity of ingested fats but also the fatty acids composition is of pivotal importance for human health. Here both contributed to determining the effects of lipid modulation in different commercial vegetable oils [28–32].

Saturated fat was used to modulate the set diet in this study, more specifically lard-rich in oleic acid (C18 : 1 n-9, 36, 92%), which is the featured representative of monounsaturated fatty acids, followed by SFAs, palmitic acid in particular (C16 : 0.23, 86%). As expected, extravirgin olive oil had greater final sums of MUFAs, in which the most abundant one is the oleic acid (C18 : 1 n-9, 69.82%), followed by saturated fatty acids (13%), (C18 : 3 n-3; 1.14%), as it has been demonstrated by others as well [33]. Soybean oil is rich in C18 : 2 n-6 (57.52%), MUFAs (C18 : 1 n-9, 23.25%), and omega-6 (22%), which has been also reported in literature [13]. Finally, canola oil is rich in C18 : 1 n-9 (60.01%) followed by PUFAs (19.7% C18 : 2 n-6 and 8.02% C18 : 3 n-3, especially in EPA *e* DHA) as well as MUFAS, n-9, in agreement with reported data so far [34].

Meanwhile, the three vegetable oils used in the present study yielded positive results regarding the metabolic syndrome-related parameters. The HFHFr group showed an increase in weight compared to control and the remaining groups. The animals treated with the respective oils maintained a gradual and homogeneous weight gain similar to control. Food intake varied throughout the experiment and it was positively correlated with energy intake. However, diet intake affected weight gain only in the group receiving

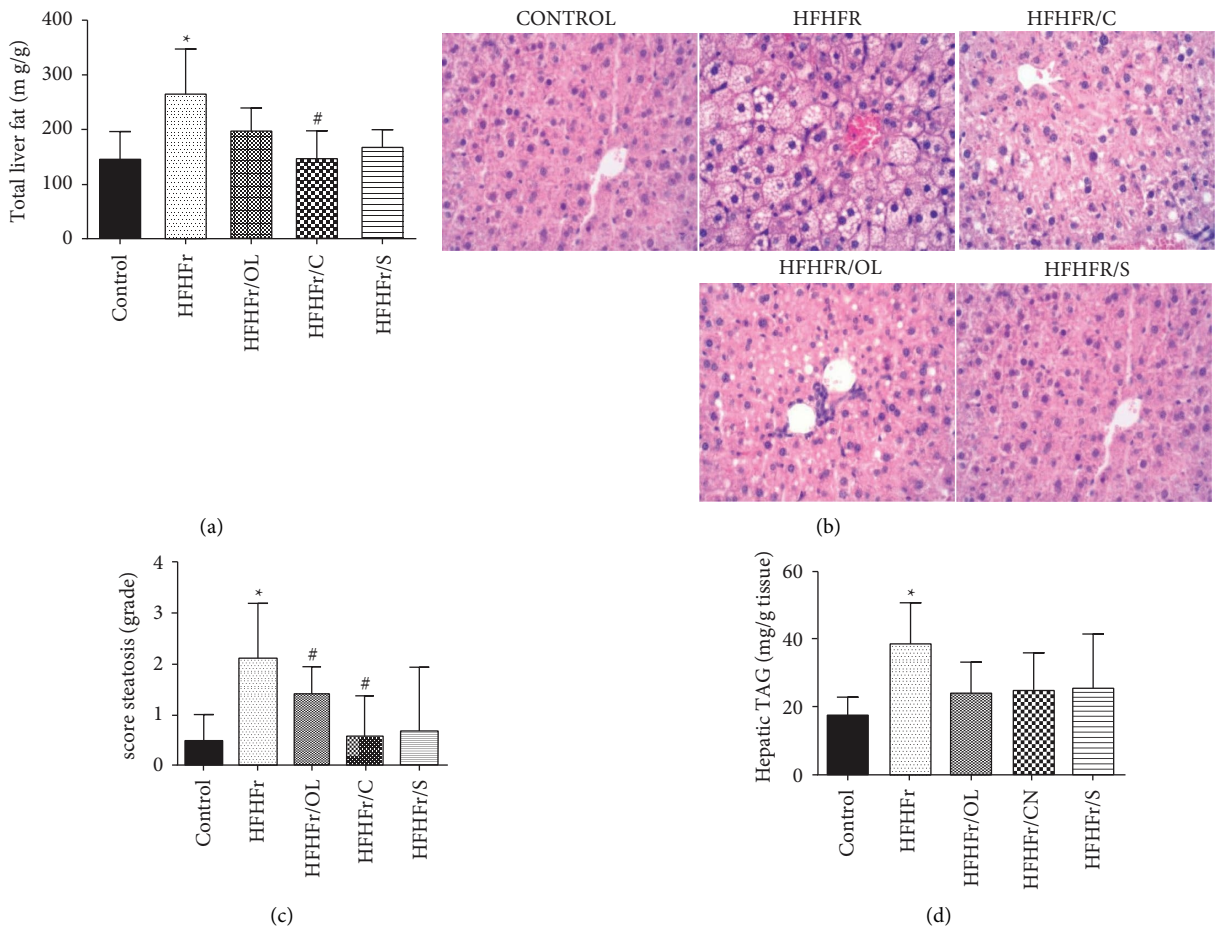

Figure 2: Analysis of hepatic parameters. Percent total hepatic fat (a). Liver photomicrograph (b). Steatosis score (c). Hepatic triacylglycerols (d). Data are reported as mean ± standard deviation for a period of 16 weeks. * $p \leq 0.05$ vs. control; # $p \leq 0.05$ vs HFHFr.

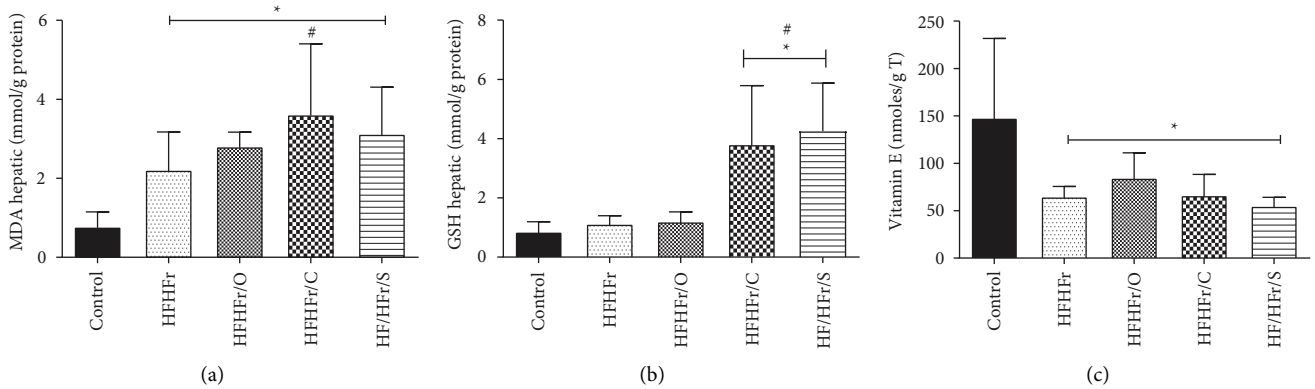

Figure 3: Hepatic content of MDA, GSH, and vitamin E in investigated animals (a). Hepatic GSH (b). Hepatic vitamin E (c). Data are reported as mean ± standard deviation for a period of 16 weeks. * $p \leq 0.05$ vs. control; # $p \leq 0.05$ vs. HFHFr.

western diet, whereas this did not occur in the groups receiving PUFAs and MUFAs, as determined by the diet efficiency rate [35].

Different types of fatty acids have different oxidation and deposition rates that may contribute to fat accumulation and weight gain. Reports have suggested positive effects of monounsaturated fatty acids (MUFAs) on weight control by increasing postprandial fat oxidation and diet-induced thermogenesis compared to SFAs or n-3 polyunsaturated fatty acids (PUFAs; flaxseed oil-rich in linolenic acid) [36]. Fatty acids regulate lipogenesis through various transcription factors and nuclear receptors, including PPARs, hepatocyte nuclear factor (HNF)-4, liver *X* receptor (LXR), and sterol response element-binding proteins (SREBPs) [37].

Table 4: Liver' fatty acid composition (wt% of total methyl esters).

Fatty acids	Control	HFHFr	HFHFr/OL	HFHFr/CN	HFHFr/S
C14 : 0	0.44 ± 0.05	0.32 ± 0.07	0.23 ± 0.06*	0.22 ± 0.07*	0.21 ± 0.05*
C16 : 0	27.38 ± 1.39	25.85 ± 1.35	23.09 ± 0.58*#	22.43 ± 0.38*#	23.72 ± 0.32*#
C18 : 0	6.56 ± 1.78	5.76 ± 3.40	6.89 ± 2.76	8.67 ± 4.23	7.04 ± 2.82
∑SFA	36.36 ± 2.04	33.56 ± 3.66	31.51 ± 2.88	33.03 ± 4.35	32.99 ± 2.45
Monounsaturated fatty acids (MUFAS)					
C16 : 1	3.21 ± 0.63	1.15 ± 0.33*	0.89 ± 0.28*	0.66 ± 0.30*	0.65 ± 0.15*
C18 : 1 n-9	25.43 ± 7.97	36.17 ± 8.73	40.57 ± 7.27*#	33.67 ± 11.03	23.53 ± 4.87
∑MUFAs	29.49 ± 8.61	38.28 ± 9.23	42.69 ± 8.14*#	35.27 ± 11.78	24.94 ± 5.21
Polyunsaturated fatty acids (PUFAS)					
C18 : 2 n-6	21.90 ± 3.92	18.19 ± 1.55	14.31 ± 1.43*	18.48 ± 2.64	29.64 ± 1.44*#
18 : 3 n-3	0.67 ± 0.13	0.34 ± 0.05*	0.23 ± 0.04*	1.23 ± 0.10*#	1.00 ± 0.19*#
C20 : 4 n-6	0.18 ± 0.12	0.05 ± 0.03*	0.03 ± 0.02*	0.03 ± 0.01*	0.04 ± 0.02*
EPA (20 : 5 n-3)	0.16 ± 0.05	0.10 ± 0.01	0.07 ± 0.01*	0.33 ± 0.06*#	0.18 ± 0.02*
DHA (22 : 6 n-3)	3.35 ± 1.08	2.63 ± 1.34	3.21 ± 1.15	4.04 ± 1.52	3.24 ± 1.13
∑PUFAs	34.18 ± 7.29	28.17 ± 5.93	25.80 ± 5.33	31.70 ± 7.42	42.08 ± 2.78*

Data are mean ± SD. Data for the five groups received different vegetable oils compared by ANOVA with Tukey's test.*Compared with control and #compared with high fatty and high fructose ($p < 0.05$). SFA, saturated fatty acids; MUFA, monounsaturated fatty acids; PUFA, polyunsaturated fatty acids; HFHFr, high fatty + fructose group; HFHFr/OL, fructose and 25% olive oil and 25% lard group; HFHFr/CN, fructose and 25% canola oil and 25% lard group; HFHFr/S, fructose and 25% soybean and 25% lard group; and control, receiving 7% soybean oil.

Moreover, a previous study showed that oil with a high P/S ratio was relevant to lower body fat accumulation, and high-MUFA oil with a high P/S ratio (HMHR; consisting of 60% MUFAs from the total fatty acids with a ratio of 5) may prevent HFD-induced increased in body weight and body fat. Therefore, quantity of ingested fats, as well as composition of fatty acids, feature a pivotal role in human health [36].

PUFAs affect essential fatty acids intake and adipose tissue lipolysis. The present findings for the groups receiving different oils demonstrate that there was no change in epididymal adipose tissue. Even though retroperitoneal adipose tissue was lower in the group receiving the canola oil diet, animals receiving western diet developed a greater volume of retroperitoneal adipose tissue and sum of adipose tissues. According to the chromatography findings in this study, canola oil is rich in n-3, especially in regard to the major incorporation of EPA and DHA. Such fatty acids regulate lipogenesis through various transcription factors and nuclear receptors, including PPARs. As it is known, PPAR is highly expressed in white adipose tissue, and its activation plays a key role in adipocyte development and differentiation resulting in lipolysis as consequence [36].

Several studies have demonstrated that omega-6 and omega-3 fatty acids suppress lipogenesis and NAFLD development by inhibiting SREBP1c and transcriptional genes involved in lipogenesis [13, 38–42]. In the present study, it was the HFHFr group that showed greater liver weight as well as greater accumulation of total hepatic fat and of hepatic triacylglycerols. It was the HFHFr/S group that otherwise featured lower accumulation of total hepatic fat and also lower steatosis score. Nevertheless, these data were positively correlated with histological analysis, as in accordance with macro and micro vesicular steatosis the present steatosis was classified as mild in HFHFr/S and HFHFr/CN groups and as moderate in HFHFr/OL group. The therapeutic effects of low dietary omega 6 : 3 ratio have been observed in animal models and in clinical trials with NAFLD/NASH patients. The significance of balanced omega 6 : 3 ratio was more evident in recent trials in which treatment of NAFLD patients with omega-3 fatty acids, such as eicosapentaenoic acid (EPA) or DHA, reduced steatosis [37].

According to Hijona et al. [43], the biochemical quantitation of hepatic fat shows a good correlation with the histological classification of hepatic steatosis proposed by Kleiner and Brunt [44]. The HFHFr/OL group showed higher serum levels of triacylglycerols and VLDL compared to the HFHFr groups, whereas the soybean oil group showed lower levels. Studies conducted on rodents have shown that diets enriched with extravirgin olive oil increase the activity of both acetyl-CoA carboxylase and fatty acid synthase and also reduce the activity of carnitine palmitoyltransferase, thus increasing lipogenesis and reducing β oxidation [45]. Furthermore, the reduced soybean oil values may be associated with the action of PUFAs (n-6), present in greater quantities in this vegetable oil, in terms of either both lipogenesis suppression and regulation of PPRα expression, with the consequent degradation of fatty acids [13]. Conversely, the group receiving olive oil displayed greater quantities of HDL-C. In a study carried out with 200 volunteers, Covas et al. [45] demonstrated that the consumption of extravirgin olive oil increased the plasma levels of HDL-C. Fasting glycemia and the insulin predicting factor did not differ among the groups studied. Yan et al. [46] also found no significant difference among groups in a study that compared different proportions of n-6/n-3. In the present study, canola oil did not show significant changes in the biochemical parameters among the treated groups.

The present data demonstrated a greater quantity of palmitic acid in the HFHFr/OL and HFHFr/S groups. It may be a fact related to the aforementioned described findings, with greater steatosis in the olive oil group and an increase in serum cholesterol in the soybean oil group. Palmitic acid is known for promoting increased inflammation of hepatic

cells [47]. Although the difference was not statistically significant, oleic acid levels were higher in the group receiving olive oil though. The olive oil presented lower amount of serum cholesterol. These results indicate that the molecular mechanism, through EVOO extracts, promotes a hypocholesterolemic effect through HMGCoAR activity modulation, a crucial enzyme in cholesterol biosynthesis and also the well-known target of statins [48].

Both canola oil and soybean oil induced higher EPA levels compared to control, even though these levels were higher only in the canola oil group than in the HFHFr group, while DHA showed no changes. Morrison et al. demonstrated that EPA was more effective than DHA regarding the parameters of steatosis [47]. Hanke et al. [49] demonstrated an attenuation of NAFLD through use of different quantities of canola oil and a greater hepatic quantity of EPA and DHA, alongside a reduction of inflammatory parameters. The present findings show that all the oils used for various groups' treatment increased lipid peroxidation, as demonstrated by the analysis of hepatic MDA. However, in relation to antioxidant protection based on GSH determination, an increase in hepatic GSH levels was only observed in groups treated with canola oil and soybean oil, while vitamin *E* levels were lower in the treated groups.

5. Conclusions

In summary, lipid modulation in a vegetable oil contained diet was able to reserve a number of adverse metabolic effects of high fat diet and high fructose diet, in special the usage of soybean oil and of canola oil. Therefore, canola oil is suggested to be useful to treat metabolic syndrome comorbidities and NAFLD. This appears to be an interesting low-cost and easily applicable alternative for the prevention/treatment of steatosis induced by rich western style diet in either or both patients with NAFLD and metabolic syndrome.

Data Availability

The data used to support this study are available from the corresponding author upon request.

Additional Points

Core tip: It is a fact that there is no guideline or more targeted treatment. Due to the increase in the consumption of ultra-processed foods, rich in saturated fat and fruit, the prevalence of disease increased. Thus, studied dietary methods through dietary modulation for the prevention of nonalcoholic liver disease in a wide scenario increased prevalence of nontransmissible chronic diseases.

Ethical Approval

All animal experiments conformed to the internationally accepted principles for the care and use of laboratory animals (Animal use Ethics Committee, Brazil; protocol no. No. 017/2015, The Institutional Animal Care and Use Committee at Faculdade de Medicina de Ribeirão Preto, SP, Brazil). Arrive guidelines statement: The authors have read the ARRIVE guidelines, and the manuscript was prepared and revised according to the arrival guidelines.

Conflicts of Interest

The authors declare that they have no conflicts of interest.

Authors' Contributions

M.C.S. conducted the research, wrote the article, performed the statistical analysis, and contributed to the study design and data interpretation. A.L.M.C.S and O.P.P contributed to technical support. R.L.Z contributes to the interpretation of histological data analysis. A.A.J. contributed to the technical support and data interpretation. All authors read and approved the final manuscript.

Acknowledgments

This study was supported by grant from FAPESP (Fundação de Amparo a Pesquisa do Estado de São Paulo), No. 2015/01348-6.

References

[1] W. Feng, H. Wang, P. Zhang et al., "Modulation of gut microbiota contributes to curcumin-mediated attenuation of hepatic steatosis in rats," *Biochimica et Biophysica Acta (BBA)—General Subjects*, vol. 1861, no. 7, pp. 1801–1812, 2017.

[2] A. Lonardo, C. D. Byrne, S. H. Caldwell, H. Cortez-Pinto, and G. Targher, "Global epidemiology of nonalcoholic fatty liver disease: meta-analytic assessment of prevalence, incidence, and outcomes," *Hepatology*, vol. 64, no. 4, 2016.

[3] R. Loomba, C. B. Sirlin, J. B. Schwimmer, and J. E. Lavine, "Advances in pediatric nonalcoholic fatty liver disease," *Hepatology*, vol. 50, no. 4, pp. 1282–1293, 2009.

[4] V. Marin, N. Rosso, M. Dal Ben et al., "An animal model for the juvenile non-alcoholic fatty liver disease and non-alcoholic steatohepatitis," *PLoS One*, vol. 11, no. 7, Article ID e0158817, 2016.

[5] N. Suzuki-Kemuriyama, T. Matsuzaka, M. Kuba et al., "Different effects of eicosapentaenoic and docosahexaenoic acids on atherogenic high-fat diet-induced non-alcoholic fatty liver disease in mice," *PLoS One*, vol. 11, no. 6, Article ID e0157580, 2016.

[6] P. Angulo, "Nonalcoholic fatty liver disease," *New England Journal of Medicine*, vol. 346, no. 16, pp. 1221–1231, 2002.

[7] G. C. Farrell and C. Z. Larter, "Nonalcoholic fatty liver disease: from steatosis to cirrhosis," *Hepatology*, vol. 43, no. S1, pp. S99–S112, 2006.

[8] M. Basaranoglu, G. Basaranoglu, and H. Sentürk, "From fatty liver to fibrosis: a tale of "second hit"," *World Journal of Gastroenterology*, vol. 19, no. 8, pp. 1158–1165, 2013.

[9] D. M. Torres, C. D. Williams, and S. A. Harrison, "Features, diagnosis, and treatment of nonalcoholic fatty liver disease," *Clinical Gastroenterology and Hepatology*, vol. 10, no. 8, pp. 837–858, 2012.

[10] C. P. Day and O. F. James, "Steatohepatitis: a tale of two "hits"?" *Gastroenterology*, vol. 114, no. 4, pp. 842–845, 1998.

[11] M. Basaranoglu, G. Basaranoglu, T. Sabuncu, and H. Senturk, "Fructose as a key player in the development of fatty liver disease," *World Journal of Gastroenterology*, vol. 19, no. 8, pp. 1166–1172, 2013.

[12] M. B. Vos and J. E. Lavine, "Dietary fructose in nonalcoholic fatty liver disease," *Hepatology*, vol. 57, no. 6, pp. 2525–2531, 2013.

[13] R. A. Siddiqui, Z. Xu, K. A. Harvey, T. M. Pavlina, M. J. Becker, and G. P. Zaloga, "Comparative study of the modulation of fructose/sucrose-induced hepatic steatosis by mixed lipid formulations varying in unsaturated fatty acid content," *Nutrition & Metabolism*, vol. 12, no. 1, p. 41, 2015.

[14] A. K. Leamy, R. A. Egnatchik, and J. D. Young, "Molecular mechanisms and the role of saturated fatty acids in the progression of non-alcoholic fatty liver disease," *Progress in Lipid Research*, vol. 52, no. 1, pp. 165–174, 2013.

[15] G. S. de Castro and P. C. Calder, "Non-alcoholic fatty liver disease and its treatment with n-3 polyunsaturated fatty acids," *Clinical Nutrition*, vol. 37, no. 1, pp. 37–55, 2018.

[16] T. Ueno, H. Sugawara, K. Sujaku et al., "Therapeutic effects of restricted diet and exercise in obese patients with fatty liver," *Journal of Hepatology*, vol. 27, no. 1, pp. 103–107, 1997.

[17] M. Cave, I. Deaciuc, C. Mendez et al., "Nonalcoholic fatty liver disease: predisposing factors and the role of nutrition," *The Journal of Nutritional Biochemistry*, vol. 18, no. 3, pp. 184–195, 2007.

[18] E. Juárez-Hernández, N. C. Chávez-Tapia, M. Uribe, and V. J. Barbero-Becerra, "Role of bioactive fatty acids in non-alcoholic fatty liver disease," *Nutrition Journal*, vol. 15, no. 1, p. 72, 2016.

[19] P. G. Reeves, F. H. Nielsen, and G. C. Fahey, "AIN-93 purified diets for laboratory rodents: final report of the American Institute of Nutrition ad hoc writing committee on the reformulation of the AIN-76A rodent diet," *Journal of Nutrition*, vol. 123, no. 11, pp. 1939–1951, 1993.

[20] R. Pamplona, M. Portero-Otín, D. Riba et al., "Mitochondrial membrane peroxidizability index is inversely related to maximum life span in mammals," *Journal of Lipid Research*, vol. 39, no. 10, pp. 1989–1994, 1998.

[21] E. M. Brunt, D. E. Kleiner, C. Behling et al., "Misuse of scoring systems," *Hepatology*, vol. 54, no. 1, pp. 369-370, 2011.

[22] E. G. Bligh and W. J. Dyer, "A rapid method of total lipid extraction and purification," *Canadian Journal of Biochemistry and Physiology*, vol. 37, no. 8, pp. 911–917, 1959.

[23] T. Lewis, P. D. Nichols, and T. A. McMeekin, "Evaluation of extraction methods for recovery of fatty acids from lipid-producing microheterotrophs," *Journal of Microbiological Methods*, vol. 43, no. 2, pp. 107–116, 2000.

[24] X. Fan, E. Y. Liu, V. P. Hoffman, A. J. Potts, B. Sharma, and D. C. Henderson, "Triglyceride/highdensity lipoprotein cholesterol ratio: a surrogate to predict insulin resistance and low density lipoprotein cholesterol particle size in nondiabetic patients with schizophrenia," *Journal of Clinical Psychiatry*, vol. 72, no. 06, pp. 806–812, 2011.

[25] D. Gerard-Monnier, I. Erdelmeier, K. Regnard, N. Mozehenry, J. C. Yadan, and J. Chaudière, "Reaction of 1-Methyl-2-phenylindole with malonaldehyde and 4-hydroxyalkenals: analytical applications to a colorimetric assay of lipid peroxidation," *Chemical Research in Toxicology*, vol. 11, no. 10, pp. 1176–1183, 1998.

[26] J. Sedlak and R. H. Lindsay, "Estimation of total, protein-bound, and non protein sulfhydryl groups in tissue with Ellman's reagent," *Analytical Biochemistry*, vol. 25, no. 1, pp. 192–205, 1968.

[27] J. Arnaud, I. Fortis, S. Blachier, D. Kia, and A. Favier, "Simultaneous determination of retinol, alpha-tocopherol and beta-carotene in serum by isocratic high-performance liquid chromatography," *Journal of Chromatography B: Biomedical Sciences and Applications*, vol. 572, no. 1-2, pp. 103–116, 1991.

[28] Z. M. Younossi, "Review article: current management of non-alcoholic fatty liver disease and non-alcoholic steatohepatitis," *Alimentary Pharmacology & Therapeutics*, vol. 28, no. 1, pp. 2–12, 2008.

[29] W. Peverill, L. W. Powell, and R. Skoien, "Evolving concepts in the pathogenesis of NASH: beyond steatosis and inflammation," *International Journal of Molecular Sciences*, vol. 15, no. 5, pp. 8591–8638, 2014.

[30] A. Whaley-Connell and J. R. Sowers, "Indices of obesity and cardiometa-bolic risk," *Hypertension*, vol. 58, no. 6, pp. 991–993, 2011.

[31] J. S. Wooten, T. N. Nick, A. Seija, K. E. Poole, and K. B. Stout, "High-fructose intake impairs the hepatic hypolipidemic effects of a high-fat fish-oil diet in C57BL/6 mice," *Journal of Clinical and Experimental Hepatology*, vol. 6, no. 4, pp. 265–274, 2016.

[32] G. S. De Castro, J. F. R. Cardoso, P. C. Calder, A. A. Jordão, and H. Vannucchi, "Fish oil decreases hepatic lipogenic genes in rats fasted and refed on a high fructose diet," *Nutrients*, vol. 7, no. 3, pp. 1644–1656, 2015.

[33] P. Priore, A. Cavallo, A. Gnoni, F. Damiano, G. V. Gnoni, and L. Siculella, "Modulation of hepatic lipid metabolism by olive oil and its phenols in nonalcoholic fatty liver disease," *IUBMB Life*, vol. 67, no. 1, pp. 9–17, 2015.

[34] L. Lin, H. Allemekinders, A. Dansby et al., "Evidence of health benefits of canola oil," *Nutrition Reviews*, vol. 71, no. 6, pp. 370–385, 2013.

[35] M. J. Kang, H. S. Ahn, and S. S. Lee, "Effects of polyunsaturated/saturated fatty acid ratio and antioxidant supplementation on hepatic TBARS and enzyme activities under the maintenance of dietary peroxidizability index value in young and adult rats," *Annals of Nutrition & Metabolism*, vol. 49, no. 5, pp. 304–311, 2005.

[36] S. C. Yang, S. H. Lin, J. S. Chang, and Y. W. Chien, "High fat diet with a high monounsaturated fatty acid and polyunsaturated/saturated fatty acid ratio suppresses body fat accumulation and weight gain in obese hamsters," *Nutrients*, vol. 9, no. 10, p. 1148, 2017.

[37] N. Soni, A. B. Ross, N. Scheers, I. Nookaew, B. G. Gabrielsson, and A. S. Sandberg, "The omega-3 fatty acids EPA and DHA, as a part of a murine high-fat diet reduced lipid accumulation in brown and white adipose tissues," *International Journal of Molecular Sciences*, vol. 20, no. 23, p. 5895, 2019.

[38] L. Tappy and K. A. Le, "Does fructose consumption contribute to non-alcoholic fatty liver disease?" *Clinics and Research in Hepatology and Gastroenterology*, vol. 36, no. 6, pp. 554–560, 2012.

[39] S. Kajikawa, T. Harada, A. Kawashima, K. Imada, and K. Mizuguchi, "Highly purified eicosapentaenoic acid prevents the progression of hepatic steatosis by repressing monounsaturated fatty acid synthesis in high-fat/high-sucrose diet-fed mice," *Prostaglandins, Leukotrienes and Essential Fatty Acids*, vol. 80, no. 4, pp. 229–238, 2009.

[40] J. R. Levy, J. N. Clore, and W. Stevens, "Dietary n-3 polyunsaturated fatty acids decrease hepatic triglycerides in Fischer 344 rats," *Hepatology*, vol. 39, no. 3, pp. 608–616, 2004.

[41] S. D. Clarke, D. R. Romsos, and G. A. Leveille, "Differential effects of dietary methyl esters of long-chain saturated and polyunsaturated fatty acids on rat liver and adipose tissue lipogenesis," *Journal of Nutrition*, vol. 107, no. 7, pp. 1170–1181, 1977.

[42] S. D. Clarke, M. K. Armstrong, and D. B. Jump, "Dietary polyunsaturated fats uniquely suppress rat liver fatty acid synthase and S14 mRNA content," *Journal of Nutrition*, vol. 120, no. 2, pp. 225–231, 1990.

[43] E. Hijona, L. Hijona, M. Larzabal et al., "Biochemical determination of lipid content in hepatic steatosis by the Soxtec method," *World Journal of Gastroenterology*, vol. 16, no. 12, pp. 1495–1499, 2010.

[44] D. E. Kleiner, E. M. Brunt, M. Van Natta et al., "Design and validation of a histological scoring system for nonalcoholic fatty liver disease," *Hepatology*, vol. 41, no. 6, pp. 1313–1321, 2005.

[45] M. I. Covas, K. Nyyssönen, H. E. Poulsen et al., "The effect of polyphenols in olive oil on heart disease risk factors: a randomized trial," *Annals of Internal Medicine*, vol. 145, no. 5, pp. 333–431.

[46] Li G. Yang, Z. X. Song, H. Yin et al., "Low n-6/n-3 PUFA ratio improves lipid metabolism, inflammation, oxidative stress and endothelial function in rats using plant oils as n-3 fatty acid source," *Lipids*, vol. 51, no. 1, pp. 49–59, 2016.

[47] M. C. Morrison, P. Mulder, P. M. Stavro et al., "Replacement of dietary saturated fat by PUFA-rich pumpkin seed oil attenuates non-alcoholic fatty liver disease and atherosclerosis development, with additional health effects of virgin over refined oil," *PLoS One*, vol. 10, no. 9, Article ID e0139196, 2015.

[48] C. Lammi, N. Mulinacci, L. Cecchi et al., "Virgin olive oil extracts reduce oxidative stress and modulate cholesterol metabolism: comparison between oils obtained with traditional and innovative processes," *Antioxidants*, vol. 9, p. 798, 2020.

[49] D. Hanke, P. Zahradka, S. K. Mohankumar, J. L. Clark, and C. G. Taylor, "A diet high in alpha-linolenic acid and monounsaturated fatty acids attenuates hepatic steatosis and alters hepatic phospholipid fatty acid profile in diet-induced obese rats," *Prostaglandins, Leukotrienes and Essential Fatty Acids*, vol. 89, no. 6, pp. 391–401, 2013.

[50] P. Puri, R. A. Baillie, M. M. Wiest et al., "A lipidomic analysis of nonalcoholic fatty liver disease," *Hepatology*, vol. 46, no. 4, pp. 1081–1090, 2007.

[51] T. Matsuzaka, A. Atsumi, R. Matsumori et al., "Elovl6 promotes nonalcoholic steatohepatitis," *Hepatology*, vol. 56, no. 6, pp. 2199–2208, 2012.

Hindawi
Evidence-Based Complementary and Alternative Medicine
Volume 2022, Article ID 8105306, 16 pages
https://doi.org/10.1155/2022/8105306

Research Article

Huangjia Ruangan Granule Inhibits Inflammation in a Rat Model with Liver Fibrosis by Regulating TNF/MAPK and NF-κB Signaling Pathways

Qiang Cai,[1] Zongquan Wang,[2] Rong Zhang,[1] Lili Zhang,[2] Sainan Cui,[1] Huiyuan Lin,[1] Xinran Tang,[1] Dongying Yang,[1] Xianrong Lin,[1] Shasha Bai,[1] Jin Gao,[2] and Lei Yang[1]

[1]*School of Pharmaceutical Sciences, Guangzhou University of Chinese Medicine, Guangzhou 510000, China*
[2]*Yingkerui (Hengqin) Pharmaceutical Research Institute Co., Ltd, Zhuhai 519000, China*

Correspondence should be addressed to Jin Gao; gaojin@ykrskj.com and Lei Yang; yanglei@gzucm.edu.cn

Received 25 April 2022; Revised 24 May 2022; Accepted 31 May 2022; Published 30 July 2022

Academic Editor: Chan-Yen Kuo

The Huangjia Ruangan granule (HJRG) is a clinically effective Kampo formula, which has a significant effect on liver fibrosis and early liver cirrhosis. However, the mechanism underlying HJRG in treating liver fibrosis remains unclear. In this study, carbon tetrachloride (CCl_4) was used to induce liver fibrosis in rats to clarify the effect of HJRG on liver fibrosis and its mechanism. Using network pharmacology, the potential mechanism of HJRG was initially explored, and a variety of analyses were performed to verify this mechanism. In the liver fibrosis model, treatment with HJRG can maintain the liver morphology, lower the levels of AST and ALT in the serum, and ameliorate pathological damage. Histopathological examinations revealed that the liver structure was significantly improved and fibrotic changes were alleviated. It can effectively inhibit collagen deposition and the expression of α-SMA, reduce the levels of the rat serum (HA, LN, PC III, and Col IV), and inhibit the expression of desmin, vimentin, and HYP content in the liver. Analyzing the results of network pharmacology, the oxidative stress, inflammation, and the related pathways (primarily the TNF signaling pathway) were identified as the potential mechanism of HJRG against liver fibrosis. Experiments confirmed that HJRG can significantly increase the content of superoxide dismutase and glutathione and reduce the levels of malondialdehyde and myeloperoxidase in the rat liver; in addition, HJRG significantly inhibited the content of proinflammatory cytokines (TNF-α, IL-1β, and IL-6) and reduced the expression of inflammatory regulators (Cox2 and iNOS). Meanwhile, treatment with HJRG inhibited the phosphorylation of NF-κB P65, IκBα, ERK, JNK, and MAPK P38. Moreover, HJRG treatment reversed the increased expression of TNFR1. The Huangjia Ruangan granule can effectively inhibit liver fibrosis through antioxidation, suppressing liver inflammation by regulating the TNF/MAPK and NF-κB signaling pathways, thereby preventing the effect of liver fibrosis.

1. Introduction

Liver fibrosis is a pathophysiological process. It is the abnormal proliferation of connective tissue in the liver caused by various pathogenic factors, which is a serious health problem for humans. Without intervention and treatment, liver fibrosis may progress into liver cirrhosis or even liver cancer [1]. At present, the treatment of liver fibrosis is primarily based on the original cause of the disease, such as anti-inflammatory therapy [2], regulating the body's oxidative stress [3], inhibiting the deposition of the extracellular matrix (ECM) in the liver, and promoting ECM degradation [4]. Clinical studies have shown that liver fibrosis can be reversed. Therefore, in the stage of liver fibrosis or even the advanced stage of liver fibrosis, taking preventive interventions can effectively improve the clinical results [5].

CCl_4 is a common hepatotoxin, widely used to induce toxic effects in the liver of experimental animal models, which can induce liver inflammation and fibrosis in rats [6]. Prolonged exposure to CCl_4 can promote lipid peroxidation, and reactive oxygen species (ROS) are excessively produced in the body, leading to the consumption of glutathione

(GSH), superoxide dismutase (SOD), malondialdehyde (MDA), and myeloperoxidase (MPO) formation, which causes oxidative stress [7]. The induction of CCl_4 further lures inflammation in the liver tissues, leading to the release of various inflammatory cytokines, such as tumor necrosis factor-alpha (TNF-α, IL-6, and IL-1β), and inflammatory regulators (Cox2 and iNOS), thus causing hepatitis [8]. Moreover, the increase of inflammatory cytokines leads to further aggravation in the oxidative stress, thereby maintaining a vicious circle, leading to the conversion of HSCs from a resting state to myofibroblast-like cells, then activating the myofibroblasts, which are responsible for matrix remodeling and the increasing levels of ECM proteins such as collagen, desmin, vimentin, and laminin [9], thereby leading to liver fibrosis, liver cirrhosis, and liver cancer. Therefore, medical interventions that are aimed at blocking oxidative stress and inflammation are crucial in reversing liver fibrosis.

Transcriptional regulatory nuclear factor (NF-κB P65) is an important mediator of the inflammatory signal to stimulation [10]. A large number of studies have shown that the upregulation of NF-κB P65 can stimulate the proliferation of hepatic stellate cells (HSCs) and inhibit HSC apoptosis, which plays a key role in fibrosis [11]. Meanwhile, the MAPK pathway is another major extracellular signal transduction pathway stimulated by inflammatory mediators. The MAPK family includes three components: c-Jun N-terminal kinase (JNK), extracellular signal receptor-activated kinase (ERK) 1/2, and p38 MAPK. Once stimulated by signals, ERK/JNK/p38 is phosphorylated to mediate inflammatory responses [12]. TNFR1 is thought to be the major receptor involved in the activation of the NF-κB and MAPK pathways, which in turn induces the expression of proteins of the inflammatory response and plays an important role in regulating the inflammatory response [13].

The Huangjia Ruangan granule is a pure Chinese medicine compound preparation, which is composed of *Hedysarum Multijugum Maxim* (Huangqi, HQ), *Trionyx sinensis Wiegmann* (Biejia, BJ), *Radix Puerariae* (Gegen, GG), *Radix Bupleuri* (Chaihu, CH), *Ganoderma* (Lingzhi, LZ), *Radix Paeoniae Rubra* (Chishao, CS), *Radix Salviae* (Danshen, DS), *Panax Notoginseng* (Sanqi, SQ), *Abri Herba* (Jigucao, JGC), and *Phyllanthus urinaria* L (YeXiaZhu, YXZ). HQ and CH are used to ameliorate liver injury [14, 15]; BJ can soften and disperse knots; LZ, CS, DS, and SQ can promote the blood circulation and have antioxidant and anti-inflammatory effects [16–19]; GG, JGC, and YXZ can detoxify damp-heat residual toxins [5, 20, 21]. The combination of these drugs exerts a variety of pharmacological effects, such as antioxidation, anti-inflammatory, and antifibrosis while protecting the liver and relieving depression. In addition, it is clinically used to relieve liver fibrosis and early liver cirrhosis. However, the specific mechanism of how HJRG relieves liver fibrosis remains unclear.

Chinese medicine has attracted great interest in the treatment of liver fibrosis for its efficacy and few side effects [22], but its chemical composition is complex, and it acts on multiple targets in different ways. All of these pose challenges to the understanding of underlying mechanisms [23]. Network pharmacology is based on system biology and network analysis [24]. Given the rapid development of various bioinformatics resources, network pharmacology methods have been applied to the discovery of active ingredients and molecular mechanisms of Chinese medicine [25]. Therefore, the research of Chinese medicine based on network pharmacology is worth exploring.

We first studied the pharmacodynamics of rats with liver fibrosis, and results have showed that HJRG demonstrated obvious antiliver fibrosis effects. Afterward, we searched the chemical composition and targets of HJRG through the database and then constructed a composite target-disease network combined with relevant literature to predict the mechanism of HJRG in the treatment of liver fibrosis. Finally, we verified its potential mechanism through pharmacological experiments and clarified that the Huangjia Ruangan granule can effectively inhibit liver fibrosis through antioxidation, inhibiting liver inflammation by regulating the TNF/MAPK and NF-κB signaling pathways, thereby preventing the effect of liver fibrosis.

2. Materials and Methods

2.1. Animals and Experimental Design. A total of 72 male SD rats, specific pathogen-free (SPF) grade, weighing 180–220 g, were provided by the Laboratory Animal Center of Guangzhou University of Traditional Chinese Medicine (experimental animal use license number: SYXK (Guangdong) 2018–0085; Laboratory animal production license number: SCXK (Guangdong) 2018-0034). The experimental rats were kept in an SPF animal room with suitable standard environmental temperature and humidity. During the breeding period, the rats were exposed to sunlight for 12 h every day. After 1 week, the rats were randomly divided into six groups: the control group (Control), the model group (Model), the silymarin group (Silymarin), the Huangjia Ruangan granule low-dose group (HJRG-L), the Huangjia Ruangan granule medium-dose group (HJRG-M), and the Huangjia Ruangan granule high-dose group (HJRG-H). Twelve rats were included in each group. The control group was given the corresponding olive oil two times a week for 10 weeks to induce liver fibrosis in the rat models, whereas the other groups were given a 20% CCl_4 olive oil solution (3 mL/kg) by gavage. From the second day of modeling, the administration group was given the corresponding test drug by gavage. The silymarin group was given the silymarin solution at a daily dose of 25 mg/kg/d. The Huangjia Ruangan granule low-dose group (1.16 g/kg/d), the middle-dose group (2.32 g/kg/d), and the high-dose group (4.64 g/kg/d) were given a daily dose of the Huangjia Ruangan granule solution by gavage, and the control group and the model group were given the corresponding amount of drinking water by gavage once a day for 10 weeks. Silymarin was purchased from Shanghai Macklin Biochemical Co., Ltd (Shanghai, China, cat no.S873807), and the Huangjia Ruangan granule was obtained from YingKeRui (Hengqin) Pharmaceutical Research Institute Co., Ltd (Zhuhai, China, cat no. 20190615)

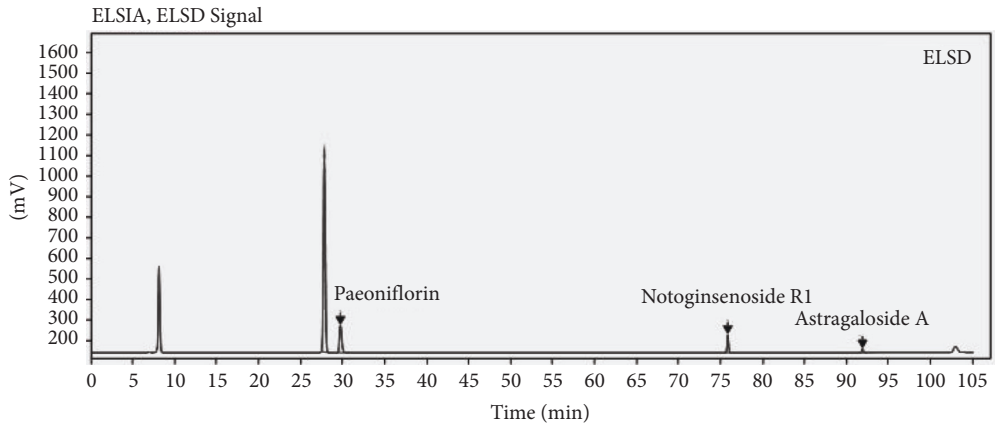

(a)

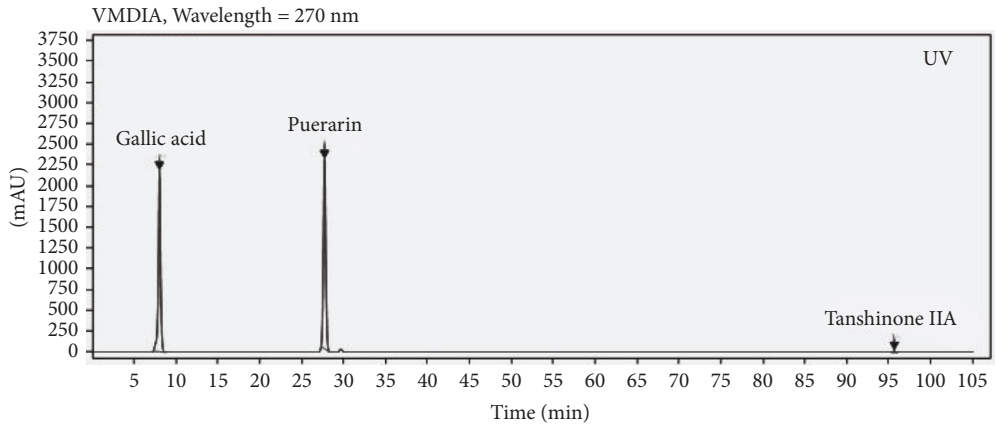

(b)

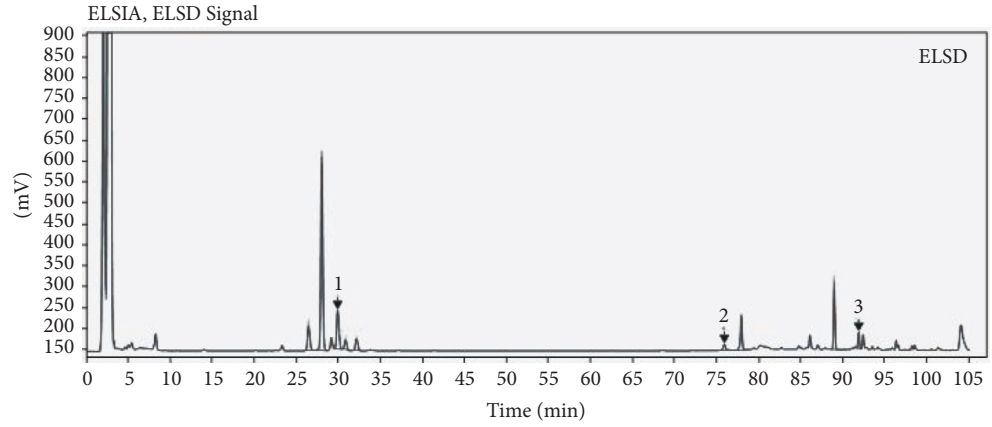

(c)

Figure 1: Continued.

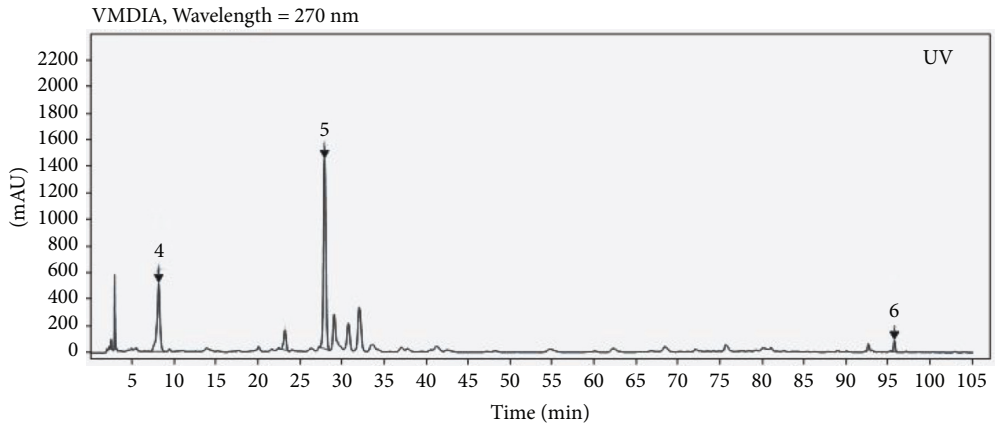

(d)

Figure 1: The results of HJRG by HPLC. (a) The reference substance of paeoniflorin, notoginsenoside R1, and astragaloside A in HPLC. (b) The reference substance of gallic acid, puerarin, and tanshinone IIA in HPLC. (c) The HPLC analysis results of HJRG. (1) Paeoniflorin; (2) notoginsenoside R1; (3) astragaloside (A). (d) The HPLC analysis results of HJRG. (4) Gallic acid. (5) Puerarin. (6) Tanshinone IIA.

2.2. HPLC Analysis. A HPLC assay was carried out using a Waters Symmetry-C18 column (250 mm × 4.6 mm, 5 μm). The phases were mobile phase A = methanol and mobile phase B = 0.1% aqueous acetic acid. Program gradient: 0–25 min, 5%–30% A; 25–50 min, 30%–35% A; 50–65 min, 35%–45% A; 65–95 min, 45%–95% A; 95–105 min, 95% A. The flow rate was 1 mL/min. The ELSD was used for paeoniflorin, notoginsenoside R1, and astragaloside. The detection wavelength was set at 270 and was used for gallic acid, puerarin, and tanshinone IIA (Figure 1).

2.3. Histopathological Analysis of the Liver. After fixing the liver with 4% paraformaldehyde, it was dehydrated with ethanol, transparent with xylene, and embedded in paraffin to prepare 4 μm-thick histopathological sections for eosin (H&E) staining (Beyotime Bio, cat no. C0105) and Sirius red staining (Legend Bio, cat no. DC0041) to observe histopathology and collagen formation. Sirius red staining was quantified by the Image J software.

2.4. Serum Biochemical Analysis and Hepatic HYP Content Analysis. After the rats were anesthetized, blood was drawn from the abdominal aorta, and the serum was obtained by centrifugation. The operation was performed according to the kit instructions to determine the contents of ALT (Nanjing Jiancheng Bio, cat no. C009-2-1) and AST (Nanjing JianchengBio, cat no. C010-2-1) in the serum, and HYP (Nanjing Jiancheng Bio, cat no. A030-2-1) in the liver tissues. The serum PC III (JiangLai Bio, cat no. JL20799), Col-IV (JiangLai Bio, cat no. JL20754), HA (JiangLai Bio, cat no. JL10946), and LN (JiangLai Bio, cat no. JL13737) contents were determined by enzyme-linked immunosorbent assay (ELISA).

2.5. Network Pharmacological Analysis. The active ingredients of the Huangjia Ruangan granule and their corresponding targets were collected on the basis of the Traditional Chinese Medicine System Pharmacology Analysis Platform (TCMSP). Relevant target information of liver fibrosis was obtained from the OMIM database, TTD database, GeneCards database, and DisGeNet database. The intersection was used to obtain the predicted target of the Huangjia Ruangan granule for the treatment of liver fibrosis, and Cytoscape software was used to construct the "C (component)-T (target)" action network diagram. The DAVID database was used to enrich the targets in the network for GO enrichment and KEGG pathway enrichment, analyze the biological treatment process of the Huangjia Ruangan granule on liver fibrosis and the signal pathway conduction process, and then predict the drug mechanism. The enrichment analysis results were visualized through OmicShare.

2.6. Analysis of Oxidative Stress Indicators. The liver tissue was accurately weighed, and nine times the volume of normal saline was added to a weight (g)-to-volume (mL) ratio of 1 : 9. The liver was cut, and the homogenate was prepared in an ice water bath, centrifuged at 3000 rpm for 10 min, and collected. The supernatant was a 10% homogenized supernatant to be tested. According to the kit instructions, the expression levels of malondialdehyde (MDA) (Nanjing Jiancheng Bio, cat no. A003-1), GSH (Nanjing Jiancheng Bio, cat no. A006-2-1), and SOD (Nanjing Jiancheng Bio, cat no. A001-3) in the rat liver tissues were determined.

2.7. Myeloperoxidase (MPO) Activity. The liver tissue was accurately weighed. The second reagent solution prepared by using the kit as the homogenization medium was used, and the homogenization medium was added to a weight-to-volume ratio of 1 : 19 to prepare a 5% tissue homogenate without centrifugation. According to the kit instructions, the MPO (Nanjing Jiancheng Bio, cat no. A044-1-1) activity in the rat liver homogenate was determined.

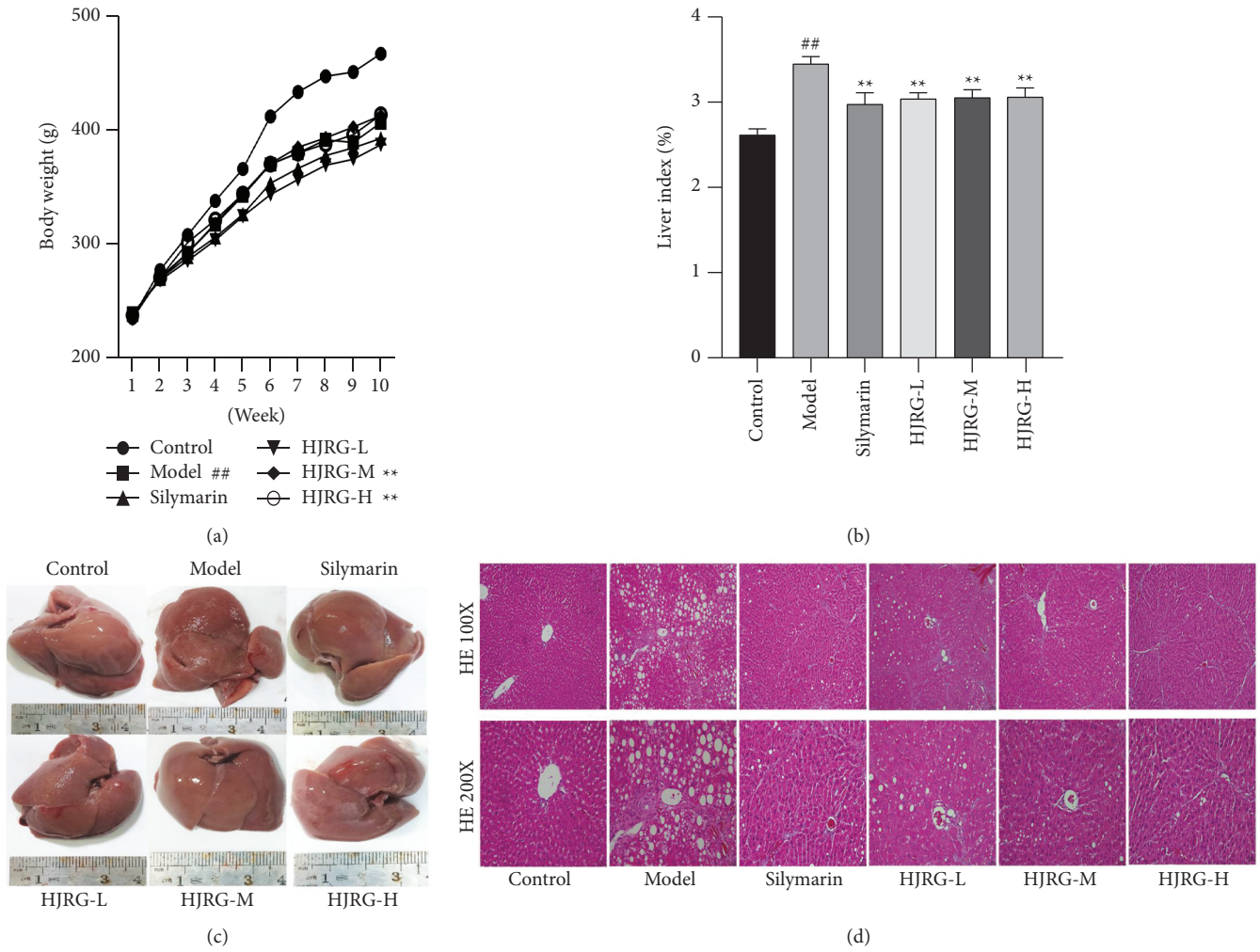

Figure 2: Continued.

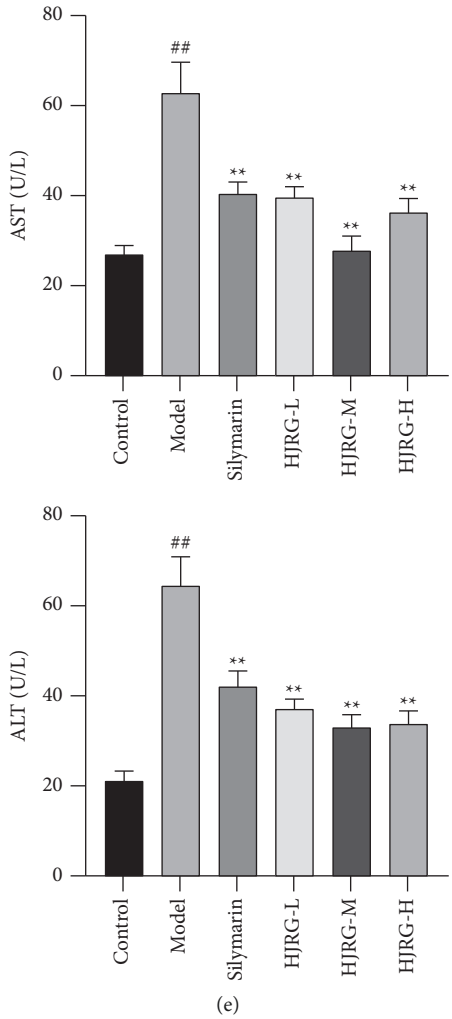

Figure 2: HJRG prevents the injury of CCl_4 in rats. (a) Comparison of the body weight of rats in each group. (b) The Liver Index of rats in different groups ($n = 12$). (c) Appearance of the isolated liver of each group of rats. (d) HE staining of the liver tissue representative images (Magnification, 100X and 200X). (e) Concentrations of AST and ALT in the serum ($n = 12$). #$p < 0.05$ and ##$p < 0.01$, compared with the control group; $^{*}p < 0.05$ and $^{**}p < 0.01$, compared with the model group. Control: control group; Model: model group; Silymarin: silymarin group; HJRG-L: Huangjia Ruangan granule low-dose group; HJRG-M: Huangjia Ruangan granule medium-dose group; HJRG-H: Huangjia Ruangan granule high-dose group.

2.8. Western Blot Analysis. The liver tissue was accurately weighed, and tissue lysate was added to a weight (mg)-to-volume (μL) ratio of 1 : 10. Then, a tissue homogenate was prepared using a tissue homogenizer and centrifuged at 12000 rpm at 4°C for 15 min. The supernatant was collected, quantified using the BCA protein assay kit (Keygen Biotech), and boiled in a metal heater at 100°C for 10 min for denaturation. Approximately 50 mg of the total protein was separated by 12% SDS-polyacrylamide gel electrophoresis and transferred to a polyvinylidene fluoride membrane. The membrane was blocked with 5% skimmed milk powder for 2 h. The primary antibody was incubated at 4°C overnight (over 12 h), and then the corresponding secondary antibody was incubated on a shaker at room temperature for 1.5 h. The bound protein was detected using the Bio-Rad imaging system. The gray value of each band relative to the internal reference protein of the same sample was analyzed on the ImageJ software. The main antibodies detected by western blotting were as follows: TNFR1 (1 : 1000, Affinity, USA), NF-κB P65 (1 : 1000, Cell Signaling Technology, USA), P-IκBα (1 : 1000, Cell Signaling Technology, USA), ERK (1 : 1000, Affinity, USA), P-ERK (1 : 1000, Affinity, USA), JNK (1 : 1000, Cell Signaling Technology, USA), P-JNK (1 : 1000, Cell Signaling Technology, USA), MAPK P38 (1 : 1000, Cell Signaling Technology, USA), P-P38 (1 : 1000, Cell Signaling Technology, USA), iNOS (1 : 1000, Affinity, USA), Cox2 (1 : 1000, Affinity, USA), TNF-α (1 : 500, Affinity, USA), IL-6 (1 : 1000, Affinity, USA), IL-1β (1 : 1000, Affinity, USA), Desmin

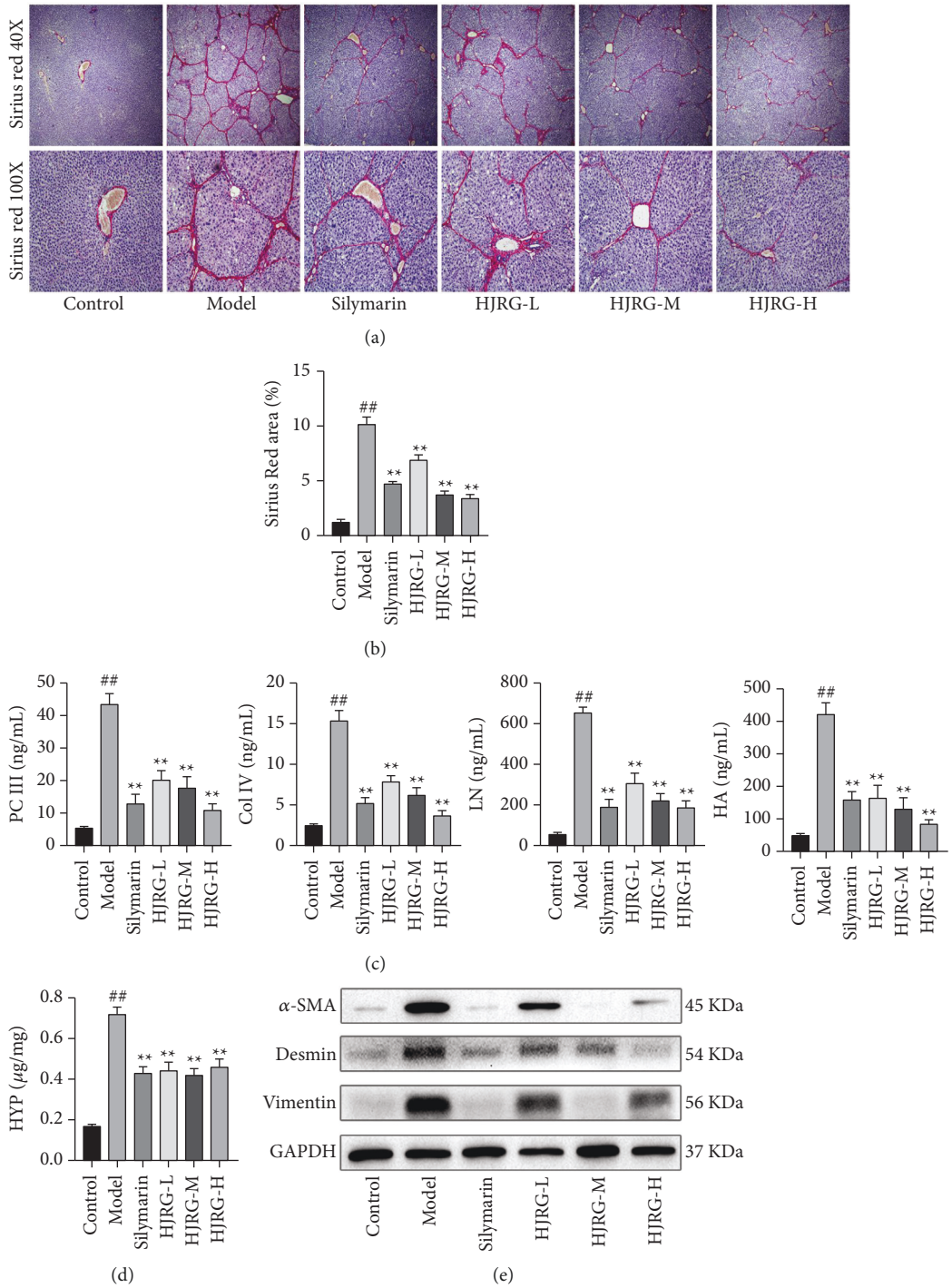

Figure 3: Continued.

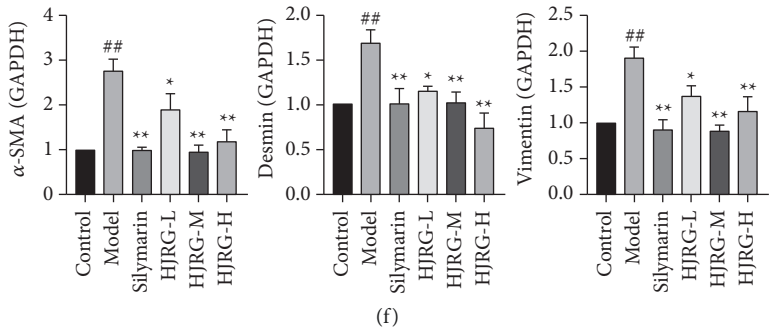

Figure 3: HJRG can reduce the progression of fibrosis. (a) Sirius red staining of liver tissue sections (magnification, 40X and 100X). (b) Quantification of collagen deposition by Sirius red staining ($n = 3$). (c) Four serum indexes of liver fibrosis: PC III, Col IV, LN, and HA ($n = 12$). (d) HYP contents in liver tissue ($n = 8$). (e) Effects of HJRG on protein levels of α-SMA, desmin, and vimentin in liver tissue. (f) Quantification of α-SMA, desmin, vimentin, and the protein expression in liver tissue ($n = 5$). #$p < 0.05$ and ##$p < 0.01$, compared with the control group; $^{*}p < 0.05$ and $^{**}p < 0.01$, compared with the model group. Control: control group; Model: model group; silymarin: silymarin group; HJRG-L: Huangjia Ruangan granule low-dose group; HJRG-M: Huangjia Ruangan granule medium-dose group; HJRG-H: Huangjia Ruangan granule high-dose group.

(1 : 1000, Affinity, USA), Vimentin (1 : 1000, Affinity, USA), and α-SMA (1 : 500, Affinity, USA).

2.9. Statistical Analysis. GraphPad Prism was used to perform Dunnett's multiple comparison test. The statistical analysis results were expressed as the mean value of SEM, and statistical analysis was analyzed by analysis of variance. $p < 0.05$ was considered statistically significant.

3. Result

3.1. Attenuating Effect of the Huangjia Ruangan Granule on CCl_4 Liver Injury. Compared with the control group, the weight of the model group increases slowly, and the last weight significantly decreased (Figure 2(a)). The Liver Index is significantly higher (Figure 2(b)), and the isolated liver is dim in color, with a rough and granular surface (Figure 2(c)). Compared with the model group, HJRG and silymarin can effectively alleviate the slow weight gain of rats, last weight gain, smooth surface, color of the liver, and significantly reduce the liver index of rats. Liver histopathological examination is the gold standard for the diagnosis of liver fibrosis. The histopathological changes in the liver tissue were detected in liver sections (Figure 2(d)). Evident changes were observed in the liver tissue of the model group, including necrosis, inflammatory cell infiltration, and diffuse fat changes. Compared with the model group, HJRG and silymarin treatment significantly ameliorated necrosis, inflammation, and steatosis. Serum AST and ALT activities are markers of liver toxicity [26]. Compared with the control group, the AST and ALT (Figure 2(e)) of the model group were significantly increased ($p < 0.01$). By contrast, HJRG and silymarin treatment significantly reduced serum AST and ALT activities. Therefore, the Huangjia Ruangan granule can regulate liver injury in rats.

3.2. Huangjia Ruangan Granule Improves Liver Fibrosis Induced by CCl_4 in Rats. As shown in the figure (Figures 3(a) 3(b)), the model group was stained with Sirius red to show the evidence of collagen accumulation, connective tissue deposition, and thin diaphragms formed between liver lobules, but under the treatment of HJRG and silymarin, the fibrous intervals, severity scores, and positive areas of collagen fibers in liver tissue were significantly reduced. PC III, Col IV, LN, and HA are considered important indicators of liver fibrosis [27], which can be used to reflect the extent of liver fibrosis. According to our results, PC III, Col IV, LN, and HA (Figure 3(c)) of the model group were significantly increased compared with those of the control group. By contrast, HJRG and silymarin treatments significantly reduced the serum PC III, Col IV, LN, and HA levels ($p < 0.05$). HYP is one of the main components of collagen tissue. The accumulation of HYP is significantly increased by collagen accumulation at the liver fibrosis sites and can be used to assess the extent of liver fibrosis [28]. The model group showed a high level of HYP content in the liver ($p < 0.01$) while the groups with HJRG and silymarin treatments reduced the HYP level in the liver (Figure 3(d)). α-smooth muscle actin (α-SMA) is known as a marker of HSC activation [29]. In the model group, the expression of α-SMA in the liver was significantly increased (Figures 3(e) and 3(f)), which indicated that HSC activated the myofibroblasts. Compared with the model group, HJRG and silymarin treatments significantly reduced the expression of α-SMA ($p < 0.05$), indicating that the myofibroblasts expressing α-SMA were inhibited. The measurement of liver desmin and vimentin indicated the production of collagen [30]. The contents of desmin and vimentin (Figures 3(e) and 3(f)) in the model group were significantly higher than those in the control group. HJRG and silymarin can reduce the desmin and vimentin content of liver fibrosis rats ($p < 0.05$). Therefore, HJRG treatment has a good effect on liver fibrosis indicators.

3.3. Network Pharmacological Analysis of Huangjia Ruangan Granule. Based on the two standards (DL ≥ 0.18 and OB ≥ 30) [31], a total of 117 compounds have been identified

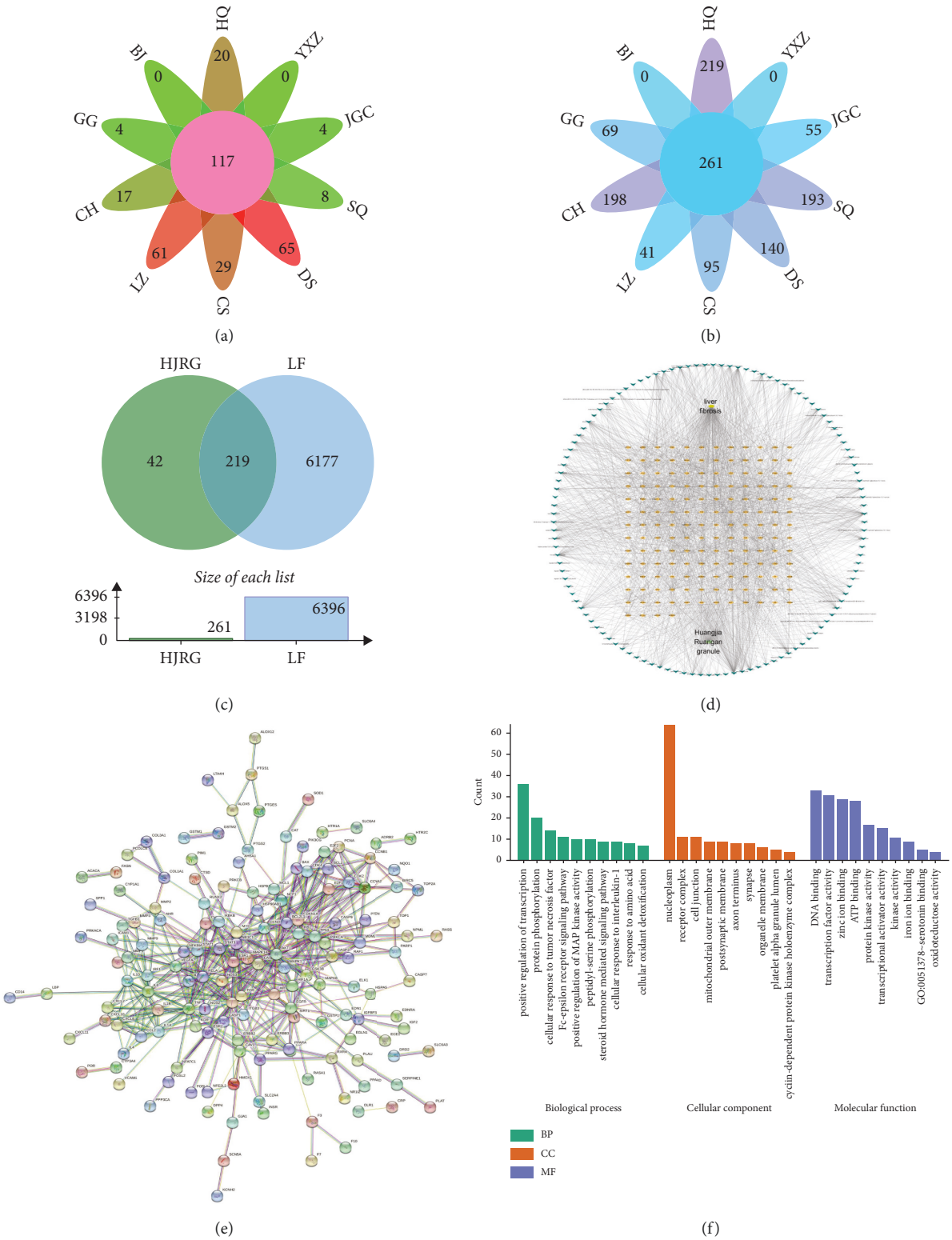

Figure 4: Continued.

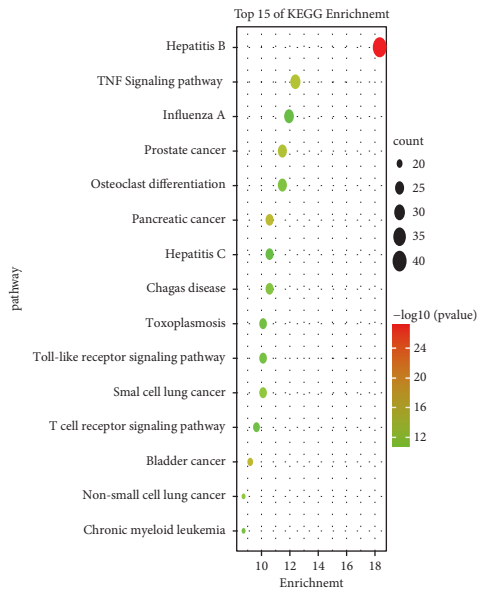

(g)

Figure 4: Analysis of network pharmacology related to HJRG. (a) The flower plot of the active ingredients in HJRG. The pink circle in the center represents the 117 active ingredients of HJRG. Each petal corresponds to the number of compounds in the corresponding Chinese medicine. (b) The flower plot of the potential target in HJRG. The pink circle in the center represents the 261 potential targets of HJRG. Each petal corresponds to the number of potential targets in the corresponding Chinese medicine. (c) A Venn diagram showing that HJRG shares 219 potential targets with the targets of liver fibrosis. (d) The component-target network. (e) PPI network analysis of potential targets. (f) Top 10 items of BP, CC, and MF in the GO enrichment analysis of potential targets. BP: biological process; CC: cellular component; MF: molecular function. (g) Top 15 items of the KEGG pathway analysis of the potential targets.

in the TCM database. In particular, 20, 0, 4, 17, 61, 29, 65, 8, 4, and 0 candidate compounds were detected in HQ, BJ, GG, CH, LZ, CS, DS, SQ, JGC, and YXZ, respectively (Figure 4(a)). Then, we further explored the potential therapeutic targets. A total of 261 potential targets were found from the TCMSP and HIT databases (Figure 4(b)). Different components of HJRG have similar activities. This finding may be due to modulation with a shared target. We further searched 6396 liver fibrosis-related targets in the OMIM database, TTD database, GeneCards database, and DisGeNet database. The VENN diagram reflects that there are in total 219 shared targets between the Huangjia Ruangan granule and liver fibrosis-related targets (Figure 4(c)). In screening the core components and targets of HJRG, the C (component)-T (target) network constructed by Cytoscape was used (Figure 4(d), or Figure 1 in the supplemental files). These targets are candidate targets for HJRG with antiliver fibrosis activity. PPI network analysis was performed (Figure 4(e), or Figure 2 in the supplemental files). In addition, the Omicshare online tool was used to perform GO enrichment analysis (Figure 4(f)) and KEGG pathway analysis (Figure 4(g)) to determine the factors inhibiting liver fibrosis and to clarify the multitarget and multipathway mechanism of HJRG on liver fibrosis. Immune inflammation (IL-6 and NF-κB) is a GO item that shows significant enrichment; in addition, the core target is the TNF signaling pathway.

3.4. Huangjia Ruangan Granule Improves Oxidative Stress in Rats with Liver Fibrosis. Liver damage is the final result of free-radical-mediated oxidative stress in the liver. CCl_4 undergoes biotransformation in the liver to produce active metabolites, leading to the generation of a large number of free radicals. After the free radicals are formed, they will trigger a series of reactions and eventually lead to lipid peroxidation reactions [32]. Oxidative stress caused by free radicals is an important mechanism of liver damage induced by CCl_4. SOD is an important antioxidant enzyme in the body, and GSH is the substrate for GSH-Px to decompose hydrogen peroxide [33]. Liver MPO activity is used as a marker of oxidative stress, inflammation, and tissue neutrophil accumulation and activation [34]. Our results showed that HJRG and silymarin had inhibitory effects on CCl_4-induced oxidative stress damage in rats. Compared with the control group, the content of GSH (Figure 5(a)) and SOD (Figure 5(b)) in the model group decreased, and the content of MDA (Figure 5(c)) and MPO (Figure 5(d)) increased significantly. Compared with the model group, the administration of HJRG and silymarin significantly increased the content of SOD and GSH, and decreased the content of MDA and MPO. The comprehensive results indicate that HJRG may reduce liver fibrosis by alleviating the oxidative stress environment.

3.5. Huangjia Ruangan Granule Reduces Inflammation in Rats with Liver Fibrosis. Inflammation usually leads to liver fibrosis, and the development of fibrosis is usually accompanied by an increase of inflammatory factors [35]. Therefore, we further evaluated the inhibitory effect of HJRG

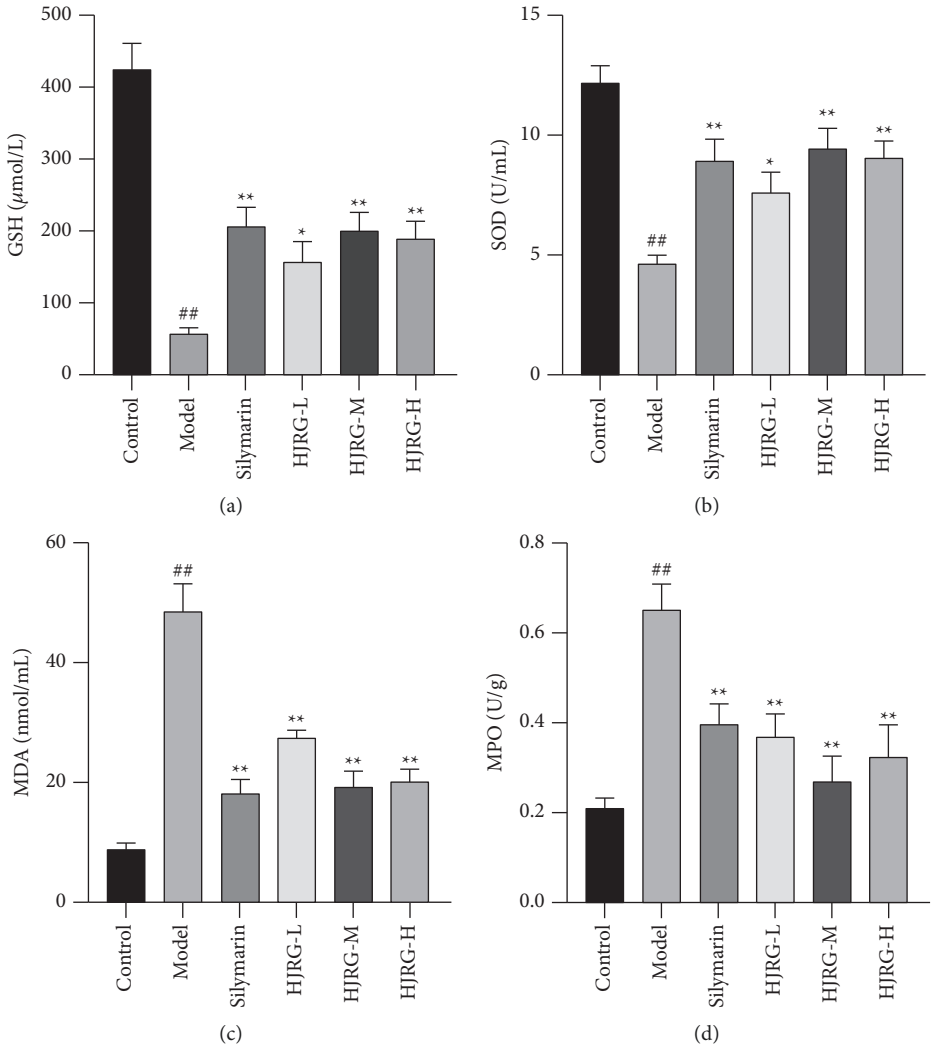

Figure 5: HJRG inhibited oxidative stress in rats. (a) Glutathione (GSH), (b) superoxide dismutase (SOD) activity, (c) malondialdehyde (MDA) content, and (d) myeloperoxidase (MPO) activity in the liver tissue. Data are presented as means ± SEM ($n = 10$ in each group). #$p < 0.05$ and ##$p < 0.01$, compared with the control group; $^{*}p < 0.05$ and $^{**}p < 0.01$, compared with the model group. Control: control group; Model: model group; Silymarin: silymarin group; HJRG-L: Huangjia Ruangan granule low-dose group; HJRG-M: Huangjia Ruangan granule medium-dose group; HJRG-H: Huangjia Ruangan granule high-dose group.

on inflammatory responses in the progression of fibrosis. Compared with the control group, the protein expression levels of TNF-α, IL-1β, IL-6, Cox2, and iNOS (Figure 6) in the liver of the model group were significantly upregulated ($p < 0.05$). Compared with the model group, the protein expression levels of TNF-α, IL-1β, IL-6, Cox2, and iNOS in the HJRG and silymarin treatment groups were significantly downregulated ($p < 0.05$). Our comprehensive results show that HJRG treatment has a great inhibitory effect on the inflammatory response induced by CCl_4.

3.6. Huangjia Ruangan Granule Regulated TNF/MAPK and NF-κB Signaling Pathways of Rats with Liver Fibrosis. To further clarify the antifibrosis mechanism of HJRG, we detected the expression of related proteins in TNF/MAPK and NF-κB signaling pathways. As shown in Figure 7, compared with the control group, the protein expression of TNFR1, p-IκBα, p-P65/P65, p-ERK/ERK, p-JNK/JNK, and MAPK p-P38/P38 in the liver tissue was markedly increased in the model group ($p < 0.05$). Compared with the model group, the protein expression levels of TNFR1, p-IκBα, p-P65/P65, p-ERK/ERK, p-JNK/JNK, and MAPK p-P38/P38 in the HJRG and silymarin treatment groups was markedly decreased ($p < 0.05$). The results indicated that HJRG could inhibit the TNF/MAPK and NF-κB signaling pathways.

4. Discussion

Liver fibrosis is a pathological process of abnormal liver connective tissue proliferation and a key step in the progression of chronic liver disease to cirrhosis. Its prognosis depends on whether it can block or reverse the progression of cirrhosis [36]. Therefore, in the early stages of hepatic fibrosis, the main treatment's main focus is on the etiological treatment and anti-inflammation hepatoprotection [37].

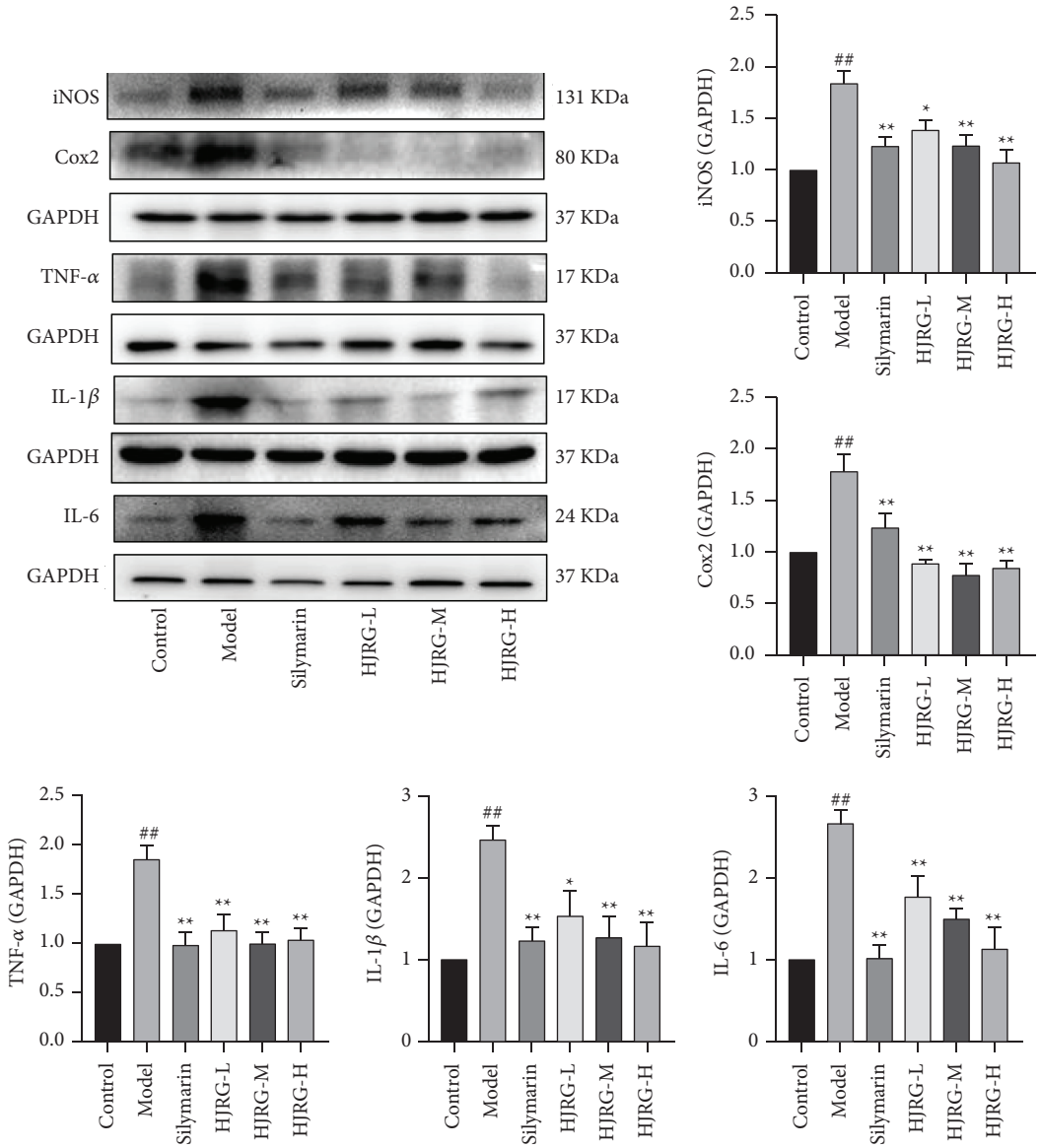

Figure 6: HJRG reduces inflammation in rats. Representative images of western blot analysis and the protein expression statistics of TNF-α, IL-1β, IL-6, Cox2, and iNOS in the liver. ($n = 5$). #$p < 0.05$ and ##$p < 0.01$, compared with the control group; $^{*}p < 0.05$ and $^{**}p < 0.01$, compared with the model group. Control: control group; Model: model group; Silymarin: silymarin group; HJRG-L: Huangjia Ruangan granule low-dose group; HJRG-M: Huangjia Ruangan granule medium-dose group; HJRG-H: Huangjia Ruangan granule high-dose group.

HJRG has the effects of relieving liver stagnation and depression and promoting blood circulation, which are important for intervening liver fibrosis and early cirrhosis. It has been effectively used in clinical practice in recent years. Evidence accumulated from animal and human studies shows that HJRG can reduce liver damage, especially by reversing liver fibrosis. However, the mechanism of HJRG's antiliver fibrosis remains unclear.

In this study, we established a liver fibrosis model in rats induced by CCl_4 and intervened with the Huangjia Ruangan granule. Silymarin is the main active ingredient of *Silybum marianum*. It is the most studied botanical drug with important antioxidant properties [38]. It has been used to treat human liver cirrhosis, reverse fibrosis, and stimulate regeneration [39]. Therefore, we selected silymarin as the positive drug. Based on the results, HJRG can not only effectively restore liver tissue abnormalities, but also reduce the concentration of ALT and AST in the serum of rats with liver fibrosis induced by CCl_4 and then prevent liver necrosis and inflammatory cell infiltration, indicating that HJRG can relieve liver damage during fibrosis.

The characteristic of liver fibrosis is due to the imbalance between ECM production and degradation, resulting in excessive deposition of ECM in the liver [40]. The activation of HSC has been identified as a key event in the development of liver fibrosis, which regulates the mass production and secretion of ECM [41]. In this study, HJRG can effectively inhibit collagen accumulation and HYP contents in liver tissues; reduce serum PC III, Col IV, LN, and HA levels, and the overexpression of α-SMA, desmin, and vimentin in the

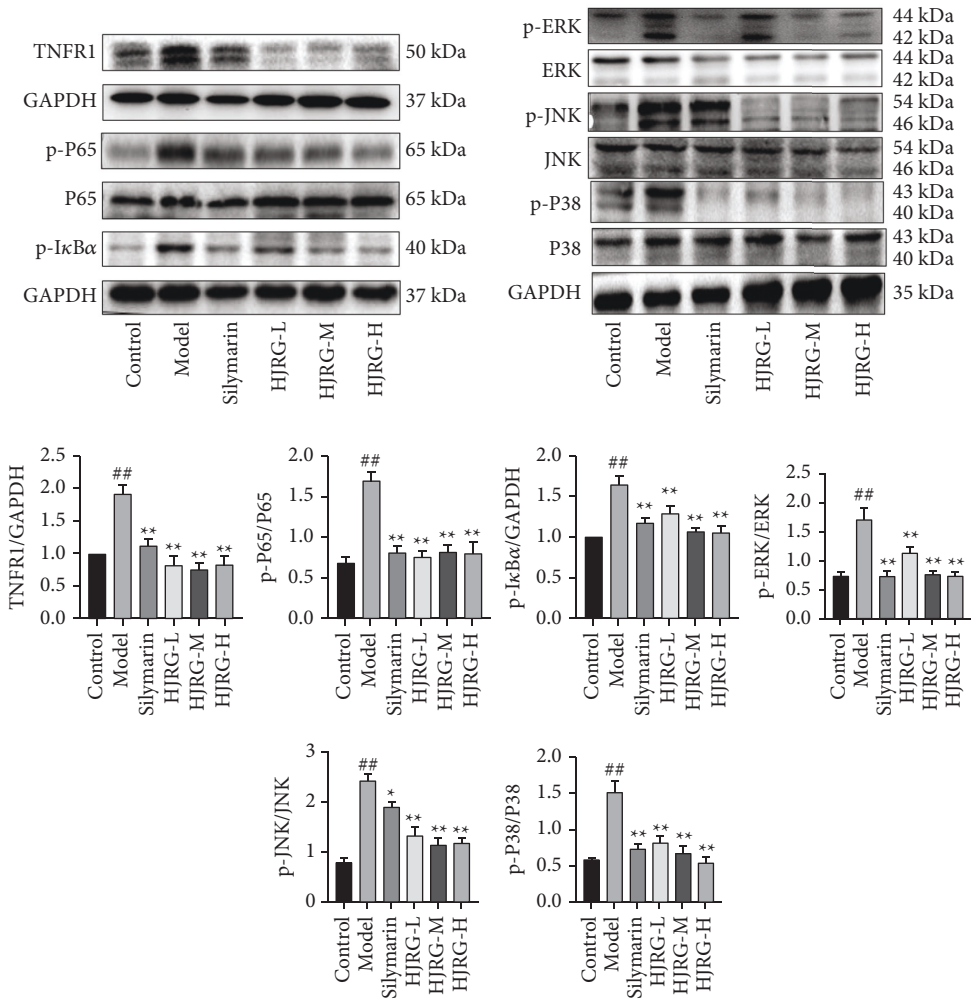

Figure 7: HJRG regulated TNF/MAPK and NF-κB signaling pathways in rats. Representative images of western blot analysis and the protein expression statistics of TNFR1, p-IκBα, p-P65/P65, p-ERK/ERK, p-JNK/JNK, and MAPK p-P38/P38 in the liver. ($n = 5$). #$p < 0.05$ and ##$p < 0.01$, compared with the control group; $^{*}p < 0.05$ and $^{**}p < 0.01$, compared with the model group. Control: control group; Model: model group; Silymarin: silymarin group; HJRG-L: Huangjia Ruangan granule low-dose group; HJRG-M: Huangjia Ruangan granule medium-dose group; HJRG-H: Huangjia Ruangan granule high-dose group.

liver tissue; inhibit the activation of HSC and ECM deposition in the liver, thereby inhibiting liver fibrosis.

The overall process of liver fibrosis is complex, and achieving an appropriate therapeutic effect on a single target is difficult. As a traditional Chinese medicine prescription, HJRG is involved in multiple levels and targets and focuses on the overall regulation and treatment of liver fibrosis. Thus, we checked the candidate components and targets of HJRG using the network pharmacological analysis and found 117 candidate compounds and 219 targets corresponding to antiliver fibrosis. Further GO enrichment analysis and KEGG pathway analysis of candidate targets showed that HJRG primarily regulated inflammation through the TNF signaling pathway and improves oxidative stress antiliver fibrosis effects.

Oxidative stress is the main pathogenesis of CCl_4-induced liver fibrosis in rats [42]. The toxicity of CCl_4 is mediated by metabolic activation, which leads to peroxidation in the body by generating highly active trichloromethyl free radicals [43]. Results showed that the level of reduced GSH in the liver tissue of the model group was significantly decreased. GSH is a major antioxidant. Glutathione reductase resists oxidative stress and protects macromolecules and cell membranes from free radical damage [44]. The examination of liver biochemical markers also shows that a large number of free radicals produced by CCl_4 interference include SOD, MDA, and MPO. SOD provides the main defense against oxidative stress by scavenging free radicals. MDA, and MPO levels reflect the oxidative damage that causes liver tissue damage [45]. However, after the administration of HJRG, the levels of GSH and SOD can be significantly restored, and the activity of MDA and MPO can be reduced, helping the body to scavenge free radicals generated by the CCl_4 stress and self-protect against the oxidative stress. Therefore, HJRG can alleviate liver fibrosis through antioxidant effects.

Hepatic immune-inflammatory mechanisms are essential to maintain liver homeostasis. Evidence shows that CCl_4

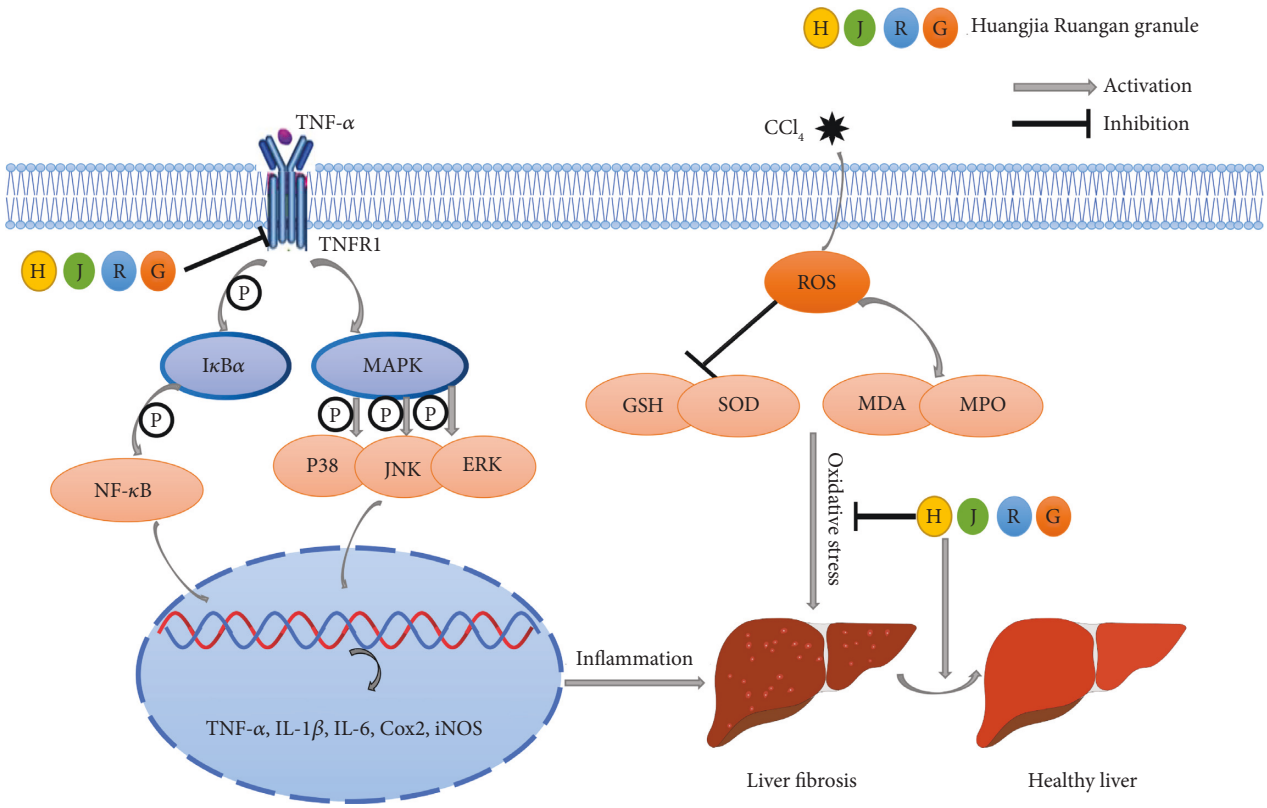

Figure 8: Schematic diagram of the proposed mechanisms underlying the protective effects of HJRG inhibiting CCl_4-induced liver fibrosis in rats. The mechanism of HJRG may be inhibiting the TNFR1-mediated MAPK and NF-κB signaling pathways, reducing the inflammatory response, and ameliorating oxidative stress, thereby inhibiting liver fibrosis.

toxicity can trigger the recruitment inflammatory mediators, such as TNF-α, IL-1β, IL-6, Cox2, and iNOS, thereby inducing liver inflammation [46]. TNF-α, IL-1β, and IL-6 mainly contribute to HSCs activation; Cox2 and iNOS are the main regulators of the inflammatory response; Cox2 induces prostaglandin E2 (PGE2) production and then mediates inflammation in the liver disease models [47]; the continuous production of NO is associated with the increased iNOS expression. In our experiment, HJRG downregulated the expression of the proinflammatory factors (TNF-α, IL-1β, and IL-6). In addition, HJRG downregulated the expression of Cox2 and iNOS in the liver tissue. That is, HJRG can prevent the recruitment of inflammatory mediators of liver fibrosis, thereby improving liver fibrosis.

Our study identified the TNF signaling pathway as the main signal pathway in the treatment of liver fibrosis with HJRG. Upregulation of TNFR1, one of the TNF signaling receptors, was correlated with incident liver fibrosis [48]. Evidence shows that TNFR1 activates the downstream MAPK signaling pathways, including ERK, JNK, and MAPK P38 pathways [49]. On the other hand, TNFR1 can also induce the phosphorylation of IκBα, which promotes the phosphorylation of NF-κB P65 to participate in the inflammatory reaction together with the MAPK signaling pathway, regulating the process of liver fibrosis [50]. Our study found that HJRG significantly inhibited the increase of p-IκBα, p-P65/P65, p-ERK/ERK, p-JNK/JNK, and MAPK p-P38/P38 ratios in the liver tissue of rats with hepatic fibrosis and the protein expression levels of TNFR1. This study demonstrates that HJRG may exert antifibrotic effects by inhibiting the activation of TNFR1 and the downstream MAPK and NF-κB pathways (Figure 8).

5. Conclusions

Our research proved that HJRG can effectively reduce the liver damage and oxidative stress caused by CCl_4, and the mechanism may be the inhibition of TNFR1-mediated MAPK and NF-κB signaling pathways to reduce the inflammatory response, thereby inhibiting liver fibrosis. The present study may provide experimental evidence for the study and usage of HJRG in liver fibrosis.

Data Availability

The datasets analyzed in this article are publicly available, and further inquiries can be directed to QC (1367084356@qq.com).

Disclosure

Qiang Cai and Zongquan Wang share first authorship.

Conflicts of Interest

The authors declare that they have no conflicts of interest.

Authors' Contributions

QC and ZW carried out the major experiment. RZ, LZ, SC, HL, XT, DY, XL, and SB assisted in completing the experiment. QC wrote the manuscript. LY and JG guided the experiments and reviewed the manuscript. Qiang Cai and Zongquan Wang have contributed equally to this work.

Acknowledgments

This work was supported by the R & D projects in key areas of the Guangdong Province (2019B020201006) and the National Science And Technology Major Special Project Of "Major New Drug Creation"(2017ZX09301017).

Supplementary Materials

Figure 4(d) can be found in Figure 1 in the supplemental files, and Figure 4(e) can be found in Figure 2 in the supplemental files. (*Supplementary Materials*)

References

[1] Y. Peng, T. Yang, K. Huang, L. Shen, Y. Tao, and C. Liu, "Salvia miltiorrhiza ameliorates liver fibrosis by activating hepatic natural killer cells in vivo and in vitro," *Frontiers in Pharmacology*, vol. 9, p. 762, 2018.

[2] D. Oro, T. Yudina, G. Fernandez-Varo et al., "Cerium oxide nanoparticles reduce steatosis, portal hypertension and display anti-inflammatory properties in rats with liver fibrosis," *Journal of Hepatology*, vol. 64, no. 3, pp. 691–698, 2016.

[3] Z. Wei, Y. Xue, Y. Xue et al., "Ferulic acid attenuates non-alcoholic steatohepatitis by reducing oxidative stress and inflammation through inhibition of the ROCK/NF-kappaB signaling pathways," *Journal of Pharmacological Sciences*, vol. 147, no. 1, pp. 72–80, 2021.

[4] V. Prestigiacomo, A. Weston, S. Messner, F. Lampart, and L. Suter-Dick, "Pro-fibrotic compounds induce stellate cell activation, ECM-remodelling and Nrf2 activation in a human 3D-multicellular model of liver fibrosis," *PLoS One*, vol. 12, no. 6, p. e179995, 2017.

[5] X. Liu, Y. Shi, Y. Hu et al., "Bupleurum marginatum Wall.ex DC in liver fibrosis: pharmacological evaluation, differential proteomics, and network pharmacology," *Frontiers in Pharmacology*, vol. 9, p. 524, 2018.

[6] A. M. Abdel-Moneim, M. A. Al-Kahtani, M. A. El-Kersh, and M. A. Al-Omair, "Free radical-scavenging, anti-inflammatory/anti-fibrotic and hepatoprotective actions of taurine and silymarin against CCl_4 induced rat liver damage," *PLoS One*, vol. 10, no. 12, Article ID e144509, 2015.

[7] A. Elkhamesy, M. Refaat, M. Gouida, S. S. Alrdahe, and M. M. Youssef, "Diminished CCl_4-induced hepatocellular carcinoma, oxidative stress, and apoptosis by co-administration of curcumin or selenium in mice," *Journal of Food Biochemistry*, vol. 46, no. 4, Article ID e13845, 2022.

[8] S. I. Ojeaburu and K. Oriakhi, "Hepatoprotective, antioxidant and, anti-inflammatory potentials of gallic acid in carbon tetrachloride-induced hepatic damage in Wistar rats," *Toxicology Reports*, vol. 8, pp. 177–185, 2021.

[9] M. S. Islam, A. Ciavattini, F. Petraglia, M. Castellucci, and P. Ciarmela, "Extracellular matrix in uterine leiomyoma pathogenesis: a potential target for future therapeutics," *Human Reproduction Update*, vol. 24, no. 1, pp. 59–85, 2018.

[10] R. S. Albeltagy, F. Mumtaz, M. A. Abdel, and O. H. El-Habit, "N-acetylcysteine reduces miR-146a and NF-kappaB p65 inflammatory signaling following cadmium hepatotoxicity in rats," *Biological Trace Element Research*, vol. 199, no. 12, pp. 4657–4665, 2021.

[11] X. Lin, Y. Li, X. Zhang et al., "Tormentic acid inhibits hepatic stellate cells activation via blocking PI3K/Akt/mTOR and NF-kappaB signalling pathways," *Cell Biochemistry and Function*, vol. 39, no. 1, pp. 77–87, 2021.

[12] K. M. Kim, S. Y. Kim, T. J. Mony et al., "Dracocephalum moldavica ethanol extract suppresses LPS-induced inflammatory responses through inhibition of the JNK/ERK/NF-kappaB signaling pathway and IL-6 production in RAW 264.7 macrophages and in endotoxic-treated mice," *Nutrients*, vol. 13, no. 12, 2021.

[13] B. Zhang, Z. Zeng, and H. Wu, "A network pharmacology-based analysis of the protective mechanism of miao medicine xuemaitong capsule against secondary brain damage in the ischemic area surrounding intracerebral hemorrhage," *Journal of Pharmacology and Experimental Therapeutics*, vol. 377, no. 1, pp. 86–99, 2021.

[14] C. Liu, G. Wang, G. Chen et al., "Huangqi decoction inhibits apoptosis and fibrosis, but promotes Kupffer cell activation in dimethylnitrosamine-induced rat liver fibrosis," *BMC Complementary and Alternative Medicine*, vol. 12, p. 51, 2012.

[15] X. Shen, Z. Zhao, H. Wang, Z. Guo, B. Hu, and G. Zhang, "Elucidation of the anti-inflammatory mechanisms of Bupleuri and scutellariae Radix using system pharmacological analyses," *Mediators of Inflammation*, vol. 2017, Article ID 3709874, 2017.

[16] Z. Qiu, D. Zhong, and B. Yang, "Preventive and therapeutic effect of Ganoderma (lingzhi) on liver injury," *Advances in Experimental Medicine & Biology*, vol. 1182, pp. 217–242, 2019.

[17] H. E. Tzeng, C. H. Tsai, T. Y. Ho et al., "Radix Paeoniae Rubra stimulates osteoclast differentiation by activation of the NF-kappaB and mitogen-activated protein kinase pathways," *BMC Complementary and Alternative Medicine*, vol. 18, no. 1, p. 132, 2018.

[18] Y. Li, Y. Chen, X. Huang et al., "Tanshinol A ameliorates triton-1339W-induced hyperlipidemia and liver injury in C57BL/6J mice by regulating mRNA expression of lipemic-oxidative injury genes," *Lipids*, vol. 55, no. 2, pp. 127–140, 2020.

[19] Q. H. Wang, N. Kuang, W. Y. Hu, D. Yin, Y. Y. Wei, and T. J. Hu, "The effect of Panax notoginseng saponins on oxidative stress induced by PCV2 infection in immune cells: in vitro and in vivo studies," *Journal of Veterinary Science*, vol. 21, no. 4, p. e61, 2020.

[20] H. Miyao, T. Arao, M. Udayama, J. Kinjo, and T. Nohara, "Kaikasaponin III and soyasaponin I, major triterpene saponins of Abrus cantoniensis, act on GOT and GPT: influence on transaminase elevation of rat liver cells concomitantly exposed to CCl_4 for one hour," *Planta Medica*, vol. 64, no. 1, pp. 5–7, 1998.

[21] Y. Wu, Y. Lu, S. Y. Li, Y. H. Song, Y. Hao, and Q. Wang, "Extract from Phyllanthus urinaria L. inhibits hepatitis B virus replication and expression in hepatitis B virus transfection model in vitro," *Chinese Journal of Integrative Medicine*, vol. 21, no. 12, pp. 938–943, 2015.

[22] L. Zhang and D. Schuppan, "Traditional Chinese Medicine (TCM) for fibrotic liver disease: hope and hype," *Journal of Hepatology*, vol. 61, no. 1, pp. 166–168, 2014.

[23] Z. Zhang, F. Lu, H. Liu et al., "An integrated strategy by using target tissue metabolomics biomarkers as pharmacodynamic surrogate indices to screen antipyretic components of Qingkaikling injection," *Scientific Reports*, vol. 7, no. 1, p. 6310, 2017.

[24] G. B. Zhang, Q. Y. Li, Q. L. Chen, and S. B. Su, "Network pharmacology: a new approach for Chinese herbal medicine research," *Evidence Based Complementary and Alternative Medicine*, vol. 2013, Article ID 621423, 2013.

[25] M. J. Shi, X. L. Yan, B. S. Dong, W. N. Yang, S. B. Su, and H. Zhang, "A network pharmacology approach to investigating the mechanism of Tanshinone IIA for the treatment of liver fibrosis," *Journal of Ethnopharmacology*, vol. 253, Article ID 112689, 2020.

[26] S. S. Sokar, M. E. El-Sayad, M. E. Ghoneim, and A. M. Shebl, "Combination of Sitagliptin and Silymarin ameliorates liver fibrosis induced by carbon tetrachloride in rats," *Biomedicine & Pharmacotherapy*, vol. 89, pp. 98–107, 2017.

[27] X. Lou, Y. Hou, H. Cao, J. Zhao, and F. Zhu, "Clinical significance of decoy receptor 3 upregulation in patients with hepatitis B and liver fibrosis," *Oncology Letters*, vol. 16, no. 1, pp. 1147–1154, 2018.

[28] Y. Zhou, R. Wu, F. F. Cai et al., "Xiaoyaosan decoction alleviated rat liver fibrosis via the TGFbeta/Smad and Akt/FoxO3 signaling pathways based on network pharmacology analysis," *Journal of Ethnopharmacology*, vol. 264, Article ID 113021, 2021.

[29] S. Wang, C. Tang, H. Zhao et al., "Network pharmacological analysis and experimental validation of the mechanisms of action of Si-Ni-san against liver fibrosis," *Frontiers in Pharmacology*, vol. 12, Article ID 656115, 2021.

[30] A. Marti-Rodrigo, F. Alegre, A. B. Moragrega et al., "Rilpivirine attenuates liver fibrosis through selective STAT1-mediated apoptosis in hepatic stellate cells," *Gut*, vol. 69, no. 5, pp. 920–932, 2020.

[31] X. Wang, X. Xu, W. Tao, Y. Li, Y. Wang, and L. Yang, "A systems biology approach to uncovering pharmacological synergy in herbal medicines with applications to cardiovascular disease," *Evid Based Complement Alternat Med*, vol. 2012, Article ID 519031, 2012.

[32] Y. Cui, X. Yang, X. Lu, J. Chen, and Y. Zhao, "Protective effects of polyphenols-enriched extract from Huangshan Maofeng green tea against CCl_4-induced liver injury in mice," *Chemico-Biological Interactions*, vol. 220, pp. 75–83, 2014.

[33] F. Ali, E. H. Saad, N. A. M. Mostafa et al., "The impact of royal jelly against hepatic ischemia/reperfusion-induced hepatocyte damage in rats: the role of cytoglobin, nrf-2/HO-1/COX-4, and P38-MAPK/NF-kappaB-p65/TNF-alpha signaling pathways," *Current Molecular Pharmacology*, vol. 14, no. 1, pp. 88–100, 2021.

[34] G. Ndrepepa, "Myeloperoxidase-A bridge linking inflammation and oxidative stress with cardiovascular disease," *Clinica Chimica Acta*, vol. 493, pp. 36–51, 2019.

[35] J. Li, T. Wang, P. Liu et al., "Hesperetin ameliorates hepatic oxidative stress and inflammation via the PI3K/AKT-Nrf2-ARE pathway in oleic acid-induced HepG2 cells and a rat model of high-fat diet-induced NAFLD," *Food & Function*, vol. 12, no. 9, pp. 3898–3918, 2021.

[36] Y. Koyama, J. Xu, X. Liu, and D. A. Brenner, "New developments on the treatment of liver fibrosis," *Digestive Diseases*, vol. 34, no. 5, pp. 589–596, 2016.

[37] H. Li, M. H. Huang, J. D. Jiang, and Z. G. Peng, "Hepatitis C: from inflammatory pathogenesis to anti-inflammatory/hepatoprotective therapy," *World Journal of Gastroenterology*, vol. 24, no. 47, pp. 5297–5311, 2018.

[38] Q. Ou, Y. Weng, S. Wang et al., "Silybin alleviates hepatic steatosis and fibrosis in NASH mice by inhibiting oxidative stress and involvement with the nf-kappaB pathway," *Digestive Diseases and Sciences*, vol. 63, no. 12, pp. 3398–3408, 2018.

[39] A. Federico, M. Dallio, and C. Loguercio, "Silymarin/silybin and chronic liver disease: a marriage of many years," *Molecules*, vol. 22, no. 2, 2017.

[40] M. Parola and M. Pinzani, "Liver fibrosis: pathophysiology, pathogenetic targets and clinical issues," *Molecular Aspects of Medicine*, vol. 65, pp. 37–55, 2019.

[41] G. Vendemiale, I. Grattagliano, M. L. Caruso et al., "Increased oxidative stress in dimethylnitrosamine-induced liver fibrosis in the rat: effect of N-acetylcysteine and interferon-alpha," *Toxicology and Applied Pharmacology*, vol. 175, no. 2, pp. 130–139, 2001.

[42] G. L. Tipoe, T. M. Leung, E. C. Liong, T. Y. Lau, M. L. Fung, and A. A. Nanji, "Epigallocatechin-3-gallate (EGCG) reduces liver inflammation, oxidative stress and fibrosis in carbon tetrachloride (CCl_4)-induced liver injury in mice," *Toxicology*, vol. 273, no. 1-3, pp. 45–52, 2010.

[43] X. Feng, M. H. Li, J. Xia et al., "Tibetan medical formula shiwei-Gan-Ning-Pill protects against carbon tetrachloride-induced liver fibrosis - an NMR-based metabolic profiling," *Frontiers in Pharmacology*, vol. 9, p. 965, 2018.

[44] I. Ceballos-Picot, V. Witko-Sarsat, M. Merad-Boudia et al., "Glutathione antioxidant system as a marker of oxidative stress in chronic renal failure," *Free Radical Biology and Medicine*, vol. 21, no. 6, pp. 845–853, 1996.

[45] A. Kumar, V. Kaur, K. Pandit et al., "Antioxidant phytoconstituents from onosma bracteata wall. (Boraginaceae) ameliorate the CCl_4 induced hepatic damage: in vivo study in male wistar rats," *Frontiers in Pharmacology*, vol. 11, p. 1301, 2020.

[46] C. Ning, X. Gao, C. Wang et al., "Hepatoprotective effect of ginsenoside Rg1 from Panax ginseng on carbon tetrachloride-induced acute liver injury by activating Nrf2 signaling pathway in mice," *Environmental Toxicology*, vol. 33, no. 10, pp. 1050–1060, 2018.

[47] A. Shehzad, S. Rehmat, S. Ul-Islam et al., "Lirioresinol B dimethyl ether inhibits NF-kappaB and COX-2 and activates IkappaBalpha expression in CCl_4-induced hepatic fibrosis," *BMC Complementary Medicine and Therapies*, vol. 20, no. 1, p. 49, 2020.

[48] P. R. Singh, E. S. Priya, S. Balakrishnan et al., "Nimbolide inhibits androgen independent prostate cancer cells survival and proliferation by modulating multiple pro-survival signaling pathways," *Biomedicine & Pharmacotherapy*, vol. 84, pp. 1623–1634, 2016.

[49] S. A. Jang, D. W. Park, E. H. Sohn, S. R. Lee, and S. C. Kang, "Hyperoside suppresses tumor necrosis factor alpha-mediated vascular inflammatory responses by downregulating mitogen-activated protein kinases and nuclear factor-kappaB signaling," *Chemico-Biological Interactions*, vol. 294, pp. 48–55, 2018.

[50] C. M. Yang, I. T. Lee, R. C. Hsu, P. L. Chi, and L. D. Hsiao, "NADPH oxidase/ROS-dependent PYK2 activation is involved in TNF-alpha-induced matrix metalloproteinase-9 expression in rat heart-derived H9c2 cells," *Toxicology and Applied Pharmacology*, vol. 272, no. 2, pp. 431–442, 2013.

Hindawi
Evidence-Based Complementary and Alternative Medicine
Volume 2022, Article ID 1833921, 15 pages
https://doi.org/10.1155/2022/1833921

Research Article

Jieduan–Niwan Formula Ameliorates Oxidative Stress and Apoptosis in Acute-on-Chronic Liver Failure by Suppressing HMGB1/TLR-4/NF-κB Signaling Pathway: A Study In Vivo and In Vitro

Peng Fang,[1] **Bo Dou**,[2] **Weixin Hou**,[2] **Xiaoyi Wei**,[2] **Jiajun Liang**,[2] **Chongyang Ma**,[2] **and Qiuyun Zhang**[2]

[1]*Department of Infectious Diseases, The First Affiliated Hospital of Zhejiang Chinese Medical University (Zhejiang Provincial Hospital of Traditional Chinese Medicine), Hangzhou 310006, Zhejiang Province, China*
[2]*Beijing Key Lab of TCM Collateral Disease Theory Research, School of Traditional Chinese Medicine, Capital Medical University, Beijing 100069, China*

Correspondence should be addressed to Qiuyun Zhang; zhangqiuyun8202@aliyun.com

Received 30 March 2022; Accepted 17 June 2022; Published 15 July 2022

Academic Editor: Chih-Yuan Ko

Jieduan-Niwan (JDNW) formula is a traditional Chinese medicine compound created by the famous Chinese medicine expert Professor Qian Ying, and has been used clinically for decades to treat acute-on-chronic liver failure (ACLF) and exhibits remarkable efficacy. However, the exact mechanism remains to be discovered. As an important hepatocyte damage-associated molecular patterns (DAMP) factor, high mobility group box 1 (HMGB1) is a potential therapeutic target as an accelerator of ACLF in the pathogenesis. Therefore, the present study investigated whether JDNW inhibits the overexpression and cytoplasmic translocation of HMGB1 in ACLF liver tissue and alleviates its mediated oxidative stress and apoptosis. In vivo, an immune-induced ACLF rat model was established, and then treated with JDNW for 5, 10, and 15 d. The results showed that a large number of cytoplasmic translocations of HMGB1 occurred in the ACLF group. And there was an increase in the expression of HMGB1 in the M-5 d group. After the intervention of JDNW, the overexpression and translocation of HMGB1 were inhibited. In vitro, D-GaLN caused an increase in the expression and translocation of HMGB1 in L02 cells. Similar to the inhibitor of HMGB1, JDNW serum alleviated this kind of increase. Further tests showed that JDNW attenuated ACLF-related oxidative stress and apoptosis, and the inhibition was associated with the regulation of TLR-4/NF-κB signaling pathway. In conclusion, our present findings suggest that the therapeutic effect of JDNW on ACLF was associated with the inhibition of high expression and cytoplasmic translocation of HMGB1 during the acute injury phase, thus, attenuating oxidative stress injury and apoptosis induced by HMGB1/TLR-4/NF-κB pathway.

1. Introduction

Acute-on-chronic liver failure (ACLF) is a life-threatening liver failure syndrome [1].

The main causes of ACLF vary widely between East and West, with hepatitis virus and alcohol abuse, respectively [2]. The pathogenesis of ACLF is very complicated, characterized by immune system disturbances and excessive inflammatory responses, which lead to the release of damage-associated molecular patterns (DAMPs) [3]. By binding to specific receptors, the inflammatory response is enhanced by DAMP and further recognized by the immune system; thereby releasing pro-inflammatory factors, triggering and aggravating the inflammatory response of the liver, which can eventually lead to liver failure [4, 5].

High mobility group box 1 (HMGB1) is a ubiquitous eukaryotic nuclear DNA-binding protein with diverse functions in and out of cells [6]. When infection or sterile

injury occurs, HMGB1 translocates extracellularly, either actively by macrophages or by passive pathways in damaged cells, thereby becoming a DAMPs factor that binds to atopic receptors. It acts as a damage announcer, transmitting damage signals to adjacent cells [7]. Likewise, HMGB1 is a hepatocyte DAMP that modulates cell death patterns [8]. HMGB1 in peripheral blood of ACLF patients was much more than that of chronic hepatitis patients, which may be a potential target for improving the prognosis of ACLF [9]. In addition to its pro-inflammatory role, which has been extensively studied, recent studies have demonstrated that HMGB1 also plays an important role in mediating oxidative stress and apoptosis [10]. As a prooxidant, NF-κB is induced and activated by recombinant HMGB1 through TLR-4-dependent NADPH oxidase to generate a large amount of intracellular reactive oxygen species [11]. In addition, HMGB1 is also related to apoptosis. By binding to DNA, HMGB1 is released in late apoptotic cells [12]. In hepatic ischemia-reperfusion injury, the released HMGB1 activates caspase-3-dependent apoptosis through the TLR-4 pathway [13].

Clinical treatment of ACLF is still limited, and liver transplantation is the only established treatment, but it is only suitable for a small number of patients (~5%) due to scarcity of donor organs, cost, and contraindications. Traditional Chinese medicine (TCM) has irreplaceable advantages in the treatment of ACLF and is an important complementary and alternative therapy at present. Qian Ying, a master of traditional Chinese medicine, based on his lifelong learning and medical experience, created the Jieduan-Niwan (JDNW) formula to treat ACLF, which has a unique curative effect. JDNW was significantly better than the general treatment group in improving liver function and reducing mortality in ACLF patients [14]. JDNW is designed for the ACLF's pathogenesis of TCM "poison damage to the liver" and "loss of righteous qi." In the formula, the role of bitter *Phyllanthus vulgaris*, Trichosanthis, Lysimachia, and Turmeric are used for "attacking and replenishing, detoxification, removing blood stasis and dampness, and strengthening righteousness turmeric." *Salvia miltiorrhiza* are used for "clearing away heat and detoxification," "removing phlegm and dampness," "promoting gallbladder and reducing jaundice," and "cooling blood and removing blood stasis." Therefore, they share the responsibility of "Jieduan," that is, preventing the disease from worsening. *Astragalus* and *Panax notoginseng* are used for "invigorating the spleen and qi" and "promoting blood circulation and regulating the liver." Mistletoe, dried rehmannia root, and aconite "nourishes the yin of the liver and kidney, and the yang of the spleen and kidney." Thus, it played the role of "Niwan," which means to replenish the righteousness and exorcise evil [15]. Due to the good clinical effect of JDNW, the ACLF treatment guidelines of Integrative Chinese and Western Medicine propose that JDNW is the key method to treat ACLF [16]. However, the underlying scientific reasons for JDNW to alleviate ACLF have not been well studied, limiting our generalization and application of it. Several of our previous experiments showed that JDNW can reduce 24-hour mortality, reduce liver inflammation, and excessive apoptosis in ACLF model rats [17–19]. However, whether the specific mechanism of JDNW's treatment of ACLF is related to HMGB1, the important hepatocyte DAMP molecule remains unknown and thus warrants further research.

2. Materials and Methods

2.1. Animals. Specific pathogen-free male Wistar rats were purchased from Vital River Laboratory Animal Technology Co. Ltd. All the rats were housed in the Department of Laboratory Animals, Capital Medical University. They were reared under environmental conditions of temperature ($25 \pm 3^{\circ}$C) and humidity ($60 \pm 10\%$) with a 12-hour light-dark cycle. The animal feeding and handling were carried out in accordance with the "Guidelines for the Care and Use of Laboratory Animals." The animal experiment ethics were approved by the Animal Care and Use Committee of Capital Medical University (No. AEEI-2019-067).

2.2. Preparation of JDNW. The formulation ingredients and herbal doses of each dose of JDNW are listed in Supplementary Table S1. The preparation of JDNW was as previously described. Briefly, soak all the herbs in distilled water for 4 hours. After boiling the aconitum with 1 L of distilled water for 30 minutes, add the rest of the herbs and boil for another 45 minutes to obtain the concoction of the first decoction. The herbs were then boiled again in 1 L of distilled water for 30 minutes to collect the second decoction. After mixing the two decoctions evenly, the preparation of JDNW was completed. Based on the results of our previous study, the optimal dose of JDNW formulation per rat was 21.7 g/kg/d. After concentrating the decoction to 4.34 g/mL, it was refrigerated at 4°C for intragastric administration of rats [17].

The protocol for the identification and qualification of the main chemical components of it were as previously described. Briefly, we established a fingerprint using HPLC-MS analysis to characterize the compounds of the JDNW formula and control the quality. Seven kinds of JDNW compounds, including catalpol, gallic acid, 3,4-dihydroxybenzaldehyde, chlorogenic acid, notoginsenoside R1, salvianolic acid B, and ginsenoside Rb1 were characterized and quantified [19].

2.3. Animal Modeling and Drug Administration. A total of 90 rats were randomly divided into the normal control group ($n = 6$) and the treatment group ($n = 82$). Immune liver injury induced by injection of human serum albumin (HSA) in the treatment group. As a xenogeneic serum, HSA elicits an immune response in rats, and the formed immune complex deposits stimulate collagen proliferation and cause liver fibrosis. The procedure consists of two steps: subcutaneous injection for sensitization (one injection on 0, 13, 23, and 33 d, respectively, each injection of HSA 4 mg) and tail vein injection to induce immune fibrosis (twice a week for a total of 6 weeks, the dose of HSA was gradually increased by 2.5 mg $\longrightarrow$ 3 mg $\longrightarrow$ 3.5 mg $\longrightarrow$ 4 mg $\longrightarrow$ 4.5 mg, and then maintained at 4.5 mg). After 6 weeks, the survived 74 rats in

the treatment group were intraperitoneally injected with 400 mg/kg D-GaLN and 100 μg/kg LPS for acute liver injury to establish an ACLF model, as described previously [19]. After the ACLF model was established, the survived 72 rats were randomly divided into the JDNW group and Model (M) group. The above two groups were randomly divided into three subgroups, namely the JDNW/M group (5, 10, and 15 d; $n = 12$ per group). JDNW treatment started 24 hours after the acute injury, and the treatment group was given intragastric administration for 5, 10, and 15 d. The NC group and the M group were continuously given a 0.9% equal dose of normal saline. Samples for research were collected from rats in each group at 5, 10, and 15 d after treatment for analysis. The non-JDNW intervention groups were given the same amount of normal saline by gavage. After anesthesia with 1% sodium pentobarbital (40 mg/kg), blood was drawn from the abdominal aorta, placed at room temperature for 30 minutes, and centrifuged (3000 rpm, 15 minutes) to separate and collect serum. Liver tissue was rapidly collected and frozen in liquid nitrogen. The euthanasia method for rats was performed by cervical dislocation. The obtained specimens were stored at −80°C.

2.4. Determination of Serum Alanine Aminotransferase (ALT), Aspartate Aminotransferase (AST), Total Bilirubin (TBiL), and Prothrombin Times (PTs). Serum and plasma were collected in non-anticoagulated and anticoagulated tubes, and centrifuged for 15 minutes at 3000 rpm (Sigma, USA). Levels of ALT, AST, TBiL, and PT were detected by assay kits. All steps are followed as per the manufacturer's instructions.

2.5. Histological Evaluation. After fixation, paraffin-embedded, sectioned 5 μm thick, stained with hematoxylin and eosin (H and E), and the pathological pictures were acquired with a panoramic scanner (Leica Aperio AT2) for pathological sections.

2.6. JDNW Serum Preparation. To further explore the pharmacodynamic mechanism of JDNW, we prepared JDNW serum for in vitro experiments. Briefly, rats were given an equal amount of distilled water and 21.7 g JDNW crude drug/kg/day by gavage for 7 d to obtain control serum and JDNW serum, respectively. After anesthetizing the rats with a small animal anesthesia machine (Matrx VMR, Midmark), the abdominal aortic blood collection method was used for sterile collection. After standing vertically at 4°C for 4 hours, the blood sample was centrifuged at 3000 rpm/min for 30 minutes at 4°C, and then inactivated at 56°C for 30 minutes. Filtered by a microfiltration membrane (0.22 um), the samples were stored at −80°C.

2.7. MDA and GSH Content in ACLF Rats. MDA and GSH in liver tissues were detected with assay kits, respectively (Beyotime, China; cat: S0131; Beyotime, China; cat: S0053). Measure the content of MDA and GSH with a microplate reader at the absorption wavelengths of 532 and 412 nm, respectively. The contents of MDA and GSH are expressed as nmol/mg protein.

2.8. Cell Culture. Normal human hepatocytes (L02 cells) were used for in vitro experiments. L02 cells were obtained from the Cell Bank of Type Culture Collection of the Chinese Academy of Sciences (Shanghai, China) and were maintained in DMEM media supplemented with 10% (v/v) fetal bovine serum (FBS), 37°C, 5% CO_2. L02 cells in the logarithmic growth phase were digested with 0.25% trypsin to prepare cell suspension. The cells were inoculated with 3×10^6 cells in 6-well plates and incubated in an incubator for 12 hours. The L02 cells were randomly divided into the NC group, D-GaLN group, JDNW group, and HMGB1 inhibitor (glycyrrhizin, GLY) group. Cultivating intervention conditions: NC group and D-GaLN group were in the medium containing 10% control serum, GLY group was treated with 10% control serum medium (containing 1 mmol/L GLY), and JDNW group was treated with JDNW serum at different concentrations (2.5%, 5%, and 10%), the total serum concentration was supplemented to 10% with the control serum. The intervening concentration of D-GaLN was screened by cell viability assay.

2.9. CCK-8. The Cell Counting Kit-8 (CCK8) assay (Beijing, China; catalog: AQ308) was used to evaluate the effect of D-GaLN and JDNW serum on L02 cell viability. After treatment with D-GaLN and/or JDNW serum for the indicated times, cells from different groups were incubated with the CCK-8 reagent for 2 hours. Measure the optical density of each well by using a microplate reader (Thermo Scientific, USA).

2.10. Western Blot. Total protein was extracted from L02 cells and liver tissue samples by radioimmunoprecipitation assay lysis buffer (RIPA; Applygen, China; cat: C1053). The nuclear and cytoplasmic protein extraction kit (Beyotime, China; catalog: P0028) was used to separate cytoplasmic and nuclear proteins. Protein concentration was determined with bicinchoninic acid (BCA) protein reagent (Beyotime, China; catalog: P0012). The protein lysate was electrophoresed, transferred to the membrane, and blocked with nonfat milk powder. The primary antibody was incubated overnight at 4°C, and after washing with TBST, the secondary antibody was incubated for 1 hours. Finally, a chemiluminescence reagent (NCM Biotech, China; cat: P10100) was used to detect the reaction. An ImageQuantLAS4000 (GE Co., USA) chemiluminescence imaging system was used to acquire visual images of target proteins. Quantify protein expression using Image J software version 1.80, and expressed as a percentage of the control.

2.11. Immunostaining of 4-HNE and HMGB1. After deparaffinization and antigen retrieval, paraffin sections were incubated with bovine serum albumin (BSA) and blocked. For L02 cells, after exposure to the indicated experimental conditions, they were then fixed with 4% paraformaldehyde

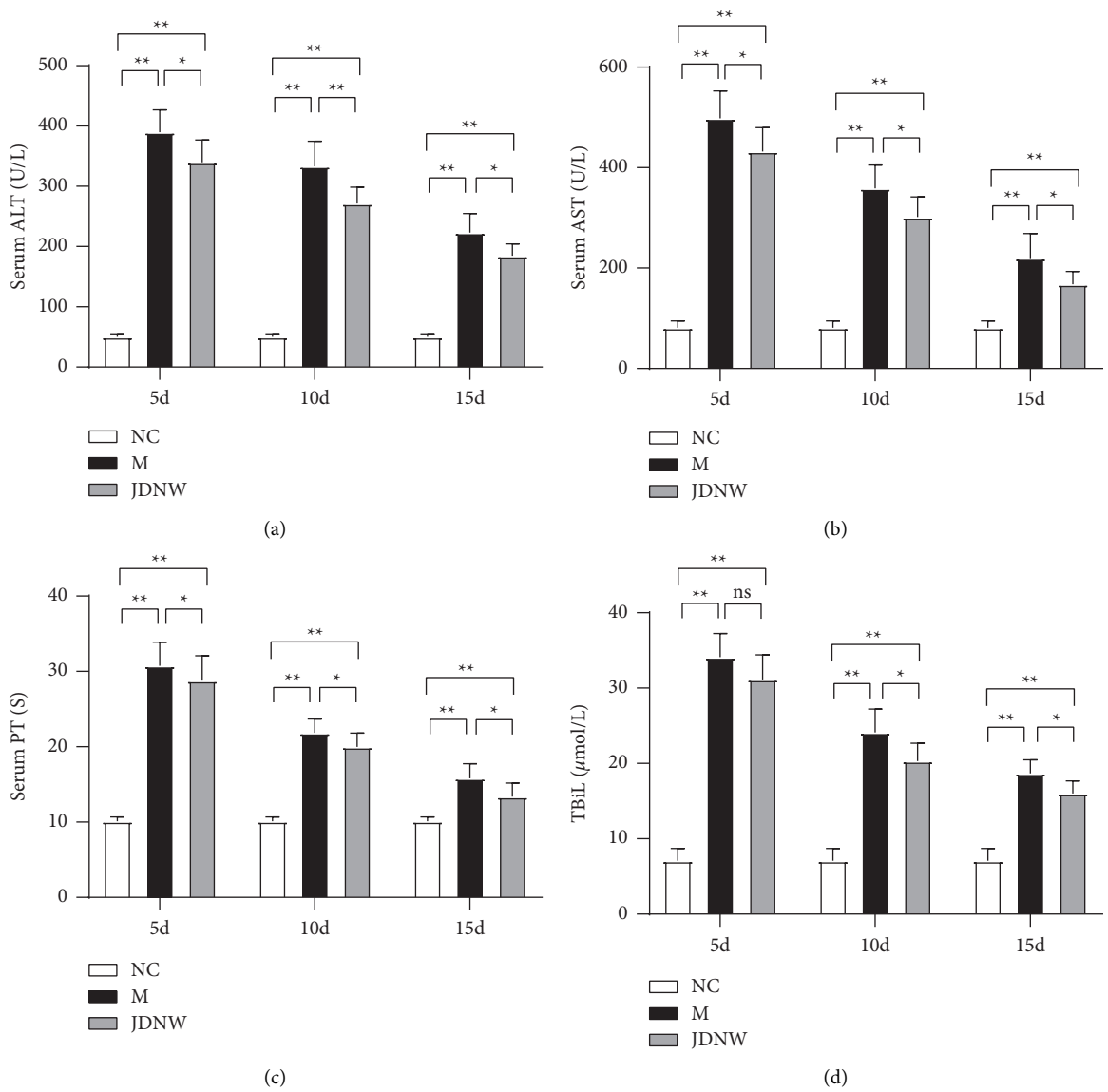

Figure 1: Effects of Jieduan-Niwan (JDNW) formula intervention on liver function in acute-on-chronic liver failure (ACLF) rats at different time points. (a) The serum levels of alanine aminotransferase (ALT); (b) the serum levels of aspartate aminotransferase; (c) the serum levels of total bilirubin (TBiL); (d) prothrombin times (PTs). Each bar represents the mean ± SD of $n = 5$–6 ($^{*}p < 0.05$, $^{**}p < 0.01$, "ns" $p > 0.05$).

and blocked with 5% BSA. Pathological sections and cell slides were incubated with primary antibodies overnight at 4°C. After being washed with PBS, the slides were incubated with TIRTC-labeled secondary antibodies for 2 hours at 37°C in the dark. Anti-fluorescence decay sealing solution (contains DAPI) sealed the slides. Fluorescence images were acquired with a confocal microscope (Leica TCS SP8) and quantified with Image J software version 1.80.

2.12. Real-Time Quantitative Polymerase Chain Reaction (qRT-PCR) to Detect the Expression of HMGB1. Total mRNA from liver tissue was extracted with RNA prep pure Tissue Kit (TIANGEN Biotech, China; catalog: DP431) and reverse transcribed into cDNA. The qRT-PCR reaction system was established by SuperReal PreMix Plus Kit (Tiangen Biotechnology, China; catalog: FP215) with GAPDH as the internal control. The amplification procedure was as follows: pre-denaturation: 95°C, 5 minutes, 1 cycle; amplification: 95°C, 10 s, 60°C, 30 s, a total of 40 cycles. As final, statistical analysis of gene expression was performed by the $2^{-\Delta\Delta CT}$. The specific primer sequences are in Supplementary Table S2.

2.13. Tunel. TdT-mediated dUTP Nick end labeling (TUNEL) detection and fluorescein in situ cell death assay kit (KeyGEN BioTECH, China; catalog: KGA7072) were used to detect the apoptotic response of L02 cells and liver tissues, according to the manufacturer's instructions.

2.14. Measurement of Reactive Oxygen Species (ROS). ROS in L02 cells was measured by using a reactive oxygen species detection kit (Beyotime, China; cat: S0033). Seeded

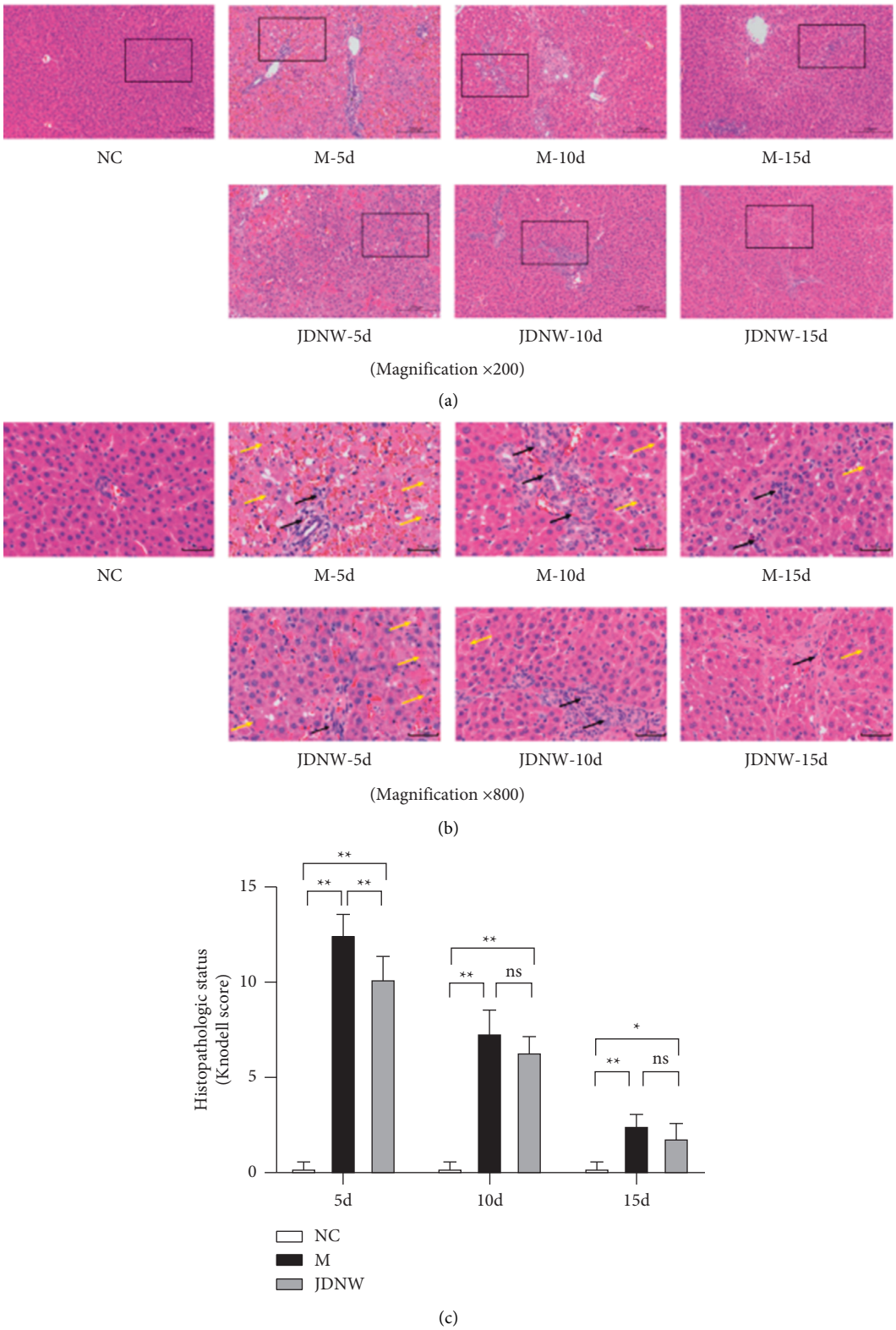

Figure 2: Effects of JDNW intervention on liver histopathology in ACLF rats at different time points. (a, b) Hematoxylin and eosin (H&E) staining to evaluate the pathological changes in rat's liver. Magnification 200x, 800x; scale bar: 200 μm, 50 μm. Infiltration of inflammatory cells (Black arrows), necrotic hepatocytes (Yellow arrows). (c) Evaluation of histopathological status (Knodell score). Each bar represents the mean ± SD of $n = 5$–6, ($^{*}p < 0.05$, $^{**}p < 0.01$, "ns" $p > 0.05$).

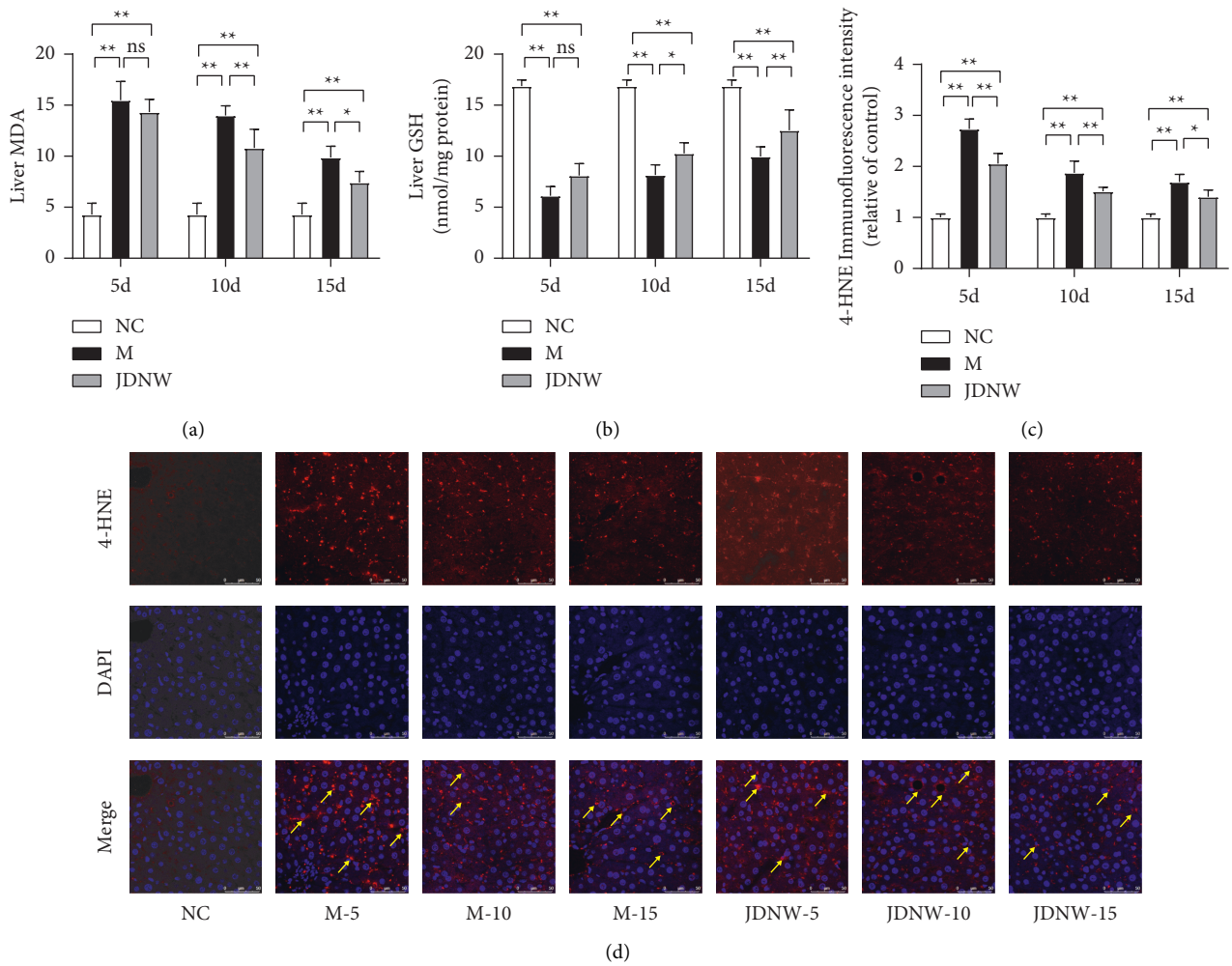

Figure 3: Effects of JDNW on oxidative stress injury of liver tissue in ACLF rats. (a) Malondialdehyde (MDA) content; (b) glutathione (GSH); (c, d) immunofluorescence results of 4-hydroxynonenal (4-HNE). Magnification 400x scale bar: 50 μm. Each bar represents the mean ± SD of $n = 5$–6 ($^{*}p < 0.05$, $^{**}p < 0.01$, "ns" $p > 0.05$).

the cells in a 6-well plate, after being exposed to the specified experimental conditions, incubated with 10 mM DCFH-DA at 37°C for 30 minutes. The cells were then harvested by trypsinization and centrifugation, and the level of intracellular ROS was detected by flow cytometry.

2.15. Statistical Analysis. All the data were analyzed by Prism 8.0 and expressed as mean ± standard deviation (SD). Statistical comparison among multiple groups was performed using one-way ANOVA followed by Tukey's post hoc test (data are normally distributed and homogeneity of variance, results were expressed as mean ± standard deviation (SD)) or Kruskal–Wallis test followed by Dunn's test (data are non-normally distributed or without homogeneity of variance, results were expressed as the median (min − max)). $p < 0.05$ is considered statistically significant.

3. Results

3.1. Effects of JDNW on Liver Function and Pathology in ACLF Rats. As shown in Figure 1, serum levels of ALT, AST, TBiL, and PT were determined to evaluate the effect of JDNW on liver function. Compared with the model group, at the same time point, the liver function of the JDNW treatment group was significantly improved at 5, 10, and 15 d. Pathologically, liver cells in the ACLF group were arranged disorderly, inflammatory cells were infiltrated, hepatic sinusoids were dilated and hemorrhaged, and a large number of necrotic liver cells were present. Next, we performed a histopathological status assessment (Knodell score) to assess the level of inflammation and necrosis in liver tissue. Compared with the model group, the treatment of JDNW statistically reduced the Knodell score of liver tissue in the 5 d group (Figure 2).

3.2. Effects of JDNW on Oxidative Stress. As shown in Figure 3, the content of MDA and GSH, as well as the accumulation level of 4-HNE were examined to evaluate the effect of JDNW on oxidative stress. Compared with the NC group, 4-HNE had more accumulation in ACLF model liver tissue. Likewise, the MDA contents of the ACLF group

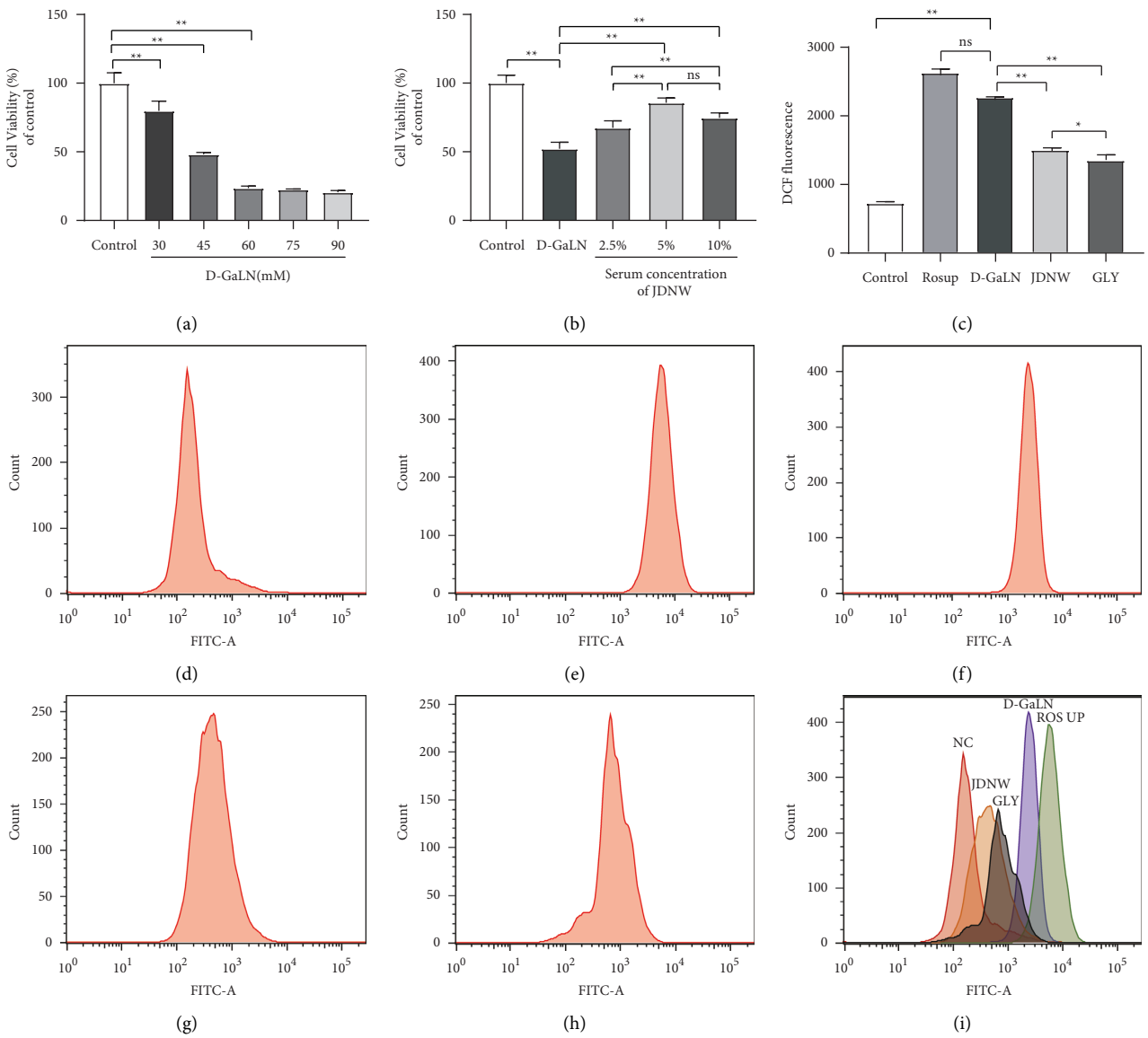

Figure 4: Effects of JDNW on D-galactosamine (D-GaLN)-induced cell damage and reactive oxygen species production in L02 cells. (a, b). The Cell Counting Kit-8 (CCK8) test was used to analyze cell viability. (a) Cells were treated with different concentrations of D-GaLN (30, 45, 60, 70, and 90 mM) and (b) pretreated with different concentrations of JDNW serum (2.5%, 5%, and 10%) for 12 hours and then cotreated with D-GaLN (45 mM) for 11 hours. (C–I) Flow cytometric analysis of ROS levels in L02 cells. (c) ROS statistics, (d) control group, (e) Rosup group, (f) D-GaLN (45 mM) group, (g) cotreated with JDNW (5%) and D-GaLN (45 mM) group, (h) cotreated with GLY (1 mM) and D-GaLN (45 mM), (i) aggregate results. Each bar represents the mean ± SD of $n = 3$ ($^{*}p < 0.05$, $^{**}p < 0.01$, "ns" $p > 0.05$).

increased, while the contents of GSH decreased, which was obvious in the M-5 d group. After JDNW treatment, the levels of 4-HNE and MDA in liver tissue decreased, and the level of GSH increased, indicating that the intervention of JDNW significantly reduced the oxidative stress damage in ACLF liver tissue.

Meanwhile, we conducted a CCK-8 test in vitro, and confirmed that JDNW serum can attenuate D-GaLN damage to L02 cells (Figures 4(a) and 4(b)). Next, to further observe the effect of JDNW serum on oxidative stress damage, we measured the fluorescence intensity of DCF by flow cytometry to analyze the accumulation of ROS in L02 cells in vitro. As shown in (Figures 4(c)–4(i)), D-GaLN significantly increased the accumulation of ROS in L02 cells, while the JDNW group was similar to glycyrrhizin (GLY; a specific HMGB1 inhibitor) [20, 21], significantly reduced the accumulation of ROS in L02 cells.

3.3. The Amelioration of Apoptosis by JDNW May be Related to Mitochondrial Pathway. Next, we performed TUNEL staining to detect the apoptosis of ACLF rat liver tissue and L02 cells. As shown in (Figures 5(a) and 5(b)), the apoptosis rate of hepatocytes (TUNEL-positive cell rate) of the ACLF group increased, and the M-5 d group was the highest. After JDNW treatment, the apoptosis rate of hepatocytes was

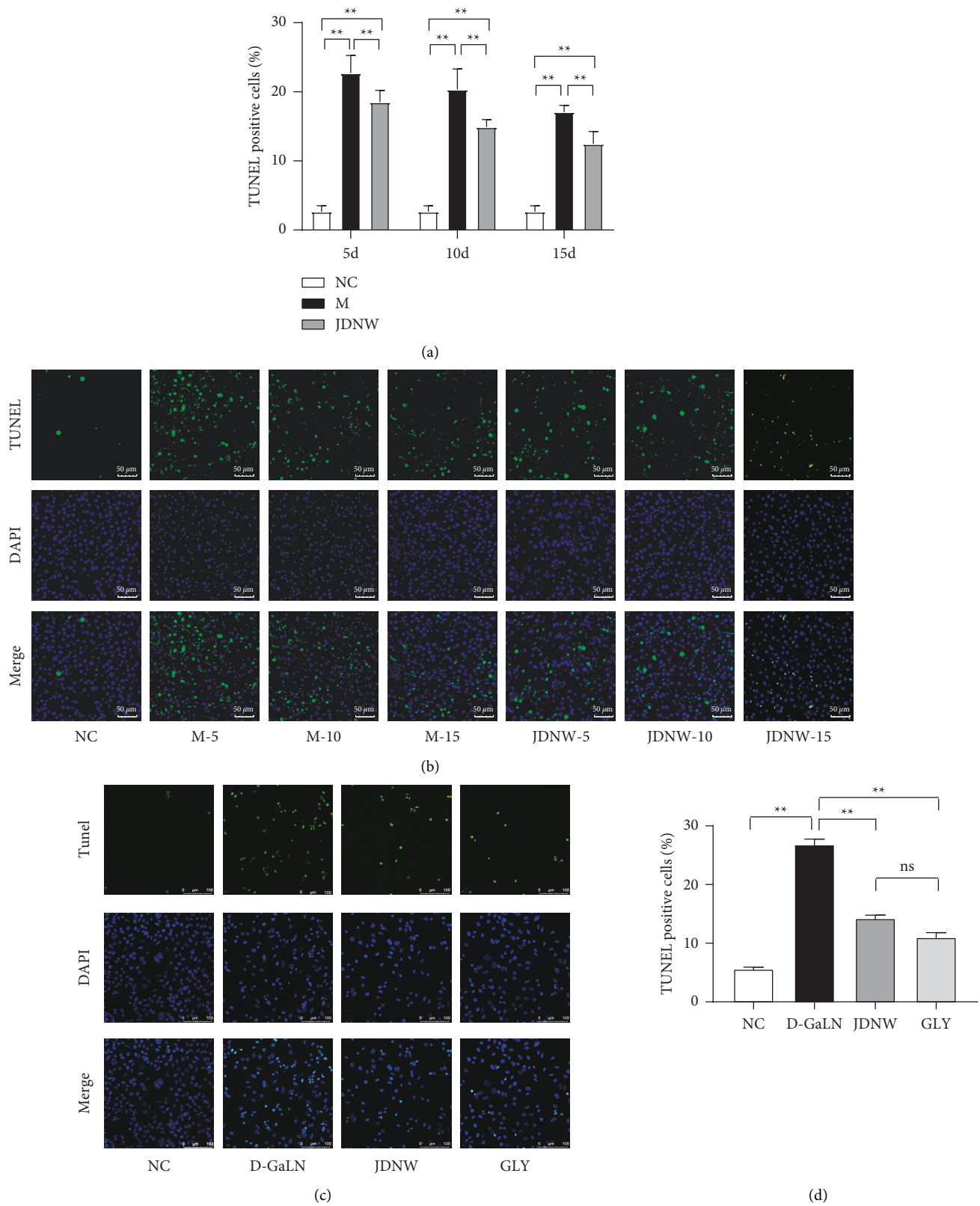

Figure 5: TdT-mediated dUTP Nick end labeling (TUNEL) staining to detect the effect of JDNW on the apoptosis rate of hepatocytes. (a, b) The effect of treatment at different time points on hepatocyte apoptosis in ACLF rats: 10 random fields/per slice, 3 random slices/per sample, representative of 5–6 rats/group. (c, d) Effects of JDNW serum on apoptosis of L02 cells induced by D-GaLN. Data are presented from three independent experiments. TUNEL-positive cells (green fluorescence). Each bar represents the mean ± SD ($^{*}p < 0.05$, $^{**}p < 0.01$, "ns" $p > 0.05$).

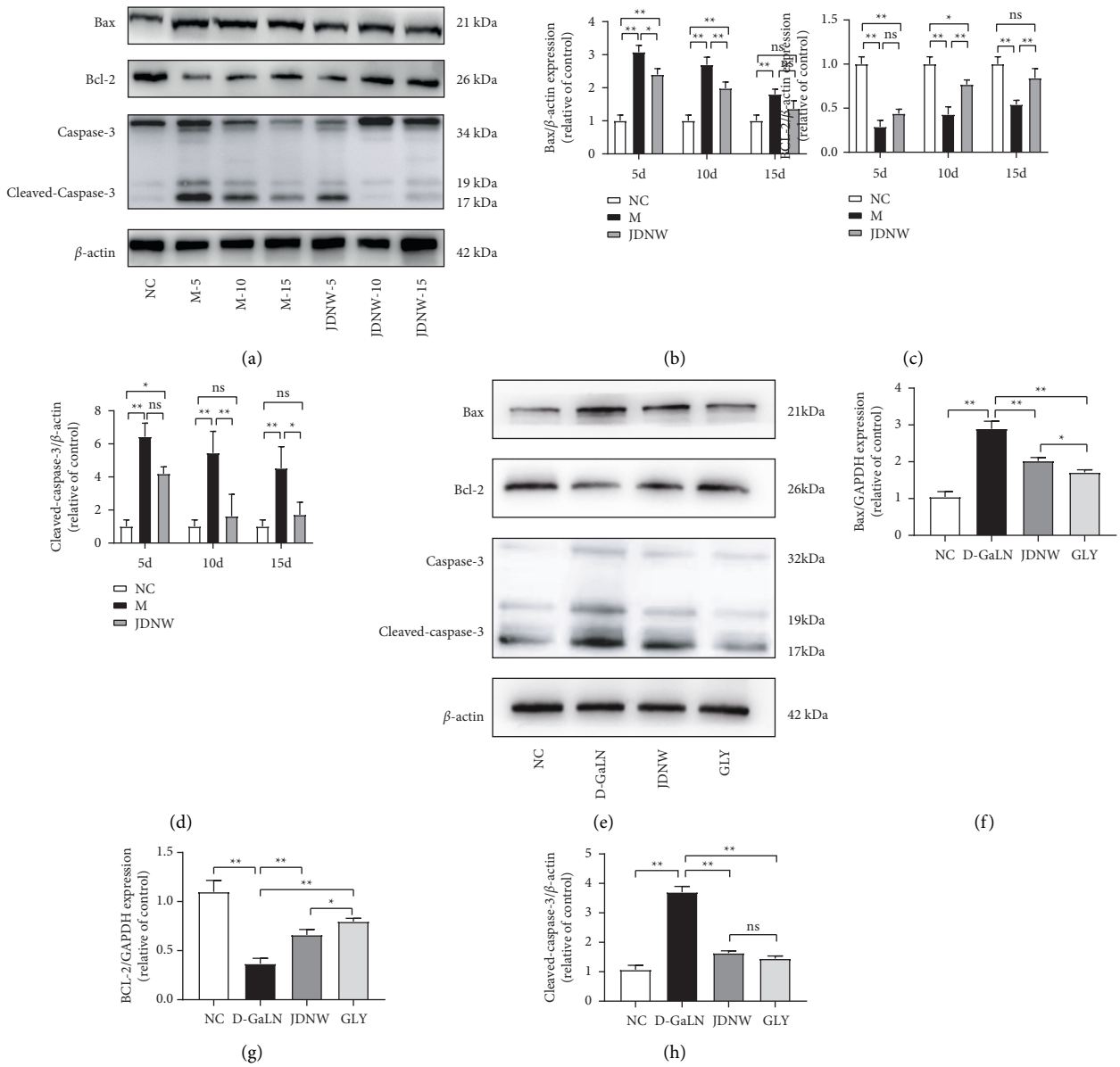

Figure 6: Effects of JDNW on the expression of Bax, Bcl-2, and Caspase-3 in vitro and in vivo. (a–d) Effects of JDNW treatment at different time points on mitochondrial apoptosis-related proteins in liver tissues of ACLF rats. (e–h). Effects of JDNW serum on mitochondrial apoptosis-related proteins of L02 cells. The data on quantified protein expressions were normalized by related β-actin. Each bar represents the mean ± SD of $n = 3$ ($^{*}p < 0.05$, $^{**}p < 0.01$, "ns" $p > 0.05$).

significantly lower than that of the model group at the same time point. Likewise, in vitro, the intervention of JDNW serum significantly reduced the apoptosis of L02 cells caused by D-GaLN, and its effect was similar to that of GLY (Figures 5(c) and 5(d)).

Further, we examined the effect of JDNW on mitochondrial pathway apoptosis-related proteins. As shown in (Figures 6(a)–6(d)), in ACLF rats' liver tissue, the expression of cleaved-caspase-3 and Bax increased, and the anti-mitochondrial pathway apoptosis protein Bcl-2 decreased. While the treatment of JDNW reversed this kind of change compared with the model group during the same period. In vitro, the intervention of JDNW serum also reversed the increase of cleaved-caspase-3 and Bax, and the decrease in Bcl-2 caused by D-GaLN, similar to the effect of an inhibitor of HMGB1 (GLY; Figures 5(e)–5(h)).

3.4. Effects of JDNW on HMGB1. Our previous study showed the expression and translocation of HMGB1 were associated with oxidative stress and mitochondrial pathway apoptosis [22]. Therefore, we performed immunofluorescence, qRT-PCR, and western blotting to detect the expression and distribution of HMGB1, and the results (Figure 7) showed that the cytoplasmic distribution of HMGB1 in the ACLF group increased significantly. The total expression of HMGB1 in the M-5 d group was significantly increased, indicating that there was an overexpression of HMGB1 in

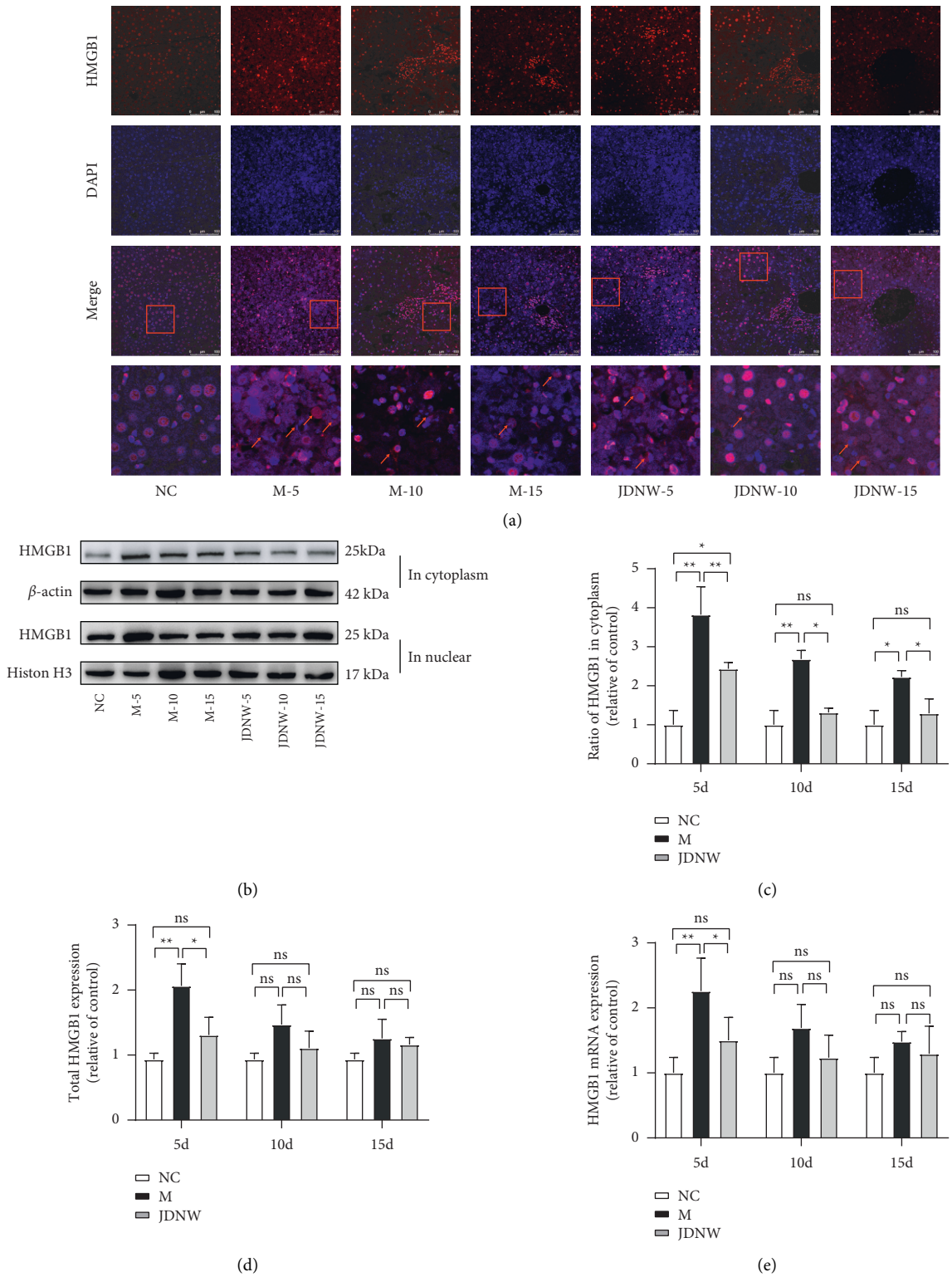

Figure 7: Effects of JDNW on the expression and translocation of HMGB1 in ACLF rats. (a) Immunofluorescence staining of HMGB1 at different time points. Scale bar: 100 μm; HMGB1 in the cytoplasm (red arrows). (b) Western blot detection of HMGB1. (c) Ratio of HMGB1 in the cytoplasm and (d) total HMGB1 by western blot assay. (e) HMGB1 mRNA expression was detected by qRT-PCR. Each bar represents the mean ± SD of $n = 3$ ($^{*}p < 0.05$, $^{**}p < 0.01$, "ns" $p > 0.05$).

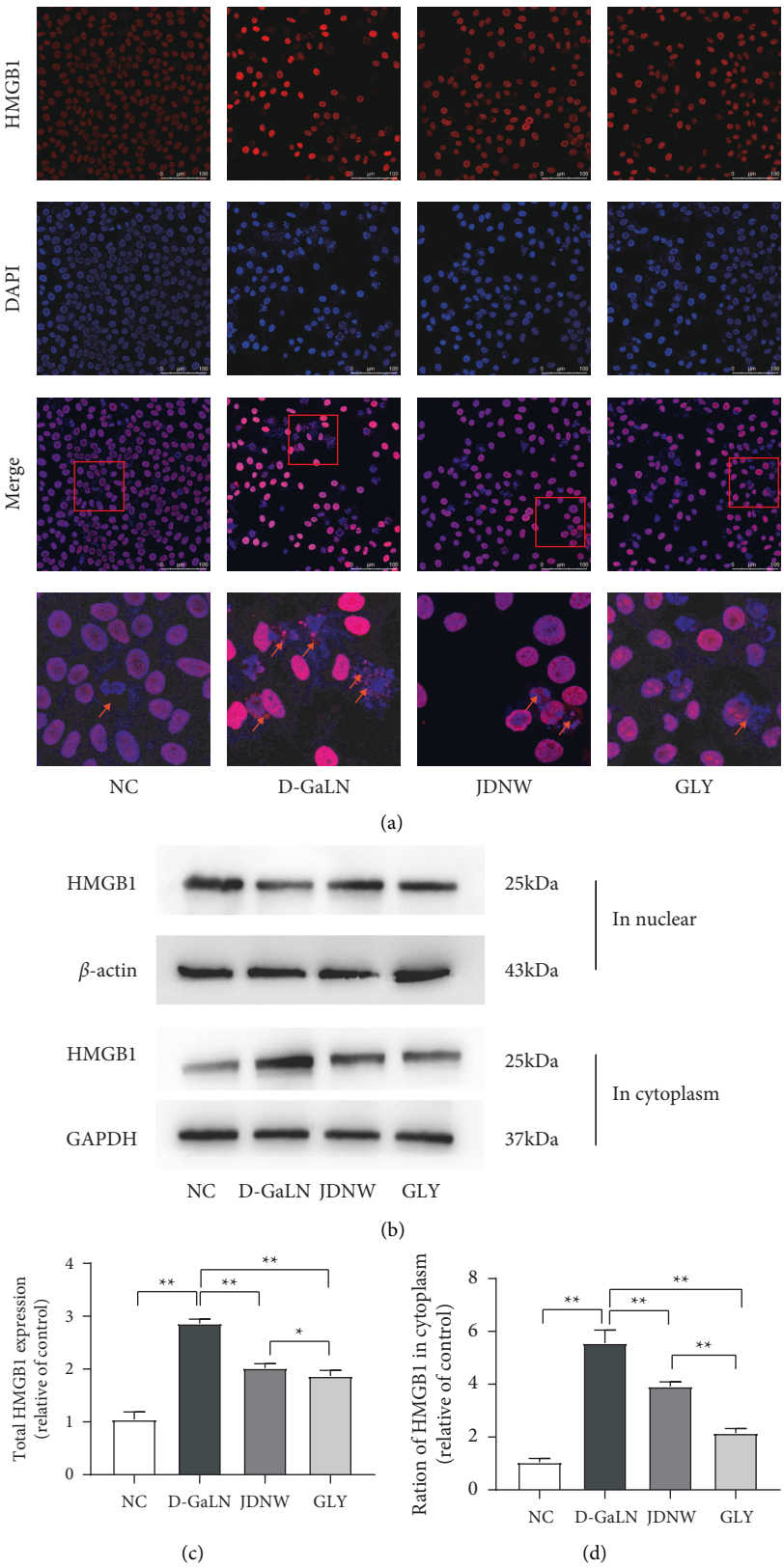

Figure 8: The effect of JDNW serum on the expression and translocation of HMGB1 in L02 cells. (a) Immunofluorescence staining of HMGB1. Scale bar: 100 μm; HMGB1 in the cytoplasm (red arrows). (b) Western blot detection of HMGB1. (c) Total HMGB1 and (d) ratio of HMGB1 in the cytoplasm by western blot assay. Each bar represents the mean ± SD of $n = 3$ ($^{*}p < 0.05$, $^{**}p < 0.01$, "ns" $p > 0.05$).

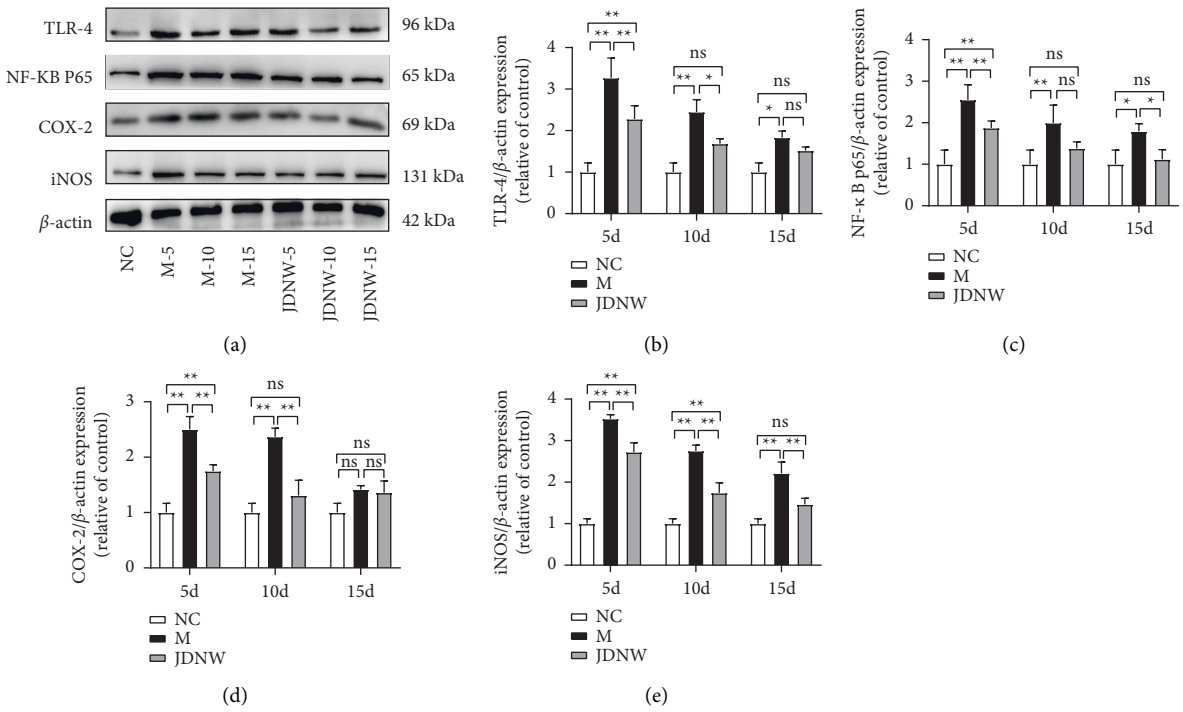

Figure 9: Effect of JDNW on HMGB1/TLR-4/NF-κB pathway in ACLF rats. The protein expression levels in liver tissues of TLR-4, NF-κB P65, iNOS, and COX-2 were evaluated by western blotting. (a) Representative immunoblots. (b–e) The relative protein expression results of TLR-4, NF-κB P65, iNOS, and COX-2. Each bar represents the mean ± SD of $n = 3$ ($^{*}p < 0.05$, $^{**}p < 0.01$, "ns" $p > 0.05$).

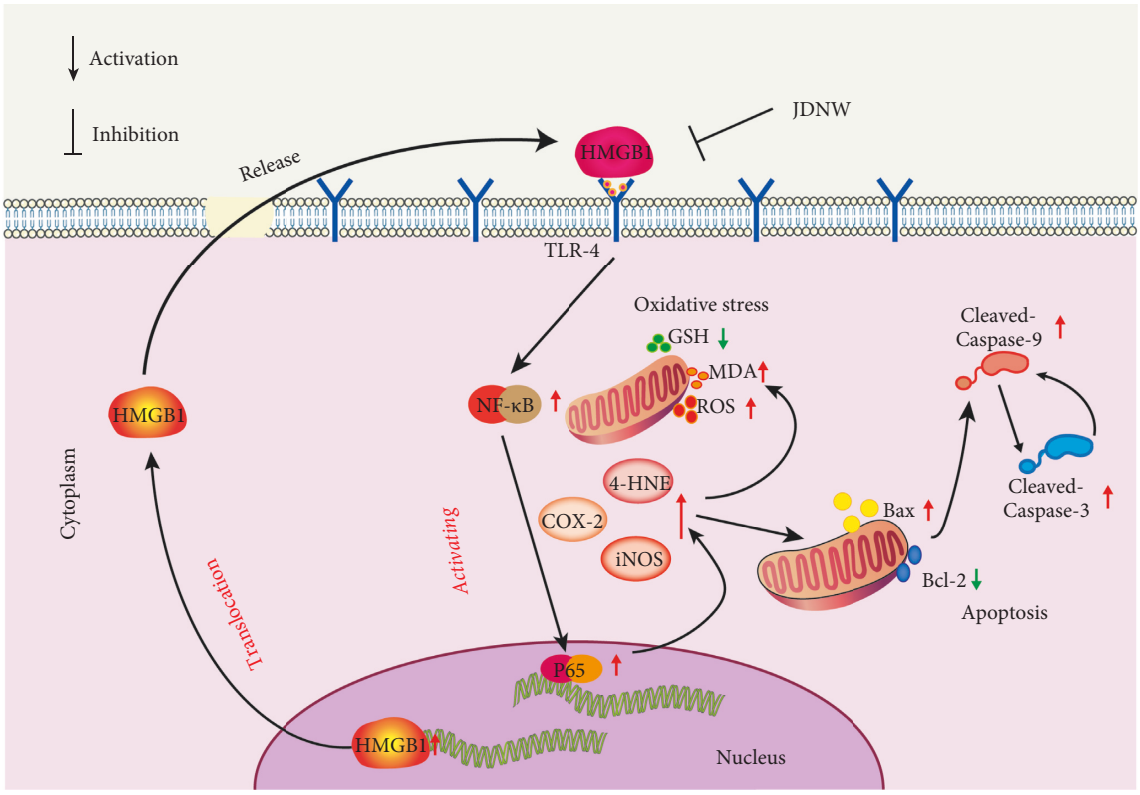

Figure 10: The mechanisms of JDNW inhibit HMGB1 overexpression and translocation, thus the oxidative stress and apoptosis are mediated by the HMGB1/TLR-4/NF-κB pathway in ACLF.

the early period of ACLF injury. After JDNW treatment, the intracytoplasmic translocation and the overexpression of HMGB1 were significantly reduced. Also, the overexpression of HMGB1 in the early stage of ACLF injury was significantly reduced. In vitro, the intervention of D-GaLN resulted in the overexpression and the translocation of HMGB1 in L02 cells. However, after the intervention of JDNW serum and HMGB1 inhibitor-GLY, the increase was suppressed (Figure 8). These results indicated that JDNW inhibited the overexpression and intracytoplasmic translocation of HMGB1.

3.5. Effects of JDNW on HMGB1/TLR-4/NF-κB Signaling Pathway. Western Blot was used to detect the expression of TLR4, the main receptor of HMGB1, and the key downstream factors NF-κB P65, COX-2, and iNOS, in order to observe the effect of JDNW on the HMGB1-mediated oxidative stress pathway. The results (Figure 9) showed that the expressions of TLR-4, NF-κB P65, COX-2, and iNOS in the ACLF group were significantly increased, the M-5d group being the most obvious. After JDNW treatment for 5, 10, and 15 d, the expression of related signaling pathway proteins was inhibited compared with the model group at the same time point.

4. Discussion

The pathological mechanism of ACLF is far from clear, but immune system-related factors are the key cause of ACLF has been widely recognized. ACLF patients have two immune-related pathophysiological characteristics: a state of excessive systemic response and susceptibility to infection [23]. Due to factors such as acute triggers (usually bacterial infections) and pathogens directly or indirectly activate immune cells. In turn, the systemic inflammatory response is aggravated, and a cytokine storm is induced, causing liver cell damage, necrosis, and even extrahepatic tissues. Eventually, liver failure and even the failure of extrahepatic organs are induced [3, 4].

As an important DAMPs factor, extracellular HMGB1 aggravates ACLF progression [24]. Translocation to the cytoplasm is a key process before HMGB1 is released outside the cell membrane. In the current study, we found that in the early injury stage of the ACLF model, the total expression of HMGB1 and the proportion of it in cytoplasm increased significantly and the treatment of JDNW alleviated this increase. A similar increase of HMGB1 is seen in the cytoplasm of L02 cells when D-GaLN damage occurs in vitro. After the intervention of GLY and JDNW serum, the total amount and proportion of HMGB1 in the cytoplasm were significantly reduced. By binding to the TLR4 receptor and increasing transcription activity following release from the cell membrane, HMGB1 regulates the expression of IKB-α and NF-kB p65 [25]. As a result, COX-2 and iNOS are activated, and 4-HNE is accumulated, causing lipid peroxidation and oxidative stress [26, 27].

Besides necrosis of hepatocytes plus infiltration of inflammatory cells, excessive apoptosis is another pathological characteristic of ACLF. Studies have confirmed that the intrinsic apoptotic pathway affects the occurrence and development of ACLF [28]. Activating the intrinsic pathway of apoptosis requires mitochondria and is induced by excess ROS and oxidative stress. Bcl-2 counteracts the pro-apoptotic effects of Bax, which digs holes in the mitochondrial outer membrane. Through inhibition of cytochrome c cytoplasmic release, as well as cytochrome c-mediated caspase cascades (caspase-9 is initiated during apoptosis by caspase-3), apoptosis is induced [29]. We previously found that HMGB1 might worsen liver injury in ACLF rats via oxidative stress and then mitochondrial dysfunction, leading to apoptosis [30]. The current study confirmed that extensive apoptosis occurred in ACLF liver tissue, whereas JDNW intervention reduced oxidative stress and apoptosis both in vivo and in vitro. In the ACLF group, the expression of TLR-4, NF-κB p65, COX-2, iNOS, activated caspase-3, and Bax increased, while the anti-mitochondrial pathway apoptosis protein Bcl-2 decreased. The expression of related proteins was reversed after JDNW treatment.

The active components of JDNW may be responsible for this effect through a related mechanism. HPLC was used to analyze the main components of JDNW and their concentrations, including catalpol (CTP; 0.1324 mg/mL), gallic acid (GA; 0.0902 mg/mL), 3,4-dihydroxybenzaldehyde (0.0073 mg/mL), chlorogenic acid CA (0.0266 mg/mL), notoginsenoside R1 (NG-R1; 0.1905 mg/mL), salvianolic acid B (Sal B; 0.5436 mg/mL), and ginsenoside Rb1 (GRb1; 0.1834 mg/mL) [19]. Here, SalB confers protection against hepatic steatosis and inflammation through SIRT1-mediated HMGB1 deacetylation [31]. Sal B significantly ameliorated myocardial I/R injury in a dose-dependent manner, improved cardiac function, attenuated the inflammatory response, and cardiomyocyte apoptosis and expression of the apoptosis proteins Bcl-2 and Bax, as well as HMGB1 and TLR4 [32]. In addition to regulating Caspase-3, Bax, and Bcl-2 expression, Sal B also maintains the permeability of the mitochondrial membrane and ensures basic cellular energy metabolism by regulating their expression [33]. NG-R1 treatment inhibited HMGB1/TLR4/NF-κBp65, lowered MPO activity, and reduced the severity of acute lung injury [34]. GRb1 inhibits caspase3 activation, downregulates cleaved caspase 3, Bax to reduce hepatocyte apoptosis, and upregulates Bcl-2 protein expression in the liver [35]. By affecting the miR-142/HMGB1/TLR4/NF-κB pathway, CTP protects muscles from SCI by suppressing apoptosis, oxidative stress, and inflammation [36]. HMGB1 induces the production of ECM in human hepatic sinusoids and human umbilical vein endothelial cells when CA is administered [37]. Furthermore, CA activates SIRT1 to inhibit nuclear translocation of HMGB1 and M2 polarization, thereby alleviating *Klebsiella pneumoniae*-induced pneumonia in AMs [38]. It is suggested that the main components of the JDNW formula can inhibit the expression and translocation of HMGB1 and its mediated HMGB1/TLR-4/NF-kB pathway, and have anti-apoptotic and oxidative stress effects. This may partially explain the potential material basis of JDNW ameliorating ACLF liver injury by reducing oxidative stress and apoptosis by inhibiting the HMGB1/TLR-4/NF-κB pathway.

Taken together, in the current study, by revealing that JDNW inhibits the overexpression and translocation of HMGB1, an important DAMP molecular and further affects its mediated oxidative stress injury and apoptosis, it can partially explain the theory of "toxic damage to the liver." But, the current study still has some limitations. The improvement of oxidative stress and apoptosis by JDNW was demonstrated in this research, as well as its inhibition of Bcl-2 and inhibition of Bax and cleaved caspase-3, indicating the inhibition of apoptosis by JDNW may be associated with the mitochondrial pathway. However, we have not done relevant research on mitochondrial outer membrane permeabilization and mitochondrial functions, which deserves further refinement in future research.

5. Conclusion

In summary, our current results indicate that JDNW reduced liver injury in ACLF rats, and this effect was a result of its inhibition of the HMGB1/TLR-4/NF-κB pathway, thereby reducing oxidative stress and the occurrence of hepatic apoptosis (Figure 10).

Data Availability

The data used to support the findings of this study are available from the corresponding author upon reasonable request.

Conflicts of Interest

The authors declare that they have no conflicts of interest.

Authors' Contributions

P. F., B. D., and Q. Z. conceived and designed the experiments; W. H., J. L., and X. W. were involved in the experimental study design, preparation, and review of this manuscript. All authors have reviewed and approved the final version of the manuscript. P. F. and B. D. authors contributed equally to this work.

Acknowledgments

This research was funded by Natural Science Foundation of Beijing Municipality (Grant no. 7192024).

Supplementary Materials

Table 1 Constituents of the JDNW formula. Table 2 Primer sequences for qRT-PCR analyses. (*Supplementary Materials*)

References

[1] S. K. Sarin, A. Choudhury, M. K. Sharma et al., "Acute-on-chronic liver failure: consensus recommendations of the Asian Pacific association for the study of the liver (APASL): an update," *Hepatology International*, vol. 13, no. 4, pp. 353–390, 2019.

[2] R. Moreau, B. Gao, M. Papp, R. Bañares, and P. S. S. Kamath, "Acute-on-chronic liver failure: Acute-on-chronic liver failure: A distinct clinical syndrome distinct clinical syndrome," *Journal of Hepatology*, vol. 75, no. Suppl 1, pp. S27–S35, 2021.

[3] X. Du, Y. Shi, Y. Yang et al., "DAMP molecular IL-33 augments monocytic inflammatory storm in hepatitis B-precipitated acute-on-chronic liver failure," *Liver International*, vol. 38, no. 2, pp. 229–238, 2018.

[4] C. Engelmann, J. Clària, G. Szabo, J. Bosch, and M. Bernardi, "Pathophysiology of decompensated cirrhosis: portal hypertension, circulatory dysfunction, inflammation, metabolism and mitochondrial dysfunction," *Journal of Hepatology*, vol. 75, no. Suppl 1, pp. S49–S66, 2021.

[5] W. Wu, S. Sun, Y. Wang et al., "Circulating neutrophil dysfunction in HBV-related acute-on-chronic liver failure," *Frontiers in Immunology*, vol. 12, Article ID 620365, 2021.

[6] H. Wang, O. Bloom, M. Zhang et al., "HMG-1 as a late mediator of endotoxin lethality in mice," *Science*, vol. 285, no. 5425, pp. 248–251, 1999.

[7] H. Yang, D. J. Antoine, U. Andersson, and K. J. Tracey, "The many faces of HMGB1: molecular structure-functional activity in inflammation, apoptosis, and chemotaxis," *Journal of Leukocyte Biology*, vol. 93, no. 6, pp. 865–873, 2013.

[8] H. Yang, H. Wang, S. S. Chavan, and U. Andersson, "High mobility group box protein 1 (HMGB1): the prototypical endogenous danger molecule," *Molecular Medicine*, vol. 21, no. S1, pp. S6–S12, 2015.

[9] T. Yamamoto and Y. Tajima, "HMGB1 is a promising therapeutic target for acute liver failure," *Expert Review of Gastroenterology and Hepatology*, vol. 11, no. 7, pp. 673–682, 2017.

[10] S. Zhang, Z. Feng, W. Gao et al., "Aucubin attenuates liver ischemia-reperfusion injury by inhibiting the HMGB1/TLR-4/NF-κB signaling pathway, oxidative stress, and apoptosis," *Frontiers in Pharmacology*, vol. 11, Article ID 544124, 2020.

[11] F. Artru, A. Louvet, and I. Ruiz, "Liver transplantation in the most severely ill cirrhotic patients: a multicenter study in acute-on-chronic liver failure grade 3," *Journal of Hepatology*, vol. 67, pp. 708–715, 2017.

[12] B. Khambu, S. Yan, N. Huda, and X. M. Yin, "Role of high mobility group box 1 in liver pathogenesis," *International Journal of Molecular Sciences*, vol. 20, no. 21, Article ID 5314, 2019.

[13] Y. Shi, X. Guo, J. Zhang, H. Zhou, B. Sun, and J. Feng, "DNA binding protein HMGB1 secreted by activated microglia promotes the apoptosis of hippocampal neurons in diabetes complicated with OSA," *Brain, Behavior, and Immunity*, vol. 73, pp. 482–492, 2018.

[14] H. J. Hua, Q. Ying, and Y. Naili, "Treatment of chronic severe hepatitis B by Jieduan Niwan method," *Chinese Journal of Integrated Traditional and Western Medicine on Liver Diseases*, vol. 4, no. 20, pp. 200–203, 2010.

[15] Y. Qian, "Using Jieduan-Niwan method treats chronic severe hepatitis," *Beijing Journal of Traditional Chinese Medicine*, vol. 27, no. 2, pp. 85–87, 2008.

[16] X. Wang, "Expert consensus on the diagnosis and treatment of acute on chronic liver failure with integrated traditional Chinese and Western medicine(CAIM)," *Joournal of clinical hepatology*, vol. 37, no. 9, pp. 2045–2053, 2021.

[17] W. Yang, Y. Hao, W. Hou, X. Fang, P. Fang, and T. Jiang, "Jieduan-niwan formula reduces liver apoptosis in a rat model of acute on chronic liver failure by regulating the E2F1-mediated intrinsic apoptosis pathway," *Evidence Based Complement and Alternative Medicine*, vol. 2019, Article ID 8108503, 2019.

[18] J. Liang, M. Wu, C. Bai, C. Ma, P. Fang, and W. Hou, "Network pharmacology approach to explore the potential mechanisms of jieduan-niwan formula treating acute-on-chronic liver failure," *Evidence Based Complement and Alternative Medicine*, vol. 2020, Article ID 1041307, 2020.

[19] W. Hou, Y. Hao, W. Yang et al., "The jieduan-niwan (JDNW) formula ameliorates hepatocyte apoptosis: a study of the inhibition of E2F1-mediated apoptosis signaling pathways in acute-on-chronic liver failure (ACLF) using rats," *Drug Design, Development and Therapy*, vol. 15, pp. 3845–3862, 2021.

[20] L. Mollica, F. De Marchis, A. Spitaleri et al., "Glycyrrhizin binds to high-mobility group box 1 protein and inhibits its cytokine activities," *Chemistry and Biology*, vol. 14, no. 4, pp. 431–441, 2007.

[21] R. Smolarczyk, T. Cichoń, S. Matuszczak, I. Mitrus, M. Lesiak, and M. Kobusińska, "The role of glycyrrhizin, an inhibitor of HMGB1 protein, in anticancer therapy," *Archivum Immunologiae et Therapiae Experimentalis*, vol. 60, no. 5, pp. 391–399, 2012.

[22] P. Fang, J. Liang, X. Jiang et al., "Quercetin attenuates d-GaLN-induced L02 cell damage by suppressing oxidative stress and mitochondrial apoptosis via inhibition of HMGB1," *Frontiers in Pharmacology*, vol. 11, p. 608, 2020.

[23] J. Trebicka, J. Fernandez, M. Papp et al., "The PREDICT study uncovers three clinical courses of acutely decompensated cirrhosis that have distinct pathophysiology," *Journal of Hepatology*, vol. 73, no. 4, pp. 842–854, 2020.

[24] Y. B. Hu, D. P. Hu, and R. Q. Fu, "Correlation between high mobility group box-1 protein and chronic hepatitis B infection with severe hepatitis B and acute-on-chronic liver failure: a meta-analysis," *Minerva Medica*, vol. 108, no. 3, pp. 268–276, 2017.

[25] W. J. Liang, H. W. Yang, H. N. Liu, W. Qian, and X. L. Chen, "HMGB1 upregulates NF-kB by inhibiting IKB-α and associates with diabetic retinopathy," *Life Sciences*, vol. 241, Article ID 117146, 2020.

[26] S. M. Chuang, J. H. Lu, K. L. Lin et al., "Epigenetic regulation of COX-2 expression by DNA hypomethylation via NF-κB activation in ketamine-induced ulcerative cystitis," *International Journal of Molecular Medicine*, vol. 44, no. 3, pp. 797–812, 2019.

[27] S. S. Singhal, S. P. Singh, P. Singhal, D. Horne, J. Singhal, and S. Awasthi, "Antioxidant role of glutathione S-transferases: 4-hydroxynonenal, a key molecule in stress-mediated signaling," *Toxicology and Applied Pharmacology*, vol. 289, no. 3, pp. 361–370, 2015.

[28] F. Li, L. Miao, H. Sun, Y. Zhang, X. Bao, and D. Zhang, "Establishment of a new acute on chronic liver failure model," *Acta Pharmaceutica Sinica B*, vol. 7, no. 3, pp. 326–333, 2017.

[29] C. K. Kontos, M. I. Christodoulou, and A. Scorilas, "Apoptosis-related BCL2-family members: key players in chemotherapy," *Anti Cancer Agents in Medicinal Chemistry*, vol. 14, no. 3, pp. 353–374, 2014.

[30] H. Wei, X. Wei, and J. Liang, "HMGB1-induced hepatocyte pyroptosis expanding inflammatory responses contributes to the pathogenesis of acute-on-chronic liver failure (ACLF)," *Journal of Inflammation Research*, vol. 23, pp. 1178–7031, 2021.

[31] W. Zeng, W. Shan, L. Gao et al., "Inhibition of HMGB1 release via salvianolic acid B-mediated SIRT1 up-regulation protects rats against non-alcoholic fatty liver disease," *Scientific Reports*, vol. 5, no. 1, Article ID 16013, 2015.

[32] H. Liu, W. Liu, H. Qiu et al., "Salvianolic acid B protects against myocardial ischaemia-reperfusion injury in rats via inhibiting high mobility group box 1 protein expression through the PI3K/Akt signalling pathway," *Naunyn-Schmiedeberg's Archives of Pharmacology*, vol. 393, no. 8, pp. 1527–1539, 2020.

[33] Y. Gong, D. Li, L. Li et al., "Smad3 C-terminal phosphorylation site mutation attenuates the hepatoprotective effect of salvianolic acid B against hepatocarcinogenesis," *Food and Chemical Toxicology*, vol. 147, Article ID 111912, 2021.

[34] J. He, M. W. Liu, Z. Y. Wang, and R. J. Shi, "Protective effects of the notoginsenoside R1 on acute lung injury by regulating the miR-128-2-5p/Tollip signaling pathway in rats with severe acute pancreatitis," *Innate Immunity*, vol. 28, no. 1, pp. 19–36, 2022.

[35] B. Song, Y. Sun, Y. Chu et al., "Ginsenoside Rb1 alleviated high-fat-diet-induced hepatocytic apoptosis via peroxisome proliferator-activated receptor γ," *BioMed Research International*, vol. 2020, Article ID 2315230, 2020.

[36] H. Xia, D. Wang, X. Guo, K. Wu, F. Huang, and Y. Feng, "Catalpol protects against spinal cord injury in mice through regulating MicroRNA-142-mediated HMGB1/TLR4/NF-κB signaling pathway," *Frontiers in Pharmacology*, vol. 11, Article ID 630222, 2020.

[37] H. Miao, H. Ouyang, Q. Guo et al., "Chlorogenic acid alleviated liver fibrosis in methionine and choline deficient diet-induced nonalcoholic steatohepatitis in mice and its mechanism," *The Journal of Nutritional Biochemistry*, vol. 106, Article ID 109020, 2022.

[38] Q. R. Li, S. R. Tan, L. Yang et al., "Mechanism of chlorogenic acid in alveolar macrophage polarization in *Klebsiella pneumoniae*-induced pneumonia," *Journal of Leukocyte Biology*, vol. 112, no. 1, pp. 9–21, 2022.

Hindawi
Evidence-Based Complementary and Alternative Medicine
Volume 2022, Article ID 2264394, 16 pages
https://doi.org/10.1155/2022/2264394

Research Article

Mechanical Study of Jian-Gan-Xiao-Zhi Decoction on Nonalcoholic Fatty Liver Disease Based on Integrated Network Pharmacology and Untargeted Metabolomics

Yong-Jun Cao,[1] Han-Zhou Li,[2] Jie Zhao,[3] Yu-Meng Sun,[1] Xiao-Wen Jin,[1] Shu-Quan Lv,[4] Jun-Yu Luo,[3] Xi-Xing Fang,[5] Wei-Bo Wen,[3] and Jia-Bao Liao[6]

[1]*Department of Endocrinology, Nantong Hospital Affiliated to Nanjing University of Chinese Medicine, Nantong, China*
[2]*Graduated School, Chengde Medical University, Chengde, China*
[3]*Department of Endocrinology, Yunnan Provincial Hospital of Chinese Medicine, Kunming, China*
[4]*Department of Endocrinology, Cangzhou Hospital of Integrated Traditional Chinese Medicine and Western Medicine of Hebei Province, Cangzhou, China*
[5]*College of Traditional Chinese Medicine, Changchun University of Traditional Chinese Medicine, Changchun, China*
[6]*Department of Emergency, Jiaxing Hospital of Traditional Chinese Medicine, Jiaxing, China*

Correspondence should be addressed to Wei-Bo Wen; wenweibo2020@163.com and Jia-Bao Liao; 403233670@qq.com

Received 9 May 2022; Revised 10 June 2022; Accepted 14 June 2022; Published 8 July 2022

Academic Editor: Chih-Yuan Ko

Jian-Gan-Xiao-Zhi decoction (JGXZ) has demonstrated beneficial effects on nonalcoholic fatty liver disease (NAFLD). However, the mechanisms by which JGXZ improve NAFLD are still unclear. *Methods.* In this study, we first used a high-fat diet (HFD) to establish a NAFLD rat model to clarify the therapeutic effect of JGXZ on NAFLD. Secondly, we used network pharmacology to predict the potential targets of JGXZ on NAFLD, and then the key targets obtained from network pharmacology were verified. Finally, we used untargeted metabolomics to study the metabolic regulatory mechanism of JGXZ. *Results.* JGXZ treatment could decrease body weight and ameliorate dyslipidemia in NAFLD model rats. H&E and oil red O staining indicated that JGXZ reduced steatosis and infiltration of inflammatory cells in the liver. In addition, network pharmacology research found that the potential targets of JGXZ on NAFLD pathway were mainly associated with improving oxidative stress, apoptosis, inflammation, lipid metabolism disorders, and insulin resistance. Further experimental verification confirmed that JGXZ could inhibit inflammation and improve oxidative stress, insulin resistance, and lipid metabolism disorders. Serum untargeted metabolomics analyses indicated that the JGXZ in the treatment of NAFLD may work through the linoleic acid metabolism, alpha-linolenic acid metabolism, tryptophan metabolism, and glycerophospholipid metabolism pathways. *Conclusions.* In conclusion, this study found that JGXZ has an ameliorative effect on NAFLD, and JGXZ alleviates the inflammatory response and oxidative stress and lipid metabolism disorders in NAFLD rats. The mechanism of action of JGXZ in the treatment of NAFLD may be related to the regulation of linoleic acid metabolism, tryptophan metabolism, alpha-linolenic acid metabolism, and glycerophospholipid metabolism.

1. Introduction

Nonalcoholic fatty liver disease (NAFLD) is a chronic metabolic stress liver disease, and it is one of the most common liver diseases [1]. In 2020, the global prevalence of NAFLD was as high as 25%, and it is increasing every year [2]. The widespread prevalence of NAFLD has directly led to an increase in the incidence of cirrhosis, liver cancer, and cardiovascular disease, posing a serious threat to human life and health, as well as a significant economic burden on patients, families, and society [3]. Therefore, it is essential to establish practical interventions early to interrupt or delay the progression of NAFLD.

Traditional Chinese medicine (TCM) formulas have the characteristics of having multiple ingredients, multiple targets, and multiple pathways of actions. Traditional

research methods cannot illustrate the effectiveness of drugs at the molecular level, and the research results cannot effectively elucidate the complex interactions among the efficacy of prescriptions, substance components, and the biological network of the organism. Network pharmacology can explain the material basis and mechanism of action of TCM herbal formulas from the perspective of macro-systematic and complex correlation [4]. Metabolomics allows for the comprehensive analysis of endogenous small molecules in biological samples and multivariate analysis of the overall changes in endogenous metabolites after stimulation or disturbance of the organism [5]. By combining network pharmacology with metabolomics, the mechanism of action of herbal formulas can be interpreted in depth at various levels, such as molecular, pathway, and metabolism, and this combination has become very important to study the mechanism of herbal formulas. He et al. [6] discovered the mechanism of action of *Coptis chinensis* Franch., a classic formula for the treatment of type 2 diabetes mellitus, using network pharmacology combined with an untargeted metabolomics approach. Liu et al. [7] elucidated the characteristics of metabolic abnormalities in depression models through a combination of metabolomics and network pharmacology, confirming the antidepressant mechanism of Free Wanderer Powder and providing evidence to support its further clinical applications.

Jiangan Xiaozhi decoction (JGXZ) consists of *Salvia miltiorrhiza Bunge*, *Panax notoginseng*, *Curcuma zedoaria*, *Hawthorn*, *Astragalus membranaceus*, *Vatica mangachapoi Blanco*, *Radix Paeoniae Rubra*, *Curcuma longa*, *Rhizoma Alismatis*, *Dendranthema morifolium*, *Lotus leaf*, and *Glycyrrhiza uralensis Fisch* [8]. It has significant therapeutic effects on NAFLD and can effectively improve patients' clinical indicators. A previous study demonstrated that JGXZ can improve dyslipidemia and insulin resistance in an NAFLD rat model [9]. However, the multi-ingredient and multi-targeting nature of herbal medicines plays a common role in their efficacy, and it is difficult to effectively elucidate the potential mechanism of JGXZ. Therefore, in this study, we first generated a NAFLD rat model using high-fat chow to clarify the role of JGXZ in the treatment of NAFLD. Second, we used network pharmacology to predict the main targets of JGXZ for the treatment of NAFLD and validated the key targets using western blotting and other methods. Finally, untargeted metabolomics was employed to study the changes in metabolite levels in the serum of NAFLD rats treated with JGXZ. The network pharmacology results were correlated with the metabolomics results to investigate the integrated mechanism of JGXZ for the treatment of NAFLD from the molecular metabolite perspective and to investigate the mechanism of the integrative effect of JGXZ in the treatment of NAFLD.

2. Materials and Methods

2.1. Prediction of Potential Targets for JGXZ and NAFLD. We used the TCM systems pharmacology database and analysis platform (TCMSP) to screen the drug ingredients and their action targets of *Salvia miltiorrhiza Bunge*, *Panax notoginseng*, *Curcuma zedoaria*, *Hawthorn*, *Astragalus membranaceus*, *Vatica mangachapoi Blanco*, *Radix Paeoniae Rubra*, *Curcuma longa*, *Rhizoma Alismatis*, *Dendranthema morifolium*, *Lotus leaf*, and *Glycyrrhiza uralensis Fisch* in the compound formula with an oral bioavailability of ≥30% and drug-likeness of ≥0.18 [10]. As *Hawthorn* was not included in the TCMSP database, we chose the bioinformatics analysis tool for molecular mechANism of traditional Chinese medicine (BATMAN-TCM) database with a cutoff score of ≥20 [11]. This was used as the criterion to screen the active ingredients of *Hawthorn* and their targets. Then, we searched for disease-related disease targets by entering the keywords "nonalcoholic fatty liver disease" in the online Mendelian inheritance in man (OMIM) (http://omim.org/) and GeneCards (https://www.genecards.org/) database to eliminate duplicate genes and identify disease targets.

2.2. Target Screening and Pathway Network Construction. The obtained formula targets were intersected with the screened disease targets to obtain the potential targets of action of the compound formula against NAFLD. A network of compounds, formulas, active ingredients, target-of-action, and diseases was constructed using Cytoscape 3.8.2 software.

2.3. Reagents. HFD (17.7% sucrose, 17.7% fructose, 19.4% protein, and 40% fat) was purchased from Beijing Huafukang Bioscience Co., Ltd. (Beijing, China), Aspartate aminotransferase (AST; cat. no. C010-2-1), alanine aminotransferase (ALT; cat. no. C009-2-1), triglyceride (TG; cat. no. A110-1-1), and total cholesterol (TC; cat. no. A111-1-1) test kits were purchased from Nanjing Jiancheng Bioengineering Institute (Nanjing, China). The oil red O staining kit (cat. no. G1261) was obtained from Solarbio Biotechnology Co., Ltd. (Beijing, China). Superoxide dismutase (SOD; cat. no. A001-3-1), methane dicarboxylic aldehyde (MDA; cat. no. A003-1-1), and glutathione peroxidase (GSH-Px; cat. no. A005-1) assay test kits were obtained from Nanjing Jiancheng Biological Engineering Institute (Nanjing, China). Rat IL-1β (cat. no. E02I0010), IL-6(cat. no. E02I0006), tumor necrosis factor alpha (TNF-α; cat. no. E02T0008), and enzyme-linked immunosorbent assay (ELISA) kit was obtained from Shanghai BlueGene Biotech Co., Ltd. (Shanghai, China). Rabbit anti-NFκB-p65 (cat. no. 51–0500), rabbit anti-phospho-NFκB-p65 (cat. no. 44–711G), rabbit anti-GSK3β (cat. no. 44–610), rabbit anti-Fas (cat. no. MA5-14882), rabbit anti-Leptin (cat. no. PA1-051), rabbit anti-CYP2E1 (cat. no. PA5-52652), rabbit anti-cytochrome C (cat. no. 45–6100), rabbit anti- SREBP1(cat. no. MA5-11685), rabbit anti-c-JUN (cat. no. MA5-15881), rabbit anti-c-JUN (cat. no. MA5-15881), rabbit anti-JNK (cat. no. 44–690G), and primary antibodies were purchased from Invitrogen (USA).

2.4. Preparation of JGXZ. JGXZ contained 20 g of *Radix Paeoniae Rubra*, 15 g of *Dendranthema morifolium*, 15 g of *Salvia miltiorrhiza Bunge*, 20 g of *Hawthorn*, 6 g of *Panax*

notoginseng, 15 g of *Rhizoma Alismatis*, 20 g of *Astragalus membranaceus*, 15 g of *Curcuma zedoaria*, 15 g of *Lotus leaf*, 10 g of *Vatica mangachapoi Blanco*, 12 g of *Curcuma longa*, and 6 g of *Glycyrrhiza uralensis Fisch*. These herbs were soaked in 500 mL of distilled water for 10 min and decocted for 30 min. The water extract of JGXZ was then filtered and concentrated to 4 g crude herb/mL.

2.5. Animals. Thirty specific-pathogen free 6–8-week-old male Sprague–Dawley rats, weighing 200 ± 20 g, were provided by Beijing Huafukang Biotechnology Co., Ltd (Production License No.: SCXK (Beijing) 2019–0008). The housing environment was maintained at 25 ± 2°C, 50 ± 15% relative humidity, and a 12 h light and dark cycle, with free access to water and food. During the domestication and study periods, all the animals had free access to food and water, and were kept on a 12 h light/dark cycle (21 ± 2°C and 45 ± 10% relative humidity). This study has been approved by the Ethics Committee of Animal Medicine and Animal Care of Nanjing University of traditional Chinese medicine.

2.6. Generation and Grouping of the NAFLD Rat Model. After 1 week of acclimatization, the NAFLD rat model was replicated according to a previously described method [12]. Thirty rats were randomly divided into control ($n = 10$), model ($n = 10$), and JGXZ groups ($n = 10$). The control group was given normal chow, and the other groups were given high-fat chow (4% cholesterol, 10% lard, 5% sugar, 0.5% sodium cholate, 0.2% propylthiouracil, and 80.3% basal feed), both for 12 weeks. During the 12-week model generation period along with the drug intervention, the control and model groups were given 2 mL/day saline via intragastric administration, and the JGXZ group was given 16 g of JGXZ/kg of body weight [13] via intragastric administration for 12 consecutive weeks. The body weight of the rats was recorded every 2 weeks during the experiment.

2.7. Biochemical Indicators and Liver Index Assay. After model generation and drug administration, all the rats were fasted for 24 h and anesthetized via intraperitoneal injection of 1% phenobarbital (10 mL/kg of body weight). Blood samples were collected from the abdominal aorta and centrifuged at 4°C at 3,000 rpm for 10 min, and the serum was separated. A kit was used to determine the levels of ALT, AST, TG, and TC in the rat serum. The liver index was calculated using the following formula: liver index (%) = liver weight (g)/body weight (g) × 100%.

2.8. Liver Histology. Immediately after rat model generation and drug administration, liver tissues from the same part of the left lobe of the liver was removed, cleaned, fixed in 10% formalin, and dehydrated for paraffin embedding. They were cut into 5 μm sections using a microtome, routinely stained with hematoxylin–eosin (H&E), transparently sealed, and observed under a light microscope to assess pathological changes in the liver.

2.9. Determination of Liver Oxidative Stress Parameters. One-hundred micrograms of liver tissue was added to 900 μL of saline, homogenized by ultrasonication, and centrifuged at low temperature for 15 min; the supernatant was collected. The levels of SOD, GSH-Px, and MDA in the tissue homogenate were determined using the BCA kit according to the kit instructions.

2.10. ELISA. The levels of the cytokines TNF-α, IL-1β, and IL-6 in the serum of each group of rats were determined using ELISA according to the kit instructions.

2.11. Western Blotting. Western blotting was performed to detect NF-κB P65 phosphorylation and the expressions of JNK1/2, SREBP1, leptin, Fas, cytochrome C, GSK3β, and CYP2E1 proteins in the liver tissues. Liver tissues were collected from each group, weighed at approximately 20 mg, added to 150 μL of RIPA protein lysis buffer, and centrifuged. The proteins were retained after centrifugation of the homogenate. The total protein concentration was determined using the BCA protein assay kit. An equal amount of protein (10 μg) was taken from each sample. The proteins were separated using SDS-PAGE electrophoresis, transferred to PVDF membranes, blocked with 5% skimmed milk for 2 h at room temperature, and incubated with rabbit anti-rat primary antibody P65 (1 : 1,000), p-P65 (1 : 1,000), JNK1/2 (1 : 2,000), SREBP1 (1 : 1,000), leptin (1 : 1,000), Fas (1 : 1,000), cytochrome C (1 : 2,000), GSK3β (1 : 1,000), CYP2E1 (1 : 1,000), and β-action (1 : 2,000) overnight at 4°C. After washing the membrane, the membrane was incubated with the secondary antibody (goat anti-rabbit IgG; 1 : 8,000) at room temperature for 2 h. After washing the membrane with Tris-buffered saline, enhanced chemiluminescence was added to develop and detect the bands with Image-Pro plus 6.0 software for quantitative analysis of the grayscale values [14].

2.12. Untargeted Metabolomics Assay. Untargeted metabolomics analysis was performed with 100 μL serum sample using liquid chromatography-mass spectrometry. The specific sample processing procedures, chromatographic and mass spectrometric conditions, data processing, and analysis were performed as described in our previous study [15].

2.13. Statistical Analysis. The experimental data were analyzed using SPSS 20.0 (IBM SPSS Statistics for Windows, Version 20.0; Armonk, NY, USA). Data were expressed as mean ± standard deviation. The t-test was performed for comparisons between groups, and one-way analysis of variance was performed for comparisons among multiple groups. Differences were considered statistically significant at $p < 0.05$.

3. Results

3.1. Therapeutic Effect of JGXZ on NAFLD Rats. Compared with that in the control group, the body weight of the rats in the model group was significantly increased

($p < 0.01$, Figure 1(a)); compared with that in the model group, the body weight of the rats in the JGXZ group was significantly reduced ($p < 0.01$, Figure 1(a)). Compared with that in the control group, the hepatic indicators significantly increased in the model group, and compared with that in the model group, the hepatic indicators in the JGXZ group decreased ($p < 0.01$, Figure 1(b)). As shown in Figure 1(c), the liver of the rats in the control group was structurally intact, with hepatocytes arranged neatly in a radial pattern; the morphology of hepatocytes around the portal area and central vein was clear and intact, and the nuclei were uniform in size and shape and located in the center of the hepatocytes. The liver of rats in the model group showed a significant extent of steatosis in the hepatocytes, the hepatocytes were distinctly swollen and rounded, the nuclei were squeezed to one side, the cytoplasm was filled with a large number of fat vacuoles, the lipid droplets were of different sizes and even fused into large droplets, and inflammatory cell infiltration was observed. Treatment in the JGXZ group significantly alleviated steatosis and inflammatory cell infiltration caused by the high-fat chow diet (Figure 1(c)). The results of oil red O staining (Figures 1(d) and 1(e)) indicated that no red lipid droplets appeared in hepatocytes in the control group, red lipid droplets appeared in hepatocytes in the model group, and the number of red lipid droplets in hepatocytes in the JGXZ group were significantly reduced. In addition, the activity of serum AST and ALT and the levels of TC and TG were significantly increased in the model group compared with those in the control group (all $p < 0.01$, Figure 1(f)). Compared with that in the model group, JGXZ significantly reduced the levels of AST, ALT, TC, and TG (all $p < 0.01$, Figure 1(f)).

3.2. Network Pharmacology Results

3.2.1. Active Ingredients and Targets of Action in the Compound Formula. Based on the TCMSP and BATMAN-TCM databases, there were 343 compounds in 12 Chinese herbs of the JGXZ formula (Figure 2(a)), including 66 in *Salvia miltiorrhiza Bunge*, 8 in *Panax notoginseng*, 4 in *Curcuma zedoaria*, 21 in *Astragalus membranaceus*, 14 in *Vatica mangachapoi Blanco*, 29 in *Radix Paeoniae Rubra*, 3 in *Curcuma longa*, 10 in *Rhizoma Alismatis*, 20 in *Dendranthema morifolium*, 15 in *Lotus leaf*, 96 in *Glycyrrhiza uralensis Fisch*, and 57 in *Hawthorn*. After removing the duplicate ingredients, a total of 32 compounds were obtained. The detailed results are shown in Supplementary Table S1. After pairwise comparison of the TCMSP and BATMAN-TCM databases, a total of 1186 active targets of JGXZ compounds were obtained, and 240 active targets of JGXZ compounds were obtained by uniport comparison and de-duplication. In addition, 1179 NAFLD targets were obtained from the OMIM and GeneCards databases, where the compound formula and disease were further intersected to obtain component targets (Figure 2(b)), which screened out a total of 156 active ingredients with potential anti-NAFLD activity in the formula, 176 targets in the compound formula, and 1,392 targets of disease, and 66 potential targets of anti-NAFLD activity in the formula were obtained after intersecting the two.

3.3. Network Analysis. Cytoscape 3.8.2 was used to construct a compound–formula–active-ingredient–target-of-action–disease network, and the core nodes were screened based on the network topological features (Figure 2(c)). We analyzed these targets against "NAFLD (map04932)" in the Kyoto Encyclopedia of Genes and Genomes database (Figure 2(d)) and found that JGXZ targets in the NAFLD pathway mainly included P65, JNK1/2, C-JUN, SREBP1, leptin, GSK3β, CYP2E1, Fas, and cytochrome C. These targets are mainly associated with oxidative stress, apoptosis, inflammation, lipid metabolism disorders, insulin resistance, and insulin resistance. We selected oxidative stress and apoptosis-related proteins Fas and cytochrome C, inflammation-related proteins P65 and JNK1/2, lipid metabolism disorder-related proteins SREBP1 and leptin, and insulin resistance-related proteins GSK3β and CYP2E1 for subsequent experimental validation.

3.4. Effects of JGXZ on Oxidative Stress and Apoptosis in the NAFLD Rat Model. We evaluated the effects of JGXZ on oxidative stress and apoptosis in NAFLD rats by measuring the activities of SOD and GSH-Px and levels of MDA, Fas, and cytochrome C in the liver tissues of the rats in each group. Compared with that in the control group, the SOD and GSH-Px activities in the liver of rats in the model group were significantly decreased ($p < 0.01$), and MDA levels were significantly increased ($p < 0.01$). JGXZ treatment significantly increased the SOD and GSH-Px activities and decreased the MDA level in the liver of NAFLD rats ($p < 0.01$ and $p < 0.05$, Figure 3(a)). Western blotting results showed that the levels of Fas and cytochrome C were elevated in the liver of rats in the model group compared with those in the control group ($p < 0.01$, Figure 3(b)) and were significantly decreased after JGXZ treatment compared with those in the model group ($p < 0.01$, Figure 3(b)). These results suggest that JGXZ inhibits oxidative stress and apoptosis in NAFLD by downregulating the protein expressions of Fas and cytochrome C in the liver tissues.

3.5. Effects of JGXZ on Inflammation in the NAFLD Rat Model. To investigate the effects of JGXZ on the inflammatory response in the liver tissues of NAFLD rats, we performed ELISA to determine the levels of the proinflammatory factors IL-6, IL-1β and TNF-α in the liver tissues. The levels of IL-6, IL-1β and TNF-α were significantly increased in the liver tissues of rats in the model group compared with those in the control group ($p < 0.01$), and JGXZ treatment significantly reduced the levels of IL-6, IL-1β, and TNF-α in the liver tissues of NAFLD rats compared with that in the model group ($p < 0.01$ and $p < 0.05$, Figure 3(c)). We performed western blotting to determine the levels of inflammation-related protein NF-κB p65 phosphorylation, JNK1/2, and C-JUN levels in the liver tissues. NF-κB p65 phosphorylation, JNK1/2, and C-JUN

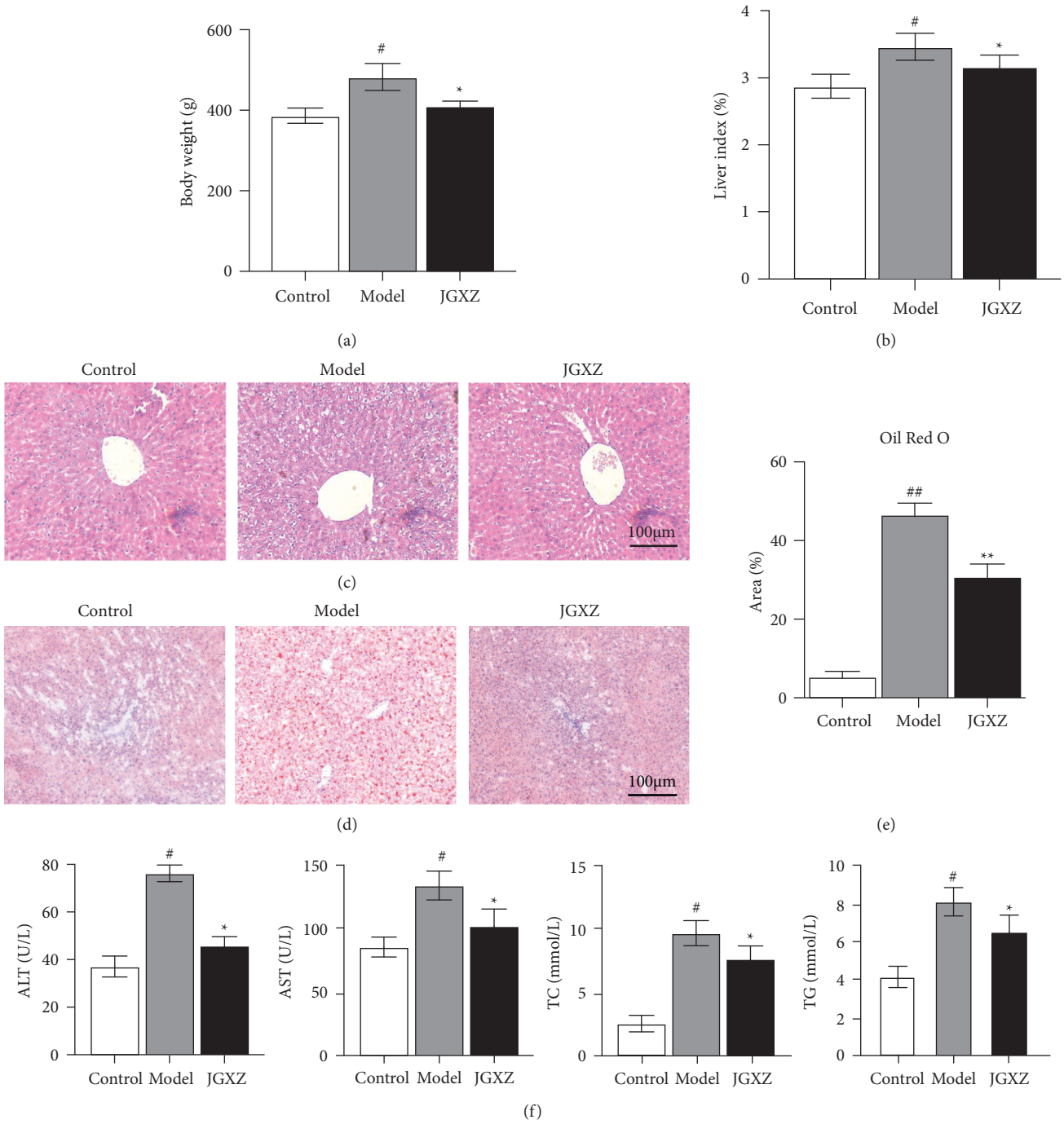

Figure 1: JGXZ treatment reduced body weight gain and improved liver steatosis in NAFLD model rats. (a) JGXZ treatment decreased the body weight in NAFLD model rats. (b) JGXZ treatment decreased the liver index in NAFLD model rats. (c) H&E staining indicated that JGXZ treatment ameliorated liver steatosis in NAFLD model rats (100 ×). (d, e) oil red O staining showed that after JGXZ treatment, the liver lipid content of NAFLD model rats decreased(100 ×). (f) JGXZ treatment decreased the levels of ALT, AST, TG, and TC in NAFLD model rat serum. Control, model, and JGXZ groups ($n = 10$ per group). Data are presented as the mean ± SD. #$p < 0.05$ compared to the control group. ##$p < 0.01$ compared to the control group. *$p < 0.05$ compared to the experimental model group.**$p < 0.01$ compared to the experimental model group.

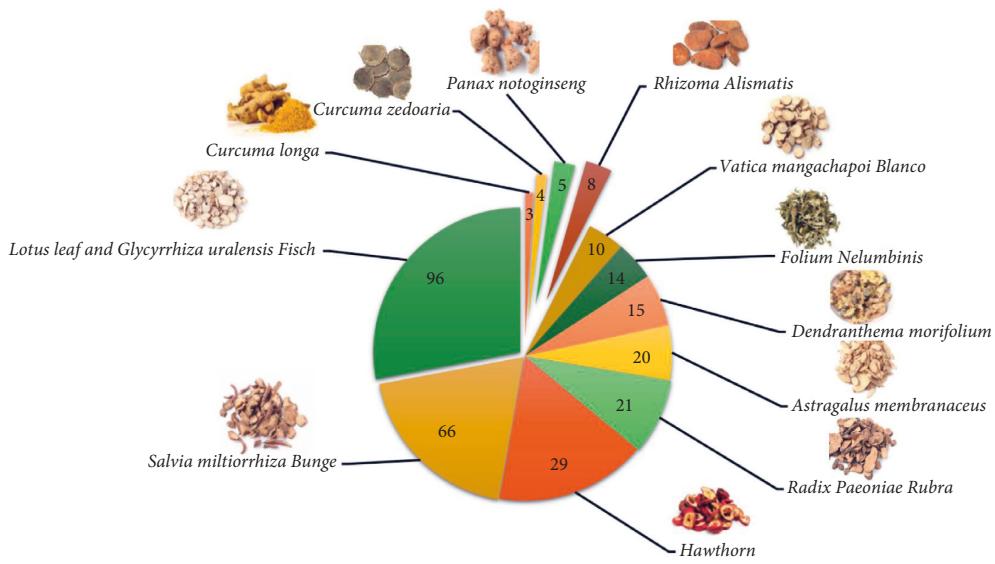

(a)

Potential targets of JGXZ on NAFLD

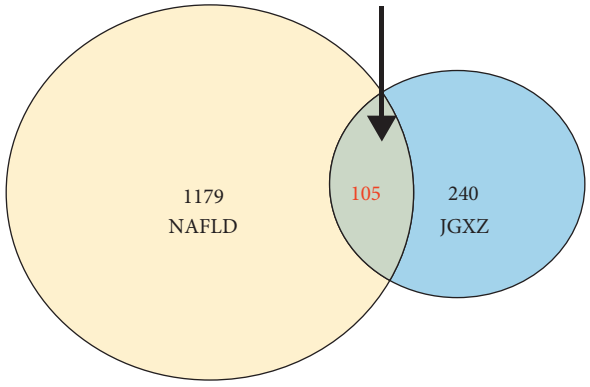

(b)

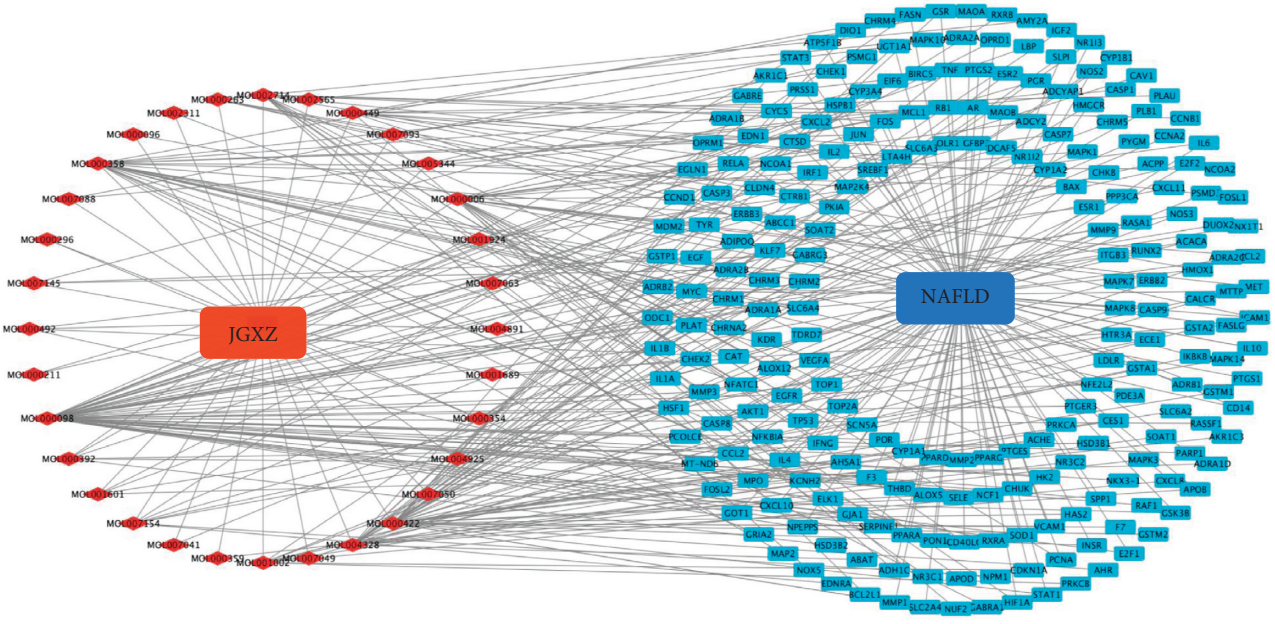

(c)

Figure 2: Continued.

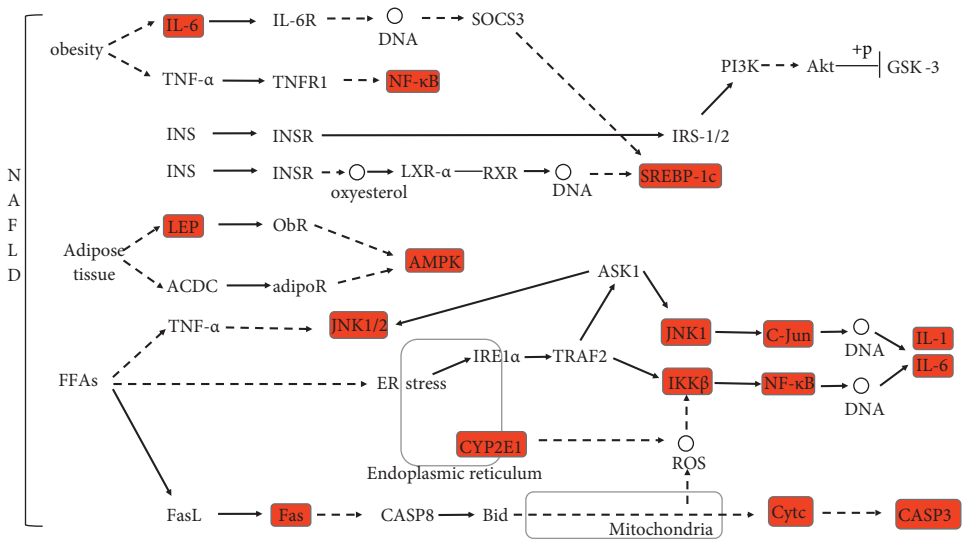

(d)

Figure 2: (a) The number of active ingredients of each herb in JGXZ obtained from TCMSP (OB ≥ 30%, DL ≥ 0.18) and BATMAN-TCM(score cutoff ≥20). (b) Veen diagram of compound targets of JGXZ and NAFLD-related targets. (c) Drug-component-disease-target network (Red diamond nodes represented the active ingredient in JGXZ and blue rectangle nodes represented the potential targets). (d) Overview of potential targets of JGXZ on NAFLD pathway (map04932) based on KEGG analysis (the potential targets are shown in red).

levels were elevated in the liver tissues of rats in the model group compared with that in the control group ($p < 0.01$, Figure 3(d)), which were significantly decreased after JGXZ treatment compared with that in the model group ($p < 0.01$, Figure 3(d)). These results indicate that JGXZ may alleviate the inflammatory response to NAFLD by downregulating NF-κB p65 phosphorylation, JNK1/2, and C-JUN levels in the liver tissues and reducing inflammatory cytokine levels.

3.6. Effects of JGXZ on Lipid Metabolism in the NAFLD Rat Model. Western blotting was performed to determine the levels of SREBP1 and leptin in the liver tissues. The results showed that the levels of related proteins were increased in the model group compared with those in the control group ($p < 0.01$, Figure 3(e)), and JGXZ treatment significantly reduced the levels of related proteins compared with those in the model group ($p < 0.01$, Figure 3(e)). These results suggest that JGXZ alleviates NAFLD insulin resistance by inhibiting SREBP1 and leptin activity.

3.7. Effects of JGXZ on Insulin Resistance in the NAFLD Rat Model. We calculated the homeostatic model assessment for the insulin resistance (HOMA-IR) index. The results showed that the fasting insulin (FINS) level and HOMA-IR index were significantly increased in the model group rats compared with those in the control group ($p < 0.05$), and JGXZ treatment significantly reduced the levels of FINS and HOMA-IR index in the model group ($p < 0.05$ and $p < 0.01$, respectively, Figure 3(f)). We performed western blotting to determine the levels of GSK3β and CYP2E1 in the liver tissues. The results showed that the model group had elevated levels of related proteins compared with those in the control group. Compared with those in the model group, the levels of related proteins were significantly reduced after JGXZ treatment ($p < 0.01$ and $p < 0.05$, Figure 3(g)). These results suggest that JGXZ alleviates NAFLD insulin resistance by inhibiting GSK3β and CYP2E1 activity.

3.8. Effects of JGXZ on Serum Metabolite Levels in the NAFLD Rat Model. Principle component analysis (PCA) plots showed that the control group was well distinguished from the model group and that the model group was well distinguished from the JGXZ group (Figures 4(a), 4(b)). An orthogonal partial least squares discriminant analysis (OPLS-DA) model was used for differential metabolite identification, and the explanatory rate (R^2) and predictive power (Q^2) of the model were evaluated by applying seven-round cross validation and 200 repetitions of RPT under the established OPLS-DA model. R^2 was 0.0, R0.221 and Q^2 was 0.0, −0.564 between the control and model groups(Figures 4(c) and 4(d)), and R^2 was 0.0, 0.313 and Q^2 was 0.0, −0.627 between the model and JGXZ groups (Figures 4(e), 4(f)).

Furthermore, differential metabolites ($p < 0.05$ and VIP >1) were identified based on our previous study [16], as shown in Table 1. Compared with the control group, the serum levels of L-proline, L-lysine, citrulline, L-tryptophan, L-isoleucine, L-valine, L-arginine, sphingosine-1-phosphate, L-leucine, glycocholic acid, uric acid, stearic acid, glyceryl phosphoryl ethanolamine, palmitic acid, TG (18 : 0/20 : 4 (5Z,8Z,11Z,14Z)/20 : 4 (5Z,8Z,11Z,14Z)), phosphatidylethanolamine, and glycerol. The contents of 12(R)-HETE and D-galactose were significantly increased; while the contents of acetylcholine, linoleic acid, eicosapentaenoic acid, alpha-linolenic acid, gluconic acid, choline, phosphatidylcholine, and L-threonine were significantly decreased. The contents

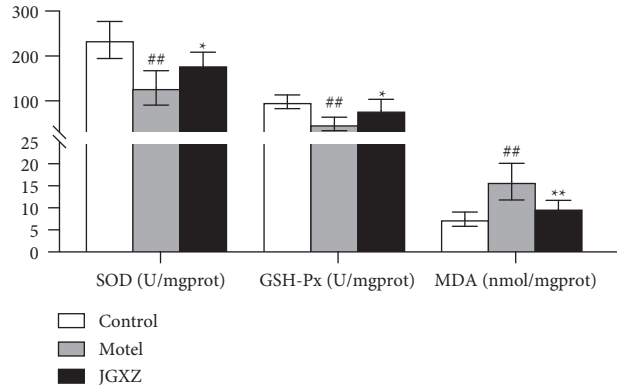

(a)

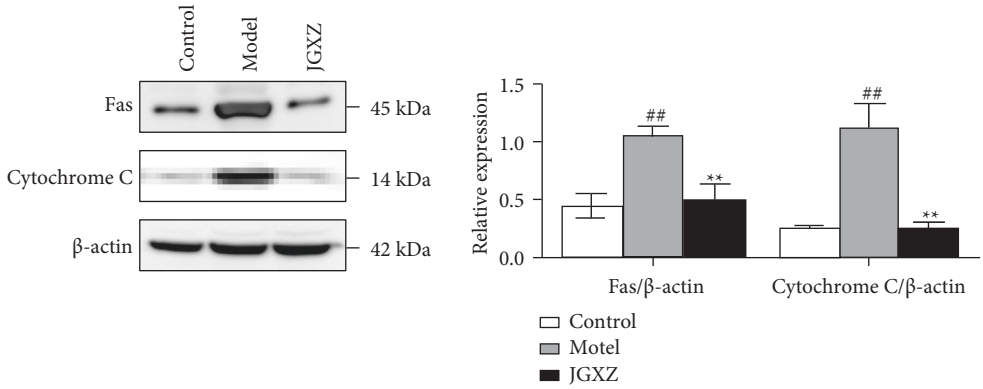

(b)

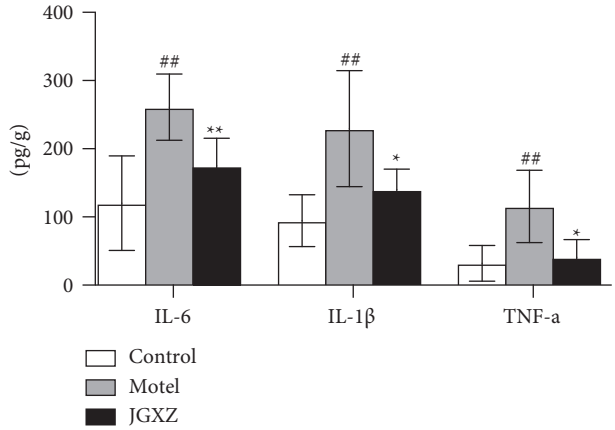

(c)

Figure 3: Continued.

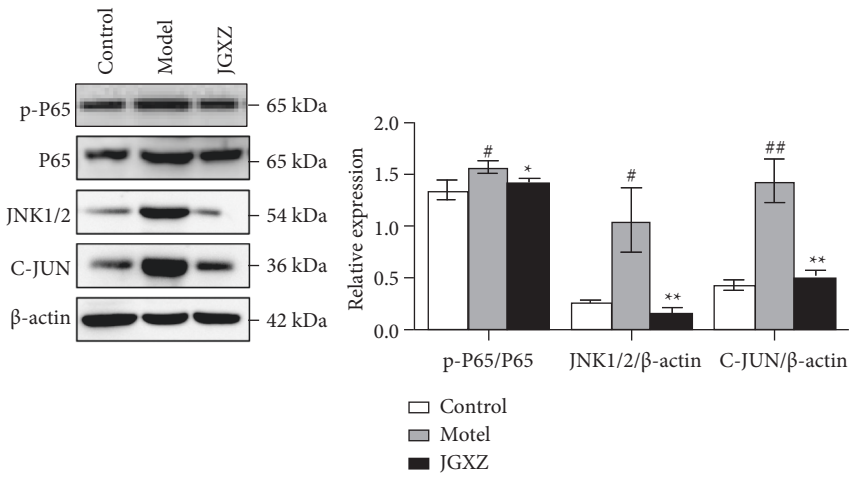

(d)

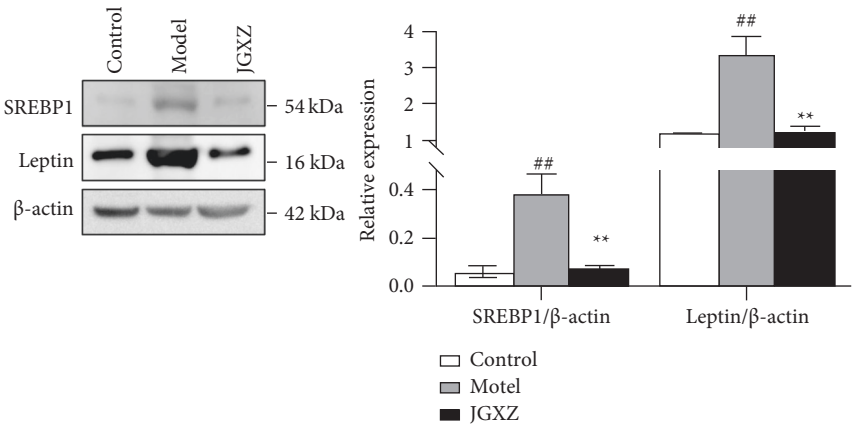

(e)

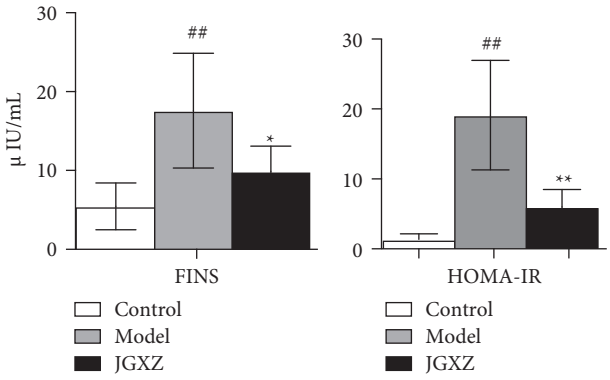

(f)

Figure 3: Continued.

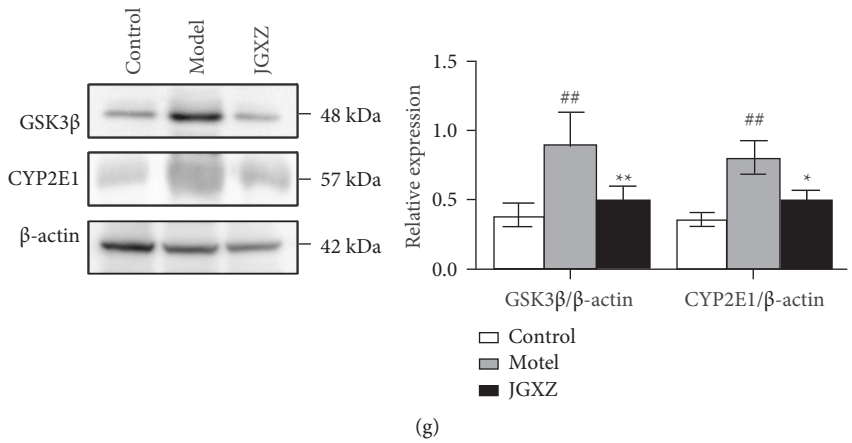

Figure 3: Experimental validation of network pharmacology analysis (a) JGXZ treatment increased the SOD and GSH-Px activities, and reduced the MDA level in the liver tissue homogenate. (b) JGXZ downregulated the protein expressions of Fas and Cytochrome C expression in the liver tissue. (c) JGXZ treatment decreased the levels of pro-inflammatory cytokines in the liver tissues. (d) JGXZ downregulated the protein expressions of NF-κB p65 phosphorylation, JNK1/2, and C-JUN in the liver tissue. (e) JGXZ downregulated the protein expressions of SERBP1 and Leptin in the liver tissue. (f) JGXZ treatment reduced the FINS level and HOMA-IR in NAFLD model rats. (g) JGXZ downregulated the protein expressions of GSK3β and CYP2E1 in the liver tissue.

of L-threonine, acetylcholine, linoleic acid, eicosapentaenoic acid, alpha-linolenic acid, gluconic acid, and choline in the rat serum were significantly increased, L-proline, L-lysine, citrulline, L-tryptophan, L-Iioleucine, *L* -valine, L-arginine, sphingosine-1-phosphate, L-leucine, glycocholic acid, uric acid, stearic acid, glyceryl phosphoryl ethanolamine, palmitic acid, TG(18 : 0/20 : 4(5Z,8Z,11Z,14Z)/20 : 4(5Z, 8Z, 11Z, 14Z)), phosphatidylethanolamine, glycerol, and 12 (R)-HETE, D-galactose were significantly decreased (Table 1).

Metabolite pathway enrichment analysis of differential metabolites in NAFLD model rats was conducted using Metabo Analyst website (Figures 4(g) and 4(h)). Differential metabolic pathways (Pathway impact >0.10, $p < 0.05$) were identified based on our previous study [16]and the differential metabolic pathways between the control group and the model group included linoleic acid, tryptophan metabolism, alpha-linolenic acid metabolism, arginine biosynthesis, glycerophospholipid metabolism, glycerolipid metabolism. The differential metabolic pathways between the model group and the JGXZ group include linoleic acid metabolism, tryptophan metabolism, alpha-linolenic acid metabolism, glycerophospholipid metabolism, galactose metabolism, arginine and proline metabolism. Among them, the pathways of linoleic acid metabolism, alpha-linolenic acid metabolism, tryptophan metabolism, and glycerophospholipid metabolism are the pathways shared by normal and model, model and JGXZ group. These pathways were selected as the metabolic pathways of JGXZ interfering with NAFLD and discussed.

4. Discussion

In this study, a high-fat chow diet was used to establish an NAFLD rat model. The TG, TC, ALT, and AST levels were significantly elevated in the liver tissues of rats in the model group. Pathological examination also showed significant steatosis and cellular damage in hepatocytes in the model group, suggesting the successful generation of the NAFLD model, in agreement with previous studies [15]. The JGXZ group had lower TG, TC, ALT, and AST levels after treatment and improved liver pathological alterations, which suggests that JGXZ has a therapeutic impact on NAFLD, which is consistent with our previous research findings.

Oxidative stress and apoptosis are important factors during the NAFLD development [17]. We found that JGXZ was able to increase the SOD and GSH-Px activities and decrease the MDA level in NAFLD rats, which suggested that JGXZ could attenuate oxidative stress and apoptotic responses in NAFLD rats. MDA is a product of lipid peroxidation caused by free radicals or reactive oxygen species (ROS) in cells under oxidative stress, and MDA levels indirectly reflect the degree of oxidative damage in cells [18]. SOD and GSH-Px are antioxidant enzymes that respond to antioxidant capacity [19]. SOD acts as an intracellular oxygen radical scavenger, catalyzing the formation of O_2^- from O_2 and H_2O_2, thereby protecting the organism from superoxide anions. GSH-Px catalyzes the conversion of reduced GSH to oxidized glutathione, protecting cells from disruption and damage caused by peroxide. The network pharmacology results identified Fas and cytochrome C, which are important proteins related to oxidative stress and apoptosis. Our results revealed that the levels of Fas and cytochrome C in NAFLD rats decreased by varying extents after JGXZ treatment. Fas acts as a protein receptor molecule on the cell surface. FasL is a ligand for Fas and can bind with Fas to initiate apoptotic signaling after stimulated by lipotoxicity factors [20]. Cytochrome C is an important protein that reflects cellular oxidative stress and apoptosis. Upon release into the cytoplasm, cytochrome C binds to apoptosis protease-activating factor-1, activates caspase-9 and triggers apoptosis [21].

The inflammatory response is an important pathological process in NAFLD, and the imbalance of inflammatory factors in NAFLD is an important pathological basis for

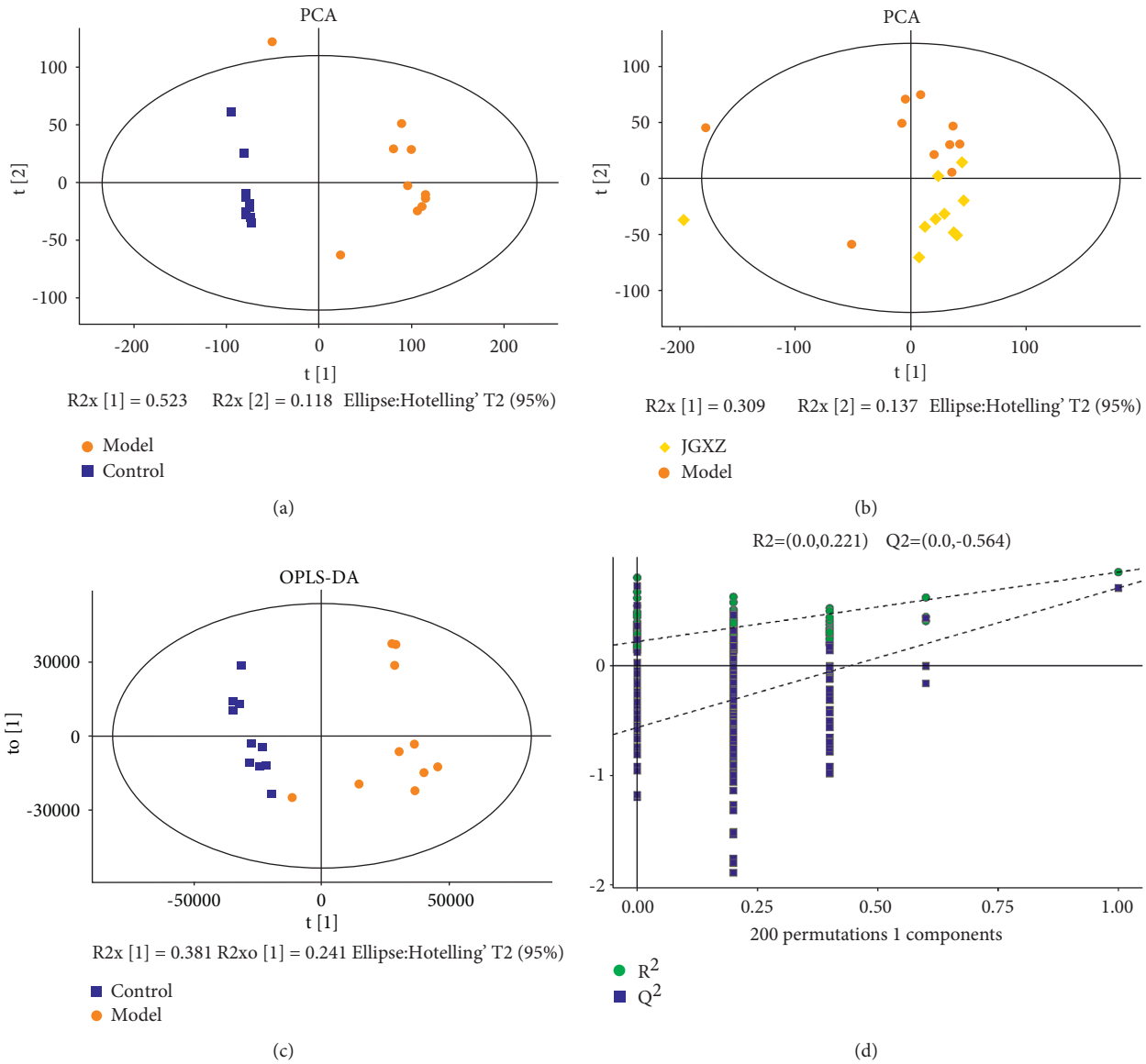

Figure 4: Continued.

hepatocyte damage during the progression of the disease [22]. Proinflammatory factors such as IL-6, IL-1β, and TNF-α exacerbate NAFLD hepatocyte damage in response to increased inflammation [23]. We found that JGXZ reduced the levels of IL-6, IL-1β, and TNF-α in NAFLD model rats. The results of network pharmacology revealed that the inflammation-related proteins P65 and JNK1/2 may be the targets of action of JGXZ. Further experimental validation revealed that JGXZ significantly reduced NF-κB p65 phosphorylation and JNK1/2 levels in the liver. P65 is an important subunit involved in NF-κB activation and is normally in a nonactivated state. Upon stimulation, NF-κB p65 phosphorylation degrades IκB, leading to the nuclear translocation of NF-κB, which in turn stimulates the release of inflammatory cytokines and exacerbates inflammatory damage. Jun N-terminal kinases (JNK) are members of the p38 mitogen-activated protein kinase family [9]. Phosphorylation of JNK regulates the activity of downstream products, which affects the activation of inflammatory cells and the release of inflammatory cytokines, e.g., TNF-α, IL-1β, and IL-6 [24]. A study found that inhibition of JNK activation improved the inflammatory response in a mouse model of inflammation and found that the release of inflammatory markers, such as IL-1β, TNF-α, and IL-6, was significantly reduced [25].

Disorders of lipid metabolism are one of the causes of the NAFLD development [26]. The results of network pharmacology revealed that SREBP1 and leptin, important regulatory proteins of lipid metabolism, may be the targets of action of the JGXZ formula, and further experimental validation confirmed that JGXZ can decrease SREBP1 and leptin levels. SREBP1 is an important transcriptional regulator that regulates lipid synthesis and exists as an inactive precursor in the endoplasmic reticulum after synthesis [27]. When the insulin signaling

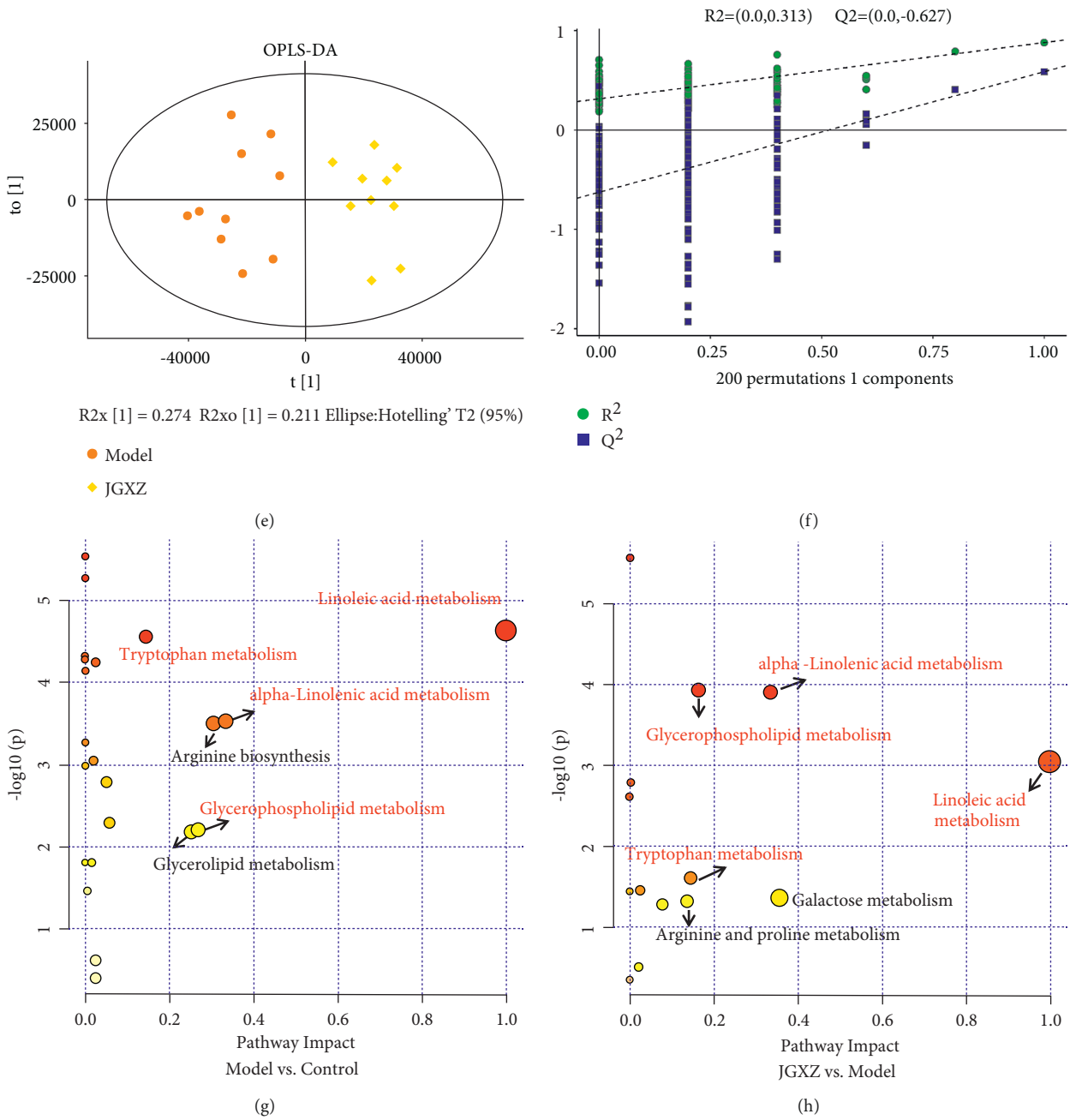

Figure 4: (a) PCA scores of control group and model group. (b) PCA scores of JGXZ group and model group. (c, d) OPLS-DA score and load coefficient diagram of control group and model group. (e, f) OPLS-DA score and load coefficient diagram of model group and JGXZ group. (g) Pathway analysis diagram of control group and model group. (h) Pathway analysis diagram of model group and JGXZ group. (a) linoleic acid metabolism; (b) tryptophan metabolism; (c) alpha-linolenic acid metabolism; (d) arginine biosynthesis; (e) glycerophospholipid metabolism; (f) glycerolipid metabolism; (g) galactose metabolism; (h) arginine and proline metabolism. The common pathways have been marked in red.

pathway is activated, SREBP1 can be transported from the endoplasmic reticulum to the golgi apparatus, where it is processed and cleaved by proteases. After maturation, N-SREBP1 enters the nucleus and induces the expression of genes related to lipid synthesis. Leptin exerts its biological effects through the mediation of specific receptors (Ob-R), which are class I cytokine receptors. Studies have shown that at least five subtypes of Ob-R (Ob-Ra, Ob-Rb, Ob-Rc, Ob-Rd, and Ob-Rf) are present in humans. In lipid metabolism, leptin regulates lipid metabolism by binding to Ob-Rb, activating Janus kinase signaling and signal transducer and activator of transcription pathways in both directions and affecting the secretion of various neuroendocrine hormones, such as neuropeptide [28].

Insulin resistance is closely related to the development of NAFLD. The imbalance between energy intake and

Table 1: The differential metabolites in the serum after JGXZ treatment.

m/z	Rt (min)	Formula	Metabolites	VIP		FC		Trend		Pathway
				M vs. C	J vs. M	M vs. C	J vs. M	M vs. C	J vs. M	
116.07	1.06	$C_5H_9NO_2$	L-Proline	2.43	1.07	4.47	0.49	$\uparrow^{\#\#}$	$\downarrow^{**}$	*h*
120.07	0.92	$C_4H_9NO_3$	L-Threonine	1.18	1.29	0.27	2.30	$\downarrow$	$\uparrow^{**}$	—
147.11	0.76	$C_6H_{14}N_2O_2$	L-Lysine	1.38	0.45	2.14	0.99	$\uparrow^{\#\#}$	$\downarrow$	—
146.12	1.05	$C_7H_{15}NO_2$	Acetylcholine	1.18	0.43	0.68	1.07	$\downarrow^{\#}$	$\uparrow$	*e*
198.08	0.96	$C_6H_{13}N_3O_3$	Citrulline	1.47	0.89	3.13	0.77	$\uparrow^{\#\#}$	$\downarrow$	*d*
203.08	5.77	$C_{11}H_{12}N_2O_2$	L-Tryptophan	1.52	2.02	2.62	0.59	$\uparrow^{\#\#}$	$\downarrow^{**}$	*b*
132.10	2.69	$C_6H_{13}NO_2$	L-Isoleucine	2.94	0.55	2.19	0.86	$\uparrow^{\#\#}$	$\downarrow$	—
118.09	1.43	$C_5H_{11}NO_2$	L-Valine	2.79	0.66	2.72	0.85	$\uparrow^{\#\#}$	$\downarrow$	—
281.25	0.71	$C_{18}H_{32}O_2$	Linoleic acid	1.28	1.02	0.76	2.05	$\downarrow^{\#\#}$	$\uparrow^{**}$	*a*
175.12	0.88	$C_6H_{14}N_4O_2$	L-Arginine	2.77	1.45	1.87	0.48	$\uparrow^{\#}$	$\downarrow^{**}$	*d*, *h*
380.25	9.54	$C_{18}H_{38}NO_5P$	Sphingosine-1-phosphate	2.17	1.60	1.97	0.51	$\uparrow^{\#\#}$	$\downarrow^{**}$	—
132.10	2.92	$C_6H_{13}NO_2$	L-Leucine	3.89	1.74	1.77	0.68	$\uparrow^{\#}$	$\downarrow$	—
301.22	10.42	$C_{20}H_{30}O_2$	Eicosapentaenoic acid	1.06	1.79	0.31	2.86	$\downarrow^{\#\#}$	$\uparrow^{**}$	—
464.30	8.80	$C_{26}H_{43}NO_6$	Glycocholic acid	1.73	1.78	2.31	0.25	$\uparrow^{\#}$	$\downarrow^{**}$	—
169.03	2.30	$C_5H_4N_4O_3$	Uric acid	2.37	0.09	3.31	0.90	$\uparrow^{\#\#}$	$\downarrow$	—
283.26	14.23	$C_{18}H_{36}O_2$	Stearic acid	2.30	2.07	1.72	0.61	$\uparrow^{\#}$	$\downarrow^{*}$	—
216.06	6.60	$C_5H_{14}NO_6P$	Glyceryl phosphoryl ethanolamine	1.22	1.96	2.58	0.49	$\uparrow^{\#}$	$\downarrow^{*}$	*e*
255.23	11.44	$C_{16}H_{32}O_2$	Palmitic acid	2.09	0.61	2.83	0.84	$\uparrow^{\#\#}$	$\downarrow$	—
277.22	10.50	$C_{18}H_{30}O_2$	Alpha-linolenic acid	1.60	1.98	0.44	2.11	$\downarrow^{\#\#}$	$\uparrow^{**}$	*c*
241.06	9.83	$C_6H_{12}O_7$	Gluconic acid	1.23	0.43	0.63	1.08	$\downarrow^{\#\#}$	$\uparrow$	—
948.80	0.84	$C_{61}H_{102}O_6$	TG(18 : 0/20 : 4(5Z,8Z,11Z,14Z)/20 : 4(5Z,8Z,11Z,14Z))	1.96	0.59	2.24	0.95	$\uparrow^{\#\#}$	$\downarrow$	*f*
104.11	10.17	$C_5H_{13}NO$	Choline	2.19	1.84	0.70	1.76	$\downarrow^{\#}$	$\uparrow^{**}$	*e*
766.48	10.58	$C_{45}H_{70}NO_8P$	Phosphatidylcholine	1.33	0.56	0.36	1.02	$\downarrow^{\#\#}$	$\uparrow$	*e*
738.55	9.33	$C_{42}H_{80}NO_8P$	Phosphatidylethanolamine	1.13	1.08	2.74	0.46	$\uparrow^{\#\#}$	$\downarrow^{**}$	*a*, *c*, *e*
115.04	1.06	$C_3H_8O_3$	Glycerol	0.25	0.04	2.79	0.98	$\uparrow^{\#\#}$	$\downarrow$	*f*
319.23	9.43	$C_{20}H_{32}O_3$	12(R)-HETE	0.68	1.90	2.44	0.56	$\uparrow^{\#\#}$	$\downarrow^{**}$	—
181.07	10.14	$C_6H_{12}O_6$	D-Galactose	0.16	1.14	1.30	0.71	$\uparrow^{\#\#}$	$\downarrow^{**}$	*g*

Control, model, and JGXZ ($n = 10$ per group) groups. $^{\#}p < 0.05$ as compared to the control group; $^{\#\#}p < 0.01$ as compared to the control group; $^{*}p < 0.05$ as compared to the model group; $^{**}p < 0.01$ as compared to the model group; ↑: content increased; ↓: content decreased; vs.: versus; C: control group; M:model group; J:JGXZ group; Rt: retention time; VIP: variable importance of projection; FC: fold change *a*: linoleic acid metabolism; *b*: tryptophan metabolism; *c*: alpha-linolenic acid metabolism; *d*: arginine biosynthesis; *e*: glycerophospholipid metabolism; *f*: glycerolipid metabolism; *g*: galactose metabolism; *h*: arginine and proline metabolism.

expenditure leads to insulin resistance in liver tissue, causing fat accumulation in the liver and exacerbating NAFLD [29]. The results of network pharmacology showed that the regulation of insulin-related proteins GSK3β and CYP2E1 was the target of action of JGXZ. JGXZ significantly reduced the protein levels of GSK3β and CYP2E1. GSK-3 is a protein kinase that includes two isoforms, GSK-3α, and GSK-3β. GSK-3β is a key enzyme in hepatic glucose metabolism, and under physiological conditions, insulin functions to promote glycogen synthesis by inactivating GSK-3β through phosphorylation in the insulin signaling pathway. In contrast, in the presence of insulin resistance in the body, insulin sensitivity decreases and dephosphorylated GSK-3β increases, resulting in reduced glycogen synthesis and increased blood glucose [30]. CYP2E1 is a key enzyme in liver diseases, and excessive activation of CYP2E1 increases the formation of "electron leakage" in mitochondria, leading to massive production of ROS, which induces oxidative stress injury when the production of ROS exceeds the capacity of the cellular antioxidant defense system [31]. Then, via oxidative alteration of important insulin downstream signaling pathways, it inhibits insulin signaling function and contributes to the development of insulin resistance [32].

4.1. Metabolomics Analysis. Serum untargeted metabolomics was employed to investigate the effects of JGXZ on metabolites in the serum of NAFLD rats. PCA and OPLS-DA analyses indicated that the serum metabolism of NAFLD mice showed significant changes and that the serum metabolism level of NAFLD mice could be significantly affected after JGXZ treatment. Further differential metabolite analysis showed that JGXZ could affect the levels of glyceryl phosphoryl ethanolamine, alpha-linolenic acid, phosphatidylethanolamine, choline, and 27 other metabolites. Metabolic pathway analysis of the differential metabolites using MetaboAnalyst showed that the linoleic acid metabolism, alpha-linolenic acid metabolism, tryptophan metabolism, and glycerophospholipid metabolism pathways changed in the control, model, and JGXZ groups, which suggests that the effects of the JGXZ in the treatment of NAFLD may work through these pathways.

4.2. Linoleic Acid Metabolism. JGXZ elevated the serum level of linoleic acid in NAFLD rats. Linoleic acid is the most abundant polyunsaturated fatty acid. As an essential nutrient, linoleic acid is mainly present in vegetable oils and has a variety of biological activities, which are important for metabolic disorders. G-protein coupled receptor120 (GPR120) is a specific receptor for long-chain polyunsaturated fatty acids in the body. Linoleic acid activates two downstream signaling pathways, Gaq and β-arrestin-2, by binding to GPR120, which plays a role in regulating lipid metabolism, increasing insulin sensitivity, and has anti-inflammatory effects [33]. Studies have shown that linoleic acid modifies the activity of lipoprotein lipase to regulate lipid metabolism homeostasis. Lipoprotein lipase degrades TG to glycerol and free fatty acids, which is a key enzyme in lipid metabolism [34]. Its main derivative, conjugated linoleic acid, improves high-fat diet-induced hepatic lipid accumulation by increasing hepatic TAG secretion rate (TAG-SR) and β-oxidation as well as reducing hepatic fatty acid uptake [35]. In a mouse model of lipopolysaccharide (LPS) induced acute inflammation, regulation of linoleic acid metabolism by promoting FADS1/FASDS2/ELOV2 expression and decreasing PLA2 expression ameliorated LPS-induced acute inflammation and multiorgan injury [36]. The regulation of JGXZ in lipid metabolism disorders and its anti-inflammatory effects may be related to linoleic acid metabolism.

4.3. Alpha-Linolenic Acid Metabolism. JGXZ elevated the serum alpha-linolenic acid level in NAFLD rats. Alpha-linolenic acid is a plant-derived n-3 polyunsaturated fatty acid that has important roles in reducing TG levels, increasing fatty acid catabolism, and inhibiting inflammation. Alpha-linolenic acid increases mitochondrial activity and reduces intracellular oxidative stress. Alpha-linolenic acid ester of plant sterols (PS-ALA) is a derivative of alpha-linolenic acid that improves mitochondrial function and oxidative stress and exerts a protective effect against NAFLD [37]. *In vivo* experiments showed that alpha-linolenic acid was effective in alleviating endoplasmic reticulum stress and improving mitochondrial function, thereby improving NAFLD [38]. The alleviation of oxidative stress by the JGXZ formula may be related to alpha-linolenic acid metabolism.

4.4. Tryptophan Metabolism. JGXZ significantly reduced the serum L-tryptophan level in NAFLD rats. Tryptophan is one of the 20 common amino acids and an essential amino acid that is metabolized in humans mainly through the kynurenine metabolic pathway [39]. Tryptophan and its metabolites were found to have significant anti-inflammatory and antioxidant effects [40]. In animal liver, tryptophan is involved in protein synthesis, especially when there is an acute inflammatory response in the liver. Increased protein synthesis leads to an increased demand for tryptophan, which leads to a decrease in plasma levels of tryptophan. The alleviation of inflammation and oxidative stress may be potentially associated with tryptophan metabolism.

4.5. Glycerophospholipid Metabolism. JGXZ elevated the serum acetylcholine (ACh) levels in glycerophospholipid metabolism in NAFLD rats. Glycerophospholipids are the most abundant phospholipids in the organism and are the main components of biological membranes, participating in various biological processes, such as membrane fusion, endocytosis, and membrane transport [41]. ACh is the transmitter of the cholinergic nervous system, and the ACh receptor binds to ACh. ACh receptors are categorized into muscarinic ACh receptors (M receptors) and nicotinic ACh receptors (N receptors) according to their receptor structure and response to drug treatment. ACh has been suggested to play an important role in regulating the inflammatory response. The inflammatory stimulus signal is transmitted to the brain via the vagus nerve. After sophisticated integration by the central nervous system, ACh is released from the efferent vagal nerve terminals, and cholinergic receptors bind to and activate the transmitter, further reducing the production and release of various inflammatory cytokines and regulating the local and systemic inflammatory response of the body. Thus, JGXZ can regulate ACh levels and improve the inflammatory response in NAFLD through the glycerophospholipid metabolism pathway.

In conclusion, this study found that JGXZ has an ameliorative effect on NAFLD, and JGXZ alleviates the inflammatory response and oxidative stress and lipid metabolism disorders in NAFLD rats. The mechanism of action of JGXZ in the treatment of NAFLD may be related to the regulation of linoleic acid metabolism, tryptophan metabolism, alpha-linolenic acid metabolism, and glycerophospholipid metabolism.

Control, model, and JGXZ ($n = 10$ per group) groups. Data are presented as the mean ± SD. $^{\#}p < 0.05$ as compared to the control group; $^{\#\#}p < 0.01$ as compared to the control group; $^{*}p < 0.05$ as compared to the model group; $^{**}p < 0.01$ as compared to the model group.

5. Conclusion

This study found that JGXZ has an ameliorative effect on NAFLD, and JGXZ alleviates the inflammatory response and oxidative stress and lipid metabolism disorders in NAFLD rats. The mechanism of action of JGXZ in the treatment of NAFLD may be related to the regulation of linoleic acid metabolism, tryptophan metabolism, alpha-linolenic acid metabolism, and glycerophospholipid metabolism.

Data Availability

The raw data supporting the conclusions of this article will be made available by the corresponding authors, without undue reservation.

Conflicts of Interest

The authors declare that they have no conflicts of interest.

Authors' Contributions

Yong-Jun Cao and Han-Zhou Li are co-first authors on this work.

Acknowledgments

This work was supported by the Young Scientists Fund of the National Natural Science Foundation of China (Grant No. 82104802), the Scientific Research Program of the Jiangsu Province Administration of Traditional Chinese Medicine (Grant No. YB2020065), and the Yunnan Province Major Science and Technology Special Project (Grant No. 2019ZF005) .

Supplementary Materials

Information of active ingredients in JGXZ (Table S1). (*Supplementary Materials*)

References

[1] S. H. Gerges, S. A. Wahdan, D. A. Elsherbiny, and E. El-Demerdash, "Non-alcoholic fatty liver disease: an overview of risk factors, pathophysiological mechanisms, diagnostic procedures, and therapeutic interventions," *Life Sciences*, vol. 271, Article ID 119220, 2021.

[2] E. E. Powell, V. W. Wong, and M. Rinella, "Non-alcoholic fatty liver disease," *The Lancet*, vol. 397, 2021.

[3] A. Mantovani, E. Scorletti, A. Mosca, A. Alisi, C. D. Byrne, and G. Targher, "Complications, morbidity and mortality of nonalcoholic fatty liver disease," *Metabolism*, vol. 111, Article ID 154170, 2020.

[4] Z. Zhou, B. Chen, S. Chen et al., "Applications of network pharmacology in traditional Chinese medicine research," *Evidence-Based Complementary and Alternative Medicine*, vol. 2020, Article ID 1646905, 7 pages, 2020.

[5] C. H. Johnson, J. Ivanisevic, and G. Siuzdak, "Metabolomics: beyond biomarkers and towards mechanisms," *Nature Reviews Molecular Cell Biology*, vol. 17, no. 7, pp. 451–459, 2016.

[6] T. He, M. Wang, J. Kong et al., "Integrating network pharmacology and non-targeted metabolomics to explore the common mechanism of coptis categorized formula improving T2DM zebrafish," *Journal of Ethnopharmacology*, vol. 284, Article ID 114784, 2022.

[7] X. Liu, F. Wei, H. Liu, S. Zhao, G. Du, and X. Qin, "Integrating hippocampal metabolomics and network pharmacology deciphers the antidepressant mechanisms of xiaoyaosan," *Journal of Ethnopharmacology*, vol. 268, Article ID 113549, 2021.

[8] W. Weibo, J. Mengxue, and F. Fang, "Clinical research of jiangan xiaozhi granule in treating nonalcoholic fatty liver disease of type of qi stagnancy and blood stasis," *China Medical Herald*, vol. 11, no. 27, pp. 78–82, 2014.

[9] X. H. Xie, J. B. Liao, F. Fang et al., "Jian-Gan-Xiao-Zhi decoction ameliorates high-fat high-carbohydrate diet-induced non-alcoholic fatty liver disease and insulin resistance by regulating the AMPK/JNK pathway," *Traditional Medicine Research*, vol. 6, 2021.

[10] J. Ru, P. Li, J. Wang et al., "TCMSP: a database of systems pharmacology for drug discovery from herbal medicines," *Journal of Cheminformatics*, vol. 6, 2014.

[11] Z. Liu, F. Guo, Y. Wang et al., "BATMAN-TCM: a Bioinformatics analysis Tool for molecular mechANism of traditional Chinese medicine," *Scientific Reports*, vol. 6, no. 1, Article ID 21146, 2016.

[12] Y. T. Li, H. T. Cui, L. Yang et al., "Hua-Zhuo-Kai-Yu decoction inhibits apoptosis in nonalcoholic fatty liver disease," *Traditional Medicine Research*, vol. 1, 2020.

[13] J. Liao, X. Xie, J. Gao et al., "Jian-Gan-Xiao-Zhi decoction alleviates inflammatory response in nonalcoholic fatty liver disease model rats through modulating gut microbiota," *Evidence-Based Complementary and Alternative Medicine*, vol. 2021, Article ID 5522755, 13 pages, 2021.

[14] Z. Y. Chen, Q. Lan, S. Chen et al., "Effects of Dendrobium candidum polysaccharides on microRNA-125b and mitogen-activated protein kinase signaling pathways in diabetic cataract rats," *Traditional Medicine Research*, vol. 6, no. 5, p. 45, 2021.

[15] H. Cui, Y. Li, Y. Wang et al., "Da-chai-hu decoction ameliorates high fat diet-induced nonalcoholic fatty liver disease through remodeling the gut microbiota and modulating the serum metabolism," *Frontiers in Pharmacology*, vol. 11, Article ID 584090, 2020.

[16] H. Cui, Y. Li, M. Cao et al., "Untargeted metabolomic analysis of the effects and mechanism of nuciferine treatment on rats with nonalcoholic fatty liver disease," *Frontiers in Pharmacology*, vol. 11, p. 858, 2020.

[17] Z. Chen, R. Tian, Z. She, J. Cai, and H. Li, "Role of oxidative stress in the pathogenesis of nonalcoholic fatty liver disease," *Free Radical Biology and Medicine*, vol. 152, 2020.

[18] D. Tsikas, "Assessment of lipid peroxidation by measuring malondialdehyde (MDA) and relatives in biological samples: analytical and biological challenges," *Analytical Biochemistry*, vol. 524, 2017.

[19] M. Wang, X. Zhang, W. Jia et al., "Circulating glutathione peroxidase and superoxide dismutase levels in patients with epilepsy: a meta-analysis," *Seizure*, vol. 91, 2021.

[20] S. Malarkannan, "Molecular mechanisms of FasL-mediated "reverse-signaling"," *Molecular Immunology*, vol. 127, 2020.

[21] R. Santucci, F. Sinibaldi, P. Cozza, F. Polticelli, and L. Fiorucci, "Cytochrome c: an extreme multifunctional protein with a key role in cell fate," *International Journal of Biological Macromolecules*, vol. 136, 2019.

[22] L. Yang, J. B. Liao, and A. Q. Liu, "Advances in traditional Chinese medicine for liver disease therapy in 2020," *Traditional Medicine Research*, vol. 6, no. 3, p. 30, 2021.

[23] Q. Hu, W. Zhang, Z. Wu et al., "Baicalin and the liver-gut system: pharmacological bases explaining its therapeutic effects," *Pharmacological Research*, vol. 165, Article ID 105444, 2021.

[24] M. B. Hammouda, A. E. Ford, Y. Liu, and J. Y. Zhang, "The JNK signaling pathway in inflammatory skin disorders and cancer," *Cells*, vol. 9, no. 4, p. 857, 2020.

[25] J. L. Wang, C. H. Ren, J. Feng, C. H. Ou, and L. Liu, "Oleanolic acid inhibits mouse spinal cord injury through suppressing inflammation and apoptosis via the blockage of p38 and JNK MAPKs," *Biomedicine & Pharmacotherapy*, vol. 123, Article ID 109752, 2020.

[26] K. Pei, T. Gui, D. Kan et al., "An overview of lipid metabolism and nonalcoholic fatty liver disease," *BioMed Research International*, vol. 2020, Article ID 4020249, 12 pages, 2020.

[27] J. Han, E. Li, L. Chen et al., "The CREB coactivator CRTC2 controls hepatic lipid metabolism by regulating SREBP1," *Nature*, vol. 524, 2015.

[28] S. Pereira, D. L. Cline, M. M. Glavas, S. D. Covey, and T. J. Kieffer, "Tissue-specific effects of leptin on glucose and lipid metabolism," *Endocrine Reviews*, vol. 42, 2021.

[29] Y. Sakurai, N. Kubota, T. Yamauchi, and T. Kadowaki, "Role of insulin resistance in MAFLD," *International Journal of Molecular Sciences*, vol. 22, 2021.

[30] Y. Zhang, N. Q. Huang, F. Yan et al., "Diabetes mellitus and Alzheimer's disease: GSK-3β as a potential link," *Behavioural Brain Research*, vol. 339, pp. 57–65, 2018.

[31] R. Harjumäki, C. S. Pridgeon, and M. Ingelman-Sundberg, "CYP2E1 in alcoholic and non-alcoholic liver injury. Roles of ROS, reactive intermediates and lipid overload," *International Journal of Molecular Sciences*, vol. 22, no. 15, 2021.

[32] G. H. Lee, K. J. Oh, H. R. Kim et al., "Effect of BI-1 on insulin resistance through regulation of CYP2E1," *Scientific Reports*, vol. 6, Article ID 32229, 2016.

[33] H. Karakuła-Juchnowicz, J. Róg, D. Juchnowicz, and J. Morylowska-Topolska, "GPR120: mechanism of action, role and potential for medical applications," *Postępy Higieny I Medycyny Doświadczalnej*, vol. 71, 2017.

[34] H. C. Lee, S. C. Yu, Y. C. Lo, I. H. Lin, T. H. Tung, and S. Y. Huang, "A high linoleic acid diet exacerbates metabolic responses and gut microbiota dysbiosis in obese rats with diabetes mellitus," *Food & Function*, vol. 10, no. 2, pp. 786–798, 2019.

[35] K. S. Ibrahim and E. M. El-Sayed, "Dietary conjugated linoleic acid and medium-chain triglycerides for obesity management," *Journal of Biosciences*, vol. 46, no. 1, 2021.

[36] Y. J. Liu, H. Li, Y. Tian et al., "PCTR1 ameliorates lipopolysaccharide-induced acute inflammation and multiple organ damage via regulation of linoleic acid metabolism by promoting FADS1/FASDS2/ELOV2 expression and reducing PLA2 expression," *Laboratory Investigation*, vol. 100, no. 7, 2020.

[37] H. Han, X. Li, Y. Guo, M. Zheng, T. Xue, and L. Wang, "Plant sterol ester of α-linolenic acid ameliorates high-fat diet-induced nonalcoholic fatty liver disease in mice: association with regulating mitochondrial dysfunction and oxidative stress via activating AMPK signaling," *Food & Function*, vol. 12, no. 5, 2021.

[38] H. Han, Y. Guo, X. Li et al., "Plant sterol ester of α-linolenic acid attenuates nonalcoholic fatty liver disease by rescuing the adaption to endoplasmic reticulum stress and enhancing mitochondrial biogenesis," *Oxidative Medicine and Cellular Longevity*, vol. 2019, Article ID 8294141, 14 pages, 2019.

[39] M. Platten, E. A. A. Nollen, U. F. Röhrig, F. Fallarino, and C. A. Opitz, "Tryptophan metabolism as a common therapeutic target in cancer, neurodegeneration and beyond," *Nature Reviews Drug Discovery*, vol. 18, no. 5, 2019.

[40] A. Fiore and P. J. Murray, "Tryptophan and indole metabolism in immune regulation," *Current Opinion in Immunology*, vol. 70, 2021.

[41] S. Wang, K. Tang, Y. Lu et al., "Revealing the role of glycerophospholipid metabolism in asthma through plasma lipidomics," *Clinica Chimica Acta*, vol. 513, pp. 34–42, 2021.

Hindawi
Evidence-Based Complementary and Alternative Medicine
Volume 2022, Article ID 1745244, 11 pages
https://doi.org/10.1155/2022/1745244

Research Article

Protective Mechanism of *Nostoc sphaeroides* Kütz. Polysaccharide on Liver Fibrosis by HFD-Induced Liver Fat Synthesis and Oxidative Stress

Litao Yang and Bo Zhang

Beijing Key Laboratory of Bioactive Substances and Functional Foods, Beijing Union University College of Biochemical Engineering, Beijing, China

Correspondence should be addressed to Bo Zhang; zhangbo_wl@buu.edu.cn

Received 27 March 2022; Revised 21 May 2022; Accepted 14 June 2022; Published 5 July 2022

Academic Editor: Chih-Yuan Ko

Nostoc sphaeroides Kütz. polysaccharide (NSKP) is one of the main components of *Nostoc sphaeroides* Kütz. and is often used as health food. We investigated whether NSKP interferes with the progression of liver fibrosis. Male mice were randomly divided into 4 groups: control (C), high-fat diet (M), high-fat diet + 0.4 g/kg NSKP (L), and high-fat diet + 0.8 g/kg NSKP (H). C was fed standard diet, M was fed high-fat diet, and L and H were fed high-fat diet in addition to gavage of 0.4 g/kg or 0.8 g/kg NSKP, respectively, for 22 weeks. At the end of the experiment, the serum and liver oxidative stress, fat accumulation, and fibrosis indexes were detected. The histopathology of liver was also observed. The results showed that the rice of NSKP, compared with M, improved blood lipid level, liver total cholesterol (TC), triglyceride (TG), and liver antioxidant capacity and effectively interfered with liver fibrosis related indicators. So it is interesting to note that NSKP appeared to be effective in liver injury; further experiments are necessary to clarify the exact mechanisms involved.

1. Introduction

The excessive intake of high-fat and high-calorie foods increases the prevalence of hyperlipidemia, obesity, nonalcoholic fatty liver, type 2 diabetes, hypertension, coronary heart disease, and atherosclerotic disease [1, 2]. As an important organ of the human body, the liver plays an important role in metabolism, excretion, immunity, detoxification, and so on. Hyperlipidemia caused by dyslipidemia is an independent risk factor for chronic liver injury [3]. Chronic liver injury can initiate a vicious circle of hepatocyte apoptosis and death, inflammation, oxidative stress injury, and fibrosis and eventually lead to liver cirrhosis or hepatocellular carcinoma [4–6]. The early stage of lipid metabolic disorder caused by high-fat diet is mainly characterized by abnormal accumulation of fat; with continuous accumulation of fat, it may lead to oxidative damage of hepatocytes, lipid peroxidation, endoplasmic reticulum stress, mitochondrial dysfunction, hepatocyte apoptosis, or liver inflammation, thus leading to liver fibrosis to the degree of liver cirrhosis [7].

Hyperlipidemia is an important factor in liver fibrosis [8]. In addition, defects of ApoE genes lead to excessive production of potential lipids and lipoproteins, which disrupt lipid metabolism in the body and easily lead to hyperlipidemia and obesity [9]. Therefore, $ApoE^{-/-}$ mice are often used to study lipid metabolism disorders and diseases caused by lipid metabolism disorders in various organs such as liver, kidney, artery, and brain nerves [10, 11]. Liver is the main site of lipid metabolism, and there is a close relationship between its injury and $ApoE^{-/-}$ [12]. The occurrence of liver fibrosis is mainly due to the transformation of hepatic stellate cells to hepatic myofibroblasts, the proliferation of myofibroblasts, and the imbalance between the deposition and decomposition of extracellular matrix [13]. In the liver, hepatic stellate cells (HSC) are the main source

of myofibroblasts that produce extracellular matrix; its main components are fibronectin (*FN*), collagen I (*Col-I*), and so on. Long-term liver injury will not only induce the transformation of hepatic stellate cells, but also cause a large amount of proliferation of transformed myofibroblasts [14, 15], and myofibroblasts are the main cells secreting extracellular matrix [16]. As one of the common symptoms of liver injury, hyperlipidemia can cause abnormal fat synthesis in the liver. A large amount of fat deposition in the liver can induce oxidative damage to hepatocytes, which triggers the secretion of transforming growth factor-β, a key factor for fibrosis, leading to the activation of hepatic stellate cells, characterized by the emergence of a large number of myofibroblasts expressing α-smooth muscle actin (α-*SMA*) [17, 18]. Some studies have shown that the emergence of a large number of myofibroblasts causes the deposition of extracellular matrix and leads to liver fibrosis [19].

Nostoc sphaeroides Kütz. is a kind of lower unicellular cyanobacteria belonging to Cyanophyta, Cyanophyceae, Hormogonales, Nostocaceae, and *Nostoc*. It is commonly known as Nostoc sphaeroids or water fungus [20]. It is a kind of functional food for reducing fat, with anti-inflammation, anti-oxidation, and anti-atherosclerosis functions. It can be planted artificially, and it is a kind of economic cyanobacteria with high edible value [21, 22] and is rich in proteins, amino acids, fatty acids, vitamins, and other nutrients, of which the most important components are proteins and polysaccharides. Polysaccharides are important substances in *Nostoc sphaeroides* Kütz. [23]. A lot of studies have shown that plant polysaccharide extracts can protect the liver by improving the levels of lipids in serum and liver or anti-oxidation in the liver in animals with a high-fat diet [24]. Tang et al. have shown that the isolated polysaccharides from *Pueraria lobata* have the effect of scavenging free radicals [25]. Li Haifeng and others proved that NSKP has the function of anti-oxidation by using the *Caenorhabditis elegans* model [26]. Therefore, it is of great significance to study NSKP as a dietary supplement in the intervention of chronic diseases.

The main purpose of this study is to explore whether NSKP can interfere with liver fibrosis caused by long-term high-fat diet with improving oxidative stress caused by fat deposition in the liver of high-fat mice.

2. Materials and Methods

2.1. Materials. NSKP sample purity is 96.95% (provided by Hunan Yandi Bioengineering Co., Ltd., Hunan, China). The preparation method was as follows: 500 times the volume of distilled water was added to Kudzu rice powder that had been dried and crushed, extracted at 100°C for 2 hours, and then centrifuged at 9000 r/min for 15 min, and the supernatant was collected. After 10-time concentration, the supernatant was precipitated overnight in 40% (v/v) ethanol at 4°C and centrifuged at 9000 r/min for 15 min, and the supernatant and precipitate were collected and washed four times with 45% (v/v) ethanol. The precipitate was dissolved in distilled water and precipitated again in 40% (v/v) ethanol overnight at 4°C. After centrifugation at 9000 r/min for 15 min, the precipitate was collected, washed twice with 45% (v/v) ethanol, freeze-dried, and crushed into NSKP powder [23].

Assay kits used to measure total cholesterol (TC), triglyceride (TG), aspartate transaminase (AST), alanine transaminase (ALT), superoxide dismutase (SOD), glutathione (GSH), and malondialdehyde (MDA) were purchased from Nanjing Jiancheng Bioengineering Institute (Nanjing, China). Antibodies *GAPDH* (No. G3206-1OD), anti-transforming growth factor-beta 1 (*TGF-β1*, No. GB111876), *α-SMA* (No. GB13044), and anti-fibronectin (*FN*, No. GB11091); Sirius red staining kit; H&E staining kit; and oil red O staining kit were all provided by Wuhan Servicebio Co., Ltd. (Wuhan, China).

2.2. Animals and Experiment. The Animal Research Committee of Beijing Union University approved this study (license number: 201913). Eight-week-old male ApoE$^{-/-}$ mice were purchased from Beijing Charles River Experimental Animal Technology Co., Ltd. (Beijing, SCXK (Jing) 2016–0006). The mice were placed in the SPF animal room of Beijing Union University and were freely provided with feed and drinking water in a 12-hour light-dark cycle at a constant temperature of 22°C ± 2°C.

After 40 ApoE$^{-/-}$ mice were fed adaptively for one week with standard diet (SD), the mice were divided into 4 groups with 10 mice in each group. They were control group (C), high-fat diet (HFD) group (M), HFD + 0.4 g/kg BW group (L), and HFD + 0.8 g/kg BW group (H). During the 22-week study, the C was fed the SD, the M was fed the HFD, the L and H were fed HFD and given 0.4 g/kg BW or 0.8 g/kg BW NSKP, respectively, once a day, at 8 : 00 am, for 22 weeks. The SD and HFD were purchased from Medicience Ltd., Jiangsu, China (SD Product model: MD12014; HFD Product model: MD12015A; Certificate No. 2018–10030, Table 1). The experimental process is shown in Table 2, and the dose of NSKP was determined according to the previous experimental results.

Animals were weighed before and after experiment, and their food intake was measured. At the end of 22 weeks, all animals were fasted for 6 hours. At 6 am the next day, phenobarbital was injected intraperitoneally to anesthesia, and blood samples were collected. The animals were dissected, and the liver was quickly removed, weighed, and partially fixed in 4% paraformaldehyde phosphate buffer solution for histopathological examination. The rest of the liver was immediately placed in liquid nitrogen and stored at −80°C for later experiments.

2.3. Serum and Liver Indexes. After blood collection, the supernatant was centrifuged at 4°C, 3000 r/min, for 10 min to be used as serum, and AST and ALT were detected using kits.

The liver tissue frozen at −80°C was accurately weighed and mechanically homogenized in a ratio of weight (g) to homogenate medium (mL) of 1 : 9 under ice water bath. The homogenized tissue was prepared at 2500 r/min and centrifuged for 10 min. The supernatants were taken to detect the contents of TG, TC, AST, and ALT in liver tissue according to the corresponding kit. Protein concentrations were determined using the bicinchoninic acid (BCA) protein

Table 1: The ingredient of the diet (g/100 g).

Ingredient	Standard diet	High-fat diet
Cornstarch	20.96	5.00
Casein	19.47	19.47
Maltodextrin	9.98	9.98
Anhydrous milk fat	3.97	19.72
Corn oil	1.28	0.99
Sucrose	34.00	34.00
Fiber	4.99	4.99
Mineral mix	3.88	3.88
Vitamin mix	1.47	1.47
Cholesterol	0	0.5

Table 2: Procedure of experiment.

	Diet	ApoE$^{-/-}$			
0th week-1th week	SD	√			
	HFD	—			
		C	M	L	H
2nd week –22nd week	SD	√	—	—	—
	HFD	—	√	√	√
	0.4 g/kg NSKP	—	—	√	—
	0.8 g/kg NSKP	—	—	—	√

Note. C: SD; M: HFD; L: HFD + 0.4 g/kg NSKP; H: HFD + 0.8 g/kg NSKP.

assay kit (Thermo Fisher Scientific). The data were normalized against the total protein level. Normal saline was used as homogenate to detect liver AST and ALT, and anhydrous ethanol was used as homogenate to detect liver TG and TC. Unless otherwise stated, the kits were purchased from Nanjing Jiancheng Institute of Biological Engineering.

2.4. Oxidative Stress Indicators. According to the ratio of weight (g) to normal saline (mL) of 1 : 9 and mechanical homogenate under ice water bath, the tissue homogenate prepared was 2500 r/min, centrifuged for 10 min. Taking supernatant and the appropriate dilution concentration was selected according to the corresponding kit for the detection of SOD, GSH, and MDA in liver according to the kit manufacturer's steps. Protein concentrations were determined using the bicinchoninic acid (BCA) protein assay kit (Thermo Fisher Scientific). The concentrations of SOD, GSH, and MDA in liver were calculated according to the data of total protein concentration.

2.5. Histopathology. The liver was fixed in 4% paraformaldehyde phosphate buffer solution to prepare 4 μm cross-cut slices. Histopathological evaluation was performed by H&E staining, oil red O staining, and Sirius red staining. H&E staining was used to evaluate the morphology of liver tissue, oil red O staining was used to evaluate the lipid accumulation in liver tissue, and Sirius red staining was used to evaluate the degree of fibrosis in liver tissue. The Olympus D1027 microscope was used to randomly select 5 nonoverlapping fields, and Image-Pro Plus 6.0 graphic analysis software was used to calculate the percentage of positive area of fibrosis.

2.6. Immunohistochemical Staining. Liver fixed in 4% paraformaldehyde phosphate buffer solution was used to prepare 4 μm cross-cut slices. The samples were randomly selected from each group. The *α-SMA* and *FN* of liver were determined according to the instructions of the immunohistochemical kit, and the immunohistochemical staining sections were quantified. The positive expression of brown-yellow or yellow particles was taken as positive expression. Five fields were randomly selected from each section, and the average optical density of positive staining area was detected by Image-Pro Plus 6.0 analysis software (Area Optical Density = IOD/Area).

2.7. Western Blotting (WB). The liver at −80°C was used. The cytokine *TGF-β1* (with the dilution ratio of antibody concentration being 1 : 1000) in liver was detected, and *β*-actin was used as a normalize control for protein loading. Total protein was extracted from liver samples by homogenization with RIPA extraction buffer (Servicebio, Wuhan, China). The protein concentration of liver samples was measured using a BCA method (Nanjing Jiancheng Bioengineering Institute, Nanjing, China). Protein samples were then subjected to 10% sodium dodecyl sulfate–polyacrylamide gel electrophoresis separation (SDS-PAGE) and transferred to nitrocellulose membranes. Membranes were blocked for 1 h using 5% bovine serum albumin (BSA)/phosphate buffered saline (PBS), after which they were probed overnight with appropriate primary antibodies at 4°C. Blots were then washed using PBS and probed using appropriate horseradish peroxidase-linked secondary antibodies. The membrane bands were displayed by chemiluminescence (micropores), and the strip intensity of each channel was quantified by ImageJ 6.0 software.

2.8. Reverse Transcription-Polymerase Chain Reaction (RT-PCR). Liver tissue cryopreserved at −80°C was used. TRIzol was used to extract total RNA from mouse liver, and the concentration and purity of RNA were measured by nucleic acid protein analyzer at 260/280 nm. Then, the cDNA was reverse-transcribed by Fast Pfus PCR Master Mix and then operated according to the kit. The primers *GAPDH*, sterol regulatory element binding transcription factor 1 (*SREBP-1c*), fatty acid synthesis (*FAS*), *TGF-β1*, *α*-smooth muscle actin (*α-SMA*), fibronectin (*FN*), and collagen I (*Col-I*) were designed by DNAMAN software. The primers were synthesized by Wuhan Sewell Biotechnology Co., Ltd., and detected by Bio-Rad CFX96™ fluorescence quantitative PCR system. PCR procedure was as follows: 95°C for 2 min; 95°C for 20 s, 55°C for 20 s, 72°C for 20 s, 30 cycles; 72°C for 10 s. Using *GAPDH* as internal reference, the relative expression levels of the genes to be measured were expressed as $2^{-\Delta\Delta Ct}$. $^{\Delta\Delta}$ Ct = [Ct target gene (sample to be tested) – reference within Ct (sample to be tested)] – [Ct target gene (calibration sample) – reference within Ct (calibration sample)]. Primer sequences are shown in Table 3.

2.9. Statistical Analysis. Statistical analysis was conducted using SPSS software for Windows (version 22). Data were assessed using one-way ANOVA and Newman–Keuls pairwise

Table 3: Primers used for RT-PCR

Accession ID	Genes	Forward (5′ to 3′)	Reverse (5′ to 3′)
NM_008084.2	*GAPDH*	CCTCGTCCCGTAGACAAAATG	TGAGGTCAATGAAGGGGTCGT
NM_001313979.1	*SREBP-1c*	TCTGTGAGAAGGCCAGTGGGTA	GAGCTGTGGCCTCATGTAGGAATA
NM_007987.2	*FAS*	TAGAACCTCCAGTCGTGAAACCA	ATCTCATCTATCTTGCCCTCCTTG
NM_011577.2	*TGF-β1*	TAATGGTGGACCGCAACAAC	CCACATGTTGCTCCACACTTGAT
NM_007392.3	*α-SMA*	GTACCACCATGTACCCAGGC	GAAGGTAGACAGCGAAGCCA
NM_001276408.1	*FN*	ACACGGTTTCCCATTACGCC	GGTCTTCCCATCGTCATAGCAC
NM_007742.4	*Col-I*	GAGAGGTGAACAAGGTCCCG	AAACCTCTCTCGCCTCTTGC

Table 4: Effects of NSKP on body weight and food intake of high-fat mice.

	Body weight (g)		Total food intake (g)
	0th week	22nd week	
C	23.26 ± 0.78	29.79 ± 1.52	515.73 ± 31.91^{a}
M	23.05 ± 0.46	30.06 ± 1.81	463.51 ± 37.23^{ab}
L	23.19 ± 0.72	31.76 ± 1.78	444.34 ± 26.27^{b}
H	22.72 ± 0.55	32.79 ± 2.07	456.65 ± 18.53^{ab}

Values represent mean ± SEM; $n = 10$ in each group.

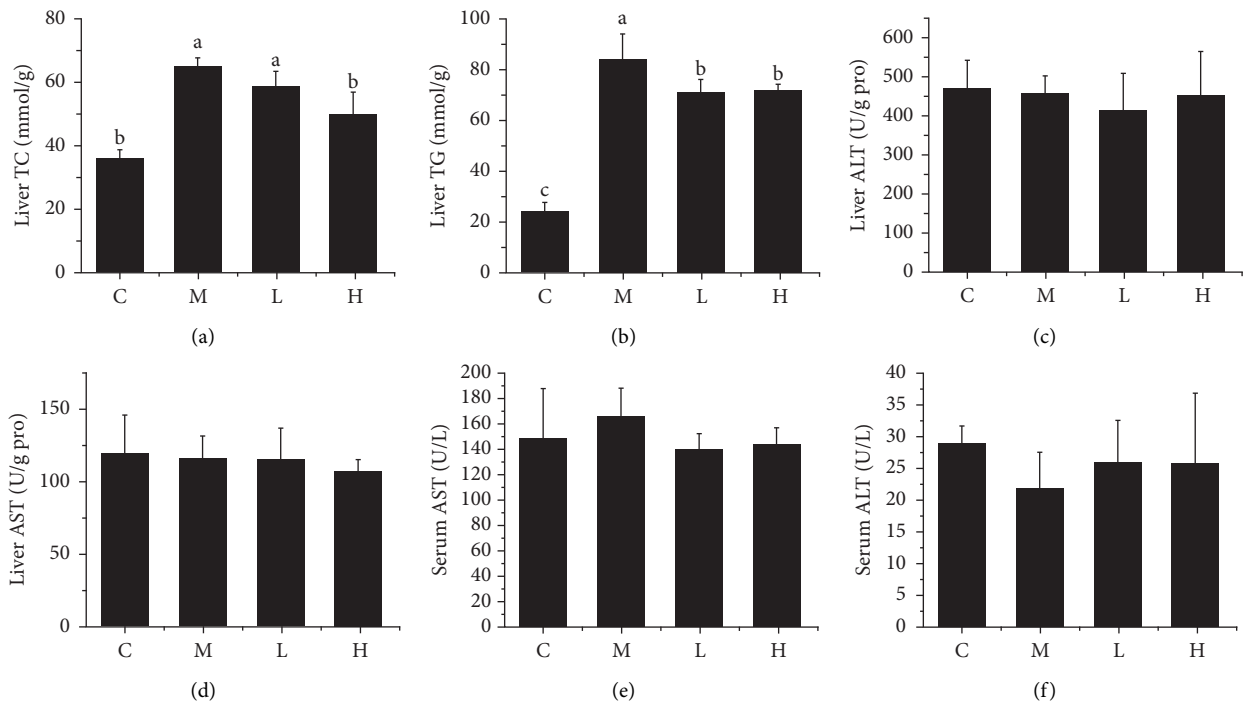

Figure 1: Effects of NSKP on serum and liver indexes of high-fat mice. (a) Liver TC. (b) Liver TG. (c) Liver ALT. (d) Liver AST. (e) Serum ALT. (f) Serum AST. Bars marked with different letters represent statistically significant ($P < 0.05$), whereas bars labeled with the same letter indicate no statistically significant difference between the groups ($P > 0.05$). Values represent mean ± SEM; $n = 10$ in each group.

comparison. $P < 0.05$ values were considered significant differences. All data from these assays are shown as mean ± SEM.

3. Results

3.1. Effects of NSKP on Body Weight and Food Intake. As shown in Table 4, compared with group M, groups L and H had no significant differences in the final body weight and total food intake ($P > 0.05$), indicating that NSKP had no effect on the body weight and total food intake of high-fat diet mice.

3.2. Effects of NSKP on Lipid and Transaminase in the Serum and Liver of High-Fat Diet Mice. Lipids and transaminases in serum and liver were detected at the end of 22 weeks. Our previous study has concluded that NSKP significantly reduced serum TC, TG, and LDL-C and increased HDL-C

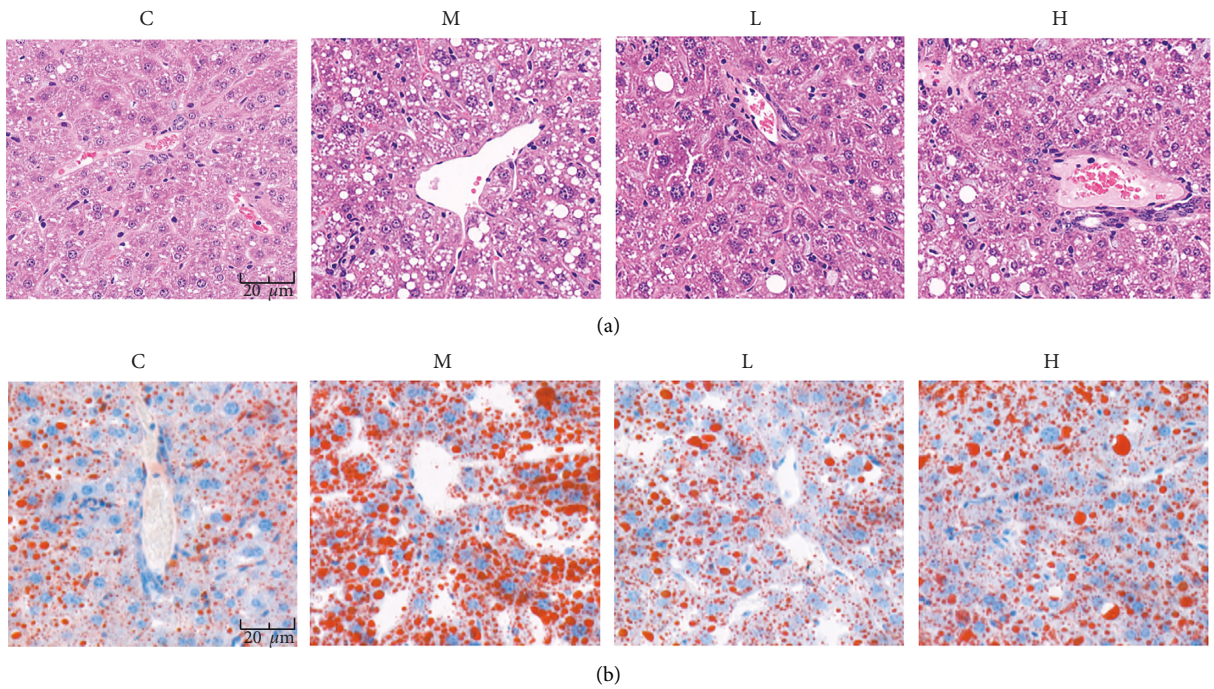

Figure 2: Effects of NSKP on liver of high-fat mice. (a) H&E staining in the liver. (b) Oil red O staining in the liver. Original magnification: 400x.

content in mice fed a high-fat diet for 22 weeks (title: Effects of *Nostoc sphaeroides* Kütz. Polysaccharide on Renal Fibrosis in High-Fat Mice, accepted). As shown in Figures 1(a) and 1(b), liver TC and TG in group M were significantly increased compared with group C, indicating that 22-week high-fat diet led to liver lipid metabolism disorder, but gavage of different doses of NSKP (L and H) significantly reduced liver TC and TG contents, respectively. There was no significant difference in ALT and AST in serum and liver (Figures 1(c)–1(f)) among all groups ($P > 0.05$). The results showed that NSKP ameliorated lipid disorder in high-fat diet mice.

3.3. Effects of NSKP on Liver Tissue Structure. Histopathology can intuitively observe the morphology and structure of tissues. According to H&E staining in Figure 2(a), liver vacuolation was severe in group M compared with group C, the structure of middle liver cells was unclear and showed swelling and necrosis, and the arrangement of cells was disordered. However, the vacuolation was relatively reduced in groups L and H, and the cell structure was clearly visible after NSKP treatment. According to oil red O staining in Figure 2(b), compared with group C, group M showed increased red lipids in liver and serious lipid accumulation, but the red area and lipid accumulation were reduced in group L and H after being fed with NSKP. The results showed that NSKP improved liver injury and steatosis of high-fat diet mice.

3.4. Effects of NSKP on mRNA of Liver Fat Synthesis. Fat synthesis genes play a key role in fat synthesis. We detected the key fat synthesis genes in the liver by RT-PCR technology. As shown in Figure 3(a), compared with group C, group M showed significantly increased mRNA expression of *SREBP-1c*, but the mRNA expression of *SREBP-1c* in groups L and H was significantly decreased after gavage of NSKP ($P < 0.05$, $P < 0.05$). As shown in Figure 3(b), the mRNA expression of *FAS* in group M was significantly increased compared with group C ($P < 0.05$), indicating that *FAS* in liver of mice was increased lipid disorders, and there was a trend of decrease after gavage of NSKP, but there was no significant difference ($P > 0.05$). The results showed that NSKP reduced the key mRNA of fat synthesis in high-fat diet mice.

3.5. Effects of NSKP on Liver Oxidative Stress. Long-term high-fat diet can cause oxidative stress in mice liver. Based on the phenomenon of oxidative stress caused by dyslipidemia, we used corresponding kits to detect the indicators of oxidative stress in mice liver. It can be seen from Figure 4(a) that there was no significant difference in SOD content between group M and group C, but liver SOD contents (L) of high-fat mice fed with NSKP were significantly increased ($P > 0.05$, $P < 0.05$). As can be seen from Figures 4(b) and 4(c), liver GSH of mice was significantly decreased and liver MDA increased ($P < 0.05$, $P < 0.05$) after being fed with high-fat diet, but liver GSH of mice was significantly increased and liver MDA decreased ($P < 0.05$, $P < 0.05$) after gavage of NSKP. The results showed that NSKP improved the antioxidant capacity in liver of high-fat diet mice.

3.6. Effects of NSKP on TGF-β1, α-SMA, and FN in the Liver. *TGF-β1*, *α-SMA*, and *FN* are important markers of fibrosis, which seriously affect the development of liver fibrosis. As

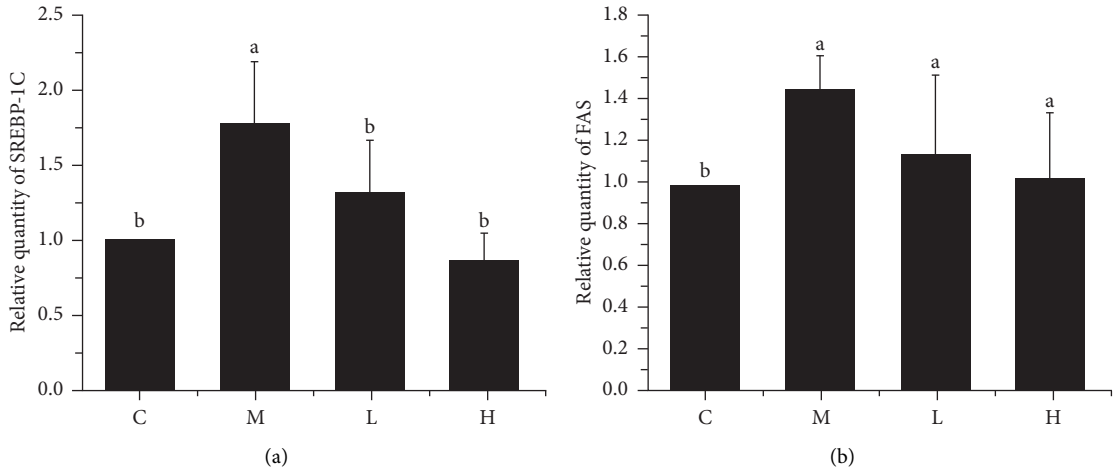

Figure 3: Effects of NSKP on mRNA of fat. (a) Relative quantity of *SREBP-1c* by RT-PCR. (b) Relative quantity of *FAS* by RT-PCR. Bars marked with different letters represent statistically significant ($P < 0.05$), whereas bars labeled with the same letter indicate no statistically significant difference between the groups ($P > 0.05$). Values represent mean ± SEM; $n = 10$ in each group (*SREBP-1c*: sterol regulatory element binding transcription factor 1-c, *FAS*: fatty acid synthesis).

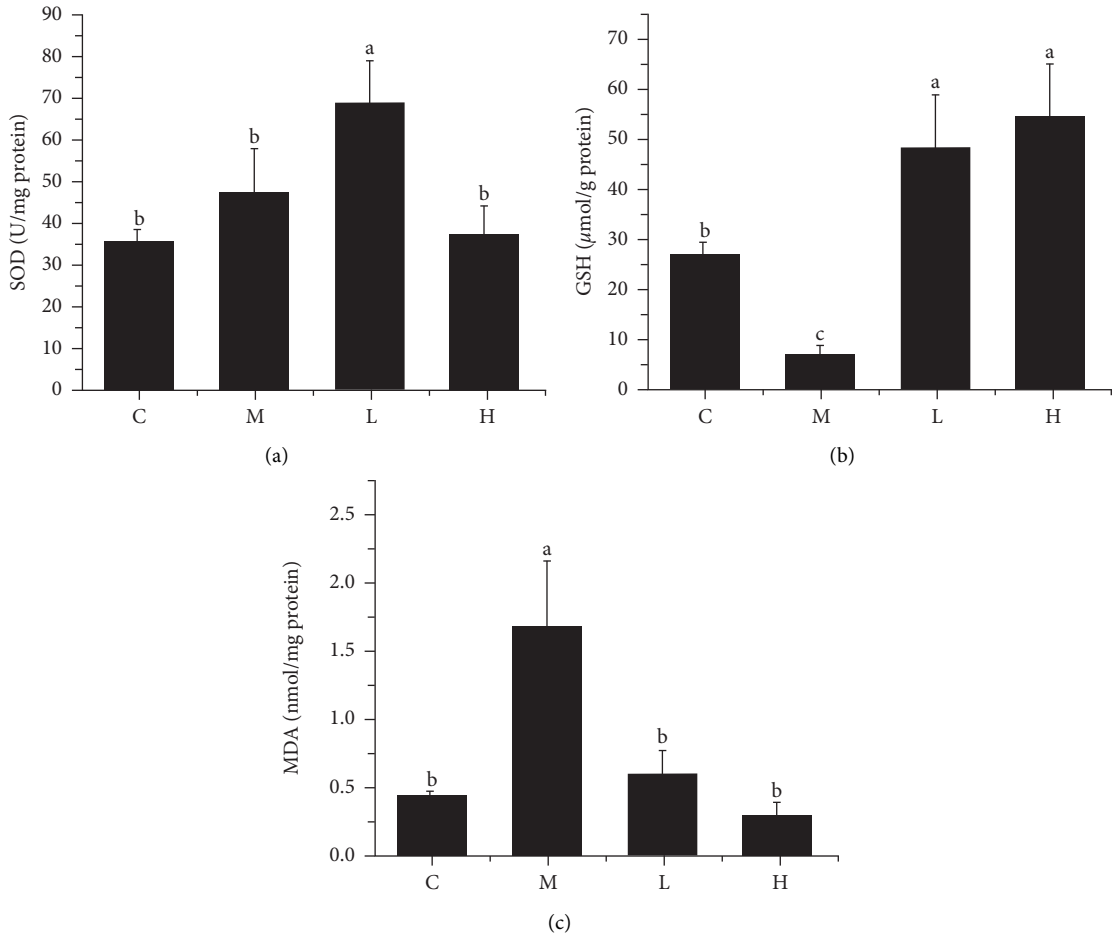

Figure 4: Effects of NSKP on liver oxidative stress in high-fat mice. (a) SOD (U/mg protein). (b) GSH (μmol/g protein). (c) MDA (nmol/mg protein). Bars marked with different letters represent statistically significant ($P < 0.05$), whereas bars labeled with the same letter indicate no statistically significant difference between the groups ($P > 0.05$). Values represent mean ± SEM; $n = 10$ in each group (SOD: superoxide dismutase, GSH: glutathione, MDA: malondialdehyde).

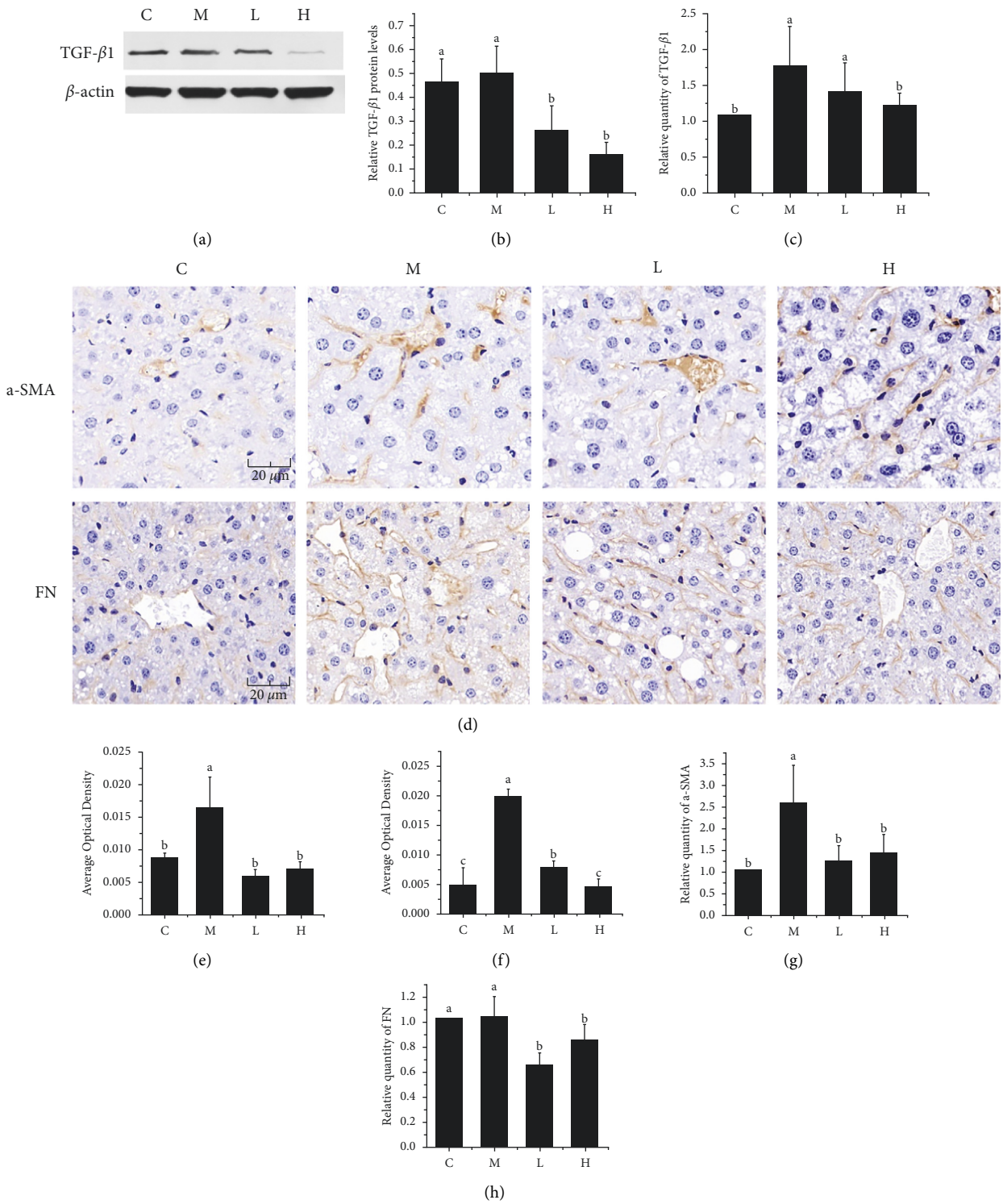

Figure 5: Effects of NSKP on hepatic *TGF-β1*, *α-SMA*, and *FN* in high-fat mice. (a) The blot of *TGF-β1* by WB. (b) Protein expression of *TGF-β1*. (c) Relative quantity of *TGF-β1* by RT-PCR. (d) Immunohistochemical staining (*α-SMA*, *FN*), original magnification: 400x. (e) Quantitative analysis of the average optical density of *α-SMA* immunohistochemical staining sections. (f) Quantitative analysis of the average optical density of *FN* immunohistochemical staining sections. (g, h) Relative quantity of *α-SMA* and *FN* by RT-PCR. Bars marked with different letters represent statistically significant ($P < 0.05$), whereas bars labeled with the same letter indicate no statistically significant difference between the groups ($P > 0.05$). Values represent mean ± SEM; $n = 10$ in each group (*TGF-β1*: transforming growth factor-beta 1; *α-SMA*: *α*-smooth muscle actin; *FN*: fibronectin).

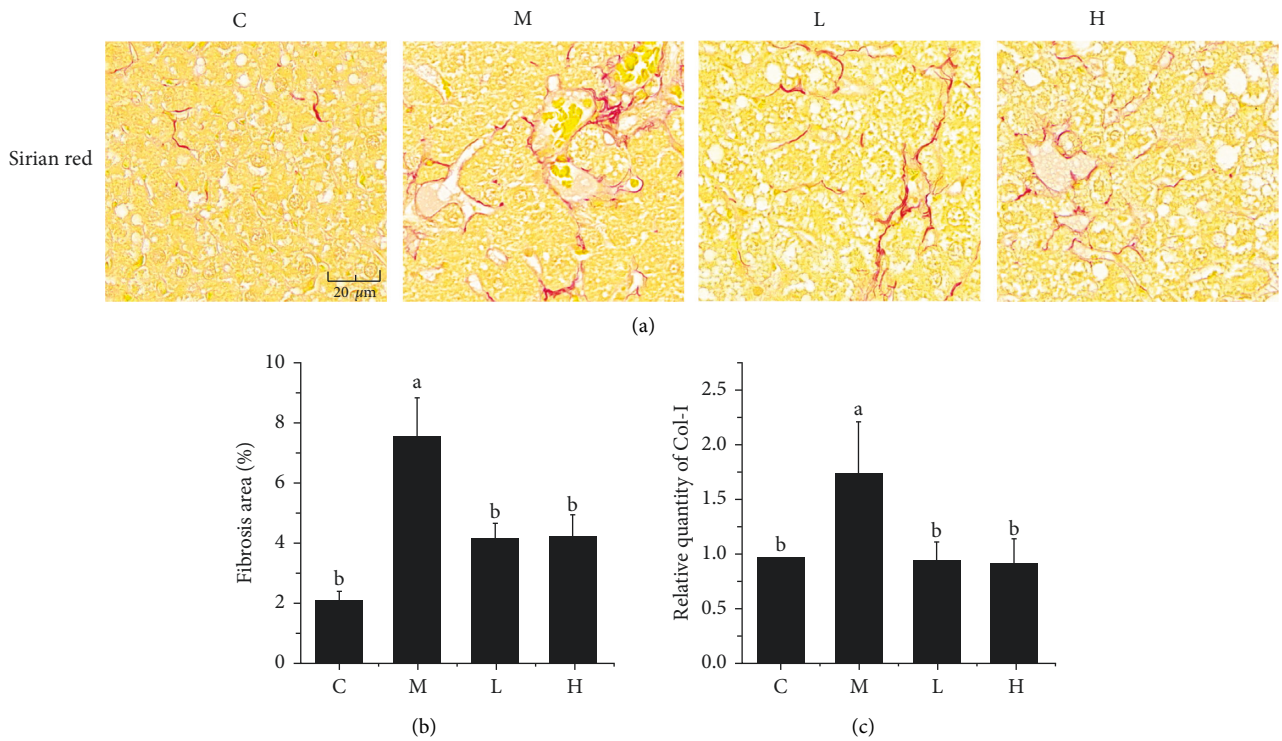

Figure 6: Effect of NSKP on hepatic collagen fibers in high-fat mice. (a) Sirius red staining of the liver; red represents collagen fibers; original magnification: 400x. (b) Fibrosis area (%). (c) The mRNA expression levels of *Col-I* were detected by RT-PCR. Bars marked with different letters represent statistically significant ($P < 0.05$), whereas bars labeled with the same letter indicate no statistically significant difference between the groups ($P > 0.05$). Values represent mean ± SEM; $n = 10$ in each group (*Col-I*: collagen I).

can be seen from Figures 5(a)–5(c), the protein expression of *TGF-β1* in group M was not significantly different compared with group C ($P > 0.05$), but the mRNA expression of *TGF-β1* was significantly increased ($P < 0.05$), and the protein expression and mRNA expression of *TGF-β1* were significantly decreased ($P < 0.05$) after feeding mice with NSKP. The results showed that NSKP decreased the expression of *TGF-β1* in liver of high-fat diet mice.

As shown in Figures 5(d)–5(f), immunohistochemical staining of *α-SMA* and *FN* showed that the positive area of *α-SMA* and *FN* in group M was increased and Area Optical Density was significantly increased compared with group C ($P < 0.05$, $P < 0.05$), but after the intervention of NSKP, the positive area of *α-SMA* and *FN* was decreased. Area Optical Density was significantly decreased ($P < 0.05$, $P < 0.05$). RT-PCR assays were performed on *α-SMA* and *FN*. As shown in Figures 5(g) and 5(h), the mRNA expressions of *α-SMA* and *FN* were significantly decreased after 22 weeks of NSKP intervention ($P < 0.05$, $P < 0.05$). The results indicated that NSKP reduced the expression of *α-SMA* and *FN* in liver of high-fat diet mice.

3.7. Effects of NSKP on Liver Fibrosis. The main cause of liver fibrosis is the accumulation of fibrin in the hepatic Disse space. According to Figures 6(a) and 6(b), compared with group C, group M showed significantly increased red part and area of fibrosis ($P < 0.05$). After 22 weeks of NSKP treatment, the red part was significantly decreased and the area of fibrosis was significantly decreased ($P < 0.05$). As shown in Figure 6(c), the mRNA expression of *Col-I* was significantly decreased in high-fat diet mice after 22 weeks of NSKP treatment ($P < 0.05$). The results showed that NSKP ameliorated liver fibrosis in high-fat diet mice.

4. Discussion and Conclusion

Liver fibrosis is the persistent result of chronic liver injury, that is, an abnormal healing reaction caused by liver injury, which is a reversible process, but if not treated in time, it will cause liver cirrhosis and eventually lead to liver failure [27]. High-fat diet can cause dyslipidemia, and dyslipidemia is another important risk factor for liver fibrosis in addition to obesity and type 2 diabetes [28]. A long-term high-fat diet can also induce chronic liver diseases such as hepatitis and liver fibrosis. Studies have shown that it can cause abnormal synthesis and accumulation of fat in the liver and induce oxidative stress and inflammatory reactions. Then, it stimulates the fiber to form a signal pathway and cause liver fibrosis [29].

As a functional food of natural biological origin, *Nostoc sphaeroides* Kütz. is a kind of single-celled blue algae and has a good lipid-lowering effect, which can directly reduce the absorption of cholesterol in the intestinal tract and inhibit atherosclerotic lesions without increasing the burden of liver metabolism [21]. Previous studies in our laboratory have proved that *Nostoc sphaeroides* Kütz. can inhibit liver injury and improve intestinal microorganisms [22, 30]. The content

of polysaccharides in *Nostoc sphaeroides* Kütz. is about 40%. The monosaccharide composition of NSKP connects arabinose, galactose, glucose, xylose, mannose, and glucuronic acid through β-1-3 glycosidic bond and β-1-4 glycosidic bond. It is an important substance in *Nostoc sphaeroides* Kütz. [26]. Some studies have shown that the important mechanism of polysaccharides extracted from *Lycium barbarum* in improving liver fibrosis induced by high-fat diet may be the improvement of oxidative stress in the liver [31]. Phaeophyceae extract can reduce liver fibrosis in high-fat male C57BL/6J mice by intervening in abnormal oxidative stress and inflammatory response induced by high-fat diet [32]. Therefore, this experiment mainly studies the effect of NSKP on liver lipid content and oxidative stress in hyperlipidemic mice, which may achieve the effect of preventing liver fibrosis.

Hepatic steatosis is caused by increased de novo fat synthesis rate and decreased fat oxidation rate [33, 34]. Two important factors of fat accumulation in the liver are blocked free fatty acid transport and abnormal increase of fat synthesis, and the genes *SREBP-1c* and *FAS* of fat synthesis play a key role in steatosis [35, 36]. It has been reported that *SREBP-1c* can regulate *FAS* expression and lead to TG synthesis, and the mechanisms underlying the effects of *SREBP-1c* on hepatic stellate cell activation and liver fibrosis were involved in its influences on the receptors for *TGF-β1* and PDGF-β and their downstream signaling, and the molecules for epigenetic regulation of genes [37]. The high-fat diet has been confirmed to cause TG and TC accumulation by increasing *SREBP-1c* and *FAS* expression [38, 39]. A large number of studies have shown that plant extracts can reduce liver steatosis by improving key genes of liver fat synthesis [40, 41]. In our experiment, NSKP reduced the lipid level of high-fat diet mice fed for 22 weeks. After histopathological staining sections, it was observed that the liver structure of high-fat mice had abnormal damage and the fat accumulation was serious. On the contrary, after NSKP feed, liver injury was alleviated and fat accumulation was improved. At the same time, the mRNA expression of *SREBP-1c* and *FAS* was decreased, suggesting that NSKP interfered with the accumulation of fat in liver by reducing *SREBP-1c* and *FAS*, which are important genes in liver fat synthesis.

The increase of liver fat load and the occurrence of lipotoxicity can lead to a high level of oxidative stress in animal models of liver fat with fibrosis, mainly due to the reduction of antioxidant level [42, 43]. According to the double-hit hypothesis, the aggravation of fat accumulation in liver cells will lead to oxidative damage of liver cells, which is one of the key mechanisms in liver fibrosis. The decrease of antioxidant secretion and the production of lipid peroxides both accelerate the damage of liver cells and the abnormal phenomena of liver tissue structure [7]. The experimental results showed that SOD increased significantly and MDA decreased significantly after NSKP feed, indicating that the antioxidant capacity of liver tissue was gradually increased and the production of lipid peroxides was decreased. Further, it was shown that NSKP alleviated the phenomenon of oxidative stress in liver tissue caused by long-term high-fat diet. Thus, the abnormal liver tissue structure and lipid accumulation were improved.

Hepatocytes can participate in the activation of hepatic stellate cells through various mechanisms, such as the stress response or inflammatory response, thus affecting liver fibrosis [44]. Studies have shown that the activation of hepatic stellate cells is generated by direct interaction with the stress or death of hepatic cells [45]. Proliferation of hepatic stellate cells is also stimulated by growth factors, such as transforming growth factor (TGF) and epidermal growth factor [46, 47]. At the same time, growth factors promote the remodeling of the extracellular matrix (ECM), leading to the formation of collagen fibrin. In normal liver, collagen IV and collagen VI are present in the Disse space of the liver. However, they are replaced by type I and II collagen and fibronectin during fiber formation [48]. *TGF-β1* is a key signal molecule of renal fibrosis and the strongest key driver of liver fibrosis [18, 49]. It is normally inactive, but when activated, it activates the signaling pathway through Smad protein to stimulate the development of fibrosis mechanism and lead to the production of collagen fibrin [50, 51]. In addition, *TGF-β1* promotes the transdifferentiation of ECM-secreting myofibroblasts [52]. The stress response of the liver caused by long-term lipid metabolism disorders leads to the massive production of *TGF-β1*, which further stimulates the activation of hepatic stellate cells. The most obvious phenomenon is the excessive secretion of *α-SMA*, which is also an indispensable key marker in the development of liver fibrosis [53]. The presence of *TGF-β1* also seriously affects the degradation mechanism of the ECM (mainly *Col-I* and *FN*), leading to excessive deposition of extracellular matrix in the liver Disse space, inducing the damage of liver tissue structure, and ultimately leading to liver fibrosis [54, 55]. It is worth noting that in this experiment, *TGF-β1* and *α-SMA* in the liver of high-fat mice were reduced to varying degrees after gavage of NSKP, indicating that NSKP regulated *TGF-β1* and *α-SMA* key cytokines in liver fibrosis of high-fat mice, so as to achieve the effect of liver fibrosis intervention. According to histopathological staining section observation of the results of this experiment, the liver tissue structure of HFD group mice fed high fat diet for a long time had abnormal changes, with serious collagen fiber deposition and severe fibrosis in liver. The expression of FN and type I collagen fibrin in mice fed high fat diet was downregulated after given NSKP. It slowed down the deposition of extracellular matrix in liver of high fat diet mice and also improved liver fibrosis.

In conclusion, the intervention of NSKP improved liver steatosis and oxidative stress and delayed the progression of liver fibrosis in mice on a long-term high-fat diet.

Data Availability

The data used to support the findings of this study are included within the article.

Conflicts of Interest

The authors declare no conflicts of interest.

References

[1] L. Li, A. L. Yu, Z. L. Wang et al., "Chaihu-Shugan-San and absorbed meranzin hydrate induce anti-atherosclerosis and behavioral improvements in high-fat diet ApoE (−/−) mice via anti-inflammatory and BDNF-TrkB pathway," *Biomedicine & Pharmacotherapy*, vol. 115, Article ID 108893, 2019.

[2] F. Zamani-Garmsiri, S. M. R. Hashemnia, M. Shabani, M. Bagherieh, S. Emamgholipour, and R. Meshkani, "Combination of metformin and genistein alleviates non-alcoholic fatty liver disease in high-fat diet-fed mice," *The Journal of Nutritional Biochemistry*, vol. 87, Article ID 108505, 2021.

[3] H. Zeng, J. Liu, M. I. Jackson, F. Q. Zhao, L. Yan, and G. F. Combs Jr., "Fatty liver accompanies an increase in lactobacillus species in the hind gut of C57BL/6 mice fed a high-fat diet," *Journal of Nutrition*, vol. 143, no. 5, pp. 627–631, 2013.

[4] X. Zhang, L. Fan, J. Wu et al., "Macrophage p38α promotes nutritional steatohepatitis through M1 polarization," *Journal of Hepatology*, vol. 71, no. 1, pp. 163–174, 2019.

[5] Z. T. Jing, W. Liu, C. R. Xue et al., "AKT activator SC79 protects hepatocytes from TNF-alpha-mediated apoptosis and alleviates d-Gal/LPS-induced liver injury," *American Journal of Physiology - Gastrointestinal and Liver Physiology*, vol. 316, no. 3, pp. G387–G396, 2019.

[6] Y. Yuan, L. Che, C. Qi, and Z. Meng, "Protective effects of polysaccharides on hepatic injury: a review," *International Journal of Biological Macromolecules*, vol. 141, pp. 822–830, 2019.

[7] C. Y. Lian, Z. Z. Zhai, Z. F. Li, and L. Wang, "High fat diet-triggered non-alcoholic fatty liver disease: a review of proposed mechanisms," *Chemico-Biological Interactions*, vol. 330, Article ID 109199, 2020.

[8] K. Mehta, D. H. Van Thiel, N. Shah, and S. Mobarhan, "Nonalcoholic fatty liver disease: pathogenesis and the role of antioxidants," *Nutrition Reviews*, vol. 60, no. 9, pp. 289–293, 2002.

[9] J. Xu, Y. Guo, X. Huang et al., "Effects of DHA dietary intervention on hepatic lipid metabolism in apolipoprotein E-deficient and C57BL/6J wild-type mice," *Biomedicine & Pharmacotherapy*, vol. 144, 2021.

[10] W. Chen, X. Zhang, M. Xu et al., "Betaine prevented high-fat diet-induced NAFLD by regulating the FGF10/AMPK signaling pathway in ApoE(−/−) mice," *European Journal of Nutrition*, vol. 60, no. 3, pp. 1655–1668, 2021.

[11] W. Li, J. Yu, J. Zhao et al., "Poria cocos polysaccharides reduces high-fat diet-induced arteriosclerosis in ApoE(−/−) mice by inhibiting inflammation," *Phytotherapy Research*, vol. 35, no. 4, pp. 2220–2229, 2021.

[12] R. Schierwagen, L. Maybuchen, S. Zimmer et al., "Seven weeks of Western diet in apolipoprotein-E-deficient mice induce metabolic syndrome and non-alcoholic steatohepatitis with liver fibrosis," *Scientific Reports*, vol. 5, no. 1, 2015.

[13] C. Y. Zhang, W. G. Yuan, P. He, J. H. Lei, and C. X. Wang, "Liver fibrosis and hepatic stellate cells: etiology, pathological hallmarks and therapeutic targets," *World Journal of Gastroenterology*, vol. 22, no. 48, p. 10512, 2016.

[14] I. Mederacke, C. C. Hsu, J. S. Troeger et al., "Fate tracing reveals hepatic stellate cells as dominant contributors to liver fibrosis independent of its aetiology," *Nature Communications*, vol. 4, no. 1, 2013.

[15] R. Schwabe and R. F. Schwabe, "Origin and function of myofibroblasts in the liver," *Seminars in Liver Disease*, vol. 35, no. 02, pp. 097–106, 2015.

[16] V. Hernandez-Gea and S. L. Friedman, "Pathogenesis of liver fibrosis," *Annual Review of Pathology: Mechanisms of Disease*, vol. 6, no. 1, pp. 425–456, 2011.

[17] A. B. Marcher, S. M. Bendixen, M. K. Terkelsen et al., "Transcriptional regulation of hepatic stellate cell activation in NASH," *Scientific Reports*, vol. 9, no. 1, 2019.

[18] E. M. Zeisberg, S. E. Potenta, H. Sugimoto, M. Zeisberg, and R. Kalluri, "Fibroblasts in kidney fibrosis emerge via endothelial-to-mesenchymal transition," *Journal of the American Society of Nephrology*, vol. 19, no. 12, pp. 2282–2287, 2008.

[19] A. El Taghdouini and L. A. van Grunsven, "Epigenetic regulation of hepatic stellate cell activation and liver fibrosis," *Expert Review of Gastroenterology & Hepatology*, vol. 10, no. 12, pp. 1397–1408, 2016.

[20] R. Ma, F. Lu, Y. Bi, and Z. Hu, "Effects of light intensity and quality on phycobiliprotein accumulation in the cyanobacterium Nostoc sphaeroides Kutzing," *Biotechnology Letters*, vol. 37, no. 8, pp. 1663–1669, 2015.

[21] C. S. Ku, B. Kim, T. X. Pham et al., "Blue-green algae inhibit the development of atherosclerotic lesions in apolipoprotein E knockout mice," *Journal of Medicinal Food*, vol. 18, no. 12, 2015.

[22] F. Wei, Y. Liu, C. Bi, and B. Zhang, "Nostoc sphaeroids Kutz powder ameliorates diet-induced hyperlipidemia in C57BL/6j mice," *Food & Nutrition Research*, vol. 63, 2019.

[23] Y. Liu, P. Su, J. Xu et al., "Structural characterization of a bioactive water-soluble heteropolysaccharide from Nostoc sphaeroids kutz," *Carbohydrate Polymers*, vol. 200, pp. 552–559, 2018.

[24] P. H. Shih, S. J. Shiue, C. N. Chen et al., "Fucoidan and fucoxanthin attenuate hepatic steatosis and inflammation of NAFLD through modulation of leptin/adiponectin Axis," *Marine Drugs*, vol. 19, no. 3, p. 148, 2021.

[25] J. Tang, Z. Y. Hu, and X. W. Chen, "Free radical scavenging and antioxidant enzymes activation of polysaccharide extract from Nostoc sphaeroides," *The American Journal of Chinese Medicine*, vol. 35, no. 5, pp. 887–896, 2007.

[26] H. Li, L. Su, S. Chen et al., "Physicochemical characterization and functional analysis of the polysaccharide from the edible microalga Nostoc sphaeroides," *Molecules*, vol. 23, no. 2, p. 508, 2018.

[27] W. C. Zhou, Q. B. Zhang, and L. Qiao, "Pathogenesis of liver cirrhosis," *World Journal of Gastroenterology*, vol. 20, no. 23, p. 7312, 2014.

[28] E. Hijona, L. Hijona, J. I. Arenas, and L. Bujanda, "Inflammatory mediators of hepatic steatosis," *Mediators of Inflammation*, vol. 2010, Article ID 837419, 7 pages, 2010.

[29] W. Liu, S. S. Baker, R. D. Baker, and L. Zhu, "Antioxidant mechanisms in nonalcoholic fatty liver disease," *Current Drug Targets*, vol. 16, no. 12, pp. 1301–1314, 2015.

[30] F. Wei, Y. Liu, C. Bi, S. Chen, Y. Wang, and B. Zhang, "Nostoc sphaeroids Kutz ameliorates hyperlipidemia and maintains the intestinal barrier and gut microbiota composition of high-fat diet mice," *Food Sciences and Nutrition*, vol. 8, no. 5, pp. 2348–2359, 2020.

[31] J. Xiao, E. C. Liong, Y. P. Ching et al., "Lycium barbarum polysaccharides protect mice liver from carbon tetrachloride-induced oxidative stress and necroinflammation," *Journal of Ethnopharmacology*, vol. 139, no. 2, pp. 462–470, 2012.

[32] N. Takatani, Y. Kono, F. Beppu et al., "Fucoxanthin inhibits hepatic oxidative stress, inflammation, and fibrosis in diet-induced nonalcoholic steatohepatitis model mice," *Biochemical and Biophysical Research Communications*, vol. 528, no. 2, pp. 305–310, 2020.

[33] H. Tilg and A. R. Moschen, "Evolution of inflammation in nonalcoholic fatty liver disease: the multiple parallel hits hypothesis," *Hepatology*, vol. 52, no. 5, pp. 1836–1846, 2010.

[34] B. N. Finck, "Targeting metabolism, insulin resistance, and diabetes to treat nonalcoholic steatohepatitis," *Diabetes*, vol. 67, no. 12, pp. 2485–2493, 2018.

[35] M. S. Strable and J. M. Ntambi, "Genetic control of de novo lipogenesis: role in diet-induced obesity," *Critical Reviews in Biochemistry and Molecular Biology*, vol. 45, no. 3, pp. 199–214, 2010.

[36] F. Ameer, L. Scandiuzzi, S. Hasnain, H. Kalbacher, and N. Zaidi, "De novo lipogenesis in health and disease," *Metabolism*, vol. 63, no. 7, pp. 895–902, 2014.

[37] S. Su, H. Tian, X. Jia et al., "Mechanistic insights into the effects of SREBP1c on hepatic stellate cell and liver fibrosis," *Journal of Cellular and Molecular Medicine*, vol. 24, no. 17, pp. 10063–10074, 2020.

[38] L. Goedeke, J. Bates, D. F. Vatner et al., "Acetyl-CoA carboxylase inhibition reverses NAFLD and hepatic insulin resistance but promotes hypertriglyceridemia in rodents," *Hepatology*, vol. 68, no. 6, pp. 2197–2211, 2018.

[39] G. Ji, X. Zhao, L. Leng, P. Liu, and Z. Jiang, "Comparison of dietary control and atorvastatin on high fat diet induced hepatic steatosis and hyperlipidemia in rats," *Lipids in Health and Disease*, vol. 10, no. 1, 2011.

[40] H. Zhang, Y. Y. Hu, and Q. Feng, "Inhibitory effects of Qushi Huayu Decoction on fatty deposition and tumor necrosis factor alpha secretion in HepG2 cells induced by free fatty acid," *Zhongguo Zhong Xi Yi Jie He Za Zhi*, vol. 27, pp. 1105–1109, 2007.

[41] H. J. Park, U. J. Jung, M. K. Lee et al., "Modulation of lipid metabolism by polyphenol-rich grape skin extract improves liver steatosis and adiposity in high fat fed mice," *Molecular Nutrition & Food Research*, vol. 57, no. 2, pp. 360–364, 2013.

[42] G. Stokman, A. M. Hoek, D. Denker Thorbekk et al., "Dual targeting of hepatic fibrosis and atherogenesis by icosabutate, an engineered eicosapentaenoic acid derivative," *Liver International*, vol. 40, no. 11, pp. 2860–2876, 2020.

[43] M. S. Choi, J. Y. Choi, and E. Y. Kwon, "Fisetin alleviates hepatic and adipocyte fibrosis and insulin resistance in diet-induced obese mice," *Journal of Medicinal Food*, vol. 23, no. 10, 2020.

[44] J. Zhang, H. Zhang, X. Deng et al., "Baicalin attenuates non-alcoholic steatohepatitis by suppressing key regulators of lipid metabolism, inflammation and fibrosis in mice," *Life Sciences*, vol. 192, pp. 46–54, 2018.

[45] B. Afsar and R. Elsurer, "Increased renal resistive index in type 2 diabetes: clinical relevance, mechanisms and future directions," *Diabetes & Metabolic Syndrome: Clinical Research Reviews*, vol. 11, no. 4, pp. 291–296, 2017.

[46] D. H. Meyer, M. G. Bachem, and A. M. Gressner, "Modulation of hepatic lipocyte proteoglycan synthesis and proliferation by kupffer cell-derived transforming growth factors type β1 and type α," *Biochemical and Biophysical Research Communications*, vol. 171, no. 3, pp. 1122–1129, 1990.

[47] K. M. Win, F. Charlotte, A. Mallat et al., "Mitogenic effect of transforming growth factor-beta 1 on human Ito cells in culture: evidence for mediation by endogenous platelet-derived growth factor," *Hepatology*, vol. 18, pp. 137–145, 1993.

[48] B. Brown, K. Lindberg, J. Reing, D. B. Stolz, and S. F. Badylak, "The basement membrane component of biologic scaffolds derived from extracellular matrix," *Tissue Engineering*, vol. 12, no. 3, pp. 519–526, 2006.

[49] S. Djudjaj and P. Boor, "Cellular and molecular mechanisms of kidney fibrosis," *Molecular Aspects of Medicine*, vol. 65, 2019.

[50] Y. Xia, B. Yu, C. Ma et al., "Yu Gan Long reduces rat liver fibrosis by blocking TGF-β1/Smad pathway and modulating the immunity," *Biomedicine & Pharmacotherapy*, vol. 106, pp. 1332–1338, 2018.

[51] X. M. Meng, D. J. Nikolic-Paterson, and H. Y. Lan, "TGF-β: the master regulator of fibrosis," *Nature Reviews Nephrology*, vol. 12, no. 6, pp. 325–338, 2016.

[52] K. Breitkopf, P. Godoy, L. Ciuclan, M. V. Singer, and S. Dooley, "TGF-beta/Smad signaling in the injured liver," *Zeitschrift für Gastroenterologie*, vol. 44, no. 1, pp. 57–66, 2006.

[53] Z. J. Xu, J. G. Fan, X. D. Ding, L. Qiao, and G. L. Wang, "Characterization of high-fat, diet-induced, non-alcoholic steatohepatitis with fibrosis in rats," *Digestive Diseases and Sciences*, vol. 55, no. 4, pp. 931–940, 2010.

[54] L. Wu, Q. Zhang, W. Mo et al., "Quercetin prevents hepatic fibrosis by inhibiting hepatic stellate cell activation and reducing autophagy via the TGF-β1/Smads and PI3K/Akt pathways," *Scientific Reports*, vol. 7, no. 1, 2017.

[55] S. L. Friedman, "Hepatic stellate cells: protean, multifunctional, and enigmatic cells of the liver," *Physiological Reviews*, vol. 88, no. 1, pp. 125–172, 2008.

Hindawi
Evidence-Based Complementary and Alternative Medicine
Volume 2022, Article ID 3294273, 10 pages
https://doi.org/10.1155/2022/3294273

Research Article

Changes in Mitochondria-Related Gene Expression upon Acupuncture at LR3 in the D-Galactosamine-Induced Liver Damage Rat Model

Yu-Mi Lee,[1] Dong-Hee Choi,[2] Min-Woo Cheon,[3] Jae Gwan Kim,[1] Jeong-Sang Kim,[2] Myung-Geun Shin,[4] Hye-Ran Kim,[2] and Daehwan Youn[2]

[1]*Department of Biomedical Science and Engineering, Institute of Integrated Technology, Gwangju Institute of Science and Technology(GIST), Gwangju, Republic of Korea*
[2]*Department of Korean Medicine, School of Dongshin University, Naju, Jeollanam-do 58245, Republic of Korea*
[3]*Department of Health Administration, Dongshin University, Naju, Jeollanam-do 58245, Republic of Korea*
[4]*Department of Laboratory Medicine, Chonnam National University Medical School and Chonnam National University Hwasun Hospital, Hwasun, Republic of Korea*

Correspondence should be addressed to Hye-Ran Kim; hrkim@dsu.ac.kr and Daehwan Youn; human22@dsu.ac.kr

Received 15 February 2022; Revised 8 June 2022; Accepted 9 June 2022; Published 29 June 2022

Academic Editor: Chan-Yen Kuo

Hepatic diseases, such as hepatonecrosis, hepatitis, and hepatocirrhosis, are associated with mitochondrial dysfunction and increased reactive oxygen species generation and inflammation, ultimately leading to liver failure. In this study, we examined if acupuncture at LR3 can affect mitochondria-related gene expression in a liver damage model of experimentally induced acute liver failure (ALF). ALF was induced by the intraperitoneal injection of D-galactosamine (D-GalN) in experimental rats, who then received either sham (ALF), manual acupuncture (MA), electroacupuncture (EA), or silymarin (PC, positive control) treatment. Liver tissues were extracted from experimental and untreated control rats for histopathological analysis and expression profiling of genes involved in mitochondrial function. Of the 168 mitochondria-related genes profiled, two genes belonging to the solute-carrier transporter family (*Slc25a15* and *Slc25a25*) and *Ndufb7* were upregulated. Gamma-glutamylcysteine synthetase was more downregulated in MA than ALF. Furthermore, MA reversed D-GalN-induced inflammatory cell infiltration, destruction of hepatic cell plates, and increase in the levels of the proinflammatory cytokine TNF-α. MA at LR3 can reduce the risk of D-GalN-induced ALF by inducing the expression of metabolic and inflammation-related genes and regulating proinflammatory factor production in hepatic mitochondria.

1. Introduction

Acupuncture is one of the most widely used treatment methods in traditional Asian medicine for preventing and relieving the symptoms of acute and chronic pathophysiological conditions owing to its efficacy and safety [1–3]. Animal model studies have suggested its therapeutic value in liver disease. Liu et al. [4] reported that electroacupuncture (EA) at PC6 mitigated endotoxin-induced liver dysfunction in rats. Yim et al. [5] reported that acupuncture at GB34 reduced CCl_4-induced liver toxicity and protected liver function. Moreover, EA at LR3 and TE4 was reported to prevent experimental acute liver failure (ALF) in rats [6], and acupuncture at LR3 prevented hepatocellular apoptosis [7].

ALF may be induced by drugs, viruses, and autoimmune infections [8], frequently leading to rapidly advancing multiorgan failure [9]. The mortality rate in ALF is high despite treatment, and patients may require a liver transplant for survival [10]. Mitochondrial dysfunction is a major contributor to hepatocellular injury in ALF [11]. Mitochondrial (mt) DNA damage causes dysfunctions in the

mitochondrial respiratory chain and tricarboxylic acid cycle by decreasing mitochondrial transcription and inhibiting mitochondrial protein synthesis, inducing cell dysfunction or necrosis [11, 12].

Several studies have demonstrated the beneficial effects of acupuncture on mitochondrial function, including increased cytochrome *c* oxidase (complex IV) activity following acupuncture at LR3 [13]. Li et al. [14] reported that acupuncture significantly improved mitochondrial bioenergetic parameters, such as respiratory control rates and membrane potential, and prevented cognitive deficits associated with hippocampal mitochondrial dysfunction. Wang et al. [15] reported that EA treatment at CV4 and ST36 and manual acupuncture (MA) at GV20 reduced hepatic mitochondrial oxygen consumption in aging animals, leading to an improved respiratory control rate and phosphorus/oxygen ratio. However, few studies have examined the effects of acupuncture on liver disease.

In this study, we examined the effects of acupuncture at LR3 on mitochondria-related gene expression in a liver damage model of experimentally induced ALF and evaluated the underlying mechanisms.

2. Materials and Methods

2.1. Animals. Pathogen-free male Wistar rats (150–180 g) were purchased from SamTako Bio (Osan, Korea) and housed under controlled temperature (24-25°C) and humidity (40%–60%) and a 12 h-12 h dark-light cycle with ad libitum access to filtered tap water and food (Pellet, GMO, Korea). All animal care and experimental protocols were approved by the College Animal Management and Use Commission of Dongshin University (approval number: DSU-2019-05-02). All efforts were made to minimize animal suffering.

2.2. Induction of ALF and Grouping. Twenty-five male Wistar rats were randomly divided into five groups, including four experimental groups (ALF, positive control (PC), MA, and EA) and one untreated control group (control). Experimental animals were first injected with D-GalN (Sigma, St. Louis, USA; 700 mg/kg, intraperitoneal injection; i.p.) to induce ALF [16] and then given sham treatment (ALF), acupuncture treatment (MA or EA performed once every 3 d, for a total of seven administrations), or silymarin (Sigma, St. Louis, USA; 700 mg/kg, p.o.) 6 h after ALF induction as PC. All rats were euthanized by anesthesia overdose 24 h after ALF was induced.

2.3. Acupuncture Stimulation. Acupuncture was conducted as described by Choi et al. [13] at LR3 following the standard method [17]. The rats were subjected to inhalation anesthesia (following induction with 5% isoflurane, anesthesia was maintained at a concentration of 2%). Settings of the EA apparatus were adjusted to 3 V and 10 Hz, and a needle was placed into the muscle layer at the acupoint at a depth of 2-3 mm. The positive charge was introduced at the right acupoint and the negative charge at the left acupoint. Stimulation was performed for 5 min.

2.4. RNA Isolation. The liver tissue was washed three times with PBS, cut into 50 mg samples, and lysed with 1 mL of TRIzol reagent (Thermo Fisher Scientific, Waltham, USA). Whole-cell RNA was extracted using a standard protocol [18], and the yield was measured using the nanodrop spectrophotometer (Thermo Fisher Scientific, Waltham, USA). Reverse transcription was performed using the RT^2 First Strand Kit (Qiagen, Valencia, USA), according to the manufacturer's instructions.

2.5. Quantitative RT-PCR Array for Mitochondria-Related Gene Expression. The Rat Mitochondria and Mitochondrial Metabolism RT^2 Profiler PCR arrays (Qiagen, Valencia, USA) were used for quantifying real-time PCR expression of 164 mitochondrial genes (84 per array). Real-time PCR for the RT^2 profiler PCR array was performed using the RT^2 SYBR Green qPCR MasterMix and oligo-dT primers (Qiagen, Valencia, USA).

2.6. Tumor Necrosis Factor-α Levels. Tumor necrosis factor-α (TNF-α) was quantified using a kit (Thermo Fisher Scientific, Waltham, USA) in plasma samples acquired 24 h after ALF induction using a microplate-based spectrophotometer (Biochrom, Cambridge, UK), according to an automated procedure [19].

2.7. Histopathological Analysis and Immunohistochemistry. Liver tissues were fixed in Bouin's solution (Sigma, St. Louis, USA), embedded in paraffin, sectioned at 6 μm, and stained using hematoxylin and eosin (H&E; Sigma, St. Louis, USA) and Masson's trichrome stain (Trichome stain kit; ScyTek Laboratories, West Logan, USA) using standard protocols [20, 21]. Nuclear counterstaining was performed using hematoxylin, and the samples were examined using light microscopy (Nikon, Tokyo, Japan). For *Slc25a15* immunostaining, the samples were incubated first with 1 : 300 dilutions of the anti-*Slc25a15* antibody (Abcam, Cambridge, UK) and then with a biotinylated anti-mouse IgG (Vectastain ABC Kit; Vector Labs, Burlingame, USA). The sections were incubated with the avidin–biotin–peroxidase complex (Vectastain ABC Kit; Vector Labs, Burlingame, USA) and DAB. The Celleste image analysis software (Thermo Fisher Scientific, Waltham, USA) was used to count the number of immunoreactive cells.

2.8. Data Analysis

2.8.1. Statistical Analyses for Arrays. Real-time PCR data were analyzed through the ΔΔCt method using the Qiagen Gene Globe Data Analysis Center portal (https://www.qiagen.com/us/shop/genesand-pathways/data-analysis-center-overview-page). Control wells of real-time PCR arrays detect genomic contamination and serve as reverse transcription and positive PCR controls. The following five reference

genes were used for data normalization: beta-actin, lactate dehydrogenase A, ribosomal protein large P1, beta-2 microglobulin, and hypoxanthine phosphoribosyltransferase 1. Genes with an absolute fold-change in expression > 2 at a $p < 0.05$ relative to other groups were considered differentially expressed and selected for comparative analysis.

2.8.2. Statistical Analyses for ELISA and IHC. The GraphPad Prism 8.4.1 Software (GraphPad Software, San Diego, USA) was used for computational and statistical analyses. Tukey's multiple comparison test was used to estimate the normality of all results. The results are expressed as mean ± SD. A p value of < 0.05 was considered statistically significant.

3. Results

3.1. Manual Acupuncture Reversed the Liver Damage-Associated Dysregulation of Mitochondrial Genes. To evaluate whether acupuncture treatment had an effect on the mitochondrial gene expression profiles of rat liver, tissues from ALF, control, PC, MA, and EA were analyzed to identify 84 mitochondria genes using the RT^2 profiler PCR arrays test.

A total of 68 genes showed statistically significant changes in comparison with those in ALF (Supplementary Table 1). In the control group, 29 genes (12 up and 17 downregulated) showed changes compared with ALF; *Bid*, BH3-interacting domain death agonist (*Bid*), and gamma-glutamylcysteine synthetase (*Gclc*) were downregulated, and *Slc25a15* and *Slc25a25* were significantly upregulated. In PC, 44 genes (1 up and 43 downregulated) showed changes compared with ALF; *Bid* and *Gclc* were downregulated. In MA, 37 genes (16 up and 21 downregulated) showed changes compared with ALF; *Gclc* was downregulated; *Slc25a15* and *Slc25a25* were upregulated. In EA, 43 genes (9 up and 34 downregulated) showed changes compared with ALF; *Bid* and *Gclc* were downregulated (Figures 1 and 2(a)).

To explore whether acupuncture treatment had any effect on expression profiles of genes involved in the mitochondrial energy metabolism of rat liver, tissues from ALF, control, PC, MA, and EA were analyzed using the RT^2 profiler PCR arrays to identify 84 mitochondrial energy metabolism genes.

A total of 38 genes showed significant changes when compared with those in ALF (Supplementary Table 2).

In the control, 28 genes (4 up and 24 downregulated) showed changes compared with ALF; *Ndufb7* and *Slc25a15* were upregulated. In PC, 21 genes (all downregulated) showed changes compared with ALF. However, there were no markers in PC among these genes. In MA, 21 genes (2 up and 19 downregulated) showed changes compared with ALF; *Ndufb7* and *Slc25a15* were upregulated. In EA, 27 genes (7 up and 20 downregulated) showed changes compared with ALF. However, there were no markers in EA among these genes (Figures 3 and 2(b)).

Therefore, results from the evaluation of mitochondria and mitochondrial energy metabolism genes revealed that *Slc25a15* is a key gene in MA.

Notably, differences in expression between MA and ALF resembled patterns between control and ALF (Figure 4), suggesting that MA reversed ALF-induced expression changes. We speculate that the reversal of ALF-associated expression changes by MA could help protect mitochondrial function, thereby reducing inflammation and tissue degeneration.

3.2. Manual Acupuncture Protects against TNF-α-Mediated Hepatic Tissue Damage by Upregulating Slc25a15. Results from H&E staining revealed higher inflammatory infiltration, congestion, and tissue collapse in the liver tissue of ALF compared with the liver tissue in the control. All treatment groups showed lesser inflammatory infiltration and tissue damage than ALF. Notably, lesser inflammatory infiltration and tissue damage were observed in MA than in other treatment groups (Figure 5(a)).

Results from Masson's trichrome staining revealed that ALF showed an increase in collagen fiber deposition in the liver tissue, with each treatment group showing lesser collagen fiber deposition than ALF. In MA, lesser fibrotic deposition and congestion were observed than in other treatment groups (Figure 5(b)).

Results from immunohistostaining revealed the distribution of *Slc25a15*, a key gene of the mitochondria and mitochondrial energy metabolism. High expression was observed in the liver in control and MA groups (Figures 5(c) and 5(d)).

Furthermore, consistent with the potential protective effect of MA-induced changes in gene expression, the increased expression of proinflammatory TNF-α in ALF compared with the control ($p < 0.0001$) was reversed in PC and MA ($p < 0.01$) (Figure 5(e)).

Notes: ALF, acute liver failure and no treatment; control, no induction and no treatment; PC, silymarin treatment; MA, manual acupuncture treatment; EA, electro-acupuncture treatment.

4. Discussion

Mitochondria dysfunction is a major driver of cellular inflammatory responses and apoptosis and thus contributes to many pathological conditions [22]. Mitochondrial factors contributing to cell death include cytochrome c, endonuclease G apoptosis-inducing factor, Smac/DIABLO, HtrA2/OMI, and adenylate kinase 2 [23]. Mutations in mtDNA caused by mitochondrial dysfunction were reported to contribute to the pathogenesis of chronic inflammatory diseases, including neuromuscular and neurodegenerative disorders [24]. However, little is known regarding the contributions of mitochondrial gene dysregulation in disease or the potential protective efficacy of reversing this dysregulation. Through this study, we demonstrated the association between liver damage and dysregulation of multiple mitochondria-associated genes using a model of experimentally induced ALF and that acupuncture can be used to reverse this dysregulation and attenuate early degeneration and immune cell infiltration of liver tissue.

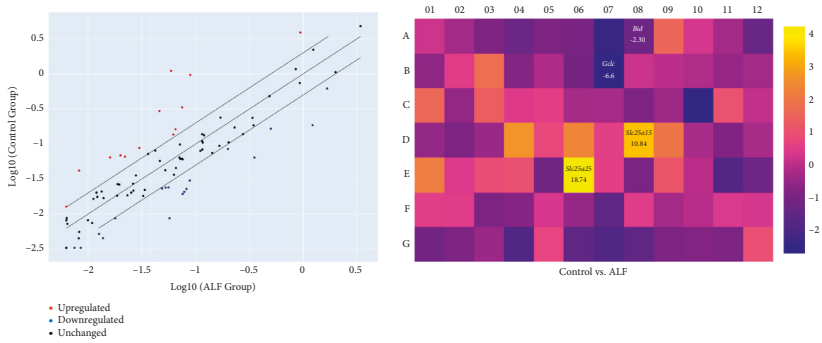

Gene symbol	Fold change	Function
Bid	-2.30	Apoptosis
Gclc	-6.60	Membrane Polarization & Potential
Slc25a15	10.84	Small Molecule Transport
Slc25a25	18.74	Small Molecule Transport

(a)

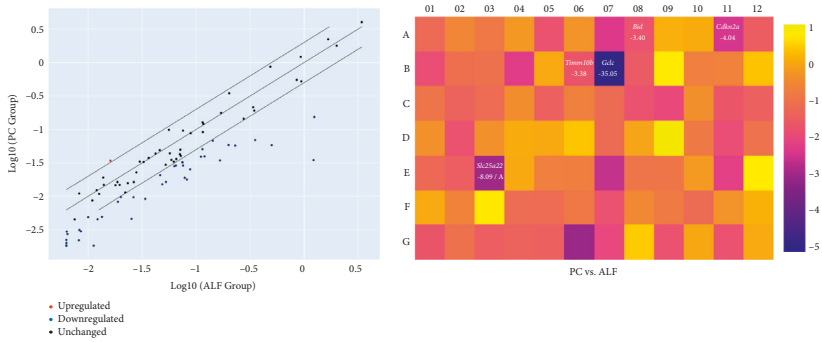

Gene symbol	Fold change	Function
Bid	-2.30	Apoptosis
Cdkn2a	-4.04	Apoptosis
Timm10b	-3.38	Inner Membrane Translocation
Gclc	-35.05	Membrane Polarization & Potential
Slc25a22	-8.09	Small Molecule Transport

(b)

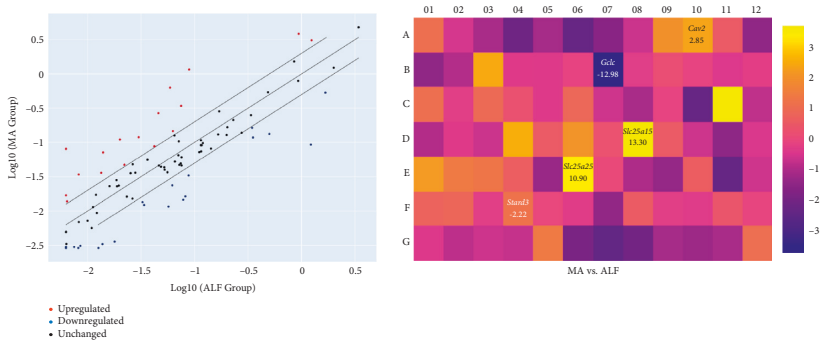

Gene symbol	Fold change	Function
Cav2	2.85	Mitochondrion Protein Import, Apoptosis
Gclc	-13.24	Membrane Polarization & Potential
Slc25a15	13.04	Small Molecule Transport
Slc25a25	10.69	Small Molecule Transport
Stard3	-2.22	Exporting cholesterol

(c)

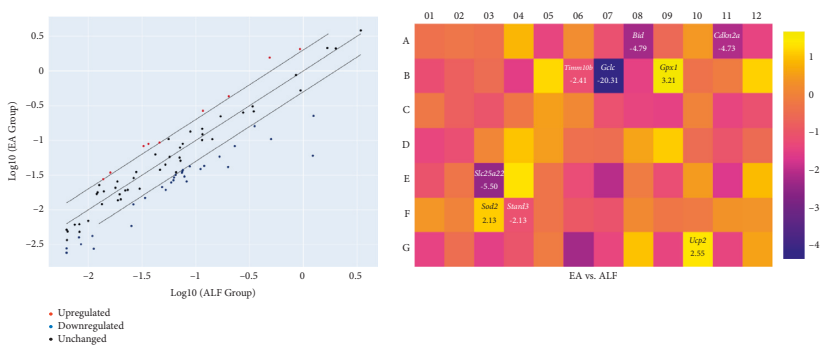

Gene symbol	Fold change	Function
Bid	-4.79	Apoptosis
Cdkn2a	-4.73	Apoptosis
Timm10b	-2.41	Inner Membrane Translocation
Gclc	-20.31	Membrane Polarization & Potential
Gpx1	3.21	Mitochondrion Protein Import, Apoptosis
Slc25a22	-5.50	Small Molecule Transport
Sod2	2.13	Apoptosis
Stard3	-2.13	Exporting cholesterol
Ucp2	2.55	Membrane Polarization & Potential, Mitochondrial

(d)

Figure 1: Expression profiles of mitochondria-related genes following chemically induced acute liver failure (ALF) were measured using a real-time PCR array. Differentially expressed genes are defined relative to ALF. (a) ALF vs. control. (b) ALF vs. silymarin (PC, positive control). (c) ALF vs. manual acupuncture (MA). (d) ALF vs. electroacupuncture (EA). The panels on the left show scatterplots ($p < 0.05$ vs. ALF); those in the middle show heatmaps of differential expression; and the ones on the right show tables of fold regulation.

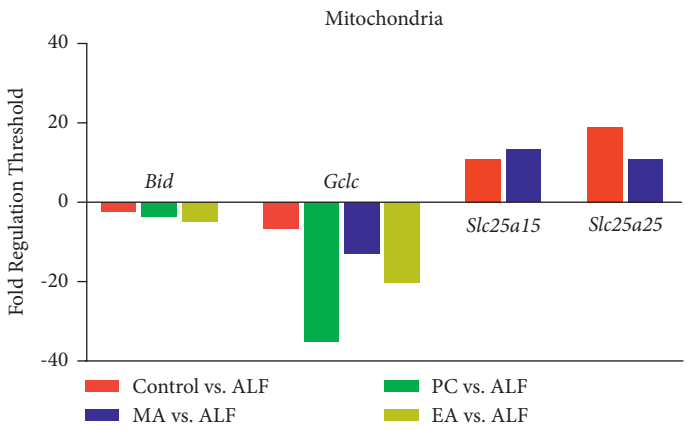

Mitochondria Key gens

Gene	Control	PC	MA	EA
Bid	-2.30	-3.4		-4.79
Gclc	-6.47	-35.05	-12.98	-20.31
Slc25a15	11.05		13.3	
Slc25a25	19.10		10.9	

(a)

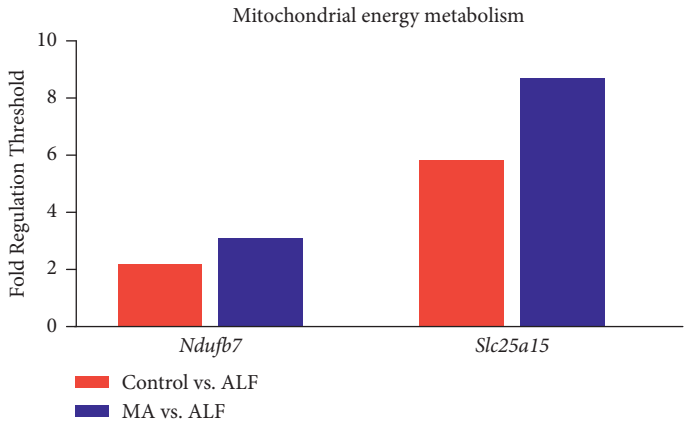

Mitochondrial energy metabolism Key gens

Gene	Control	PC	MA	EA
Ndufb7	2.21		3.1	
Slc25a15	5.81		8.7	

(b)

Figure 2: Fold-change in the expression levels of genes included in the (a) mitochondrial and (b) mitochondrial energy metabolism real-time PCR arrays. ALF, acute liver failure and no treatment; control, no induction and no treatment; PC, silymarin treatment; MA, manual acupuncture treatment; EA, electroacupuncture treatment.

D-GalN induces ALF by triggering ROS production, followed by hepatic inflammation and apoptosis [25], which are pathogenic processes implicated in many liver diseases. Thus, D-GalN-induced ALF is a widely used model of hepatic injury [26]. D-GalN reduces mitochondrial membrane fluidity and the activity of mitochondrial enzymes and ion transporters, resulting in metabolic failure and ultimately hepatic failure [27].

Silymarin is a polyphenolic flavonoid derived from milk thistle (*Silybum marianum*), and it is used as a standard agent that exhibited significant hepatoprotective activity in addition to anti-inflammatory, cytoprotective, and anti-carcinogenic effects against D-GalN [28].

In this study, we screened 168 genes, related to the mitochondria and mitochondrial energy metabolism, to analyze the effect of acupuncture at LR3 on genes that regulate the reversal of liver damage in a rat model.

Bid was cloned based on its ability to interact with both Bcl-2 and Bax. Bid only contains the BH3 domain, which is required for its interaction with the Bcl-2 family proteins and for its proapoptotic activity [29].

In this study, *Bid* expression was downregulated in all experimental groups, except in MA, compared with ALF. Unlike MA, EA affected *Bid* expression.

Gclc catalyzes the first rate-limiting step of glutathione synthesis and encodes a catalytic and light regulatory subunit. *Gclc* overexpression was reported to inhibit endoplasmic reticulum stress and the downstream inflammatory factor [30].

In this study, *Gclc* expression was downregulated in all experimental groups compared with the ALF. MA and EA may facilitate a mechanism for the maintenance of cellular GSH homeostasis.

Slc25a25 belongs to a family of calcium-binding mitochondrial carriers. The protein encoded by *Slc25a25* binds PGC-1a, which acts as an ATP carrier. *Slc25a25* is also involved in the regulation of glucagon, the deficiency or depletion of which can reduce glucose-dependent ATP production [31]. In this study, we found that the restoration of normal expression levels by MA can help maintain the ATP supply required to mitigate the effects of D-GalN.

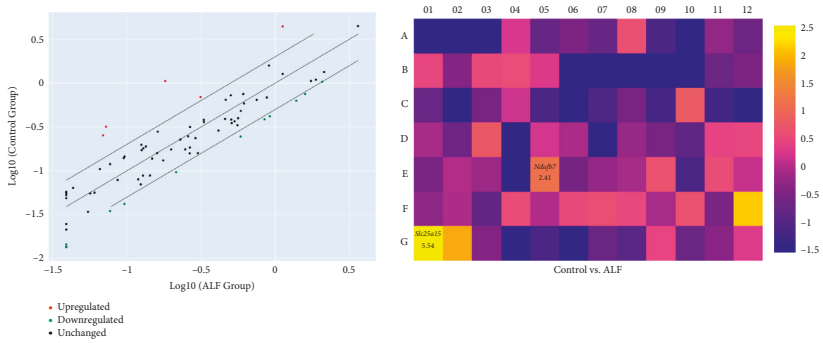

Gene symbol	Fold change	Function
Ndufb7	2.41	Complex I (NADH-Coenayme Q Reductase)
Slc25a15	5.54	Electron Transport Chain & Phosphorylation Accessory Proteins

(a)

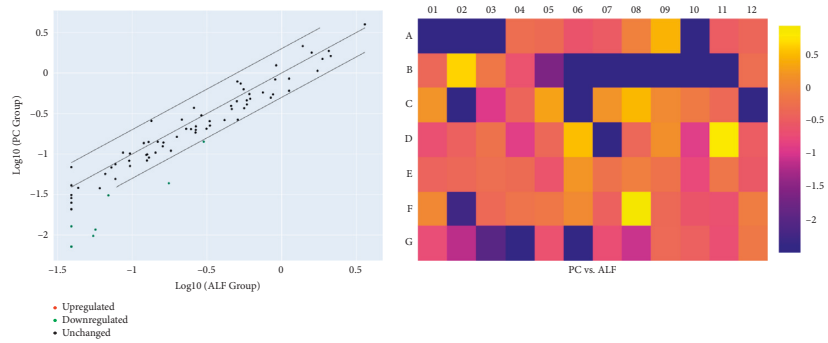

Gene symbol	Fold change	Function
Not Found		

(b)

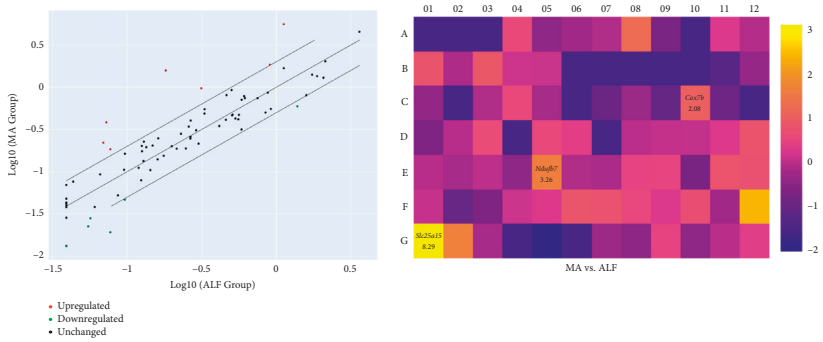

Gene symbol	Fold change	Function
Cox7b	2.08	Electron transport Chain
Ndufb7	3.26	Complex I (NADH-Coenayme Q Reductase)
Slc25a15	8.29	Electron Transport Chain & Phosphorylation Accessory Proteins

(c)

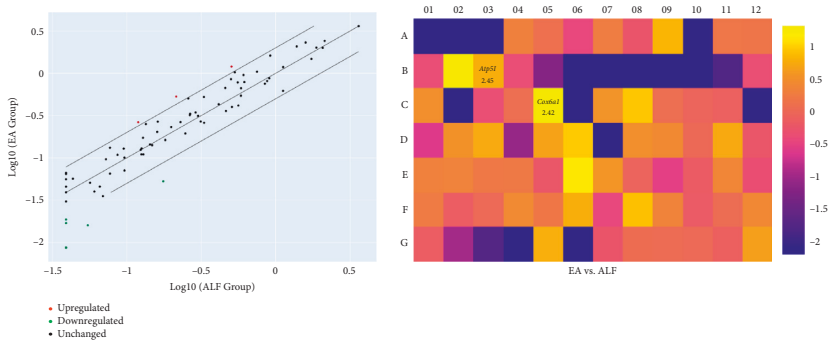

Gene symbol	Fold change	Function
Atp5I	2.45	ATP synthase, mitochondrial F0 complex
Cox6a1	2.47	Complex IV (Cytochrome c Oxidase)

(d)

Figure 3: Expression profiles of genes related to the mitochondrial metabolism following chemically induced acute liver failure (ALF), measured using real-time PCR arrays. Differentially expressed genes are defined relative to ALF. (a) ALF vs. control. (b) ALF vs. silymarin (PC, positive control). (c) ALF vs. manual acupuncture (MA). (d) ALF vs. electroacupuncture (EA). The panels on the left show scatterplots ($p < 0.05$ vs. ALF), panels in the middle show heatmaps of differential expression, and those on the right show tables of fold regulation.

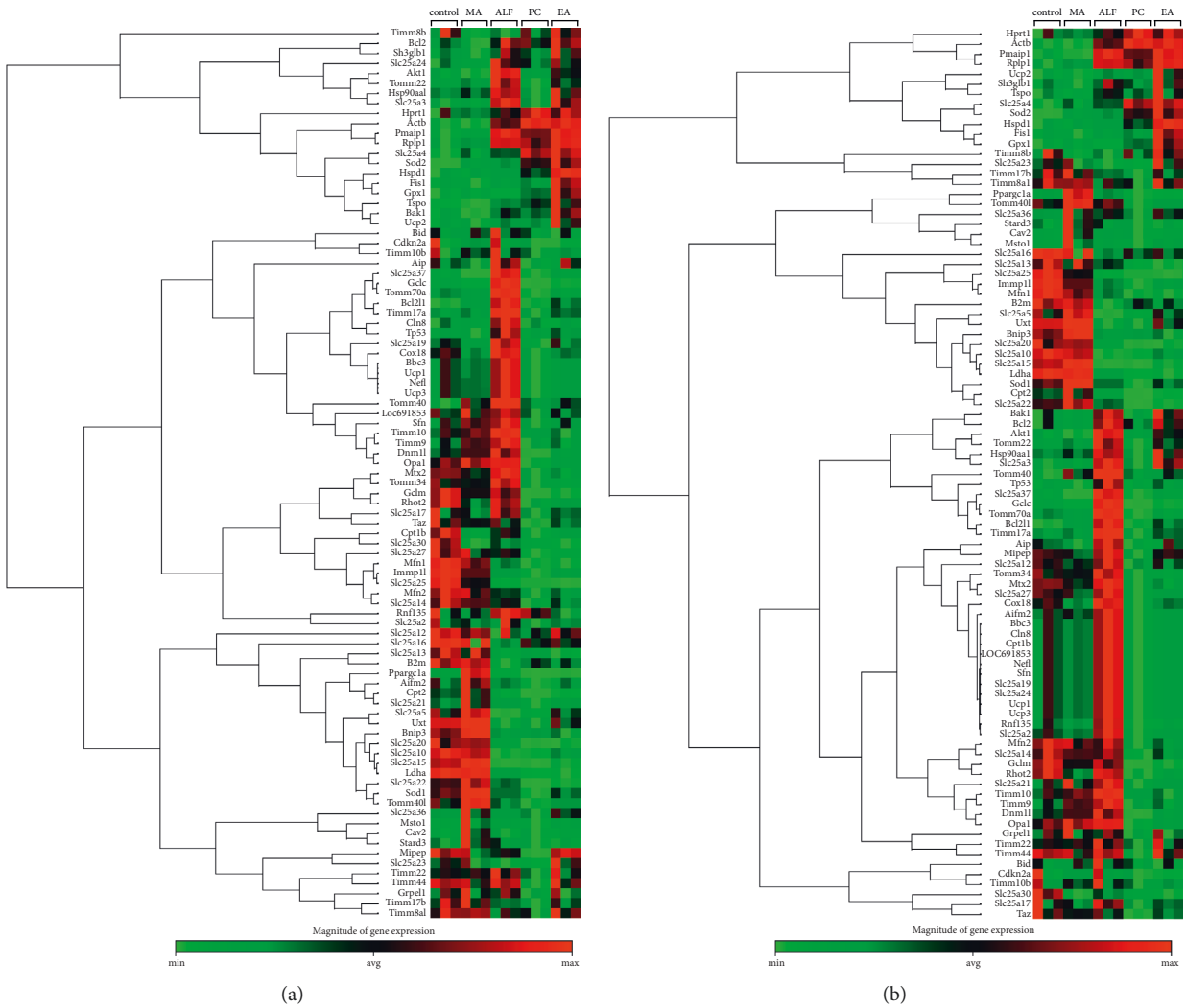

Figure 4: Clustergram of the (a) mitochondrial and (b) mitochondrial energy metabolism real-time PCR array results. The clustergram shows the nonsupervised hierarchical clustering dendrogram and heatmap identifying coregulated genes across groups. Red means higher expression and green means lower expression.

Ndufb7 contributes to the regulation of complex I (NADH-coenzyme Q reductase) functions. The absence or deficiency of *Ndufb7* induces complex I defects. Rescue of function with *Ndufb7* restores complex I activation [32]. In this study, we have shown that the restoration of *Ndufb7* expression may contribute to MA-mediated hepatoprotection by sustaining complex I activity.

Slc25a15 is a member of the mitochondrial carrier family and provides instructions for making a protein called mitochondrial ornithine transporter 1. The encoded protein transports ornithine across the inner mitochondrial membrane from the cytosol to the mitochondrial matrix. The protein is an essential component of the urea cycle and functions in ammonium detoxification and arginine biosynthesis. *Slc25a15* was reported to be associated with the involvement of ornithine in the brain energy metabolism homeostasis, cellular ATP transfer, and inflammation. [33].

In this study, *Slc25a15* expression was upregulated in MA compared with ALF in both mitochondrial and mitochondrial energy metabolism genes. MA most likely contributes to hepatoprotective effects against D-GalN by regulating the expression of proinflammatory genes.

Several mitochondrial carriers, such as *Slc25a15*, are involved in the inflammatory process [34]. Therefore, we conducted histopathological analysis and measured blood concentrations of the proinflammatory factor TNF-α. MA reversed D-GalN-induced upregulation of TNF-α, suggesting that MA protects against hepatic damage by suppressing system inflammation. Acupuncture at ST36, CV4, and KI1 was reported to reduce inflammatory factors, such as TNF-α, and inflammatory cell infiltration in a nonalcoholic fatty liver disease model [35]. Moreover, MA at ST36 regulated inflammatory factors in hepatitis models [36].

Liver damage was also assessed by using H&E with Masson's trichrome staining to evaluate the disruption of the cellular structure in the liver and fibrotic septa [37].

H&E staining revealed that inflammatory cell infiltration, destruction of hepatic cell plates, and structural

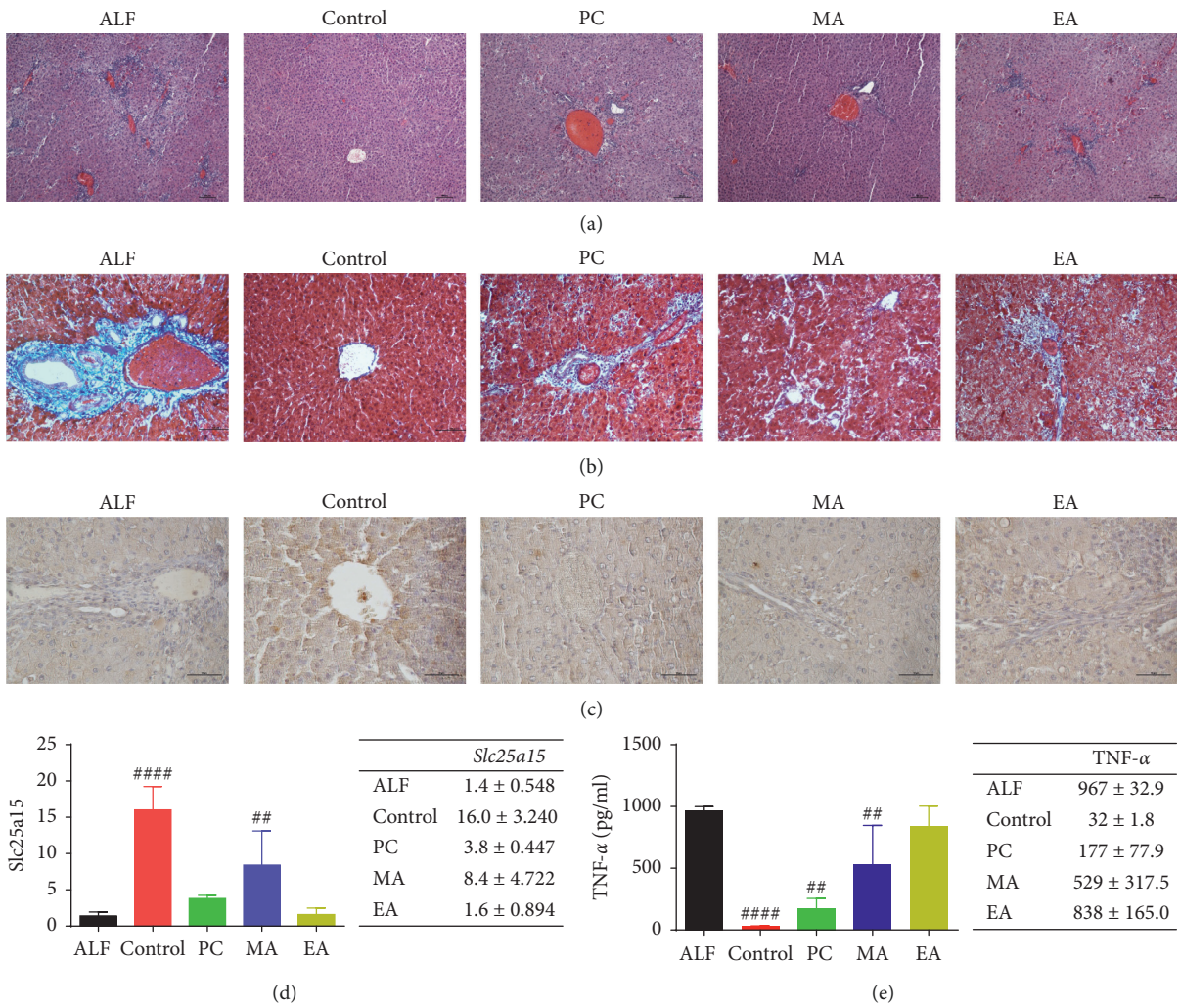

	Slc25a15
ALF	1.4 ± 0.548
Control	16.0 ± 3.240
PC	3.8 ± 0.447
MA	8.4 ± 4.722
EA	1.6 ± 0.894

	TNF-α
ALF	967 ± 32.9
Control	32 ± 1.8
PC	177 ± 77.9
MA	529 ± 317.5
EA	838 ± 165.0

Figure 5: Representative photomicrographs of liver histology. (a) Hematoxylin and eosin (magnification: 100x) and (b) Masson's trichrome (magnification: 200x) staining. (c), (d) Immunohistochemical observation of *Slc25a15* in the liver tissue. Data are presented as mean ± SD. $^{\#\#\#\#}P < 0.0001$, $^{\#\#}p < 0.01$ vs. ALF (magnification: 400x). (e) TNF-α concentration in blood samples obtained 24 h after ALF induction. Data are presented as mean ± SD. $^{\#\#\#\#}P < 0.0001$, $^{\#\#}p < 0.01$ vs. ALF.

disruption of hepatic lobules observed in ALF was mitigated by MA, and Masson's trichrome staining showed that tissue damage and fibrosis observed in ALF were mitigated by MA.

The histological observations demonstrate that the hepatoprotective effect of MA may result from the regulation of inflammatory factors.

To confirm *Slc25a15* expression, the immunohistochemical distribution of *Slc25a15* in liver tissue was observed and appeared to be similarly upregulated in control and MA in both mitochondria and mitochondria energy metabolism genes. We confirmed that the immunoreactivity of *Slc25a15* in control and MA increased compared with that in ALF, which was the same as the results of the RT^2 profiler PCR array.

In summary, our results from screening gene expression profiles and histopathological, immunohistochemical, and proinflammatory mediator analyses demonstrated that the MA-induced reduction in TNF-α reflects a reduction in hepatic inflammation due to the preservation of mitochondrial function, which in turn results from the restoration of *Slc25a15* expression levels in D-GalN-induced liver damage.

Limitations of this study include the lack of basic liver function tests, observations of inflammation-linked mechanisms or proteins related to inflammation, and observations during the recovery period following hepatic injury. Further investigations are required to confirm the hepatoprotective mechanisms of MA through cross-validation of mitochondrial genes and inflammation-related proteins.

5. Conclusions

Reduction of inflammation in liver tissue and recovery of the histological structure were observed. The MA group showed recovery compared with other experimental groups. A reduction in the TNF-α level was observed after this type of acupuncture stimulation. The recovery effect was linked to changes in the expression of *Slc25a15*, which is one of the 168 genes in the mitochondria.

Collectively, these results suggest that acupuncture can reduce liver injury by upregulating genes associated with the mitochondria and mitochondrial energy metabolism, thereby reducing inflammation and hepatic cell apoptosis.

Data Availability

The datasets used and analyzed during this study are available from the corresponding author upon request.

Conflicts of Interest

The authors declare that there are no conflicts of interest.

Authors' Contributions

Yu-Mi Lee and Dong-Hee Choi contributed equally to the writing of this article.

Acknowledgments

This work was supported by the National Research Foundation (NFR) of Korea (NRF-2018R1D1A1A02046580).

Supplementary Materials

Information on profiling genes that showed significant changes among a total of 164 mitochondrial-related genes are given in supplementary tables. Supplementary Table 1: profiling of 84 mitochondria genes related to membrane polarization and potential, mitochondrial transport, small molecule transport, targeting proteins to mitochondria, mitochondrion protein import, outer membrane translocation, inner membrane translocation, mitochondrial fission and fusion, mitochondrial localization, and apoptosis obtained identified 68 differentially expressed genes relative to the ALF group. Supplementary Table 2: profiling of 84 genes related to complex I, complex II, complex III, complex IV, electron transport chain, and oxidative phosphorylation identified 38 differentially expressed genes relative to the ALF group. (*Supplementary Materials*)

References

[1] W. Dong, W. Yang, F. Li et al., "Electroacupuncture improves synaptic function in SAMP8 mice probably via inhibition of the AMPK/eEF2K/eEF2 signaling pathway," *Evidence-Based Complementary and Alternative Medicine*, vol. 2019, Article ID 8260815, 10 pages, 2019.

[2] Z. Q. Guo, Y. Huang, H. Jiang, and W. B. Wang, "Randomized clinical trials of early acupuncture treatment of limb paralysis in traumatic brain injury patients and its mechanism," *Zhen Ci Yan Jiu*, vol. 44, no. 8, pp. 589–593, 2019.

[3] Y. Y. Zhang, X. H. Li, and M. X. Wu, "Effect of electroacupuncture at Wnt/β-catenin signaling pathway on inhibiting cartilage degeneration in rats with knee osteoarthritis," *Zhongguo Zhen Jiu*, vol. 39, no. 10, pp. 1081–1086, 2019.

[4] H. W. Liu, M. C. Liu, C. M. Tsao, M. H. Liao, and C. C. Wu, "Electro-acupuncture at "Neiguan"—(Pc6) attenuates liver injury in endotoxaemic rats," *Acupuncture in Medicine*, vol. 29, no. 4, pp. 284–288, 2011.

[5] Y. K. Yim, H. Lee, K. E. Hong et al., "Hepatoprotective effect of manual acupuncture at acupoint GB34 against CCl4-induced chronic liver damage in rats," *World Journal of Gastroenterology*, vol. 12, no. 14, p. 2245, 2006.

[6] D.-H. Youn and C.-S. Na, "Hepatoprotective effects of electroacupuncture at Taechung (LR3) and Yangji (TE4) on experimental liver injury in rats," *Korean Journal of Acupuncture*, vol. 23, pp. 167–176, 2006.

[7] H. Y. Shin, H. J. Lee, S. C. Lim et al., "The protective effects of acupuncture on the liver in the oxidative stress caused by cadmium," *The Acupuncture*, vol. 31, no. 4, pp. 33–43, 2014.

[8] S. Chu, Z. Niu, Q. Guo et al., "Combination of monoammonium glycyrrhizinate and cysteine hydrochloride ameliorated lipopolysaccharide/galactosamine-induced acute liver injury through Nrf2/ARE pathway," *European Journal of Pharmacology*, vol. 882, Article ID 173258, 2020.

[9] W. Bernal, G. Auzinger, A. Dhawan, and J. Wendon, "Acute liver failure," *The Lancet*, vol. 376, no. 9736, pp. 190–201, 2010.

[10] K. Rasineni, S. M. L. Lee, B. L. McVicker, N. A. Osna, C. A. Casey, and K. K. Kharbanda, "Susceptibility of asialoglycoprotein receptor-deficient mice to lps/galactosamine liver injury and protection by betaine administration," *Biology*, vol. 10, no. 1, p. 19, 2020.

[11] D. Pessayre, B. Fromenty, A. Berson et al., "Central role of mitochondria in drug-induced liver injury," *Drug Metabolism Reviews*, vol. 44, no. 1, pp. 34–87, 2012.

[12] D. Han, L. Dara, S. Win et al., "Regulation of drug-induced liver injury by signal transduction pathways: critical role of mitochondria," *Trends in Pharmacological Sciences*, vol. 34, no. 4, pp. 243–253, 2013.

[13] D. Choi, Y. Lee, M. Kim et al., "The effects of acupuncture at LR3 acupoint on mitochondrial complex IV oxidase activity in liver," *Korean Journal of Acupuncture*, vol. 36, no. 4, pp. 200–209, 2019.

[14] H. Li, Y. Liu, L. T. Lin et al., "Acupuncture reversed hippocampal mitochondrial dysfunction in vascular dementia rats," *Neurochemistry International*, vol. 92, pp. 35–42, 2016.

[15] H. Wang, J. Liu, J.-M. Liu, J.-F. Lü, M.-Y. Chen, and J.-Z. Wang, "Effect of electroacupuncture stimulation of "Guanyuan" (CV 4), bilateral "Housanli" (ST 36), etc. on anti-fatigue ability and liver mitochondrial respiratory function in ageing rats with Yang-deficiency," *Zhen Ci Yan Jiu*, vol. 38, no. 4, pp. 259–264, 2013.

[16] A. A. Ganai, A. A. Khan, Z. A. Malik, and H. Farooqi, "Genistein modulates the expression of NF-κB and MAPK (p-38 and ERK1/2), thereby attenuating d-galactosamine induced fulminant hepatic failure in wistar rats," *Toxicology and Applied Pharmacology*, vol. 283, no. 2, pp. 139–146, 2015.

[17] World Health Organization (WHO) Regional Office for the Western Pacific, *WHO Standard Acupuncture Point Locations in the Western Pacific Region*, World Health Organization, Geneva, Switzerland, 2008.

[18] M. K. Hyun, M. J. Mo, D. R. Hwang et al., "The effects of Jodeungsan pharmacopuncture at GB20 on cognitive impairment induced by focal brain injury in rats," *The Acupuncture*, vol. 33, no. 4, pp. 49–63, 2016.

[19] L. Chen, F. Ren, H. Zhang et al., "Inhibition of glycogen synthase kinase 3β ameliorates D-GalN/LPS-induced liver injury by reducing endoplasmic reticulum stress-triggered apoptosis," *PLoS One*, vol. 7, no. 9, Article ID e45202, 2012.

[20] J. B. Wang, H. R. Cui, R. L. Wang et al., "A systems pharmacology-oriented discovery of a new therapeutic use of the TCM formula Liuweiwuling for liver failure," *Scientific Reports*, vol. 8, p. 5645, 2018.

[21] R. Bekeredjian, C. B. Walton, K. A. MacCannell et al., "Conditional HIF-1α expression produces a reversible cardiomyopathy," *PLoS One*, vol. 5, no. 7, Article ID e11693, 2010.

[22] M. M. Faas and P. de Vos, "Mitochondrial function in immune cells in health and disease," *Biochimica et Biophysica Acta - Molecular Basis of Disease*, vol. 1866, no. 10, Article ID 165845, 2020.

[23] X. Saelens, N. Festjens, L. V. Walle, M. v. Gurp, G. V. Loo, and P. Vandenabeele, "Toxic proteins released from mitochondria in cell death," *Oncogene*, vol. 23, no. 16, pp. 2861–2874, 2004.

[24] G. Escames, L. C. López, J. A. García, L. García-Corzo, F. Ortiz, and D. Acuña-Castroviejo, "Mitochondrial DNA and inflammatory diseases," *Human Genetics*, vol. 131, no. 2, pp. 161–173, 2012.

[25] C. Li, J. Si, F. Tan, K. Y. Park, and X. Zhao, "Lactobacillus plantarum KSFY06 prevents inflammatory response and oxidative stress in acute liver injury induced by D-Gal/LPS in mice," *Drug Design, Development and Therapy*, vol. 15, pp. 37–50, 2021.

[26] Y. T. Li, J. Z. Ye, L. X. Lv et al., "Pretreatment with bacillus cereus preserves against D-galactosamine-induced liver injury in a rat model," *Frontiers in Microbiology*, vol. 10, p. 1751, 2019.

[27] K. K. Asha and K. Devadasan, "Protective effect of taurine on the mitochondria of albino rats induced with fulminant hepatic failure," *Biomedicine & Preventive Nutrition*, vol. 3, pp. 279–283, 2013.

[28] Y. P. Pei, J. Chen, and W. L. Li, "Progress in research and application of silymarin," *Medicinal and Aromatic Plant Science and Biotechnology*, vol. 3, pp. 1–8, 2009.

[29] X.-M. Yin, "Bid, a BH3-only multi-functional molecule, is at the cross road of life and death," *Gene*, vol. 369, pp. 7–19, 2006.

[30] N. Fu, D. Li, W. Li et al., "Glutamate-cysteine ligase catalytic subunit attenuated hepatitis C virus-related liver fibrosis and suppressed endoplasmic reticulum stress," *Frontiers in Molecular Biosciences*, vol. 7, p. 199, 2020.

[31] C. D. J. Tavares, S. Aigner, K. Sharabi et al., "Transcriptome-wide analysis of PGC-1α–binding RNAs identifies genes linked to glucagon metabolic action," *Proceedings of the National Academy of Sciences of the United States of America*, vol. 117, no. 36, pp. 22204–22213, 2020.

[32] S. P. Correia, M. F. Moedas, K. Naess et al., "Severe congenital lactic acidosis and hypertrophic cardiomyopathy caused by an intronic variant in NDUFB7," *Human Mutation*, vol. 42, no. 4, pp. 378–384, 2021.

[33] C. M. Viegas, A. Zanatta, L. A. Knebel et al., "Experimental evidence that ornithine and homocitrulline disrupt energy metabolism in brain of young rats," *Brain Research*, vol. 1291, pp. 102–112, 2009.

[34] A. Fu, J. C. Alvarez-Perez, D. Avizonis et al., "Glucose-dependent partitioning of arginine to the urea cycle protects β-cells from inflammation," *Nature metabolism*, vol. 2, no. 5, pp. 432–446, 2020.

[35] X. Meng, X. Guo, J. Zhang et al., "Acupuncture on ST36, CV4 and KI1 suppresses the progression of methionine-and choline-deficient diet-induced nonalcoholic fatty liver disease in mice," *Metabolites*, vol. 9, no. 12, p. 299, 2019.

[36] H. D. Lim, K. J. Kim, B. G. Jo, J. Y. Park, and U. Namgung, "Acupuncture stimulation attenuates TNF-α production via vagal modulation in the concanavalin a model of hepatitis," *Acupuncture in Medicine*, vol. 38, no. 6, pp. 417–425, 2020.

[37] D. A. Bardi, M. F. Halabi, P. Hassandarvish et al., "Andrographis paniculata leaf extract prevents thioacetamide-induced liver cirrhosis in rats," *PLoS One*, vol. 9, no. 10, Article ID e109424, 2014.

Hindawi
Evidence-Based Complementary and Alternative Medicine
Volume 2022, Article ID 2506327, 5 pages
https://doi.org/10.1155/2022/2506327

Review Article

Exercise Prescription Intervention Rehabilitation Suggestions for Fatty Liver Patients

Tian Wan, Kun-Da Hong, and Si-Yu Lu

Department of Rehabilitation Medicine, The Second Affiliated Hospital of Fujian Medical University, Quanzhou, Fujian Province, China

Correspondence should be addressed to Kun-Da Hong; hongkundafz@163.com

Received 4 February 2022; Accepted 29 March 2022; Published 16 April 2022

Academic Editor: Chan-Yen Kuo

In this study, the exercise prescription intervention rehabilitation suggestions for fatty liver patients were summarized as follows: first, basic exercises (brisk walking and jogging.), sports (swimming, badminton, and cycling), traditional Chinese medicine exercises (Taichi boxing and eight-section brocade), the aim of which is to improve overall physical strength and endurance of the body; second, exercise intensity, duration, and frequency; third, exercise precautions; and fourth, exercise prescription selection and suggestion.

1. Introduction

Fatty liver, a common liver disease in the middle-aged and elderly, refers to the pathological changes of excessive fat accumulation in hepatocytes caused by various factors. In the clinical setting, the incidence of fatty liver is increasing year-after-year with a trend towards younger age of reference. There are no specific drugs or treatment for fatty liver at this time. According to numerous references, fatty liver can be reversed, especially when the patients adhere to a proper exercise program, dietary recommendations, and/or appropriate medications [1]. It has been reported that adopting exercise therapy in an effort to ultimately stop medication may be a more scientific and ideal way to treat fatty liver [2, 3]. In the current study, an exercise prescription was initiated to probe into the rehabilitation concept of exercise prescription intervention for fatty liver patients, and suggestions on standardized rehabilitation were advanced, which are summarized as follows.

2. Exercise Items

The exercise prescription items included the following: aerobic exercises aimed at improving overall physical strength and endurance, such as brisk walking, jogging, badminton, cycling, Taichi boxing, and eight-section brocade.

2.1. Basic Exercises: Brisk Walking and Jogging. Brisk walking and jogging are currently the most popular exercises and have the advantages of easily controlled exercise intensity and volume, fewer sports injuries, and simple and easy realization, which is suitable for various populations. Brisk walking is a type of low-intensity aerobic exercise, the essentials of which are as follows: first, breathe naturally and relax the body; second, keep the head up, chest out, and abdomen in; and third, swing the arms naturally and place the center of gravity on the feet. Jogging, also known as slow-paced running, is a type of medium-intensity aerobic exercise, the essentials of which are as follows: first, breathe naturally, relax the upper limbs, and keep the muscles of the lower limbs elastic to avoid injuries; second, lean forward, relax the shoulders, and swing the arms naturally (the range should be natural and comfortable); third, land gently on the forefeet.

References have revealed that brisk walking and jogging promote fat consumption to realize fast weight loss. Brisk walking and jogging can help maintain cardiac function in the middle-aged and elderly, slow the decline in lung

elasticity, and exert positive effects in preventing diseases, such as coronary heart disease, hypertension, and arteriosclerosis [4].

2.2. Sports: Swimming, Badminton, and Cycling. Because fatty liver currently has a younger age of onset than in the past, young people can achieve quick therapeutic efficacy through sports, such as swimming, badminton, and cycling, which have the advantages of high exercise intensity and fast benefits. Experimental research has confirmed that [5, 6] sports, by regulating the lipid metabolism, antioxidation, and inflammation suppression, may ameliorate the level of blood lipids in hyperlipidemic rats. The possible mechanisms underlying swimming in treating fatty liver have been reported as follows: first, sports can repress lipid synthesis in the liver by downregulating the levels of lipid synthesis-related gene expression, such as SREBP-1c and SCD1 [7–9]; second, sports can facilitate the phosphorylation of Akt in the liver and raise the sensitivity to insulin [10–12]; third, sports can upregulate the expression of PPARα, thus enhancing the oxidation of fatty acids in the liver [13–15]. There are many references involving the treatment of fatty liver by swimming, but few studies on other sports are available. Nevertheless, badminton, cycling, and other aerobic exercises can also achieve good therapeutic efficacy on fatty liver.

2.3. Traditional Chinese Medicine (TCM) Exercises: Taichi Boxing and Eight-Section Brocade. Taichi boxing is in accordance with the principle of yin-yang change. Yin and yang interconvert into and complement each other in each move and each gesture. For this reason, Taichi boxing can recuperate yin and yang qi and blood of the entire body, soothe the liver by regulating qi, and reconcile yin and yang (Table 1).

Eight-section brocade, a regime invented by ancient Chinese medical specialists, is a type of TCM physical and breathing exercise, which is characterized by promoting the circulation of vital energy of human blood and restoring the health of human body through physical movements, such as pitching, stooping, and flexion and extension of limbs (Table 2).

Both Taichi boxing and eight-section brocade require cooperation with breathing, that is, exhalation through the mouth and inhalation through the nose. By expelling foul air through the mouth and breathing fresh air through the nose, the stale is expelled and the fresh is imbibed. Through such exhalation and inhalation, visceral movement can be enhanced, visceral microcirculation ameliorated, and liver metabolic function promoted, thus boosting rehabilitation. Hence, Taichi boxing and eight-section brocade can promote flow of qi and blood, dredge meridians, soothe the liver and gallbladder, recuperate internal organs, regulate yin and yang, prolong life, and prevent and cure diseases. Taichi boxing and eight-section brocade are very beneficial to subhealth population and the elderly, as well as fatty liver patients. A randomized controlled trial of Taichi have evaluated the effects of Taichi in ordinary adults aged 19–70 years. This study may provide valuable data on the effects of Taichi on hypertension [16]. Previous studies have showed positive effects of bone mineral density on maintaining eight-section brocade and improving functional outcome [17, 18]. It can be used to decreasing bone loss and the rate of osteoporotic fracture of patients [19]. Modern medical studies have suggested that both Taichi boxing and eight-section brocade are medium and low-intensity aerobic exercises [20, 21], and long-term practice of Taichi boxing and eight-section brocade can effectively modulate the lipid metabolism, thus ameliorating blood lipid levels, and ultimately treating fatty liver [22, 23] (Figure 1).

3. Exercise Intensity, Duration, and Frequency

3.1. Exercise Intensity. Long-term medium and low-intensity general aerobic exercises are most suitable for fatty liver patients. Because the majority of fatty liver patients are accompanied by different degrees of hypertension, overload exercise may induce cardiovascular and cerebrovascular diseases, so it is of vital importance to control the exercise intensity. Fatty liver patients should adopt different exercise intensities according to age and constitution, and the following criteria can be used for evaluation: first, the suggested heart rate variation range is 45–60 beats/min before and after exercise; second, the heart rate in the quiet state is taken as the standard, and it is suggested that the heart rate should revert to the standard level 3–5 min after exercise.

3.2. Exercise Duration and Frequency. The recommended frequency of brisk walking and jogging is 3–6 times per week for 40–90 min (or 3–6 km) each time. Attention should be paid to speed control, and it is best to sweat slightly. When the patients are out of breath, they are engaged in anaerobic exercise. In addition, the patients are suggested to do one of the sports, such as swimming, badminton, and cycling (2-3 times per week for 30–60 min each time) without feeling obvious fatigue after the sports. It is also recommended to practice one of the TCM exercises, such as Taichi boxing and eight-section brocade, 30–6 times per week for 30–45 min (2-3 repeats) each time.

4. Exercise Precautions

When creating an exercise prescription, fatty liver patients should pay attention to the following: first, undergo a physical examination regularly, which provides a basis for exercise prescription and exercise intensity control. Second, take necessary medications and do not discontinue medications abruptly. Third, develop regular and appropriate living habits and adopt a scientific and reasonable diet; no smoking, drinking alcohol, or lavish meals; and sleep regularly and do not stay up late.

5. Selection and Suggestions on Exercise Prescription

It is suggested in this study that young patients with fatty liver engage in one of the basic exercises, one of the sports,

Table 1: Specific operation of 24-style Taichi boxing.

Number	Procedure	Number	Procedure	Number	Procedure
1	Commencing form	9	Single whip	17	Push down and stand on one leg, right style
2	Part the wild horse's mane on both sides	10	Wave hands like clouds	18	Work at shuttles on both sides
3	White crane spreads its wings	11	Single whip	19	Needle at sea bottom
4	Brush knee and twist step on both sides	12	High pat on horse	20	Flash the arms
5	Play pipa	13	Kick with right heel	21	Turn, deflect downward, parry and punch
6	Repulse monkey on both sides	14	Strike opponent's ears with both fists	22	Apparent close up
7	Grasp the bird's tail, left side	15	Turn and kick with left heel	23	Cross hands
8	Grasp the bird's tail, right side	16	Push down and stand on one leg, left style	24	Closing form

Table 2: Specific operation of eight-section brocade.

Number	Procedure	Number	Procedure
1	Double hands push-up heaven	5	Thrusting the fists and making the eyes glare to enhance strength
2	Posing as an archer shooting both left- and right-handed	6	Moving the hands down the back and legs and touching the feet to strengthen the kidneys
3	Holding one arm aloft to regulate the functions of the spleen and stomach	7	Swinging the head and lowering the body to relieve stress
4	Looking backwards to prevent sickness and strain	8	Raising and lowering the heels to cure diseases

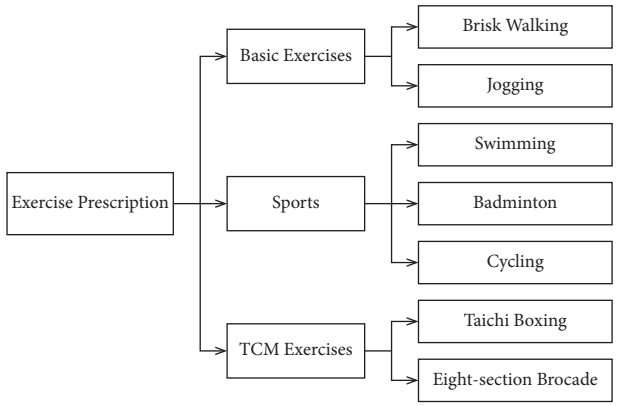

Figure 1: Exercise prescription.

and one of the TCM exercises, while elderly patients who may have cardiovascular and cerebrovascular diseases adopt one of the basic exercises plus one of the TCM exercises (they may also engage in one of the sports when necessary and the patient's physical conditions allow). Exercise training for fatty liver patients should be done in an orderly way and step-by-step, and continuous and persistent training is the most important (Figure 2).

6. Summary

As an essential organ of the human lipid metabolism, the liver is mainly responsible for excretion of lipids into blood in the form of very low-density lipoprotein and synthesis of triglycerides by absorbing free fatty acids from blood [24]. At present, people are prone to overeating due to improved living standards. As a result, excessive calories are converted into fatty acids, which enter the liver beyond the processing capacity of the liver, thus accumulating in the liver and inducing fatty liver [25]. Thus far, no specific drug for fatty liver has been developed, and exercise training plays a positive and critical role in the treatment of fatty liver. In this study, therefore, the efficacy of different exercise trainings on fatty liver patients was investigated, and suggestions were proposed regarding exercise intensity, duration, frequency, and precautions. In addition, exercise prescriptions were advanced for patients of different ages. It is expected that with the help of more standardized exercise prescription suggestions, more scientific and reasonable exercise schemes can be provided for patients.

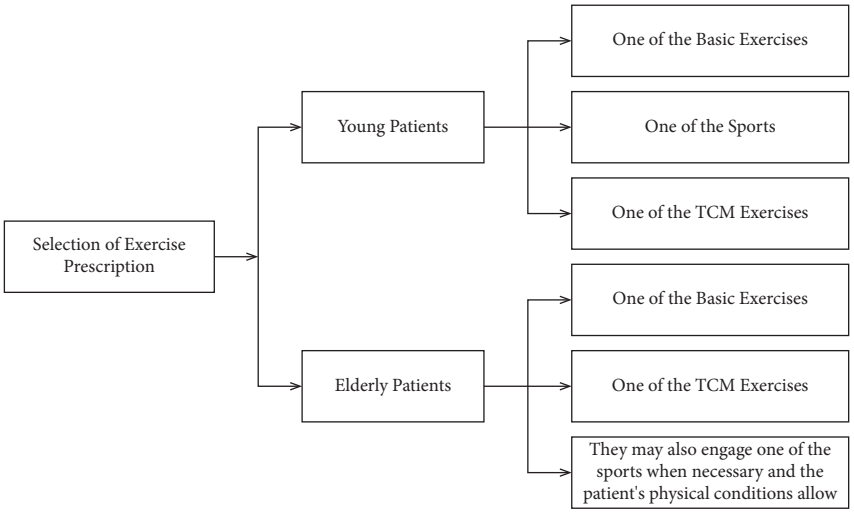

Figure 2: Selection of exercise prescription.

Data Availability

The data used to support the findings of this study are available from the corresponding author upon request.

Conflicts of Interest

The authors declare that they have no conflicts of interest.

Acknowledgments

This work was supported by The Second Affiliated Hospital of Fujian Medical University.

References

[1] K. K. Wong, S. Chen, Y. Wu, R. Bufi, and L. S. Pescatello, "Exercise as A treatment for non-alcoholic fatty liver disease: a meta-review," *Medicine and Science in Sports and Exercise*, vol. 53, p. 455, 2021.

[2] H. S. Kim, A. Ike, and J. Mathew, "Effect of exercise on the development of new fatty liver and the resolution of existing fatty liver," *Journal of Hepatology*, vol. 66, no. 3, pp. 664-665, 2016.

[3] A. Thorp and J. G. Stine, "Exercise as medicine: the impact of exercise training on nonalcoholic fatty liver disease," *Current hepatology reports*, vol. 19, no. 4, pp. 402–411, 2020.

[4] H.-J. Zhang, L.-L. Pan, Z.-M. Ma et al., "Long-term effect of exercise on improving fatty liver and cardiovascular risk factors in obese adults: a 1-year follow-up study," *Diabetes, Obesity and Metabolism*, vol. 19, no. 2, pp. 284–289, 2017.

[5] L. Zhao and X. Xu, "Effect of aerobic and resistance exercise on fatty liver in mice model: 2578 board #242 may 31 11:00 am-12:30 pm," *Medicine and Science in Sports and Exercise*, vol. 51, p. 718, 2019.

[6] F. Zheng and C. Ying, "GW29-e0215 Long-term exercise alleviates non-alcoholic fatty liver disease and insulin resistance via regulating lipid metabolism in ApoE-null mice," *Journal of the American College of Cardiology*, vol. 72, no. 16, pp. C7–C8, 2018.

[7] M. S. Gauthier, K. Couturier, J. G. Latour, and J. M. Lavoie, "Concurrent exercise prevents high-fat-diet-induced macrovesicular hepatic steatosis," *Journal of Applied Physiology*, vol. 94, no. 6, pp. 2127–2134, 1985.

[8] R. Ikaga and T. Yamazaki, "Preventive effects of exercise timing and exercise duration on high-fat diet-induced fatty liver in mice," *Nippon Eiyo Shokuryo Gakkaishi*, vol. 70, no. 2, pp. 69–75, 2017.

[9] P. Fuente, L. Quezada, C. Sepúlveda, M. Monsalves-Alvarez, and R. Troncoso, "Exercise regulates lipid droplet dynamics in normal and fatty liver," *Biochimica et Biophysica Acta (BBA)—Molecular and Cell Biology of Lipids*, vol. 1864, no. 12, pp. 158–519, 2019.

[10] Y. Koyama, P. Galassetti, R. H. Coker et al., "Prior exercise and the response to insulin-induced hypoglycemia in the dog," *American Journal of Physiology. Endocrinology and Metabolism*, vol. 282, no. 5, pp. E1128–E1138, 2002.

[11] H. Adithya, C. E. Fealy, and J. P. Kirwan, "Short-Term Exercise Improves Hepatic Insulin Extraction in Individuals with Nonalcoholic Fatty Liver Disease," *Diabetes*, vol. 67, 2018.

[12] A. Minami, N. Ishimura, N. Harada, S. Sakamoto, Y. Niwa, and Y. Nakaya, "Exercise training improves acetylcholine-induced endothelium-dependent hyperpolarization in type 2 diabetic rats, Otsuka Long-Evans Tokushima fatty rats," *Atherosclerosis*, vol. 162, no. 1, pp. 85–92, 2002.

[13] M. Rosety-Rodriguez, F. J. Ordonez, I. Rosety et al., "8-weeks training program attenuates mitochondrial oxidative stress in the liver of emotionally stressed rats," *Histology and Histopathology*, vol. 21, no. 11, pp. 1167–1170, 2006.

[14] J. Li, D. Gao, J. Sun, K. Zou, and Q. Su, "Exercise training attenuates non-alcoholic fatty liver disease in rats with diabetes via endoplasmic reticulum stress: 930 board #191 may 30 2: 00 pm-3: 30 pm," *Medicine and Science in Sports and Exercise*, vol. 50, p. 21, 2018.

[15] J. Słomko, M. Zalewska, W. Niemiro et al., "Evidence-based aerobic exercise training in metabolic-associated fatty liver disease: systematic review with meta-analysis," *Journal of Clinical Medicine*, vol. 10, no. 8, p. 1659, 2021.

[16] S.-H. Lee, B.-J. Kim, I.-H. Park et al., "Effects of taichi on grade 1 hypertension: a study protocol for a randomized controlled trial," *Trials*, vol. 21, no. 1, p. 177, 2020.

[17] B.-X. Liu, S.-P. Chen, Y.-D. Li et al., "The effect of the modified eighth section of eight-section brocade on osteoporosis in

postmenopausal women," *Medicine*, vol. 94, no. 25, p. e991, 2015.

[18] L. Zou, J. E. SasaKi, H. Wang, Z. Xiao, Q. Fang, and M. Zhang, "A systematic review and meta-analysis baduanjin qigong for health benefits: randomized controlled trials," *Evidence-based Complementary and Alternative Medicine*, vol. 2017, Article ID 4548706, 7 pages, 2017.

[19] T. Tian, Y. Cai, J. Zhou et al., "Effect of eight-section brocade on bone mineral density in middle age and elderly people: protocol for a systematic review and meta-analysis of randomised controlled trials," *Medicine*, vol. 99, no. 1, Article ID e18549, 2020.

[20] X. S. Sheng, W. Yan, Z. X. Qing, and W. H. Jun, "Influences of baduanjin exercise on the blood lipids and serum il-6,apn in the olders," *Medicine and Science in Sports and Exercise*, vol. 52, no. 7S, p. 742, 2020.

[21] J. Wen, T. Lin, C. Jiang, R. Peng, and W. Wu, "Effect of Baduanjin exercises on elevated blood lipid levels of middle-aged and elderly individuals: protocol for a systematic review and meta-analysis of randomised controlled trials," *BMJ Open*, vol. 7, no. 9, Article ID e017213, 2017.

[22] Y. N. Liu, L. Wang, X. Fan, S. Liu, Q. Wu, and Y. L. Qian, "Effects of Taijiquan on glucose and lipid metabolism in middle-aged and elderly diabetic patients: a protocol for systematic review and meta-analysis," *Medicine*, vol. 100, no. 4, Article ID e24433, 2021.

[23] J. Zhou, Y. Yu, B. Cao et al., "Characteristic of clinical studies on baduanjin during 2000-2019: a comprehensive review," *Evidence-based Complementary and Alternative Medicine*, vol. 2020, Article ID 4783915, 9 pages, 2020.

[24] Y. Xiong, Q. Peng, C. Cao, Z. Xu, and B. Zhang, "Effect of different exercise methods on non-alcoholic fatty liver disease: a meta-analysis and meta-regression," *International Journal of Environmental Research and Public Health*, vol. 18, no. 6, p. 3242, 2021.

[25] B. Rei, S. Q. Chen, and Y. Wu, "The effect of exercise on patients with non-alcohlic fatty liver disease: a meta-analysis: 1385," *Medicine and Science in Sports and Exercise*, vol. 53, 2021.

Hindawi
Evidence-Based Complementary and Alternative Medicine
Volume 2022, Article ID 6221340, 18 pages
https://doi.org/10.1155/2022/6221340

Research Article

Er-Chen Decoction Alleviates High-Fat Diet-Induced Nonalcoholic Fatty Liver Disease in Rats through Remodeling Gut Microbiota and Regulating the Serum Metabolism

Jing Miao,[1] Liying Guo,[1] Huantian Cui,[2] Li Wang,[1] Bo Zhu,[1] Jinyan Lei,[1] Peng Li,[1] Jianwei Jia,[1] and Zhaiyi Zhang[3]

[1]*Tianjin Second People's Hospital, Tianjin, China*
[2]*Shandong Provincial Key Laboratory of Animal Cell and Developmental Biology, School of Life Sciences, Shandong University, Qingdao, China*
[3]*Tianjin University of Traditional Chinese Medicine, Tianjin, China*

Correspondence should be addressed to Jianwei Jia; jiaweigt@126.com and Zhaiyi Zhang; 3461285155@qq.com

Received 10 February 2022; Accepted 10 March 2022; Published 31 March 2022

Academic Editor: Chih-Yuan Ko

Many studies have found that the dysfunction in gut microbiota and the metabolic dysfunction can promote nonalcoholic fatty liver disease (NAFLD) development. Er-Chen decoction (EC) can be used in the treatment of NAFLD. However, the mechanism of this hepatoprotection is still unknown. In this study, we constructed a rat model with NAFLD fed with high-fat chow and administered EC treatment. The therapeutic effects of EC on NAFLD were evaluated by measuring transaminases, blood lipid levels, and pathological changes in the liver. In addition, we measured the effects of EC on liver inflammatory response and oxidative stress. The changes in gut microbiota after EC treatment were studied using 16S rRNA sequencing. Serum untargeted metabolomics analysis was also used to study the metabolic regulatory mechanisms of EC on NAFLD. The results showed that EC decreased the serum transaminases and lipid levels and improved the pathological changes in NAFLD rats. Furthermore, EC enhanced the activities of SOD and GSH-Px and decreased MDA level in the liver. EC treatment also decreased the gene and protein levels of IL-6, IL-1β, and TNF-α in the liver and serum. The 16S rRNA sequencing and untargeted metabolomics indicated that EC treatment affected the gut microbiota and regulated serum metabolism. Correlation analysis showed that the effects of EC on taurine and hypotaurine metabolism, cysteine and methionine metabolism, and vitamin B6 metabolism pathways were associated with affecting in the abundance of *Lactobacillus*, *Dubosiella*, *Lachnospiraceae, Desulfovibri, Romboutsia, Akkermansia, Intestinimonas*, and *Candidatus_saccharimonas* in the gut. In conclusion, our study confirmed the protective effect of EC on NAFLD. EC could treat NAFLD by inhibiting oxidative stress, reducing inflammatory responses, and improving the dysbiosis of gut microbiota and the modulation of the taurine and hypotaurine metabolism, cysteine and methionine metabolism, and vitamin B6 metabolism pathways in serum.

1. Introduction

Nonalcoholic fatty liver disease (NAFLD) is a hepatopathy syndrome characterized by steatosis and fat accumulation in hepatocytes [1]. Recently, the NAFLD incidence has increased, and it has replaced viral hepatitis as the most common chronic liver disease worldwide, with a prevalence of 25% in adults [2]. NAFLD could also develop into type 2 diabetes, liver cirrhosis, and liver cancer in severe cases, thus, posing a great threat to human life and health, and a major economic burden to patients, families, and society [3]. Currently, the major treatments for NAFLD are exercise therapy and pharmacological therapy; however, the acceptance and sustainability of exercise therapy are still lacking [4]. For pharmacological therapy, lipid-lowering drugs (e.g., simvastatin), such as insulin inhibitors (e.g., pioglitazone), and antioxidants (e.g., vitamin E) are generally used [5–7]. However, some lipid-lowering drugs possess potential

hepatotoxicity, and some of them fail to decrease hepatic fat deposition and may even aggravate liver injury [8, 9]. Therefore, the development of traditional Chinese medicines with lipid-lowering and hepatoprotective effects would be more appropriate for treating NAFLD and have wide application prospects as well as practical significance.

Recently, gut microbiota has been widely studied as influential factors closely related to NAFLD. Gut microbiota primarily influence NAFLD development by altering the microecological composition of the gut, suppressing the expression of inflammatory factors, and regulating metabolites, such as short-chain fatty acids, bile acids, and endogenous ethanol [10]. Some probiotics, such as *Bifidobacteria*, *Lactobacillus*, and *Bacteroidetes* have essential roles in maintaining gut microbiota balance and treating NAFLD. Intestinal *Bifidobacteria* decrease intestinal cholesterol absorption by degrading bile salts and promoting fecal bile acid excretion, which affects inhibiting cholestasis and enhancing enterohepatic circulation [11]. Metabolomics allows systematic identification and quantification of metabolite levels and can elucidate the disease pathogenesis and the mechanism of drug action on metabolic levels [12]. Metabolite levels are impacted by the gut microbiota and can directly show the current metabolic state of an organ or a cell [13]. Studies have discovered that traditional Chinese medicine (TCM) has outstanding advantages in enhancing dyslipidemia in NAFLD and other aspects and has wide application value [14, 15]. Shenling Baizhu powder alleviates NAFLD through its antioxidant, anti-inflammatory, lipid-lowering, and gut microbiota regulatory effects [16–18]. Dachaihu decoction enhances the alteration of gut microbiota and regulates arachidonic acid (AA), glycerophospholipid, and glycine/serine/threonine metabolic pathways to increase metabolic disorders in NAFLD model rats [19]. Using 16S rRNA sequencing combined with metabolomics can elucidate the mechanism of action of Chinese herbal formulas through the interaction between gut microbiota and host metabolism.

Er-Chen decoction (EC), composed of *Pinellia ternata* (Thunb.) Makino, *Citrus × aurantium* L., *Smilax glabra* Roxb., and *Glycyrrhiza uralensis* Fisch. ex DC., and has been using in the treatment of NAFLD [20]. Experimental studies have indicated that EC can significantly decrease blood lipid levels, improve insulin resistance, and decrease body weight in rats on a high-fat diet [21]. Clinical observation has also discovered that EC modified formula significantly improves fat deposition, lowers blood lipids, and improves patients' quality of life in NAFLD patients [22]. However, its specific action mechanism has not been elucidated.

To better understand these mechanisms, a rat model of NAFLD was generated and the therapeutic effects of EC on NAFLD rats were evaluated, and then the effects of EC on inflammation and oxidative stress in NAFLD rats were examined. The changes in gut microbiota after EC treatment were investigated using 16S rRNA sequencing. In addition, the metabolic regulatory mechanism of EC on NAFLD was also analyzed using an untargeted metabolomics approach.

2. Materials and Methods

2.1. Reagents. Simvastatin ($C_{25}H_{38}O_5$, molecular weight: 418.57 Da, CAS No.: 79902-63-9) was obtained from Sigma-Aldrich Co., Ltd. (USA). High-fat chow (10% lard, 5% sugar, 4% cholesterol, 0.2% propylthiouracil, 0.5% sodium cholate, and 80.3% basal chow) was purchased from Beijing Sibeifu Bioscience Co., Ltd. (Beijing, China). Aspartate aminotransferase (AST), alanine aminotransferase (ALT), triglyceride (TG), total cholesterol (TC), superoxide dismutase (SOD), methane dicarboxylic aldehyde (MDA), and glutathione peroxidase (GSH-Px) test kits were purchased from Nanjing Jiancheng Biological Engineering Institute (Nanjing, China). Oil Red O Staining kit was obtained from Solarbio Biotechnology Co., Ltd. (Beijing, China). Total RNA isolation, cDNA reverse transcription, quantitative polymerase chain reaction (qPCR) kits, and primers for qPCR experiment were purchased from TianGen Biotechnology Co., Ltd. (Beijing, China). Enzyme-linked immunosorbent assay (ELISA) kits of rat interleukin (IL)-1β, IL-6, and tumor necrosis factor-alpha (TNF-α) were purchased from Shanghai BlueGene Biotech Co., Ltd. (Shanghai, China).

2.2. Preparation of Er-Chen Decoction. 15 g of *Pinellia ternata* (Thunb.) Makino, 15 g of *Citrus × aurantium* L., 9 g of *Smilax glabra* Roxb., and 4.5 g of *Glycyrrhiza uralensis* Fisch. ex DC were weighed out, and eight times the volume of water was added for 30 min of decoction and concentrated into 2 g crude herb/mL.

2.3. Animals. Specific-pathogen-free (SPF)-grade male Sprague Dawley (SD) rats aged 6–8 weeks and weighing (200 ± 20) g were provided by Beijing Huafukang Biotechnology Co., Ltd. The housing environment was maintained at 25 ± 2°C with a relative humidity of 50 ± 15% and a 12 h light-dark cycle with access to water and food *ad libitum*. The experiment was approved by the Ethics Committee of Nankai University.

2.4. Animal Grouping. After one week of adaptation rearing, the NAFLD rat model was replicated as described in the literature [23]. Fifty rats were randomly divided into control, model, simvastatin, EC low-dose, and EC high-dose groups ($n = 10$ per group). The rats in control group were fed with normal chow, and the rats in remaining four groups were given high-fat chow (4% cholesterol, 10% lard, 5% sugar, 0.5% sodium cholate, 0.2% propylthiouracil, and 80.3% basal chow), all for 12 weeks. During the 12 weeks of model establishment, drug interventions were administered simultaneously, where the control and the model groups were given 2 mL/rat of saline daily through intragastric administration. The simvastatin group was administered 1.8 mg/kg/d of simvastatin through intragastric administration [24], and the EC low and EC high-dose groups were given 4.5 g/kg/d and 9 g/kg/d (2 mL/rat) of EC through intragastric administration based on the clinically equivalent dose in

humans, all for 12 weeks. The body weight of rats was recorded every two weeks during the experiment.

2.5. Serum Biochemical Indicator Test. After modeling and drug administration, rats in each group were fasted for 24 h and anesthetized by intraperitoneal injection of 1% phenobarbital (10 mL/kg). Blood was collected from the abdominal aorta and centrifuged at 4°C and 3,000 r/min for ten minutes to separate the serum. Serum levels of ALT, aspartate transaminase (AST), triglyceride (TG), and total cholesterol (TC) were measured using reagent kits.

2.6. Liver Pathological Staining. Immediately after model establishment and drug administration, the liver tissue from the same part of the left lobe of the liver was eliminated, cleaned, fixed in 10% formalin, and dehydrated for paraffin embedding. The tissue was cut into 5 μm sections using a microtome (model RM2125 RTS, bought from Leica), routinely stained using HE, cleared, mounted, and then observed under a light microscope (model ECLIPSE E100, bought from Nikon) for pathological alterations in the liver. The pathological severity of steatosis, lobular inflammation, and hepatocyte ballooning was determined using our previously published NAFLD activity score (NAS) [25].

In addition, 10 μm-thick frozen liver tissues were cut using a cryotome (model CM3050 S, purchased from Leica) and fixed on slides to dry at room temperature for 5 min. The tissue was stained using the Oil Red O staining kit manufacturer's instructions and then immediately observed under a light microscope. The percentage of the stained area of Oil Red O was determined using Image-Pro Plus 6.0.

2.7. Antioxidant Indicator Test of the Liver Tissue. A 100 mg of liver tissues were weighed and immersed in 900 μL saline, homogenized by ultrasonication, and centrifuged at 2,000 r/min for 10 min; the supernatant was obtained. The levels of SOD, GSH-Px, and MDA in liver tissue homogenates were detected according to the manufacturer's instructions.

2.8. ELISA for Serum Inflammatory Factor Expression. The expression levels of the cytokines TNF-α, IL-1β, and IL-6 in the serum of each group were measured using ELISA. The specific methods are as described in the kit's manufacturer's instructions.

2.9. Detection of mRNA Expression of the Liver Inflammatory Factor Using qPCR. Total RNA was isolated from frozen liver tissue based on the established protocol of the kits. After testing RNA purity and concentration, the RNA was reverse transcribed into cDNA, and qPCR was conducted to detect the mRNA expression of *TNF-α* (primer sequence Forward: GAGCACGGAAAGCATGATCC; Reverse: TAGACAGAAGAGCGTGGTGG), *IL-1β* (primer sequence Forward: GGGATGATGACGACCTGCTA; Reverse: TGTCGTTGCTTGTCTCTCCT), and *IL-6* (primer sequence Forward: CTCATTCTGTCTCGAGCCCA; Reverse: TGAAGTAGGGAAGGCAGTGG) in the liver tissue. The relative expression of mRNA was computed following the relative quantification method using *β-actin* (primer sequence Forward: TCTTCCAGCCTTCCTTCCTG; Reverse: CACACAGAGTACTTGCGCTC) as an internal control. Quantification was conducted based on the $2^{-\triangle\triangle CT}$ method.

2.10. 16S rRNA Sequencing

2.10.1. Fecal Genomic DNA Extraction. The total genomic DNA of rat cecum contents was obtained using the CTAB/SDS method, and concentration and purity of DNA samples were measured using a 1% agarose gel.

2.10.2. PCR Amplification and Sequencing of 16S rRNA Gene. The 16S rRNA gene (V3 to V4 region) was amplified using universal primers 338F and 806R. The primer sequences of 338F and 806R were 5′-ACTCCTACGGGAGGCAGCAG-3′ and 5′-GGACTACHVGGGTWTCTAAT-3′, respectively. The PCR system consisted of 10 ng template DNA, 0.2-μM primers (forward and reverse, respectively), and 15 μL Phusion® High-Fidelity PCR Master Mix (New England Biolabs, Ipswich, Massachusetts, United States). The reaction conditions were predenaturation at 98°C for 1 min, denaturation at 95°C for 10 s, annealing at 50°C for 30 s, extension at 72°C for 30 s, with 15 cycles. In the end, the reaction was held at 72°C for 5 min, and then the reaction was stored at 4°C. Then, Qiagen Gel Extraction Kit (Qiagen, Germany) was used to purify the mixed PCR products. TruSeq® DNA PCR-Free Sample Preparation Kit (Illumina, USA) was used to generate the sequencing libraries, and Qubit@ 2.0 Fluorometer (Thermo Scientific) and Agilent Bioanalyzer 2100 system were used to access the library quality. Finally, 250 bp of paired-end sequences were obtained based on the Illumina NovaSeq platform.

2.10.3. Sequencing Data Analysis. Raw sequencing data were assembled using a FLASH (v1.2.7) [26], and quality control was applied to the sequence to acquire the effective tags. The tags were clustered using Uparse software (Uparse v7.0.1001) [27] at 97% similarity level. Then, the operational taxonomic units (OTUs) were obtained. The Mothur algorithm-based Silva database [28] was used to annotate the OTUs based on taxonomic information. MUSCLE software was used for multiple sequence comparisons (v3.8.31) [29]. Alpha diversity index and beta diversity analysis were subsequently conducted. Differences between groups in diversity indices were analyzed using Wilcoxon Rank Sum test, and the Kruskal–Wallis rank sum test was used (Games-Howell was selected as the posthoc test), combined with the false discovery rate of multiple testing methods to screen for differential microbiota, and differences with $P < 0.05$ were considered statistically significant. Finally, Phylogenetic Investigation of Communities by Reconstruction of Unobserved States database (PICRUSt) analysis was conducted to predict the relevant gene pathways that may be influenced by each group of differential microbiota.

2.11. Metabolomic Analysis

2.11.1. Serum Sample Processing. A 100 μL serum sample was added to 400 μL 80% methanol, vortexed and shaken, placed on an ice bath for 5 min, and centrifuged for 20 min (15,000 g at 4°C). After centrifugation, the supernatant was diluted using ultrapure water to 53% methanol, followed by centrifugation at 15,000 g at 4°C for 20 min, and the supernatant was collected as the testing sample. An equal amount of each sample was mixed and used as the quality control (QC) sample. Throughout the whole analysis, periodic analysis was conducted to monitor the stability of the instrument.

2.11.2. Chromatographic and Mass Spectrometric Conditions. The chromatography was conducted on a Hypesil Gold column (C18) and chromatographic column (1.9 μm, 2.1 mm × 100 mm) with a mobile phase comprising (A) 0.1% formic acid and (B) methanol, using a gradient elution at 0 min, 98% A, 2% B; 1.5 min, 98% A, 2% B; 12 min, 0% A, 100% B; 14 min, 0% A, 100% B; 14 min, 0% A, 100% B; 14.1 min, 98% A, 2% B; and 17 min, 98% A, 2% B. The column temperature was 40°C, the flow rate was 0.2-mL/min, and the injection volume was 2 μL. The mass spectrometry conditions were simultaneously detected in positive and negative ion mode based on the electrospray ionization (ESI) source. The ESI setting source were as follows: spray voltage: 3.2 kV; aux gasflow rate: 10-arb; sheath gas flow rate: 40-arb; capillary temp: 320°C. Polarity: positive; negative; scanning range: 100–1500 m/z. Throughout the experiment, QC was added after every six samples to analyze the stability of the experiment.

2.11.3. Data Processing. Molecular characteristic peaks were found based on mass spectrometry detection technique. The molecular peaks were identified using the combination of mzCloud, mzVault, and MassList databases. Data preprocessing of the raw files (.raw) obtained from mass spectrometry was conducted based on Compound Discoverer 3.1 (CD3.1, Thermo Fisher) software. Molecular formulas were then predicted according to the molecular ion peaks and fragment ions and compared with MassList, mzCloud, and mzVault databases, thus identifying the metabolites. Metabolites with a coefficient of variance less than 30% [30] in QC samples were then retained as final identifications for subsequent analysis. The peaks found in the samples were integrated using CD3.1 software to obtain the quantitative results of the metabolites. The data were then subjected to QC to ensure the reliability and accuracy of the data. Next, multivariate statistical analysis (principal component analysis (PCA) and orthogonal partial least squares discriminant analysis (OPLS-DA)) of the metabolites was conducted to show differences in metabolic patterns among various groups. Metabolite correlation analysis was used to show the relationship between samples and metabolites. Finally, the biological significance of metabolite correlation was explained through functional analysis, such as metabolic pathway. Metabolites ($P < 0.05$ and variable importance of projection (VIP) > 1, fold change (FC) > 1.25 or FC < 0.80) were screened as the differential metabolites. Metabolic pathway enrichment analysis of differential metabolites was conducted based on KEGG platform. Finally, pathways with $P < 0.05$ and impact >0.1 were selected as the enriched pathways.

2.11.4. Statistical Processing. Statistics and analysis were conducted using SPSS 20.0 statistical software, and data are expressed as $\overline{x} \pm s$. One-way analysis of variance was used for comparing groups. Differences with $P < 0.05$ were considered statistically significant.

3. Results

3.1. Therapeutic Effects of EC on NAFLD Rats. Compared with the control group, the body weight of rats in the model group was significantly increased ($P < 0.01$, Figure 1), and the low and high-doses of EC and simvastatin treatment significantly decreased the body weight of rats in the NAFLD model compared with the model group ($P < 0.01$, respectively, Figure 1). As indicated by HE staining, the liver of the control rats was structurally intact, and their hepatocytes were neatly arranged in a radial pattern. The hepatocytes in the portal region and around the central vein were clear and intact, and the nuclei were uniform in size and shape and located in the center of the hepatocytes. In the liver of rats in the model group, many hepatocytes indicated steatosis, where the hepatocytes were distinctively swollen and rounded; the nuclei were squeezed to one side; the cytoplasm was filled with many fat vacuoles; lipid droplets were of various sizes, which were even fused into huge lipid droplets; and inflammatory cell infiltration was observed. The EC high-dose treatment and simvastatin treatment significantly alleviated steatosis and inflammatory cell infiltration induced by high lipid chow (Figure 2(a)). Similarly, the NAS score was significantly higher in the model group than in the control group, and H&E staining in the positive control and EC groups exhibited a lower NAS score than in the model group ($P < 0.01$, Figure 2(b)). The results of Oil Red O staining proposed that the nuclei of hepatocytes in the control rats were blue, and no red lipid droplets appeared in the hepatocytes. The lipid levels in the liver tissue of rats in the model group were significantly increased compared to that in the control group ($P < 0.01$). Compared to the model group, the lipid accumulation in the hepatocytes of rats in all the dosing groups was decreased ($P < 0.01$, respectively) (Figures 2(c) and 2(d)). In addition, the results of serum biochemical indicators indicated that the serum TC and TG levels as well as ALT and AST were significantly increased in the model group compared to those in the control group ($P < 0.01$, respectively); compared to the model group, simvastatin and EC high-dose intervention significantly decreased the levels of TC levels ($P < 0.01$, $P < 0.05$, respectively), TG levels ($P < 0.01$, respectively), and the activities of ALT ($P < 0.05$, respectively), and AST ($P < 0.01$, respectively) in serum (Table 1).

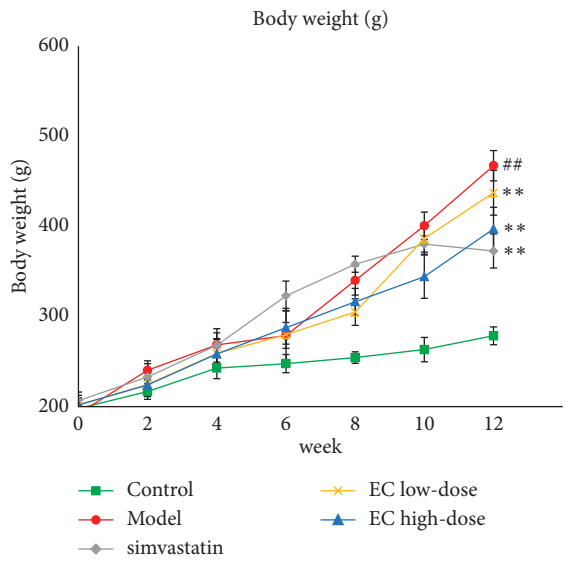

Figure 1: EC treatment decreases the body weight in NAFLD model rats. Control, model, simvastatin, EC-low dose, and EC-high dose ($n = 10$ per group) groups are shown. Data are reported as the mean ± SD. $^{\#\#}P < 0.01$ compared with the control group; $^{**}P < 0.01$ compared with the model group.

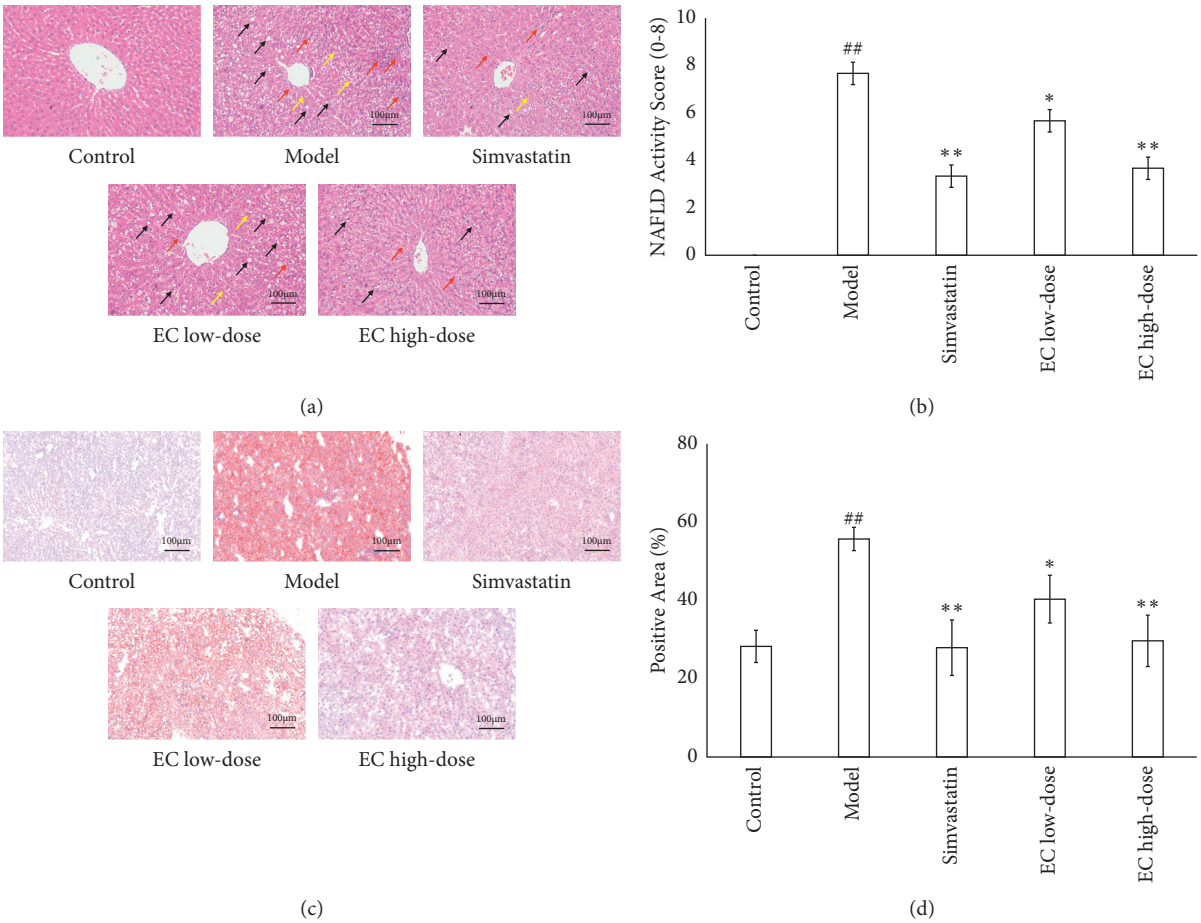

Figure 2: EC treatment improved the hepatosteatosis in NAFLD model rats. (a, b) H&E staining indicated that EC treatment ameliorated the pathological changes of the liver in NAFLD rats. Black arrows indicate the steatosis of hepatocytes, red arrows indicate lobular inflammation, and yellow arrows hepatic cord disorder (200x). (c, d) Oil Red O staining shows that EC treatment reduced the lipid accumulation in the liver (200x). Control, model, simvastatin, EC low-dose, and EC high-dose ($n = 10$ per group) groups are shown. Data are reported as the mean ± SD. $^{\#\#}P < 0.01$ compared with the control group; $^{*}P < 0.05$ compared with the model group; $^{**}P < 0.01$ compared with the model group.

Table 1: Changes in blood lipid levels and liver enzymes after EC treatment.

Group	TC (mmol/L)	TG (mmol/L)	ALT (U/L)	AST (U/L)
Control	9.48 ± 2.01	2.74 ± 0.70	28.32 ± 9.28	40.36 ± 28.87
Model	$22.92 \pm 8.91^{\#\#}$	$5.30 \pm 1.34^{\#\#}$	$58.58 \pm 26.29^{\#\#}$	$176.41 \pm 46.42^{\#\#}$
Simvastatin	$10.27 \pm 3.46^{**}$	$2.14 \pm 0.59^{**}$	$35.16 \pm 17.42^{*}$	$87.30 \pm 28.64^{**}$
EC low-dose	19.94 ± 8.85	5.02 ± 2.12	54.48 ± 19.18	143.90 ± 30.48
EC high-dose	$12.78 \pm 6.02^{*}$	$2.75 \pm 0.91^{**}$	$38.00 \pm 12.48^{*}$	$67.29 \pm 28.06^{**}$

Control, model, simvastatin, EC low-dose, and EC high-dose ($n = 10$ per group) groups are shown. Data are presented as the mean ± SD. $^{\#\#}P < 0.01$ as compared to the control group; $^{*}P < 0.05$ as compared to the model group; $^{**}P < 0.01$ as compared to the model group. TC: total cholesterol; TG: triglyceride; ALT: alanine aminotransferase; AST: aspartate aminotransferase.

3.2. Anti-Inflammatory and Antioxidative Effects of EC on NAFLD Rats. ELISA was used to detect the levels of proinflammatory factors IL-6, IL-1β, and TNF-α in the serum of rats in each group to analyze the effect of EC on the inflammatory response of NAFLD model rats. Compared to the control group, the serum levels of proinflammatory factors IL-6, IL-1β, and TNF-α were significantly increased in the model group ($P < 0.01$, respectively); compared to the model group, the interventions of simvastatin, EC low-dose, and EC high-dose significantly reduced the serum levels of IL-6 ($P < 0.01$, respectively) and IL-1β ($P < 0.01$, $P < 0.05$, $P < 0.01$, respectively); compared to the model group, the interventions of positive control drug and EC high-dose significantly decreased the serum level of IL-1β in the model group ($P < 0.01$, respectively) (Figure 3(a)). Meanwhile, the mRNA expressions of proinflammatory factors *IL-6*, *IL-1β*, and *TNF-α* in the liver tissue were detected using qPCR. Compared to the control group, the mRNA expressions of *IL-6*, *IL-1β*, and *TNF-α* in the liver were significantly upregulated in the model group ($P < 0.01$, respectively, Figure 3(b)); while the mRNA levels of *IL-6* ($P < 0.01$, $P < 0.05$, $P < 0.01$, respectively) and *IL-1β* ($P < 0.01$, $P < 0.05$, $P < 0.01$, respectively) in simvastatin, EC low-dose, and EC high-dose were significantly downregulated compared to those in the model group. Compared to the model group, the intervention of simvastatin and high-dose EC significantly reduced mRNA expression of *TNF-α* in the liver ($P < 0.01$, respectively) (Figure 3(b)).

The effects of EC on oxidative stress in rats in the NAFLD model group was evaluated by further measuring SOD, MDA, and GSH-Px levels in the liver tissue homogenates of each group. Compared to the control group, SOD and GSH-Px activities in liver tissue homogenates of rats in the model group were significantly reduced ($P < 0.01$, respectively), and MDA levels were significantly increased ($P < 0.01$, respectively). The activity of SOD in the liver homogenate was increased in simvastatin, EC low-dose, and EC high-dose groups compared with the model group ($P < 0.01$, respectively). Compared to the model group, simvastatin and high-dose of EC treatment increased the activity of GSH-Px ($P < 0.05$, $P < 0.01$, respectively) and decreased the level of MDA ($P < 0.01$, respectively) in the liver homogenate (Table 2).

Altogether, EC high-dose had a significant therapeutic effect on NAFLD rats, while significantly decreasing the inflammatory response and enhancing oxidative stress in the liver tissue; therefore, the EC high-dose group was selected for subsequent experiments to study the effects of EC on 16S rRNA sequencing and serum metabolite levels in NAFLD rats.

3.3. Effect of EC on Gut Microbiota of NAFLD Rats. To investigate the changes of EC on the gut microbiota of NAFLD rats, the fecal microbiota of different groups of rats were analyzed using 16S rRNA high-throughput sequencing. Shannon and Simpson indexes were measured to evaluate the alpha diversity of gut microbiota in each group. There were no significant differences in Shannon and Simpson indexes among each group (Figure 4(a)).

Next, the composition of microbial communities of different samples was analyzed using β-diversity and evaluated using principal coordinate analysis (PCoA) and clustering analysis. The PCoA results showed that the sample points of the model group could be completely separated from those in the control group, whereas the sample points of the EC high-dose group were very close to those in control group (Figure 4(b)). Likewise, clustering analysis indicated that the distance from the control group to the EC high-dose group was closer than the distance from the normal group to the model group (Figure 4(c)).

To further explore the α-diversity and β-diversity in the composition of gut microbiota, the number of common and unique OTUs among various groups was analyzed using Venn diagram to visualize the similarity and overlap in OTU number composition among the samples. The results are indicated in the figure, where it was found that the number of OTUs common to the normal group, the model group, and the EC high-dose group were 455 species, while the number of OTUs unique to these three groups were 3,486 species, 2,645 species, and 2,892 species, respectively (Figure 4(d)).

The composition of the gut microbiota in each sample at the phylum level is shown in Figure 4(e). *Firmicutes* and *Bacteroidetes* were dominant taxa at the phylum level. Compared with the control group, the *Firmicutes*/*Bacteroidetes* (F/B) ratio was increased in the model group ($P < 0.01$). Compared with the model group, the F/B ratio in the EC high-dose group was decreased ($P < 0.05$, Figure 4(f)). At the genus level, compared to the normal group, the model group had relatively higher abundance of *Desulfovibrio*, *Romboutsia*, and *Lactobacillus*, *Dubosiella*, *Lachnospiraceae*, and *Akkermansia* had relatively lower abundance; compared to model group, *Lactobacillus*,

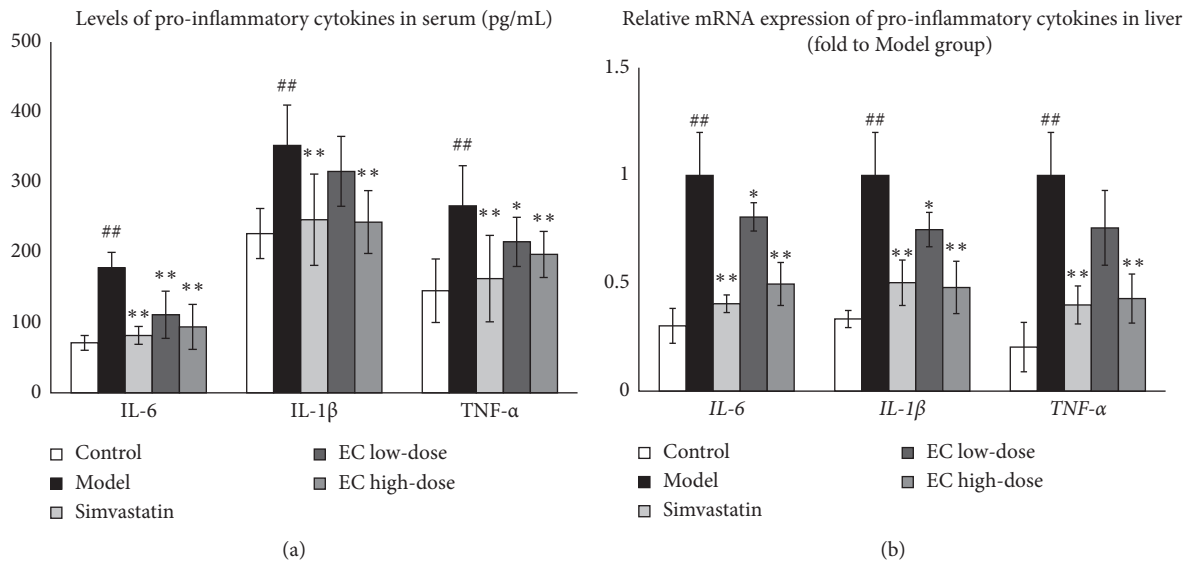

Figure 3: EC treatment reduced the inflammatory response in NAFLD model rats: (a) The levels of *IL-6*, *IL-1β*, and *TNF-α* in serum were decreased after EC treatment. (b) EC treatment downregulated the mRNA expression of *IL-6*, *IL-1β*, and *TNF-α* in the liver. Control, model, simvastatin, EC low-dose, and EC high-dose ($n = 10$ per group) groups are shown. Data are reported as the mean ± SD. $^{\#\#}P < 0.01$ compared with the control group; $^{*}P < 0.05$ compared with the model group; $^{**}P < 0.01$ compared with the model group.

Table 2: The activities of SOD and GSH-Px and the level of MDA in the rat liver homogenate after EC treatment.

Group	SOD (U/mgprot)	MDA (nmol/mgprot)	GSH-px (U/mgprot)
Control	173.07 ± 18.56	3.68 ± 0.85	96.56 ± 9.73
Model	106.52 ± 30.12$^{\#\#}$	15.95 ± 2.43$^{\#\#}$	61.75 ± 13.33$^{\#\#}$
Simvastatin	161.24 ± 23.56**	8.39 ± 3.01**	79.63 ± 18.79*
EC low-dose	144.82 ± 21.48**	13.72 ± 3.00	68.75 ± 14.48
EC high-dose	149.78 ± 33.08**	9.84 ± 4.20**	79.50 ± 5.76**

Control, model, simvastatin, EC low-dose, and EC high-dose ($n = 10$ per group) groups are shown. Data are presented as the mean ± SD. $^{\#\#}P < 0.01$ as compared to the control group; $^{*}P < 0.05$ as compared to the model group; $^{**}P < 0.01$ as compared to the model group. SOD: superoxide dismutase; MDA: methane dicarboxylic aldehyde; GSH-Px: glutathione peroxidase.

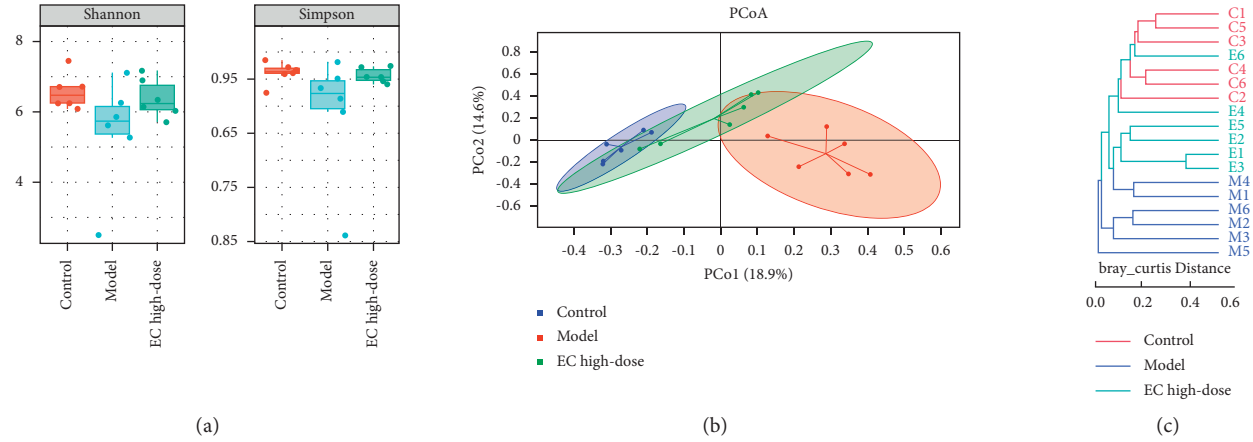

Figure 4: Continued.

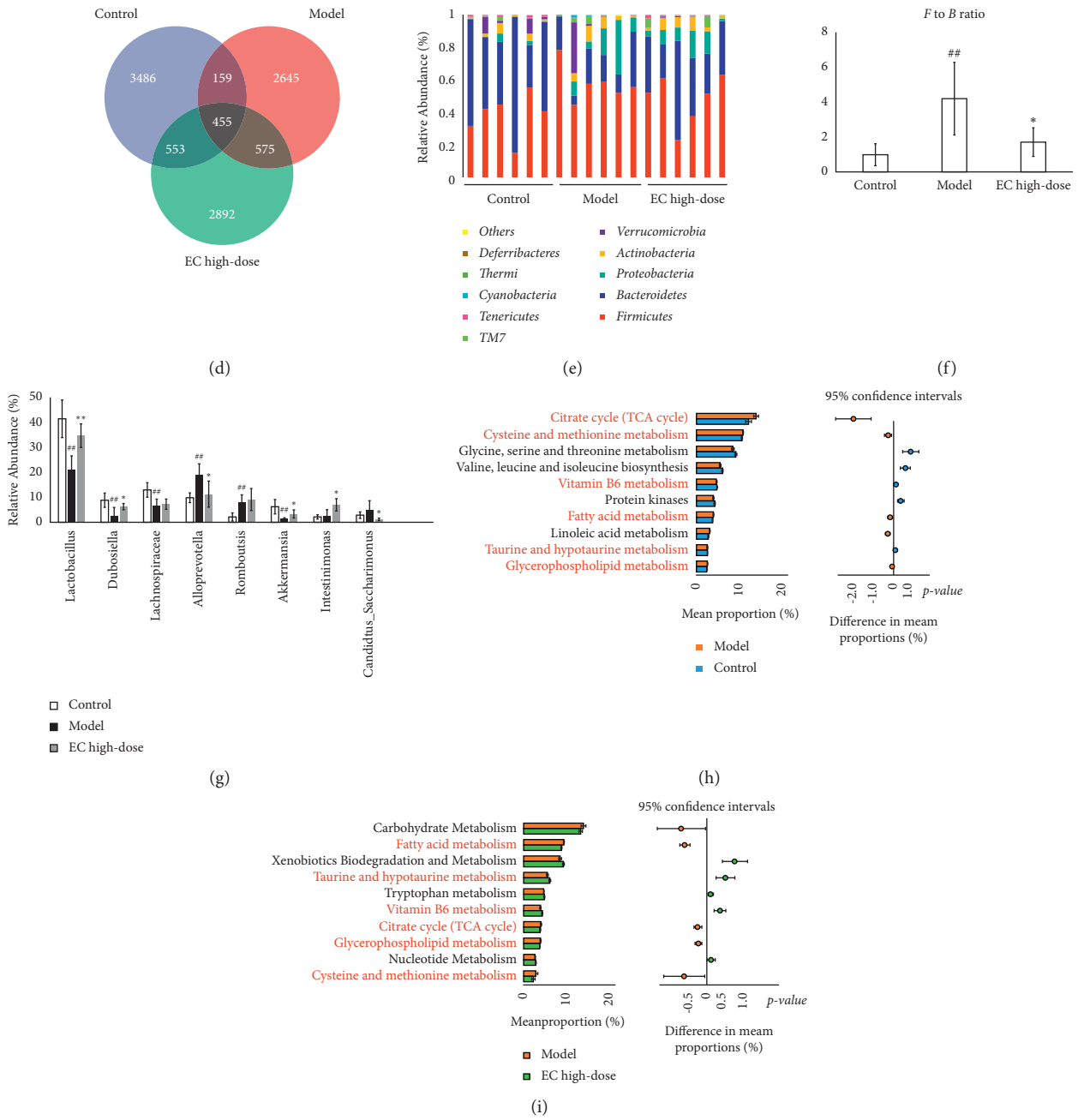

Figure 4: EC treatment affected the gut microbiota community in NAFLD model rats. (a) There were no significant differences in Shannon and Simpson indexes among each group. (b, c) PCoA and system clustering tree indicated that beta diversity of gut microbiota between EC high-dose and control groups was more similar than that between the model and control groups ("C" indicates control group; "M" indicates model group; "E" indicates EC high-dose group). (d) The different numbers of OTUs are shown using Venn diagram. (e, f) EC treatment reduced the F to B ratio in gut microbiota at the phylum level. (g) At the genus level, EC treatment affected the relative abundances of *Lactobacillus*, *Dubosiella*, *Desulfovibrio*, *Romboutsis, Intestinimonas* and *C._saccharimonas* in NAFLD rats. (h, i) The differential metabolic pathways (written in red) of EC on NAFLD were predicted using PICRUSt analysis based on the 16S rRNA sequencing data. Control, model, and EC high-dose ($n = 6$ per group) groups are shown. Data are reported as the mean ± SD. $^{\#\#}P < 0.01$ compared with the control group; $^{*}P < 0.05$ compared with the model group; $^{**}P < 0.01$ compared with the model group.

Dubosiella, *Lachnospiraceae*, *Akkermansia*, and *Intestinimonas* had relatively higher abundance in the EC high-dose group, and the abundance of *Desulfovibrio* and *C._saccharimonas* was relatively lower (Figure 4(g)).

3.4. Functional Prediction of 16S rRNA Sequencing Based on PICRUSt Analysis. PICRUSt analysis was further used to investigate the functional changes in the gut microbiota of NAFLD rats after EC high-dose treatment. Figures 4(e) and 4(f) indicated the top 10 metabolic pathways with the highest proportion and $P < 0.05$. Pathways that were changed in the normal and model groups also in the model and EC groups were considered differential metabolic pathways. Compared to the control group, the abundance of citrate cycle (TCA cycle), cysteine and methionine metabolism, and fatty acid metabolism increased in the model group. In contrast, the abundance of vitamin B6 metabolism reduced; compared with the model group, the abundance of fatty acid metabolism, TCA cycle, glycerophospholipid metabolism, cysteine, and methionine metabolism decreased in the EC high-dose group, but in contrast, the abundance of taurine and hypotaurine metabolism, and vitamin B6 metabolism improved (Figures 4(h) and 4(i)).

3.5. Changes in Serum Metabolite Levels in NAFLD Rats after EC Treatment. The PCA indicated that the control group could be well differentiated from the model group, and the model group was well differentiated from the EC high-dose group (Figure 5(a)). Furthermore, OPLS-DA model was used to identify the differential metabolites (Figures 5(b) and 5(c)). Compared with the control group, model group had explanatory rate (R^2) = 0.94 and predictive power (Q^2) = –0.60; compared to the model group, EC high-dose group had $R^2 = 0.94$ and $Q^2 = -0.49$ (Figures 5(d) and 5(e)). These results showed that the model was stable and had a good predictive ability.

The following two criteria were used to screen the differential metabolites: $P < 0.05$ and VIP >1.0, and 21 differential metabolite was identified (Table 3). Compared to the control group, the serum levels of acetoacetate, cholesterol, AA, 4-pyridoxic acid, stearic acid, taurocholic acid, prostaglandin G2, 16(R)-HETE, methionine, taurine, and pyridoxic acid were significantly improved in the model rats, while the levels of methionine, taurine, pyridoxal, L-cystine, hypotaurine, pyridoxamine, L-cysteinesulfinic acid, cholecalciferol, and α-linolenic acid were significantly reduced; compared to the model group, the serum levels of methionine, taurine, L-cystine, pyridoxamine, L-cysteinesulfinic acid, linoleic acid, calcitriol, cholecalciferol, and α-linolenic acid were significantly increased, while the levels of cholesterol, AA, APS, palmitic acid, 4-pyridoxic acid, taurocholic acid, prostaglandin G2, and 16(R)-HETE were significantly reduced (Table 3).

3.6. Analysis of Differential Metabolic Pathways in the Serum after EC Intervention in NAFLD Rats. The MetaboAnalyst analysis platform was used to conduct the enrichment analysis of the metabolic pathway for differential metabolites, and KEGG was selected as the database to screen the differential metabolic pathways based on the condition of pathway impact >0.1 and $P < 0.05$. The differential metabolic pathways between control and model groups included taurine and hypotaurine metabolism, AA metabolism, alpha-linolenic acid metabolism, cysteine and methionine metabolism, vitamin B6 metabolism, synthesis and degradation of ketone bodies, and butanoate metabolism (Figure 5(f)). The differential metabolic pathways between model and EC high-dose groups included taurine and hypotaurine metabolism, AA metabolism, alpha-linolenic acid metabolism, cysteine and methionine metabolism, vitamin B6 metabolism, sulfur metabolism, linoleic acid metabolism (Figure 5(g)). Among them, AA metabolism, taurine and hypotaurine metabolism, alpha-linolenic acid metabolism, cysteine and methionine metabolism, and vitamin B6 metabolism pathways were common between the normal and model groups, and also between the model and EC high-dose groups, where these pathways were selected to be the metabolic pathways of the EC intervention model group.

3.7. Correlation Analysis of Nontargeted Metabolomics and Gut Microbiota. Spearman's correlation analysis was used to assess the relationship between serum differential metabolites and genus levels of gut microbiota in the normal, model, and EC high-dose groups. As indicated in Figure 6, *Lactobacillus*, *Dubosiella*, *Lachnospiraceae*, *Desulfovibrio*, *Romboutsia*, *Akkermansia*, *Intestinimonas*, and *C._saccharimonas* were correlated with most of the metabolites.

3.8. Correlation Analysis of Therapeutic Effect Indicators, Oxidative Stress Indicators, and Proinflammatory Cytokines with Gut Microbiota. Spearman correlation analysis was used to assess the relationship between therapeutic effect indicators, oxidative stress levels, proinflammatory cytokines, and gut microbiota in the control, model, and EC high-dose groups. As indicated in Figure 7, *Dubosiella*, *Lactobacillus*, and *Intestinimonas* were negatively correlated with most of the physiological indicators, and *Romboutsia* and *Desulfovibrio* were positively correlated with most of the physiological indicators. In addition, *Dubosiella*, *Lactobacillus*, and *Intestinimonas* were negatively correlated with certain proinflammatory cytokines, and *Romboutsia* and *Desulfovibrio* were positively correlated with certain proinflammatory cytokines. *Dubosiella*, *Lachnospiraceae*, *Romboutsia*, *Intestinimonas*, and *C._saccharimonas* were correlated with certain oxidative stress factors.

4. Discussion

In this study, high-fat chow feeding was used to generate the NAFLD rat model, which is consistent with the previous study [31]. Compared to the control group, rats in the model group had significantly increased body weight and serum levels of TG, TC, ALT, and AST. Pathological examination also indicated significant steatosis and cellular damage in

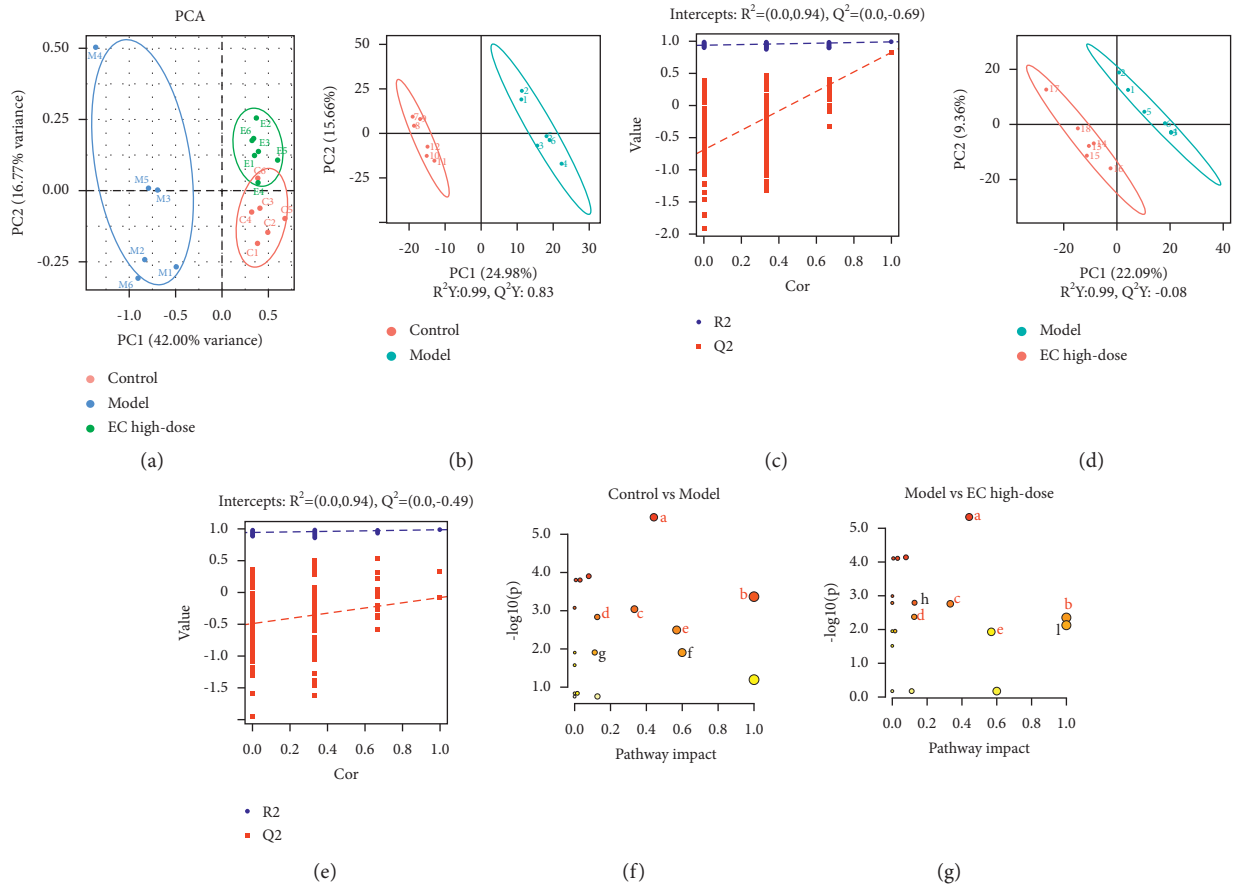

Figure 5: EC modulated the metabolites in serum in NAFLD rats. (a) PCA among groups. (b, c) OPLS-DA of untargeted metabolomics data between the control and model groups and the relative coefficient of loading plots. (d, e) OPLS-DA untargeted metabolomics data between the model and EC high-dose groups and the relative coefficient of loading plots. (f, g) Pathway analysis of differential metabolites between control and model groups (f) and between model and EC high-dose groups (g). The common pathways were written in red. a, arachidonic acid metabolism; b, taurine and hypotaurine metabolism; c, alpha-linolenic acid metabolism; d, cysteine and methionine metabolism; e, vitamin B6 metabolism; f, synthesis and degradation of ketone bodies; g, butanoate metabolism; h, sulfur metabolism; i, linoleic acid metabolism.

hepatocytes of rats in the model group, which is consistent with pathological NAFLD manifestations. Each EC dose group could decrease body weight, improve dyslipidemia, and alleviate liver pathological changes in NAFLD rats to different degrees, suggesting that EC has a therapeutic effect on NAFLD, and is most evident in the high-dose group. Simvastatin is a first-line regimen for treating NAFLD in clinical practice, which decreases body weight and increases serum ALT levels in patients with NAFLD [32]. It enhances NAFLD by increasing endothelial nitric oxide synthase (eNOS) expression, reducing inducible nitric oxide synthase (iNOS) expression, and inhibiting hepatic stellate cell (HSC) activation [33]. Therefore, simvastatin was chosen as the positive control group. The results indicated that simvastatin did not vary significantly from the EC high-dose group in improving body weight, blood lipids, and pathological changes.

Then, we evaluated the effect of EC on the level of oxidative stress and inflammation in rats with NAFLD, which has a complex pathogenesis, but the "two-hit" hypothesis is widely accepted. Fatty acids enter the liver and are deposited as TG in huge amounts in the liver parenchyma cells, and the gradual disruption of intracellular metabolism is the first hit of the disease. When cells are unable to store large amounts of free fatty acids as TG or exceed the load of cellular oxidative, the generation of large number of reactive oxygen species (ROS) from excess fatty acids inducing endoplasmic reticulum stress, oxidative stress, apoptosis, and inflammatory responses is the second hit to disease onset [34]. Our results discovered that EC could increase SOD and GSH-Px activities and reduce MDA levels in NAFLD rats, suggesting that EC can decrease oxidative stress in NAFLD model rats. As the end product of lipid peroxidation under oxidative stress, level of MDA could reflect the severity of oxidative damage in cells and organs [35]. SOD acts as an intracellular oxygen radical scavenger, catalyzing O_2^- to O_2 and H_2O_2 and protects the body from superoxide anions [36, 37]. GSH-Px catalyzes the conversion of glutathione (GSH) to oxidized glutathione (GSSG) and protects cells from oxidative stress [38].

ELISA and qPCR results indicated that EC could reduce the inflammatory response, as evidenced by the

Table 3: The differential metabolites in the serum of NAFLD rats.

No.	Formula	RT (min)	m/z	Metabolites	VIP		FC		Trend		Pathway
					M vs. C	E vs. M	M vs. C	E vs. M	M vs. C	E vs. M	
1	$C_5 H_{11} N O_2 S$	2.00	150.06	Methionine	1.49	1.46	0.63	1.30	↓#	↑*	d
2	$C_4 H_6 O_3$	1.48	101.02	Acetoacetate	1.30	1.45	1.65	1.26	↑#	↑	F, g
3	$C_{27} H_{46} O$	15.18	387.36	Cholesterol	1.22	2.10	1.75	0.54	↑##	↓**	
4	$C_{26} H_{54} N O_7 P$	10.52	568.36	Arachidonic acid	1.69	1.28	1.81	0.65	↑##	↓**	a
5	$C_{10} H_{14} N_5 O_{10} P S$	5.32	426.01	APS	1.98	2.04	1.27	0.67	↑	↓**	h
6	$C_2 H_7 N O_3 S$	1.44	124.01	Taurine	1.59	1.85	0.46	1.89	↓##	↑*	b
7	$C_{16} H_{32} O_2$	10.43	255.23	Palmitic acid	2.35	1.27	1.31	0.67	↑	↓*	
8	$C_8 H_9 N O_3$	5.27	168.06	Pyridoxal	1.17	1.29	0.79	1.26	↓#	↑*	e
9	$C_6 H_{12} N_2 O_4 S_2$	1.20	239.02	L-Cystine	1.44	1.00	0.68	1.42	↓##	↑*	d
10	$C_2 H_7 N O_2 S$	1.35	110.03	Hypotaurine	1.22	1.84	0.76	1.31	↓#	↑*	b
11	$C_8 H_{12} N_2 O_2$	1.24	169.09	Pyridoxamine	2.31	2.44	0.71	1.33	↓#	↑*	e
12	$C_{25} H_{50} N O_7 P$	14.64	566.35	L-Cysteinesulfinic acid	1.08	2.08	0.67	1.41	↓##	↑**	b, d
13	$C_8 H_9 N O_4$	3.73	184.06	4-Pyridoxic acid	1.60	1.98	1.60	0.60	↑#	↓**	e
14	$C_{18} H_{36} O_2$	11.32	283.26	Stearic acid	2.00	1.14	1.83	0.79	↑##	↓	
15	$C_{18} H_{32} O_2$	7.72	279.23	Linoleic acid	1.23	2.82	1.31	1.48	↑	↑**	i
16	$C_{27} H_{44} O_3$	14.08	415.32	Calcitriol	1.60	1.52	1.38	1.56	↑	↑*	
17	$C_{26} H_{45} N O_7 S$	8.30	516.30	Taurocholic acid	1.76	1.61	1.44	0.66	↑##	↓**	b
18	$C_{27} H_{44} O$	11.65	385.35	Cholecalciferol	1.61	1.85	0.60	1.57	↓##	↑*	
19	$C_{20} H_{32} O_6$	13.13	367.21	Prostaglandin G2	1.48	1.28	1.91	0.50	↑##	↓**	a
20	$C_{18} H_{30} O_2$	14.73	279.23	α-Linolenic acid	2.34	1.63	0.59	1.61	↓##	↑**	c
21	$C_{20} H_{32} O_3$	13.95	343.22	16(R)-HETE	1.79	2.68	1.87	0.51	↑##	↓**	a

Control, model, and EC high-dose ($n = 6$ per group) groups are shown. $^{\#}P < 0.05$ compared with the control group; $^{\#\#}P < 0.01$ compared with the control group; $^{*}P < 0.05$ compared with the model group; $^{**}P < 0.01$ compared with the model group; ↑: increase; ↓: decrease; vs.: versus; C: control group; M: model group; E: EC high-dose group; RT: retention time; VIP: variable importance of projection; FC: fold change; a: arachidonic acid metabolism; b: taurine and hypotaurine metabolism; c: alpha-linolenic acid metabolism; d: cysteine and methionine metabolism; e: vitamin B6 metabolism; f: synthesis and degradation of ketone bodies; g: butanoate metabolism h: sulfur metabolism; i: linoleic acid metabolism.

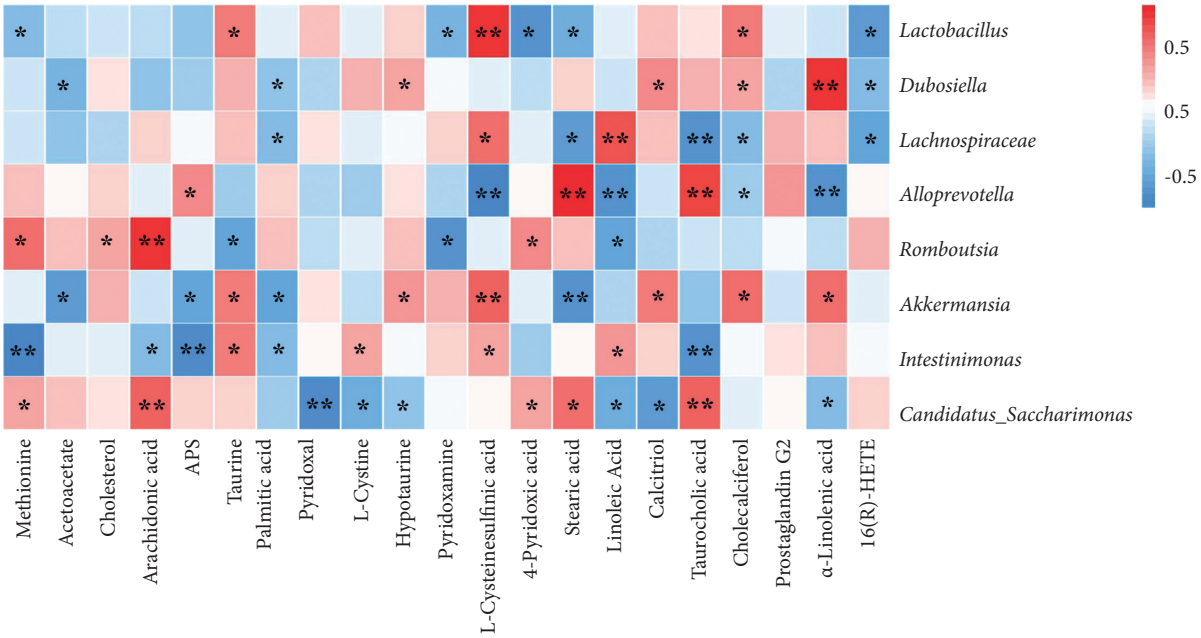

Figure 6: Spearman correlation analysis of gut microbiota with differential abundance and differential metabolites in the serum (heatmap). Red grids indicate positive correlations between gut microbiota and metabolites (correlation analysis value > 0.1), and blue grids indicate negative correlations between gut microbiota and metabolites (correlation analysis value < −0.1). $^{*}P < 0.05$; $^{**}P < 0.01$.

downregulation of gene expression of liver *IL-1β*, *IL-6*, and *TNF-α* with the decrease IL-1β, IL-6, and TNF-α levels in serum. Excessive lipid levels cause hepatocytes to produce proinflammatory factors such as IL-6, IL-1β, and TNF-α, causing NAFLD onset [39, 40]. TNF-α is closely related to the body's inflammatory response, lipid metabolism, and cell death [41]. IL-6 is also an essential proinflammatory factor that induces liver injury, causes hepatocyte apoptosis,

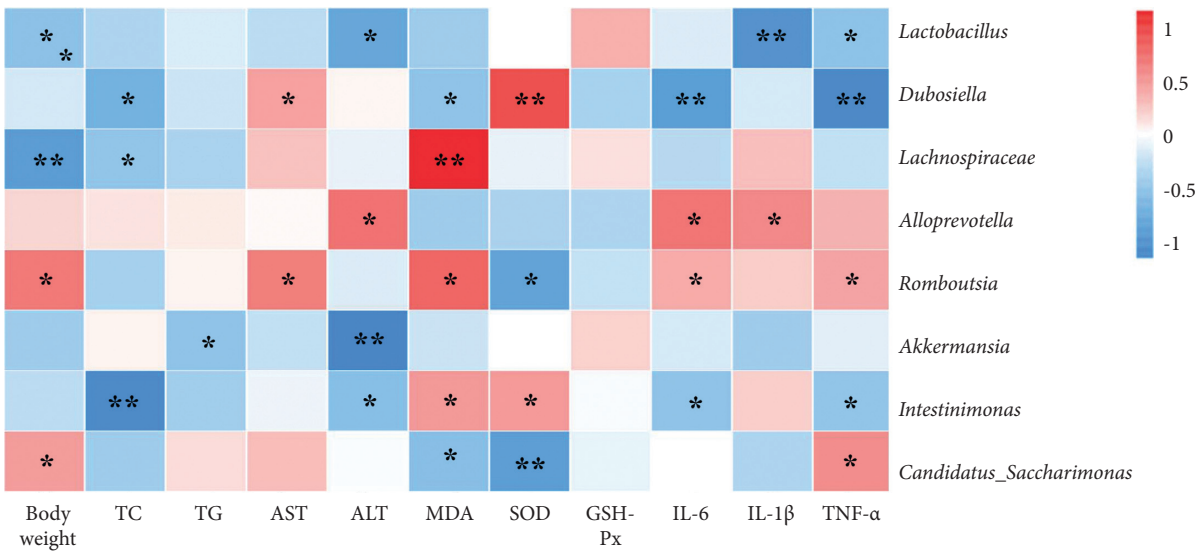

Figure 7: Spearman correlation analysis between general statement, biochemical markers, and proinflammatory cytokines and gut microbiota (heatmap). Red grids indicate positive correlations between general statement, biochemical markers, and proinflammatory cytokines and gut microbiota (correlation analysis value > 0.1), while blue grids indicate negative correlations between general statement, biochemical markers, and proinflammatory cytokines and gut microbiota (correlation analysis value < −0.1). $^{*}P < 0.05$; $^{**}P < 0.01$.

manufactures insulin resistance, and is involved in the development and progression of NAFLD [42]. IL-1β is involved in the metabolic activity of different acute liver injury symptoms and promotes hepatic steatosis [43]. These inflammatory cytokines cause compensatory hyperinsulinemia, which impairs hepatic fat metabolism and causes hepatocellular steatosis; therefore, the suppression of the inflammatory response can alleviate NAFLD [44].

The effect of the EC high-dose group on the gut microbiota of NAFLD model rats was investigated using 16S rRNA sequencing technology. The Simpson index and Shannon index reduced in the model group and increased after EC administration, proposing that EC could increase the alpha diversity of gut microbiota in NAFLD rats. The results of PCoA plot and clustering tree indicated that the beta diversity of the gut microbiota of rats in the EC group was more similar to that of the control group than to that of the model group, and these results suggested that EC could restore the beta diversity of the gut microbiota of NAFLD rats to control group's level. Further analysis of microbiota abundance indicated that at the phylum level, the main gut microbiota species in each group were *Bacteroidetes* and *Firmicutes*, and the ratio of *Firmicutes* to *Bacteroidetes* was increased in the NAFLD model rats, while EC significantly decreased the F/B ratio of gut microbiota. The F/B ratio is closely related to the inflammatory response of the organism and dyslipidemia [45]. Compared to healthy controls, patients with dyslipidemia had a significant increase in the relative abundance of *Firmicutes*, a significant reduction in *Bacteroidetes*, and an increase in the ratio [46]. Clinically, decreasing the F/B ratio in patients enhances lipids [47].

Further analysis at the genus level indicated that the abundance of *Lactobacillus*, *Dubosiella*, *Lachnospiraceae*, and *Akkermansia* was significantly reduced, and the abundance of *Alloprevotella* and *Romboutsia* was significantly increased in the model rats compared to that in the control group. EC treatment increased the abundance of *Lactobacillus*, *Dubosiella*, *Akkermansia*, and *Intestinimonas* and reduced the abundance of *Alloprevotella* and *C._saccharimonas* in NAFLD model rats. *Lactobacillus* is a major probiotic with an essential role in regulating body metabolism immunity, and so on [48–50]. The abundance of *Lactobacillus* was decreased in models of diabetes, fatty liver, and obesity, and the metabolic and inflammatory responses of the body could be enhanced by transplanting *Lactobacillus* [51]. The *Dubosiella* was decreased in mice with acute alcoholic liver injury [52]. The *Dubosiella* are potential beneficial bacteria for colitis [53], and studies have indicated that the mechanism of action of Chinese medicinal plant extracts from *Lonicera hypoglauca* and *Scutellaria baicalensis* in alleviating inflammation and oxidative stress in mice with colitis may be related to increased *Dubosiella* abundance [54]. The *Lachnospiraceae* are butyrate-producing bacteria, and one study found that the abundance of *Lachnospiraceae* was decreased in patients with NAFLD [55]. Butyrate production by bacteria is a key function in maintaining gut microbiota homeostasis, and butyrate significantly alleviates steatohepatitis by regulating gut microbiota and intestinal barrier function, thereby decreasing inflammation and oxidative damage in the liver [56]. *Desulfovibrio* promotes inflammatory responses and metabolic disorders in the organism. In a type 2 diabetes model, the abundance of *Desulfovibrio* was significantly elevated [57]. Suppression of *Desulfovibrio* abundance by microbiota transplantation may improve diabetes [58]. *Romboutsia* are bacteria associated with obesity, and some studies have indicated a positive correlation between *Romboutsia* and body fat [59]. In a high-fat diet-induced hyperlipidemia rat model, spirulina platensis 55% ethanol extract enhanced lipid metabolism by reducing the abundance of *Romboutsia* [60]. The increased

abundance of *Akkermansia* decreases the elevated lipopolysaccharide levels induced by the high-fat diet and is essential for maintaining homeostasis of glucose metabolism [61]. One study found a significant increase in the percentage of *Akkermansia* in the gut microorganisms of obese mice treated with metformin and its role in inhibiting lipid metabolic processes [62]. *Intestinimonas* are also butyrate-producing enterobacteria with antiobesity and anti-inflammatory effects [63]. *C._saccharimonas* are conditionally pathogenic bacteria that are significantly elevated in the intestine of gout patients [64]. In addition, green tea leaf powder reduces high-fat diet-induced disorders in lipid metabolism, while reducing the abundance of *C._saccharimonas* in their intestines [65]. PICRUSt analysis was used to predict the metabolic pathways associated with altered gut microbiota, including fatty acid metabolism, taurine and hypotaurine metabolism, vitamin B6 metabolism, TCA cycle, glycerophospholipid metabolism, and cysteine and methionine metabolism.

PCA and OPLS-DA of serum nontargeted metabolomics indicated that the metabolites of NAFLD model rats significantly varied from that of the control rats, and the serum metabolite levels of rats after EC intervention significantly varied from those of NAFLD model rats. The metabolic pathway analysis of the differential metabolites using MetaboAnalyst indicated that EC could affect the metabolic pathways of AA metabolism, taurine and hypotaurine metabolism, alpha-linolenic acid metabolism, cysteine and methionine metabolism, and vitamin B6 metabolism. The taurine and hypotaurine metabolism, cysteine and methionine metabolism, and vitamin B6 metabolism pathways were common pathways, proposing that EC may affect NAFLD treatment by regulating gut microbiota, which in turn affects the pathways of taurine and hypotaurine metabolism, cysteine and methionine metabolism, and vitamin B6 metabolism.

4.1. Taurine and Hypotaurine Metabolism. Taurine and hypotaurine metabolism are closely related to many diseases. In our study, it was found that taurine and hypotaurine levels were decreased in NAFLD model rats and were significantly increased after EC treatment. Taurocholic acid levels were increased and decreased after EC treatment. Taurine has different physiological functions in cells, such as improving glucolipid metabolism, immunomodulation, anti-inflammation, and antioxidation [66]. It has been shown that taurine supplementation prevents obesity and insulin resistance [67]. Taurine can decrease inflammation in adipose tissue by decreasing macrophage infiltration [68]. In addition, hepatic taurine levels affect hepatic steroid metabolism and other lipid metabolism [69–71]. Taurine is a recognized antioxidant and increases the activity of the antioxidant enzymes superoxide dismutase and glutathione peroxidase [72]. Ebrahim and Sakthisekaran showed that taurine supplementation in rats was effective in avoiding biomembrane damage induced by lipid peroxidation by increasing the antioxidant capacity of the body [73]. High concentrations of taurine may help protect the gastric mucosa from oxidative stress [74]. Taurine has a hepatoprotective effect and was found to protect against acetaminophen-induced liver injury in rats, and taurine also enhanced many liver function indicators in a carbon tetrachloride-induced liver fibrosis model by improving serum transaminase and bilirubin levels and antioxidant effects [75, 76]. Hypotaurine is a precursor of taurine synthesis that produces taurine by enzymatic action [77]. It is an antioxidant and singlet oxygen scavenger that protects cells from oxidative stress damage [78]. It has been proposed that the antioxidant effect of hypotaurine may be related to the prevention of SOD enzyme inactivation [79]. Hypotaurine decreased liver injury and fat accumulation in the NAFLD mice model, and hypotaurin supplementation was shown to increase insulin sensitivity in obese mice in an obesity model [79]. Taurocholic acid is a conjugated primary bile acid formed by bile acid binding to taurine in hepatocytes. In cholestatic liver disease, taurocholic acid-induced inflammatory response plays an essential role in disease progression [80]. Taurocholic acid levels are significantly elevated in the metabolic profile of patients with NAFLD [81]. Taurocholic acid in the liver activates sphingosine 1-phosphate receptor 2 (S1PR2)-mediated signaling pathways involved in the process of liver inflammation and fibrosis [82]. Spearman's analysis indicated that taurine was associated with *Lactobacillus*, *Akkermansia*, and *Intestinimonas*, and negatively correlated with *Romboutsia*; hypotaurine was positively correlated with *Dubosiella* and *Akkermansia* and negatively correlated with *C._saccharimonas*; and taurocholic acid was positively correlated with *Desulfovibrio* and *C._saccharimonas and* negatively correlated with *Lachnospiraceae* and *Intestinimonas.* Therefore, it was speculated that the effect of EC on taurine and hypotaurine metabolism may be related to the regulation of the abundance of *Lactobacillus*, *Akkermansia, Intestinimonas*, *Romboutsia, Dubosiella, Lachnospiraceae, Desulfovibrio,* and *C._saccharimonas*.

4.2. Cysteine and Methionine Metabolism. Cysteine and methionine metabolism is an amino acid metabolism closely related to oxidative stress and can regulate oxidative stress through the methionine/glutathione S-transferase pathway [83]. Our study found that methionine, L-cystine, and L-cysteinesulfinic acid were reduced in model group rats and increased after drug administration. Methionine and choline deficiency diet is commonly used to cause NAFLD in rodents. Methionine deficiency decreases in mice low density lipoprotein (LDL) synthesis and dysfunction of mitochondrial β-oxidation, causing rapid and massive accumulation of triacylglycerol in hepatocytes, cause hepatocyte steatosis, which constitutes the "first hit" and increases the susceptibility of the liver to other injuries [84]; hepatocyte steatosis leads to decreased mitochondrial uptake of free fatty acids, contributing to increased free fatty acid β-oxidation, causing oxidative stress and lipid peroxidation, constituting a "second hit" to the liver [85]. Methionine supplementation to a high-cholesterol diet can significantly decrease hepatic steatosis, oxidative stress, and fibrosis induced by high

choline [86]. Methionine is one of the important amino acids in the body, providing the methyl group required for the synthesis of choline in the body, which promotes phospholipid synthesis, synthesizes lipoproteins, and facilitates the transport of fat to tissues other the liver to alleviate fatty liver [87, 88]. L-cystine is a precursor of the antioxidant GSH and an essential nutrient for maintaining normal liver function. L-cystine can be converted from methionine to N-acetylcysteine (NAC) and taurine, among others, to supply the needs of cells [89, 90]. Supplementation with L-cystine reduces the elevated serum triglyceride and TC concentrations induced by liver cancer [91]. L-cystine can be converted to L-cysteine by the action of cysteine reductase [92]. Cysteine is converted to decreased glutathione (GSH) catalyzed by glutamate cysteine ligase (GCLC) and glutathione synthetase (GSS), which is involved in the decrease process of cells and phospholipid metabolism in the liver, protecting cells from lipid peroxidation damage [93]. It has been indicated that L-cysteine can upregulate GSH levels and improve oxidative stress in a high-glucose cultured hepatocyte model and in diabetic fatty liver rats [94]. Long-term supplementation with L-cysteine restores cardiovascular lesions caused by a high-fat diet in rats [95]. Dietary supplementation with L-cysteine dose-dependently promoted the antioxidant enzyme activity and decreased lipid levels in the serum and rat liver [96]. L-cysteinesulfinic acid is an intermediate in the *in vivo* oxidation of L-cystine and L-cysteine and is a precursor of taurine. Cysteine sulfinate is decarboxylated to hypotaurine by cysteine sulfinate decarboxylase, and then oxidized to taurine. Spearman's analysis indicated that methionine was positively correlated with *Romboutsia* and *C._saccharimonas* and negatively correlated with *Lactobacillus* and *Intestinimonas*; L-cystine was positively correlated with *Intestinimonas* and negatively correlated with *C._saccharimonas*; and *L-cysteinesulfinic acid* was positively correlated with *Lactobacillus*, *Lachnospiraceae*, *Akkermansia*, and *Intestinimonas*, and negatively correlated with *Desulfovibrio.* Therefore, it was speculated that the effect of EC on cysteine and methionine metabolism may be related to the regulation of the abundance of *Lactobacillus*, *Lachnospiraceae*, *Akkermansi*, *Intestinimonas*, *Romboutsia*, *Desulfovibrio*, and *C._saccharimonas*.

4.3. Vitamin B6 Metabolism. Vitamin B6 metabolism has antioxidant, hepatoprotective, blood cholesterol lowering, and anti-angiosclerosis effects [97, 98]. In our study, it was found that pyridoxal and pyridoxamine were significantly reduced in the model rats and increased after the administration of EC, while 4-pyridoxic acid was increased in the model rats and reduced after drug administration. Pyridoxal is an active form of vitamin B [99], and pyridoxal is normally converted to pyridoxal-5-phosphate (PLP) by pyridoxal kinase, which acts as a cofactor for several enzymes involved in amino acid metabolism [100]. PLP can attenuate calcium signaling *in vitro* and inhibit calcium entry into adipocytes and subsequent expression of adipocyte fatty acid synthase (FASN), thereby inhibiting lipid synthesis [101–103]. PLP treatment increased fat oxidation and insulin sensitivity in 3T3L1 adipocytes and significantly decreased oxidative and inflammatory stress [104]. Pyridoxamine is a possible inhibitor of advanced glycation end products, and is a vitamin B6 derivative and anti-glycation agent [105]. A study has indicated that pyridoxamine significantly inhibits the expression of proinflammatory genes in visceral adipose tissue of HFD mice [106]. Pyridoxamine inhibits HFD-induced weight gain and macrophage M1 polarization in obese rats and increases GLO1 expression in perivascular and visceral adipose tissue through the RAGE pathway, where it was speculated that pyridoxamine is a candidate for treating obesity or obesity-related inflammatory complications [107]. Pyridoxamine modulates oxidative stress, advanced glycosylation, inflammatory factor levels, and metabolic disorders. Also, it improves microcirculation in patients with NAFLD [108]. The 4-pyridoxic acid is the final vitamin B6 breakdown product. Vitamin B6 is metabolized to PLP in the body, which is further dephosphorylated and oxidized, and eventually generates 4-pyridoxic acid, excreted in the urine [109]. Some studies have indicated that serum 4-pyridoxic acid is elevated in renal insufficiency [110]. However, the relationship between 4-pyridoxic acid and fatty liver is unclear and requires studying in subsequent experiments. Spearman analysis indicated that pyridoxal was negatively correlated with *C._saccharimona*; pyridoxamine was negatively correlated with *Lactobacillus* and *Romboutsia*; and 4-pyridoxic acid was positively correlated with *Romboutsia* and *C._saccharimona* and negatively correlated with *Lactobacillus*. Therefore, it was speculated that the effect of EC on the TCA cycle may be related to the regulation of the abundance of *C._saccharimonas*, *Lactobacillus,* and *Romboutsia.*

5. Conclusions

In conclusion, our study showed multiple ameliorative effects of EC on NAFLD, including enhancement of liver function and blood lipids, as well as alleviation of pathological changes, oxidative stress, and inflammatory responses. The mechanism of EC for NAFLD may be related to the enhancement of gut microbiota alteration, regulation of metabolic pathways of taurine and hypotaurine metabolism, and cysteine and methionine metabolism as well as vitamin B6 metabolism.

Data Availability

The raw data supporting the conclusions of this article will be made available by the corresponding authors, without undue reservation.

Disclosure

Jing Miao and Liying Guo share the first authorship.

Conflicts of Interest

The authors declare that they have no conflicts of interest.

Acknowledgments

This work was supported by the Science and Technology projects in Key Fields of Traditional Chinese Medicine of Tianjin Municipal Health Commission (No. 2020006); Integrated Traditional Chinese and Western Medicine Scientific Research Project of Tianjin Traditional Chinese Medicine Administration Bureau, Tianjin Municipal Health Commission (2021135); Tianjin Key Medical Discipline (Specialty) Construction Project; and Chinese Foundation for Hepatitis Prevention and Control Chinese and Western Medicine Liver Disease Fund project (YGFK20210022).

References

[1] V. Bieghs, P. J. Van Gorp, K. Wouters et al., "LDL receptor knock-out mice are a physiological model particularly vulnerable to study the onset of inflammation in non-alcoholic fatty liver disease," *PLoS One*, vol. 7, no. 1, Article ID e30668, 2012.

[2] M. Eslam, P. N. Newsome, S. K. Sarin et al., "A new definition for metabolic dysfunction-associated fatty liver disease: an international expert consensus statement," *Journal of Hepatology*, vol. 73, no. 1, pp. 202–209, 2020.

[3] D. Jeon, M. Son, and J. Shim, "Dynamics of serum retinol and alpha-tocopherol levels according to non-alcoholic fatty liver disease status," *Nutrients*, vol. 13, no. 5, p. 1720, 2021.

[4] "Nonalcoholic steatohepatitis clinical research network," *Hepatology*, vol. 37, p. 224, 2003.

[5] F. Ahsan, F. Oliveri, H. K. Goud et al., "Pleiotropic effects of statins in the light of non-alcoholic fatty liver disease and non-alcoholic steatohepatitis," *Cureus*, vol. 12, no. 9, Article ID e10446, 2020.

[6] S. Francque, G. Szabo, M. F. Abdelmalek et al., "Nonalcoholic steatohepatitis: the role of peroxisome proliferator-activated receptors," *Nature Reviews Gastroenterology & Hepatology*, vol. 18, no. 1, pp. 24–39, 2021.

[7] A. J. Sanyal, N. Chalasani, K. V. Kowdley et al., "Pioglitazone, vitamin E, or placebo for nonalcoholic steatohepatitis," *New England Journal of Medicine*, vol. 362, no. 18, pp. 1675–1685, 2010.

[8] M. Yan, R. Lu, X. Jia, F. Meng, and X. Zhao, "Different serum lipid adjustment drugs for the treatment of hyperlipidemic fatty liver," *Chinese Journal of Hepatology*, vol. 9, pp. 355–357, 2001.

[9] X. W. Zhao, "Diagnosis and treatment of fatty liver in progress," *Journal of Traditional Chinese Medicine*, vol. 43, pp. 943–945, 2002.

[10] M. Shao, Z. Ye, Y. Qin, and T. Wu, "Abnormal metabolic processes involved in the pathogenesis of non-alcoholic fatty liver disease (review)," *Experimental and Therapeutic Medicine*, vol. 20, no. 5, p. 26, 2020.

[11] B. J. Perumpail, A. A. Li, N. John et al., "The therapeutic implications of the gut microbiome and probiotics in patients with NAFLD," *Diseases*, vol. 7, no. 1, pp. 1–12, 2019.

[12] G. Su, H. Wang, J. Bai, G. Chen, and Y. Pei, "A metabonomics approach to drug toxicology in liver disease and its application in traditional Chinese medicine," *Current Drug Metabolism*, vol. 20, pp. 292–300, 2018.

[13] V. Tremaroli and F. Bäckhed, "Functional interactions between the gut microbiota and host metabolism," *Nature*, vol. 489, no. 7415, pp. 242–249, 2012.

[14] L. Yang, J. Liao, A. Liu et al., "Advances in traditional Chinese medicine for liver disease therapy in 2020," *Traditional Medicine Research*, vol. 6, no. 3, p. 30, 2021.

[15] C. Liu, J.-Z. Liao, and P.-Y. Li, "Traditional Chinese herbal extracts inducing autophagy as a novel approach in therapy of nonalcoholic fatty liver disease," *World Journal of Gastroenterology*, vol. 23, no. 11, pp. 1964–1973, 2017.

[16] Y. Zhang, K. Tang, Y. Deng et al., "Effects of shenling baizhu powder herbal formula on intestinal microbiota in high-fat diet-induced NAFLD rats," *Biomedicine & Pharmacotherapy*, vol. 102, pp. 1025–1036, 2018.

[17] Y. Deng, K. Tang, R. Chen et al., "Effects of shugan-jianpi recipe on the expression of the *p*38 MAPK/NF-κB signaling pathway in the hepatocytes of NAFLD rats," *Medicines*, vol. 5, no. 3, p. 106, 2018.

[18] X. W. Gong, Y. J. Xu, Q. H. Yang et al., "Effects of soothing liver and invigorating spleen recipes on the IKK-NF-B signaling pathway in kupffer cells of nonalcoholic steatohepatitis rats," *Evidence-Based Complementary and Alternative Medicine*, vol. 2015, Article ID 687690, 9 pages, 2015.

[19] H. Cui, Y. Li, Y. Wang et al., "Da-chai-hu decoction ameliorates high fat diet-induced nonalcoholic fatty liver disease through remodeling the gut microbiota and modulating the serum metabolism," *Frontiers in Pharmacology*, vol. 11, Article ID 584090, 2020.

[20] C. Hong, Z. Chen, and R. Zhang, *Treating Fatty Liver from Phlegm and Dampness*, Fujian University of Traditional Chinese Medicine, Fuzhou, China, 2019.

[21] H. Zhang and J. Liu, "Clinical study on treating metabolic syndrome with phlegm, dampness and stasis," *China & Foreign Medical Treatment*, vol. 6, pp. 131–133, 2014.

[22] Q. Jiang and C. Liu, "Observation on the curative effect of Er-Chen decoction in treating 30 cases of non-alcoholic fat," *Medicine & People*, vol. 27, no. 8, p. 1, 2014.

[23] H. Fan, X. Ma, P. Lin et al., "Scutellarin prevents nonalcoholic fatty liver disease (NAFLD) and hyperlipidemia via PI3K/AKT-dependent activation of nuclear factor (Erythroid-Derived 2)-like 2 (Nrf2) in rats," *Medical Science Monitor*, vol. 23, 2017.

[24] H. Cheng, N. Xu, W. Zhao et al., "(-)-Epicatechin regulates blood lipids and attenuates hepatic steatosis in rats fed high-fat diet," *Molecular Nutrition & Food Research*, vol. 61, 2017.

[25] H. Cui, Y. Li, M. Cao et al., "Untargeted metabolomic analysis of the effects and mechanism of nuciferine treatment on rats with nonalcoholic fatty liver disease," *Frontiers in Pharmacology*, vol. 11, p. 858, 2020.

[26] T. Magoc and S. L. Salzberg, "FLASH: fast length adjustment of short reads to improve genome assemblies," *Bioinformatics*, vol. 27, no. 21, pp. 2957–2963, 2011.

[27] R. C. Edgar, "UPARSE: highly accurate OTU sequences from microbial amplicon reads," *Nature Methods*, vol. 10, no. 10, pp. 996–998, 2013.

[28] C. Quast, E. Pruesse, P. Yilmaz et al., "The SILVA ribosomal RNA gene database project: improved data processing and web-based tools," *Nucleic Acids Research*, vol. 41, pp. D590–D596, 2013.

[29] R. C. Edgar, "MUSCLE: multiple sequence alignment with high accuracy and high throughput," *Nucleic Acids Research*, vol. 32, no. 5, pp. 1792–1797, 2004.

[30] W. Dai, D. Xie, M. Lu et al., "Characterization of white tea metabolome: comparison against green and black tea by a nontargeted metabolomics approach," *Food Research International*, vol. 96, pp. 40–45, 2017.

[31] Y. T. Li, H. T. Cui, L. Yang et al., "Hua-Zhuo-Kai-Yu decoction inhibits apoptosis in nonalcoholic fatty liver disease," *Traditional Medicine Research*, vol. 6, p. 5, 2020.

[32] L. Eslami, S. Merat, and R. Malekzadeh, "Statins for non-alcoholic fatty liver disease and non-alcoholic steatohepatitis," *Cochrane Database of Systematic Reviews*, vol. 12, no. 12, Article ID CD008623, 2013.

[33] Y. Li, L. Liu, B. Wang, J. Wang, and D. Chen, "Metformin in non-alcoholic fatty liver disease: a systematic review and meta-analysis," *Biomedical Reports*, vol. 1, no. 1, pp. 57–64, 2013.

[34] Z.-W. Chen, L.-Y. Chen, H.-L. Dai, J.-H. Chen, and L.-Z. Fang, "Relationship between alanine aminotransferase levels and metabolic syndrome in nonalcoholic fatty liver disease," *Journal of Zhejiang University—Science B*, vol. 9, no. 8, pp. 616–622, 2008.

[35] J. Dai, H. Ma, J. Fan et al., "Crude polysaccharide from an anti-UVB cell clone of Bupleurum scorzonerifolium protect HaCaT cells against UVB-induced oxidative stress," *Cytotechnology*, vol. 63, no. 6, pp. 599–607, 2011.

[36] Z. Gao, Q. Lai, Q. Yang et al., "The characteristic, antioxidative and multiple organ protective of acidic-extractable mycelium polysaccharides by Pleurotus eryngii var. tuoliensis on high-fat emulsion induced-hypertriglyceridemic mice," *Scientific Reports*, vol. 8, no. 1, p. 17500, 2018.

[37] X. Xu, G. Yan, J. Chang et al., "Comparative transcriptome analysis reveals the protective mechanism of glycyrrhinic acid for deoxynivalenol-induced inflammation and apoptosis in IPEC-J2 cells," *Oxidative Medicine and Cellular Longevity*, vol. 2020, Article ID 5974157, 17 pages, 2020.

[38] J.-C. Tsai, Y.-A. Chen, J.-T. Wu et al., "Extracts from fermented black garlic exhibit a hepatoprotective effect on acute hepatic injury," *Molecules*, vol. 24, no. 6, p. 1112, 2019.

[39] X. H. Xie, J. B. Liao, and F. Fang, "Jian-Gan-Xiao-Zhi decoction ameliorates high-fat high-carbohydrate diet-induced non-alcoholic fatty liver disease and insulin resistance by regulating the AMPK/JNK pathway," *Traditional Medicine Research*, vol. 6, pp. 1–12, 2019.

[40] T. E. Adolph, F. Grabherr, L. Mayr et al., "Weight loss induced by bariatric surgery restricts hepatic GDF15 expression," *Journal of Obesity*, vol. 2018, Article ID 7108075, 6 pages, 2018.

[41] C. Xiaxia and B. Lei, "Dietary nucleotides protect against alcoholic liver injury by attenuating inflammation and regulating gut microbiota in rats," *Food & Function*, vol. 7, no. 6, p. 2898, 2016.

[42] R. Anty and M. Lemoine, "Liver fibrogenesis and metabolic factors," *Clinics and Research in Hepatology and Gastroenterology*, vol. 35, no. 1, pp. S10–S20, 2011.

[43] J. Wu, D. Wu, K. Ma et al., "Paeonol ameliorates murine alcohol liver disease via mycobiota-mediated Dectin-1/IL-1β signaling pathway," *Journal of Leukocyte Biology*, vol. 108, no. 1, pp. 199–214, 2020.

[44] Y. Ding, X. Sun, Y. Chen, Y. Deng, and K. Qian, "Epigallocatechin gallate attenuated non-alcoholic steatohepatitis induced by methionine-and choline-deficient diet," *European Journal of Pharmacology*, vol. 761, pp. 405–412, 2015.

[45] X. Su, W. Yu, A. Liu et al., "San-huang-yi-shen capsule ameliorates diabetic nephropathy in rats through modulating the gut microbiota and overall metabolism," *Frontiers in Pharmacology*, vol. 12, Article ID 808867, 2022.

[46] C. Kasai, K. Sugimoto, I. Moritani et al., "Comparison of the gut microbiota composition between obese and non-obese individuals in a Japanese population, as analyzed by terminal restriction fragment length polymorphism and next-generation sequencing," *BMC Gastroenterology*, vol. 15, no. 1, p. 100, 2015.

[47] P. Xu, J. Wang, F. Hong et al., "Melatonin prevents obesity through modulation of gut microbiota in mice," *Journal of Pineal Research*, vol. 62, no. 4, Article ID e12399, 2017.

[48] D. Gui, J. Huang, Y. Guo et al., "Astragaloside IV ameliorates renal injury in streptozotocin-induced diabetic rats through inhibiting NF-κB-mediated inflammatory genes expression," *Cytokine*, vol. 61, no. 3, pp. 970–977, 2013.

[49] M. B. Duran-Salgado and A. F. Rubio-Guerra, "Diabetic nephropathy and inflammation," *World Journal of Diabetes*, vol. 5, no. 3, pp. 393–398, 2014.

[50] T. Huang, X. Li, F. Wang et al., "The CREB/KMT5A complex regulates PTP1B to modulate high glucose-induced endothelial inflammatory factor levels in diabetic nephropathy," *Cell Death & Disease*, vol. 12, no. 4, p. 333, 2021.

[51] B. Zhang, G. Li, M. S. Shahid et al., "Dietary l-arginine supplementation ameliorates inflammatory response and alters gut microbiota composition in broiler chickens infected with *Salmonella enterica* serovar Typhimurium," *Poultry Science*, vol. 99, no. 4, pp. 1862–1874, 2020.

[52] Z. Yi, "Antrodin A from Antrodia camphorata modulates the gut microbiome and liver metabolome in mice exposed to acute alcohol intake," *Food & Function*, vol. 12, 2021.

[53] Z. Zhai, F. Zhang, R. Cao et al., "Cecropin A alleviates inflammation through modulating the gut microbiota of C57bl/6 mice with DSS-induced ibd," *Frontiers in Microbiology*, vol. 10, p. 1595, 2019.

[54] F. Wan, M. Wang, R. Zhong et al., "Supplementation with Chinese medicinal plant extracts from Lonicera hypoglauca and Scutellaria baicalensis mitigates colonic inflammation by regulating oxidative stress and gut microbiota in a colitis mouse model," *Frontiers in Cellular and Infection Microbiology*, vol. 11, Article ID 798052, 2022.

[55] B. Wang, X. Jiang, M. Cao et al., "Altered fecal microbiota correlates with liver biochemistry in nonobese patients with non-alcoholic fatty liver disease," *Scientific Reports*, vol. 6, no. 1, p. 32002, 2016.

[56] Y. Ji, Y. Yin, Z. Li, and W. Zhang, "Gut microbiota-derived components and metabolites in the progression of non-alcoholic fatty liver disease (NAFLD)," *Nutrients*, vol. 11, no. 8, p. 1712, 2019.

[57] Y. Li, X. Chen, T Kwan, Y. Loh, J. Singer, and Y. Liu, "Sat-160 dietary fibre and bacterial scfa modulate renal inflammation indiabetic nephropathy through activation of g-protein coupled receptors gpr43 and gpr109a," *Kidney International Reports*, vol. 5, no. 3, 2020.

[58] H.-Y. Wang, L.-X. Guo, W.-H. Hu et al., "Polysaccharide from tuberous roots of Ophiopogon japonicus regulates gut microbiota and its metabolites during alleviation of high-fat diet-induced type-2 diabetes in mice," *Journal of Functional Foods*, vol. 63, Article ID 103593, 2019.

[59] Y. Wei, J. Liang, Y. Su et al., "The associations of the gut microbiome composition and short-chain fatty acid concentrations with body fat distribution in children," *Clinical Nutrition*, vol. 40, no. 5, pp. 3379–3390, 2021.

[60] T. T. Li, A. J. Tong, and Y. Y. Liu, "Polyunsaturated fatty acids from microalgae Spirulina platensis modulates lipid metabolism disorders and gut microbiota in high-fat diet rats," *Food and Chemical Toxicology*, vol. 131, 2019.

[61] N.-R. Shin, J.-C. Lee, H.-Y. Lee et al., "An increase in the Akkermansiaspp. population induced by metformin

treatment improves glucose homeostasis in diet-induced obese mice," *Gut*, vol. 63, no. 5, pp. 727–735, 2014.

[62] H. Lee and G. Ko, "Effect of metformin on metabolic improvement and gut microbiota," *Applied and Environmental Microbiology*, vol. 80, no. 19, pp. 5935–5943, 2014.

[63] C. Wei, J. Xu, and G. Li, "Ethanol extract of propolis prevents high-fat diet-induced insulin resistance and obesity in association with modulation of gut microbiota in mice," *Food Research International*, vol. 130, Article ID 108939, 2019.

[64] T. Shao, L. Shao, H. Li, Z. Xie, Z. He, and C. Wen, "Combined signature of the fecal microbiome and metabolome in patients with gout," *Frontiers in Microbiology*, vol. 8, p. 268, 2017.

[65] J. Wang, P. Li, and S. Liu, "Green tea leaf powder prevents dyslipidemia in high-fat diet-fed mice by modulating gut microbiota," *Food & Nutrition Research*, vol. 64, 2020.

[66] A. R. Maia, T. M. Batista, J. A. Victorio et al., "Taurine supplementation reduces blood pressure and prevents endothelial dysfunction and oxidative stress in post-weaning protein-restricted rats," *PLoS One*, vol. 9, no. 8, Article ID e105851, 2014.

[67] J. E. Du, Y. A. You, E. J. Kwon et al., "Maternal malnutrition affects hepatic metabolism through decreased hepatic taurine levels and changes in HNF4A methylation," *International Journal of Molecular Sciences*, vol. 21, no. 23, p. 9060, 2020.

[68] A. M. Brennan, M. Benson, J. Morningstar et al., "Plasma metabolite profiles in response to chronic exercise," *Medicine & Science in Sports & Exercise*, vol. 50, no. 7, pp. 1480–1486, 2018.

[69] C. C. Yan, E. Bravo, and A. Cantafora, "Effect of taurine levels on liver lipid metabolism: an in vivo study in the rat," *Experimental Biology and Medicine*, vol. 202, no. 1, pp. 88–96, 1993.

[70] M. Miyata, A. Funaki, C. Fukuhara, Y. Sumiya, and Y. Sugiura, "Taurine attenuates hepatic steatosis in a genetic model of fatty liver disease," *Journal of Toxicological Sciences*, vol. 45, no. 2, pp. 87–94, 2020.

[71] C. L. Gentile, A. M. Nivala, J. C. Gonzales et al., "Experimental evidence for therapeutic potential of taurine in the treatment of nonalcoholic fatty liver disease," *American Journal of Physiology—Regulatory, Integrative and Comparative Physiology*, vol. 301, no. 6, pp. R1710–R1722, 2011.

[72] B. P. Vohra and X. Hui, "Taurine protects against carbon tetrachloride toxicity in the cultured neurons and in vivo," *Archives of Physiology and Biochemistry*, vol. 109, pp. 90–94, 2001.

[73] A. Ebrahim and D. Sakthisekaran, "Effect of vitamin E and taurine treatment on lipid peroxidation and antioxidant defense in perchloroethylene-induced cytotoxicity in mice," *The Journal of Nutritional Biochemistry*, vol. 8, no. 5, pp. 270–274, 1997.

[74] P. Anand, D. Rajakumar, M. Jeraud, A. J. Felix, and T. Balasubramanian, "Effects of taurine on glutathione peroxidase, glutathione reductase and reduced glutathione levels in rats," *Pakistan Journal of Biological Sciences: PJBS*, vol. 14, pp. 219–225, 2011.

[75] S. Ashkani-Esfahani, F. Zarifi, and Q. Asgari, "Taurine improves the wound healing process in cutaneous leishmaniasis in mice model, based on stereological parameters," *Advanced Biomedical Research*, vol. 3, p. 204, 2014.

[76] J. Miao, J. Zhang, Z. Ma, and L. Zheng, "The role of NADPH oxidase in taurine attenuation of Streptococcus uberis-induced mastitis in rats," *International Immunopharmacology*, vol. 16, no. 4, pp. 429–435, 2013.

[77] K. Sumizu, "Oxidation of hypotaurine in rat liver," *Biochimica et Biophysica Acta*, vol. 63, no. 1, pp. 210–212, 1962.

[78] P. Guérin, S. El Mouatassim, and Y. Ménézo, "Oxidative stress and protection against reactive oxygen species in the pre-implantation embryo and its surroundings," *Human Reproduction Update*, vol. 7, no. 2, pp. 175–189, 2001.

[79] H. Zhang, D. Sun, D. Li et al., "Long non-coding RNA expression patterns in lung tissues of chronic cigarette smoke induced COPD mouse model," *Scientific Reports*, vol. 8, no. 1, p. 7609, 2018.

[80] G. A. Ramm, R. W. Shepherd, A. C. Hoskins et al., "Fibrogenesis in pediatric cholestatic liver disease: role of taurocholate and hepatocyte-derived monocyte chemotaxis protein-1 in hepatic stellate cell recruitment," *Hepatology*, vol. 49, no. 2, pp. 533–544, 2009.

[81] Y. M. Vakhrushev, A. P. Lukashevich, I. A. Penkina, and E. V. Suchkova, "Comparative analysis of bile acid spectrum in non-alcoholic fatty liver disease and cholelithiasis," *Terapevticheskii Arkhiv*, vol. 91, no. 2, pp. 48–51, 2019.

[82] Y. Wang, H. Aoki, and J. Yang, "The role of S1PR2 in bile acid-induced cholangiocyte proliferation and cholestasis-induced liver injury in mice," *Hepatology*, vol. 65, 2017.

[83] M. H. Stipanuk, "Metabolism of sulfur-containing amino acids," *Annual Review of Nutrition*, vol. 6, no. 1, pp. 179–209, 1986.

[84] Q. M. Anstee and R. D. Goldin, "Mouse models in non-alcoholic fatty liver disease and steatohepatitis research," *International Journal of Experimental Pathology*, vol. 87, 2010.

[85] M. A. Gyamfi, I. Damjanov, S. French, and Y.-J. Y. Wan, "The pathogenesis of ethanol versus methionine and choline deficient diet-induced liver injury," *Biochemical Pharmacology*, vol. 75, no. 4, pp. 981–995, 2008.

[86] A. Kumar, R. Pathak, H. A. Palfrey, K. P. Stone, T. W. Gettys, and S. N. Murthy, "High levels of dietary methionine improves sitagliptin-induced hepatotoxicity by attenuating oxidative stress in hypercholesterolemic rats," *Nutrition & Metabolism*, vol. 17, no. 1, p. 2, 2020.

[87] D. Yu, X.-O. Shu, Y.-B. Xiang et al., "Higher dietary choline intake is associated with lower risk of nonalcoholic fatty liver in normal-weight Chinese women," *Journal of Nutrition*, vol. 144, no. 12, pp. 2034–2040, 2014.

[88] A. L. Buchman, M. E. Ament, M. Sohel et al., "Choline deficiency causes reversible hepatic abnormalities in patients receiving parenteral nutrition: proof of a human choline requirement: a placebo-controlled trial," *Journal of Parenteral and Enteral Nutrition*, vol. 25, no. 5, pp. 260–268, 2001.

[89] F. Jahoor, A. Jackson, B. Gazzard et al., "Erythrocyte glutathione deficiency in symptom-free HIV infection is associated with decreased synthesis rate," *American Journal of Physiology-Endocrinology and Metabolism*, vol. 276, no. 1, pp. E205–E211, 1999.

[90] J. Lyons, A. Rauh-Pfeiffer, Y. M. Yu et al., "Blood glutathione synthesis rates in healthy adults receiving a sulfur amino acid-free diet," *Proceedings of the National Academy of Sciences*, vol. 97, no. 10, pp. 5071–5076, 2000.

[91] M. Kawasaki, Y. Miura, R. Funabiki, and K. Yagasaki, "Comparison of the effects on lipid metabolism of dietary methionine and cystine between hepatoma-bearing and normal rats," *Bioscience, Biotechnology, and Biochemistry*, vol. 74, no. 1, pp. 158–167, 2010.

[92] V. Kalatzis, S. Cherqui, C. Antignac, and B. Gasnier, "Cystinosin, the protein defective in cystinosis, is a H+-

driven lysosomal cystine transporter," *The EMBO Journal*, vol. 20, no. 21, pp. 5940–5949, 2001.

[93] T. M. Seibt, B. Proneth, and M. Conrad, "Role of GPX4 in ferroptosis and its pharmacological implication," *Free Radical Biology and Medicine*, vol. 133, pp. 144–152, 2019.

[94] S. K. Jain, P. Kanikarla-Marie, and C. Warden, "L-cysteine supplementation upregulates Glutathione (GSH) and Vitamin D binding protein (VDBP) in hepatocytes cultured in high glucose and in vivo in liver, and increases blood levels of GSH, VDBP, and 25-hydroxy-Vitamin D in Zucker diabetic fatty rats," *Molecular Nutrition & Food Research*, vol. 60, 2016.

[95] C. B. Gomez, S. H. de la Cruz, G. J. Medina-Terol et al., "Chronic administration of NaHS and L-Cysteine restores cardiovascular changes induced by high-fat diet in rats," *European Journal of Pharmacology*, vol. 863, Article ID 172707, 2019.

[96] S. Lee, K.-H. Han, Y. Nakamura et al., "DietaryL-cysteine improves the antioxidative potential and lipid metabolism in rats fed a normal diet," *Bioscience, Biotechnology, and Biochemistry*, vol. 77, no. 7, pp. 1430–1434, 2013.

[97] A. R. Soylu, N. Aydogdu, U. N. Basaran et al., "Antioxidants vitamin E and C attenuate hepatic fibrosis in biliary-obstructed rats," *World Journal of Gastroenterology*, vol. 12, no. 42, pp. 6835–6841, 2006.

[98] O. Adaramoye, B. Ogungbenro, O. Anyaegbu, and M. Fafunso, "Protective effects of extracts of vernonia amygdalina, Hibiscus sabdariffa and vitamin C against radiation-induced liver damage in rats," *Journal of Radiation Research*, vol. 49, no. 2, pp. 123–131, 2008.

[99] M. Saito, "Elevated plasma concentration of homocysteine, low level of vitamin B6, pyridoxal, and vitamin D insufficiency in patients with hip fracture: a possible explanation for detrimental cross-link pattern in bone collagen," *Clinical Calcium*, vol. 16, no. 12, pp. 1974–1984, 2006.

[100] Z. Marelja, M. Dambowsky, M. Bolis et al., "The four aldehyde oxidases of Drosophila melanogaster have different gene expression patterns and enzyme substrate specificities," *Journal of Experimental Biology*, vol. 217, no. Pt 12, pp. 2201–2211, 2014.

[101] K. J. Lal, S. K. Sharma, and K. Dakshinamurti, "Regulation of calcium influx into vascular smooth muscle by vitamin B6," *Clinical and Experimental Hypertension*, vol. 15, no. 3, pp. 489–500, 1993.

[102] K. Dakshinamurti, K. Jawahar Lal, and P. K. Ganguly, "Hypertension, calcium channel and pyridoxine (vitamin B6)," *Molecular and Cellular Effects of Nutrition on Disease Processes*, vol. 188, pp. 137–148, 1998.

[103] H. Shi, N. Moustaid-Moussa, W. O. Wilkison, and M. B. Zemel, "Role of the sulfonylurea receptor in regulating human adipocyte metabolism," *The FASEB Journal*, vol. 13, no. 13, pp. 1833–1838, 1999.

[104] M. B. Zemel and A. Bruckbauer, "Effects of a leucine and pyridoxine-containing nutraceutical on fat oxidation, and oxidative and inflammatory stress in overweight and obese subjects," *Nutrients*, vol. 4, no. 6, pp. 529–541, 2012.

[105] A. A. Booth, R. G. Khalifah, and B. G. Hudson, "Thiamine pyrophosphate and pyridoxamine inhibit the formation of antigenic advanced glycation end-products: comparison with aminoguanidine," *Biochemical and Biophysical Research Communications*, vol. 220, no. 1, pp. 113–119, 1996.

[106] D. E. Maessen, O. Brouwers, K. H. Gaens et al., "Delayed intervention with pyridoxamine improves metabolic function and prevents adipose tissue inflammation and insulin resistance in high-fat diet-induced obese mice," *Diabetes*, vol. 65, no. 4, pp. 956–966, 2016.

[107] S. Oh, H. Ahn, H. Park et al., "The attenuating effects of pyridoxamine on adipocyte hypertrophy and inflammation differ by adipocyte location," *The Journal of Nutritional Biochemistry*, vol. 72, 2019.

[108] E. N. G. D. S. Pereira, R. R. Silvares, E. E. I. Flores, K. L. Rodrigues, and A. Daliry, "Pyridoxamine improves metabolic and microcirculatory complications associated with nonalcoholic fatty liver disease," *Microcirculation*, vol. 27, Article ID e12603, 2020.

[109] K. Gilany, A. Mohamadkhani, S. Chashmniam et al., "Metabolomics analysis of the saliva in patients with chronic hepatitis B using nuclear magnetic resonance: a pilot study," *Iranian Journal of Basic Medical Sciences*, vol. 22, no. 9, pp. 1044–1049, 2019.

[110] S. P. Coburn, R. D. Reynolds, M. J. Dennis et al., "Elevated plasma 4-pyridoxic acid in renal insufficiency," *American Journal of Clinical Nutrition*, vol. 1, p. 57, 2002.

Hindawi
Evidence-Based Complementary and Alternative Medicine
Volume 2022, Article ID 2447529, 5 pages
https://doi.org/10.1155/2022/2447529

Review Article

Clinical Experience of Acupuncture Treatment for Non-Alcoholic Fatty Liver Disease

Kun-Da Hong, Tian Wan, and Si-Yu Lu

Department of Rehabilitation Medicine, The Second Affiliated Hospital of Fujian Medical University, Quanzhou, Fujian, China

Correspondence should be addressed to Tian Wan; wantianfz@163.com

Received 19 January 2022; Accepted 18 February 2022; Published 11 March 2022

Academic Editor: Chan-Yen Kuo

Based on the authors' clinical experience, the acupuncture treatment of non-alcoholic fatty liver disease mainly includes the following three aspects. (1) The etiology and pathogenesis of non-alcoholic fatty liver disease are based on "deficiency in origin and excess in superficiality." The deficiency in origin means deficiency of the spleen and stomach, and the excess in superficiality is caused by hepatobiliary disorders. (2) The application of the theory of strengthening the spleen and mobilizing transportation should be considered for the treatment of non-alcoholic fatty liver disease by acupuncture and moxibustion. Therefore, the use of "treatment from the spleen" often has miraculous effects. (3) Skillful use of acupuncture, shallow acupuncture, acupoint thread embedding, and other traditional Chinese medicine therapies are used to regulate the liver and spleen. In addition, warm acupuncture is reused to warm the Yang and strengthen the body.

1. Introduction

Non-alcoholic fatty liver disease (NAFLD), also known as metabolic dysfunction-associated fatty liver disease (MAFLD), refers to the exclusion of alcohol and other clear liver damage factors. Clinicopathological syndromes in which diffuse hepatocyte bullous fat becomes the main feature include simple fatty liver disease and its evolution of steatohepatitis, fatty liver fibrosis, and cirrhosis [1]. Studies have shown that the prevalence of NAFLD is as high as 25.24% [2]. Relevant studies in recent years have shown that traditional acupuncture therapy has a positive role in the treatment of NAFLD, and its adverse reactions are mild, simple, and effectively treated [3]. The authors have accumulated experience in clinical acupuncture and moxibustion treatment of NAFLD, which is summarized as follows.

2. Etiology and Pathogenesis

The etiology and pathogenesis of non-alcoholic fatty liver disease are based on the "deficiency in origin and excess in superficiality": the deficiency in origin refers to deficiency of the spleen and stomach, and the excess in superficiality is caused by stagnation of the liver and Qi (Figure 1).

2.1. Deficiency of the Spleen and Stomach Is the Root. Spleen and stomach are the acquired foundation. The spleen and stomach are weak in transporting water and grains, and the circulation of Qi and blood is not smooth, which leads to the deposition of phlegm and dampness in the liver and blood stasis in the liver. In disorders of the spleen and stomach, the turbidity is cleared without distinction, condensing the "cream" and forming fatty liver; hyperlipidemia occurs when turbid Qi enters the blood. Modern research has also shown that gastrointestinal function is closely related to NAFLD [4]. Research has found that an imbalance of the gastrointestinal flora is highly correlated with the progression of NAFLD. The imbalance of intestinal flora may affect the expression of an endogenous biologically active substance (adiponectin) secreted by adipocytes, leading to the occurrence of NAFLD [5].

2.2. Irregular Liver and Gallbladder Are the Targets. The liver is responsible for dredging and drainage. With the onset of disease, the liver is unbalanced, the Qi does not run smoothly, the Qi is blocked by phlegm, and bile excretion is not smooth. This worsens fatty liver. Modern medical research has also confirmed that disorders of lipid metabolism

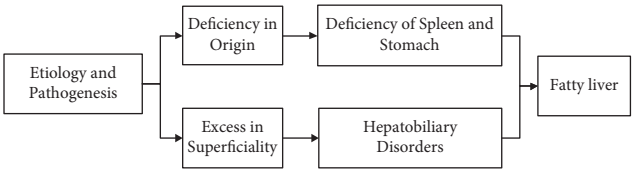

Figure 1: Etiology and pathogenesis of NAFLD.

and hepatocyte steatosis are related to NAFLD [6, 7]. Human cells produce reactive oxygen species (ROS) during the metabolic process. There are more ROS in the livers of patients with fatty liver disease. Lipid peroxidation products and ROS increase and compromise mitochondrial membrane permeability, which eventually leads to liver cell apoptosis [8]. Excess lipid peroxidation products can directly lead to necrosis or apoptosis of liver cells. The process of peroxidation-necrosis directly promotes the development of liver fibrosis. On the other hand, the normal metabolism of bile acids is an important factor in ensuring normal glucose and lipid metabolism and the inhibition of liver fat accumulation. Disorders of bile acid metabolism affect liver glucose and lipid metabolism by changing the signalling pathway of TGR5 (a G-protein-coupled bile acid receptor). Therefore, bile acid metabolism is closely related to the formation and development of NAFLD [9].

3. Considering the Spleen for Treatment and Treating Disease from the Root

The pathogenesis of non-alcoholic fatty liver disease is led by spleen deficiency. Although the disease is located in the liver, it is inseparable from the spleen. Physiologically, the movement and transformation of the spleen depend on the maintenance of the Qi of the liver, and the dispersion of the liver and blood storage needs the spleen and stomach to metabolize and produce essence for nourishment. This reflects the roles and relationship of the liver and spleen in the function of dispersion and transportation and in blood production and blood storage. Regarding the meridian and collaterals, the "Lingshu·Meridian" points out that the spleen meridian "traces the tibia, then detours to the front of the Jueyin meridian," and the liver meridian "is eight inches above the ankle and then detours to the back of the Taiyin meridian." The Foot Taiyin Spleen Meridian and Foot Jueyin Liver Meridian cross and circulate on the inner side of the calf. The two meridians influence each other, which also fully reflects the close relationship between liver and spleen functions. In terms of pathology, Dongyuan Li mentioned in "Spleen and Stomach Theory" that "[with] internal injury to the spleen and stomach, all diseases arise." If the spleen and stomach show insufficiency and dysfunction of transportation and chemistry, water dampness and turbid phlegm are inevitable; it can also affect liver failure and release, leading to the syndrome of "Tuyong Muyu." Reflecting the pathological importance of the spleen, the signs and symptoms of NAFLD are mostly the manifestations of splenic failure. In the treatment of NAFLD, spleen strengthening should be the entry point [10, 11]. The spleen and stomach are the foundation of the acquired nature and the source of Qi and blood metaplasia, which can directly affect patient recovery and the outcome of the disease. The above shows that spleen deficiency is closely related to the occurrence and development of NAFLD, and the treatment should be based on the spleen.

4. Skillful Utilization of Acupuncture and Unique Acupoint Selection

The authors believe that acupuncture and moxibustion are effective in treating NAFLD, and they chose unique therapies—shallow acupuncture, acupoint embedding, and warm needle moxibustion. At the same time, the unique selection of acupoints can be effective (Figure 2).

4.1. Making Good Use of Shallow Needle Therapy. "Binghuang Wu's shallow acupuncture" has been included in the protection of intangible heritage. Shallow acupuncture can treat a variety of diseases, and its method of flattening, replenishing, and reducing is unique in the treatment of NAFLD. The principle of shallow acupuncture is to stimulate the meridian blood circulation through the physical stimulation of the meridian points by the needle tip, adjust the functional balance of the meridians and viscera, and play the role of strengthening the body, eliminating pathology and curing diseases [12, 13]. This is basically the same as the principle of acupuncture treatment. The difference is that shallow acupuncture produces a benign stimulus to the more sensitive floating collaterals and sun collaterals of the twelve skin regions with a gentle continuous tremor. Therefore, although the patient's local acupuncture sensation is not very obvious, the result depends on the amount of effective stimulation. In other words, it is no worse than the stimulation intensity produced by acupuncture and is mainly achieved by the duration and frequency of continuous effective stimulation. The weak tremor of shallow needles can produce resonance, which not only spreads to the surrounding area through the vibration wave centered on the meridian but also can follow the meridian circulation route in both directions to achieve the purpose of effective stimulation. *Treatment Method*. (1) Acupoint selection: Danzhong point. Point selection basis: Danzhong acupoint is the mu acupoint of the pericardium (the place where the Qi of the pericardium meridian gathers), the Qihui acupoint (the place where the Qi gathers), and the rendezvous point of the Ren channel, foot taiyin, foot shaoyin, hand taiyang, and hand shaoyang. The Danzhong point can regulate qi, activate blood and dredge the collaterals, and regulate the function of the Qi of the whole body. (2) Operation: the thumb is used to press the needle tail, the index finger and the middle finger to hold the needle handle, and the needle tip to press on the meridian skin. Use your middle finger nail to make continuous up and down movements on the needle handle. Reducing method: (a) the needle body is not perpendicular to the plane of the meridian points (i.e., the included angle is less than 90°); (b) the middle finger nail is scraped up the needle handle with a strong force, but the

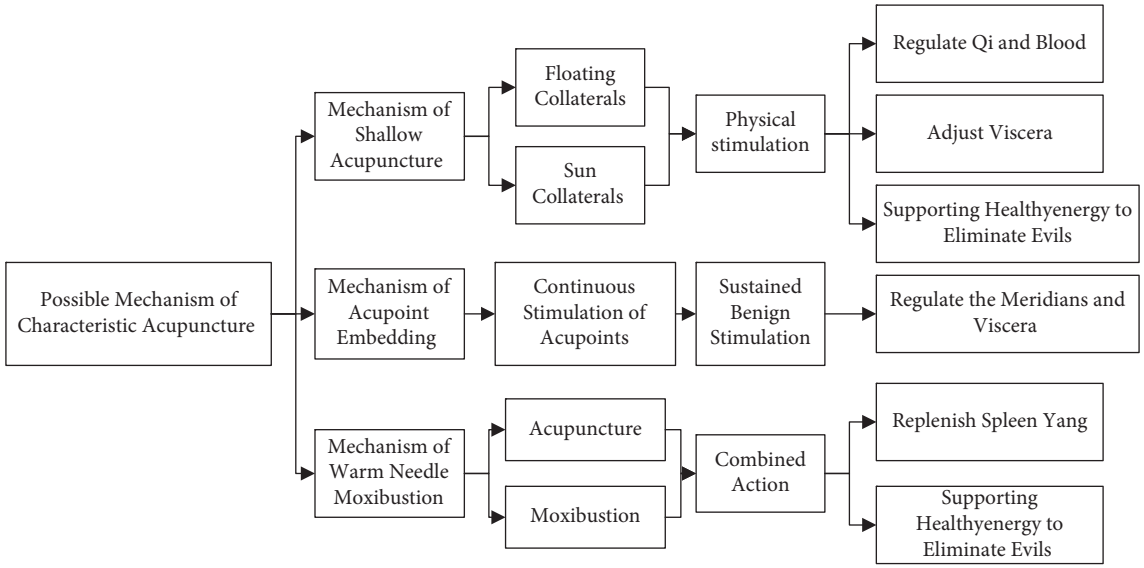

Figure 2: Possible mechanism of characteristic acupuncture.

downward force is small (i.e., weighing and scraping). Push gently. (c) After completing the stimulation of each meridian point, the thumb leaves the tail of the needle, while the middle finger keeps clamping the needle handle, and the needle tip is kept on the acupuncture point. Rotate six times in a counterclockwise arc. (3) Precautions: during the entire operation, the thumb should be kept lightly against the tail of the needle, so as not to increase the pressure involuntarily when the stimulation is applied and cause the needle to pierce the skin and cause pain. At the same time, when the middle finger nail is scraped and pushed on the needle handle, always keep the needle handle still in order to avoid irregular beating. The amplitude of the scraping and pushing should be large (that is, the full length of the needle handle is scraped and pushed), and the finger force must be soft and even; the speed should not be too fast or slow. The punctured part should always maintain a soft and even slight tremor, so that the patient can feel acupuncture and feel comfortable.

4.2. Clever Use of Acupoints to Embed Thread. The authors often use catgut embedding at acupoints to treat NAFLD, and the effect is stronger. Acupoint embedding therapy involves placement of absorbable surgical sutures into the viscera, meridians, and collaterals to infuse the Qi into a special part of the body surface, to produce continuous stimulation to the human body, so as to achieve the purpose of preventing and curing diseases. *Treatment Method.* (1) Acupoint selection: Zhongwan, Zusanli, Sanyinjiao, Fenglong, and Taichong. Point selection basis: Zhongwan is the mu point of the stomach meridian and the Fuhui of eight influential points. Zhongwan has the effect of regulating the spleen and stomach. Zusanli is the point of the stomach meridian. Zusanli can regulate the spleen and stomach and, when combined with Sanyinjiao, it can relieve the dampness of the Yangming Meridian and Taiyin Meridian and support the function of spleen and stomach transportation and transfusion. The Fenglong point is the luo point of the foot Yangming stomach meridian, and the point is also connected to the foot Taiyin spleen meridian. Therefore, this point can treat the two meridian disorders of the spleen and stomach and regulate Qi of the spleen and stomach meridian to ensure that the Qi is running and the body fluid is spreading. The spleen meridian governs transportation and transformation, and crosses out the wet and phlegm. The Taichong point is the original point of the liver meridian. It can soothe the liver, regulate the Qi, and regulate the channels of Qi. (2) Operation: the patient takes the supine position, the skin of the abdomen and lower limbs is fully exposed, and the acupoints are disinfected with Aner iodine or 75% alcohol. After washing and disinfecting the hands, the doctors put on sterile gloves. Needle selection: No. 7 injection needle (specification 0.7 mm × 32 mm) is used as a cannula, and an acupuncture needle (specification 0.30 mm × 50 mm) has the needle cut off as a needle core to make a simple embedding needle. Use sterile forceps to take the sterilized collagen thread with a length of 2 cm, place the needle tip into the injection needle, pierce the needle with the protein thread into the acupuncture point, push in the needle core, withdraw the needle tube, and pull the collagen thread. Embed the acupuncture points, put pressure on the needle hole with a cotton swab for a while after the needle is taken out, and then apply a sticking plaster to the needle hole. This is usually done once a week, for a total of 3 months of treatment. (3) Precautions: keep the needle eye position dry for 24 hours after embedding the thread to prevent infection.

4.3. Reusing Warm Acupuncture Treatment. Acupuncture and moxibustion treatment of NAFLD should focus on replenishing the spleen and stomach and treat the spleen from the perspective of "the spleen and stomach are the foundation of the acquired." Therefore, warm acupuncture and moxibustion are chosen; this combines the dual effects of acupuncture and moxibustion, which has the effect of

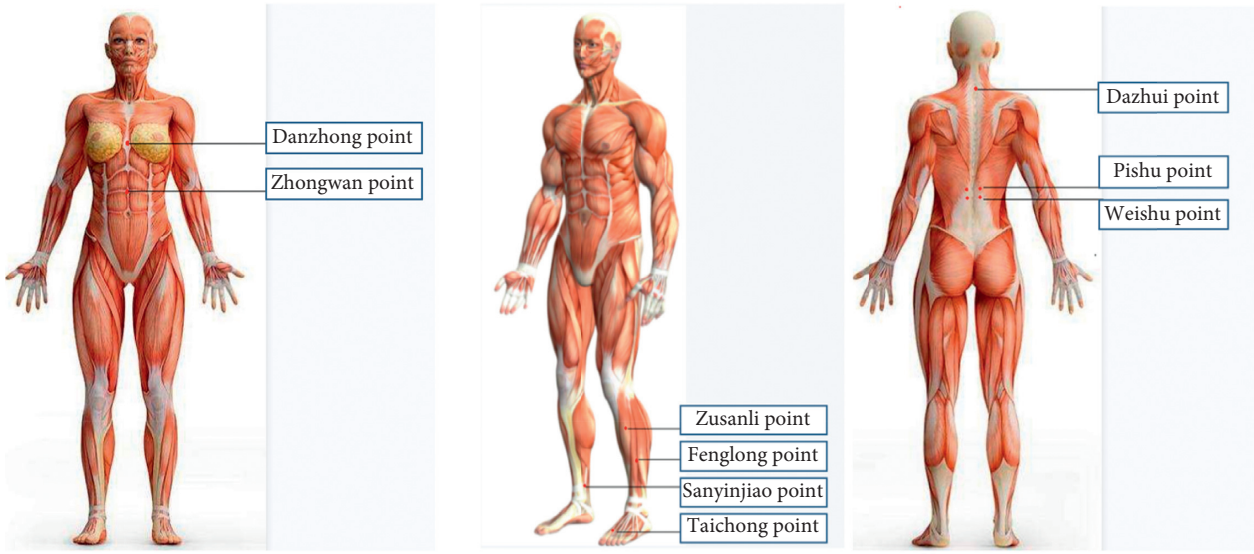

Figure 3: Acupoint location map.

warming and invigorating the spleen Yang. Based on the theory of traditional Chinese medicine, Professor Wu pointed out that warming acupuncture or the moxibustion of strong points has the effect of replenishing spleen Yang, strengthening the body and eliminating pathology, so as to improve the immune function of the body [14]. Modern medicine shows that immune cells are also closely related to NAFLD. Both specific immunity and non-specific immunity are involved in the pathogenesis of NAFLD. The activation of immunogenic cells is positively correlated with the lipid content in the liver. The interaction between the endocrine system and immune cells may be an important mechanism for the occurrence and development of NAFLD [15]. *Treatment Method*. (1) Acupoint selection: Dazhui, Pishu, and Weishu. Point selection basis: Dazhui point is the meeting of the three Yang of the hands and feet and the governor channel, and it controls the Yang Qi of the whole body. Pishu is the beishu point of the spleen and Weishu is the beishu point of the stomach. They are the main points for the treatment of spleen and stomach diseases. Both belong to the tai Yang of the feet bladder meridian, so that they have a good effect of nourishing Yang. (2) Operation: the patient lies in the prone position, the skin on the back is exposed, and the acupuncture points are thoroughly disinfected. Routinely insert the needle, insert and twist, using the replenishing and reducing method; take a 2 cm long (one strong) moxa section, insert it on the needle, and light it. Moxibustion is performed for two strong moxibustions each time, and the needles are retained for 30 minutes. (3) Precautions: protect the skin with a piece of hard paper to prevent skin burns. If burned, apply moist scald cream (Figure 3).

5. Typical Case

A female patient XX, who was 35 years old, visited the doctor on May 11, 2020. Main complaint was fullness of the flanks for 2 weeks. Although the patient is a young woman, she feels obvious fatigue, and she sweats even more after exercise. She also reports anorexia, swelling, and excessive sleep. She is 157 cm tall, weighs 70 kg, and has a body mass index (BMI) of 28.4 kg/cm2. Previous physical examination revealed fatty liver for more than 1 year; the patient denied a history of viral hepatitis and other medical history and had no history of drinking alcohol. The tongue is pale, there are tooth marks on the sides, the fur is white and greasy, and the pulse is smooth. Western medicine diagnosis was non-alcoholic fatty liver disease; Chinese medicine diagnosis was liver pi (spleen deficiency, phlegm-dampness syndrome). Treatment method: invigorate the spleen and stomach and transport and resolve phlegm and dampness. Acupuncture methods used were shallow acupuncture, acupoint embedding, and warm needle moxibustion. Symptoms improved after 3 weeks, and after more than 3 months of treatment, the symptoms improved significantly, and the patient's weight decreased to 64.2 kg.

6. Summary

Acupuncture treatment of non-alcoholic fatty liver disease is simple and effective. The authors have conducted research on the treatment of NAFLD with acupuncture. The etiology and pathogenesis of NAFLD are based on "deficiency in origin and excess in superficiality": deficiency in origin means deficiency of the spleen and stomach, and excess in superficiality is caused by hepatobiliary disorders.

Given that the spleen and stomach are the foundation of the acquired nature and that spleen deficiency and loss of transport are the internal basis of the disease, "treatment from the spleen, seeking the root of the disease" can show a miraculous effect. Acupuncture can regulate the Qi of the meridians and viscera to restore normal physiologic function. We summarize the characteristic therapies of traditional Chinese medicine acupuncture on the basis of our long-term clinical experience. We make good use of shallow acupuncture and acupoint embedding therapy to regulate

the spleen and stomach, dredging the Qi of the whole body. Additionally, we reuse warm acupuncture for warming Yang, strengthening the spleen, and improving immune function. This study provides a reference for clinical treatment and provides a basis and foundation for the clinical promotion of acupuncture and moxibustion in the treatment of NAFLD.

Conflicts of Interest

The authors declare that they have no conflicts of interest.

Acknowledgments

We thank International Science Editing (http://www.internationalscienceediting.com) for editing this manuscript.

References

[1] A. Mantovani, E. Scorletti, and A. Mosca, "Complications, morbidity and mortality of nonalcoholic fatty liver disease," *Metabolism*, vol. 111, Article ID 154170, 2020.

[2] Z. M. Younossi, "Non-alcoholic fatty liver disease - a global public health perspective," *Journal of Hepatology*, vol. 70, no. 3, pp. 531–544, 2019.

[3] H. Y. Wang, C. M. Liang, and J. W. Cui, "Acupuncture improves hepatic lipid metabolism by suppressing oxidative stress in obese nonalcoholic fatty liver disease rats," *Zhen ci yan jiu = Acupuncture research*, vol. 44, no. 3, pp. 189–194, 2019.

[4] T. V. Koval, I. V. Chopey, M. M. Hechko, and A. V. Kurakh, "NON-ALCOHOLIC fatty liver disease IN the context OF altered gut microbiota," *Wiadomosci Lekarskie*, vol. 74, no. 4, pp. 1007–1010, 2021.

[5] Y. Ni, L. Ni, F. Zhuge, and Z. Fu, "The gut microbiota and its metabolites, novel targets for treating and preventing non-alcoholic fatty liver disease," *Molecular Nutrition & Food Research*, vol. 64, no. 17, Article ID e2000375, 2020.

[6] B. L. Copple and T. Li, "Pharmacology of bile acid receptors: evolution of bile acids from simple detergents to complex signaling molecules," *Pharmacological Research*, vol. 104, pp. 9–21, 2016.

[7] K. M. Hasan, P. D. Meher Parveen, and B. Alondra Pena, "Carf (cdkn2aip) regulates hepatic lipid metabolism and protects against development of non-alcoholic fatty liver diseases," *Journal of the Endocrine Society*, vol. 5, no. 1, p. A284, 2021.

[8] R. M. Carr and A. E. Reid, "FXR agonists as therapeutic agents for non-alcoholic fatty liver disease," *Current Atherosclerosis Reports*, vol. 17, no. 4, p. 500, 2015.

[9] F. G. Schaap, M. Trauner, and P. L. M. Jansen, "Bile acid receptors as targets for drug development," *Nature Reviews Gastroenterology & Hepatology*, vol. 11, no. 1, pp. 55–67, 2014.

[10] H.-s. Li and Y.-y. Hu, "Intestinal microecology: an important target for Chinese medicine treatment of non-alcoholic fatty liver disease," *Chinese Journal of Integrative Medicine*, vol. 26, no. 10, pp. 723–728, 2020.

[11] J. Xu, R. Wang, S. You et al., "Traditional Chinese medicine Lingguizhugan decoction treating non-alcoholic fatty liver disease with spleen-yang deficiency pattern: study protocol for a multicenter randomized controlled trial," *Trials*, vol. 21, no. 1, p. 512, 2020.

[12] S. Y. Qi, D. Lin, and L. L. Lin, "Using nonlinear dynamics and multivariate statistics to analyze eeg signals of insomniacs with the intervention of superficial acupuncture," *Evidence-based Complementary and Alternative Medicine*, vol. 2020, Article ID 8817843, , 2020.

[13] D. Lin, X. Z. Huang, W. Y. Zhuang, Y. Y. Yu, and Q. Wu, "Analysis on insomniac electroencephalogram data after treatment with superfificial needling based on approximate entropy and correlation dimensionality," *Zhen Ci Yan Jiu =Acupuncture Research*, vol. 43, no. 3, pp. 180–184, 2018.

[14] Z. Wang, D. Gong, X. Yu, and S. Cai, "Wu Binghuang's academic thought and clinical experience of regulating immune function by acupuncture and moxibustion," *Zhongguo zhen jiu = Chinese acupuncture & moxibustion*, vol. 36, no. 8, pp. 861–863, 2016.

[15] R. Xu, Z. Zhang, and F.-S. Wang, "Liver fibrosis: mechanisms of immune-mediated liver injury," *Cellular and Molecular Immunology*, vol. 9, no. 4, pp. 296–301, 2012.

Hindawi
Evidence-Based Complementary and Alternative Medicine
Volume 2022, Article ID 2245491, 8 pages
https://doi.org/10.1155/2022/2245491

Review Article

Research Progress and Treatment Status of Liver Cirrhosis with Hypoproteinemia

Jianxia Wen,[1,2] **Xing Chen**,[2,3] **Shizhang Wei**,[2] **Xiao Ma**,[4] **and Yanling Zhao**[2]

[1]*School of Food and Bioengineering, Xihua University, Chengdu 610039, China*
[2]*Department of Pharmacy, Chinese PLA General Hospital, Beijing 100039, China*
[3]*Pharmacy Department, Chongqing Emergency Medical Center, Chongqing University Central Hospital, Chongqing 400014, China*
[4]*College of Pharmacy, Chengdu University of Traditional Chinese Medicine, Chengdu 611137, China*

Correspondence should be addressed to Yanling Zhao; zhaoyl2855@126.com

Received 14 January 2022; Revised 8 February 2022; Accepted 9 February 2022; Published 24 February 2022

Academic Editor: Chan-Yen Kuo

Liver cirrhosis is the 14th leading cause of death in adults worldwide. The liver is an important organ for the metabolism of sugar, protein, and fat. Liver cirrhosis with hypoproteinemia (LCH) can lead to metabolic disorders of the nutrients such as sugar, protein, and fat, as well as insufficient protein intake, digestion and absorption disorders, and continuous leakage of plasma protein into the abdominal cavity. Severe hypoproteinemia leads to a poor prognosis in patients. For every 10 g/L decrease in peripheral blood albumin, the risk of secondary liver disease complications will increase by 89% and the mortality rate increased by 24%–56%. Therefore, it is necessary to take urgent measures to treat liver cirrhosis with hypoalbuminemia and effectively treat and reverse the deterioration of the disease caused by hypoalbuminemia, so as to reduce the burden of secondary liver disease. Emerging evidence suggests that protein balance disorders, auxin resistance, and hyperleptinemia are key steps in the development of cirrhosis and hypoproteinemia. This study comprehensively analyzed the common complications, pathogenic mechanisms, and treatment status of cirrhosis caused by hypoproteinemia and proposed research prospects for dealing with this increasingly serious problem.

1. Introduction

Liver cirrhosis with hypoproteinemia (LCH) is a common clinical manifestation of liver cirrhosis, which is a chronic liver disease caused by continuous and repeated actions on the liver by a single or a complex cause. In patients with liver cirrhosis, due to the decline of liver cell function and the decrease in the number of liver cells, the protein synthesis including albumin and various coagulation factors is insufficient, resulting in hypoproteinemia [1]. A substantial reduction in the content of albumin in the body will accelerate the progression of liver insufficiency, decrease immunity, and increase the chance of infection, ascites, and hypovolemia, reduce organ dysfunction, and so forth [2], which seriously affects patient prognosis and long-term survival, and the fatality rate is high. Studies have shown that a reduction in serum albumin could increase the mortality of patients. For every 2.5 g/L decrease in peripheral albumin, the risk of secondary liver disease complications increased by 89% and the mortality rate increases by 24%–56% [3].

Currently, the improvement of hepatic protein synthesis function and hypoalbuminemia through drug therapy has become the focus of many hepatologists. However, clinical treatment faces problems such as shortage of blood product resources, high price, blood disease infection, and blood transfusion reaction. Therefore, the treatment of LCH still has certain limitations, and other alternative treatments are urgently needed. The research progress on LCH at home and abroad is summarized as follows.

2. Methods

The databases, including PubMed, SINOMED, Web of Science, EMBASE, China National Knowledge Infrastructure (CNKI), Wanfang, Chinese Biomedical Database (CBM), and VIP medicine information system (VMIS), were comprehensively searched. The following search terms were used: "liver cirrhosis" [Mesh terms] OR "hypoproteinemia" [Mesh terms]. Studies concerning the research progress and treatment status of cirrhotic hypoproteinemia were picked out manually. Two investigators independently reviewed studies after reading the title, abstract, and full text of the related studies. Any relevant disagreements were resolved by consultation with Professor Zhao.

3. Complications of LCH

3.1. Gastrointestinal Bleeding. Gastrointestinal bleeding is closely associated with the complicated course of LCH, which reflects the severity of bleeding events [4, 5]. Patients with liver cirrhosis are usually accompanied by portal hypertension, gastric ulcer, gastric lesions, and other diseases. Esophageal and gastric fundus veins are prone to rupture in the varices and cause gastrointestinal bleeding. In addition, gastric mucosa is also prone to erosive bleeding, and patients with LCH complicated with gastrointestinal bleeding have a higher mortality rate [6, 7].

3.2. Spontaneous Peritonitis. Patients with cirrhosis and hypoalbuminemia often have ascites or edema when the plasma albumin concentration is lower than 30 g/L, and ascites is bound to occur when it is lower than 25 g/L. Due to the impaired liver function, the body's defense function is low, intestinal bacteria multiply and translocate, and bacterial infection is complicated [8, 9]. Spontaneous peritonitis (SBP) is the most common complication of liver cirrhosis. The onset of SBP is relatively insidious, early diagnosis is difficult, and the end-stage cure rate is low. Therefore, it is also the leading cause of hospitalization and death in advanced patients [10].

3.3. Hepatorenal Syndrome. Hepatorenal syndrome is a serious complication of LCH. It is a syndrome characterized by renal failure caused by liver dysfunction, decreased renal blood perfusion, and abnormal endogenous vascular activity. It is associated with many factors such as secondary infections, liver damage caused by drugs, varicose vein rupture, and bleeding. The incidence of hepatorenal syndrome in LCH is 18% and 40% in 1 and 5 years, respectively [11]. Once it occurs, the prognosis is extremely poor. Studies [12] have shown that the mortality rate of hepatorenal syndrome in cirrhosis is as high as 52% to 90%, and the mortality rate can reach 100% without inappropriate interventions.

4. Pathogenesis of LCH

4.1. Impaired Protein Balance. Patients with liver cirrhosis often have symptoms of gastrointestinal dysfunction such as abdominal distension, loss of appetite, nausea, and vomiting, as well as gastrointestinal mucosal diseases such as portal hypertensive gastropathy, small bowel disease, and enteropathy, resulting in decreased protein intake and protein absorption. In liver cirrhosis, the original liver lobules are destroyed, forming false lobules, and the sinusoidal channels are disordered, which reduce the nutrient supply and oxygen supply of liver cells, aggravate the necrosis of liver cells, and reduce the synthesis of blood albumin by more than 50% [13, 14]. Studies have shown [15] that patients with liver cirrhosis are in a state of high metabolism and high decomposition, and their protein metabolism and decomposition are significantly faster than those of normal people, and the protein decomposition speed is faster than the synthesis rate. In addition, the liver glycogen content in patients with liver cirrhosis is only 1/2 of that of the normal liver, and there are obstacles to glucose utilization. Plasma insulin, glucagon, and epinephrine levels increase, which promotes early protein gluconeogenesis to maintain the body. There is a need to further reduce the serum albumin level in humans. In addition, complications such as ascites, peritonitis, and gastrointestinal bleeding can lead to substantial protein loss. Therefore, a variety of factors lead to impaired protein balance in patients with liver cirrhosis, which induces LCH.

4.2. Growth Hormone Resistance. Growth hormone (GH) is the main hormone that promotes protein synthesis in the body. In recent years, domestic and foreign scholars have studied the growth hormone-insulin-like growth factor (IGF-I) axis and found that it regulates the energy metabolism of glucose, protein, and fat. GH, which plays an important role, is mostly mediated by IGF-I, while the synthetic release of IGF-I is caused by GH stimulation, and IGF-I is mainly synthesized and released by hepatocytes. There is growth hormone resistance in patients with liver cirrhosis, which leads to obstacles in the synthesis of IGF-I and its binding protein in the liver, resulting in decreased liver albumin synthesis and decreased glucose gluconeogenesis and glycogen synthesis. It is currently believed that insulin resistance and high peripheral blood growth hormone levels play an important role in malnutrition due to liver cirrhosis [2].

4.3. Hyperleptinemia. Leptin is a protein product of obesity-related genes. It is mainly produced and secreted in adipose tissue. It senses the energy reserves of fat cells and is an important regulator of the hypothalamic axis involved in the regulation of food intake. In recent years, a number of studies have shown that hyperleptinemia is closely related to the occurrence and development of hypoalbuminemia cirrhosis [16]. Wang et al. [17] indicated that serum leptin levels in patients with hypoalbuminemia in liver cirrhosis are significantly increased, and peripheral leptin receptors can promote low protein levels by suppressing appetite, promoting fat consumption and carbohydrate conversion, and reducing body weight and the development of blood diseases. Campillo et al. [18] found that blood leptin levels are positively correlated with related indicators of

hypoalbuminemia, indicating that hyperleptinemia plays an important role in cirrhotic malnutrition, and to a certain extent can be used as an effective diagnosis of hypoalbuminemia in liver cirrhosis index. In addition, Feng et al. [19] explored the relationship between leptin, liver cirrhosis, and hepatocellular carcinoma (HCC), confirming that leptin is an independent risk factor for the progression of hepatitis B cirrhosis to liver cancer and is involved in evaluating the body's nutritional level. Hepatitis B cirrhosis is a potential serum factor for HCC.

5. Treatment of LCH

5.1. Modern Medical Treatment of LCH

5.1.1. Antivirus. Antiviral therapy is the most routine intervention in the treatment of LCH in modern medicine [20]. Antiviral drugs can reduce hepatitis B (HBV) replication, prevent further necrosis of liver cells, improve liver function to varying degrees, promote the recovery of liver synthesis function, and increase serum albumin concentration. Shang [21] reported the application of lamivudine combined with conventional liver protection measures to treat 93 patients with cirrhosis and hypoalbuminemia, and serum albumin increased significantly after 6 months of treatment. Lamivudine can significantly improve the liver function of patients with liver cirrhosis and increase the level of serum albumin. Another group of clinical controlled studies have shown that entecavir has strong anti-hepatitis B virus activity and is well tolerated [22]. It can effectively inhibit HBV replication, reduce hepatocyte inflammatory response, and improve vascular endothelial cell function. The treatment effect for hypoproteinemia, abdominal effusion, and portal hypertension is remarkable.

5.1.2. Human Albumin or Plasma Infusion. Infusion of human albumin or plasma is currently one of the most commonly used methods for the treatment of hypoalbuminemia in liver cirrhosis. A number of studies have clearly shown that albumin can effectively improve hemodynamic disorders and various complications caused by advanced liver cirrhosis. All exhibited this common characteristic. Salerno et al. [23] confirmed the efficacy of albumin in improving the outcome of SBP patients through meta-analysis and significantly improved the survival rate of hospitalized patients. When liver cirrhosis is complicated by HRS, albumin combined with vasoconstrictor (mainly Terlipressin) can improve the survival of patients in a short period of time. It can improve renal function in about 40% of cases and cure HRS in about 30% of cases [24]. Bernardi et al. [25] analyzed 17 trials and found that albumin infusion was more effective in reducing circulatory dysfunction after paracentesis and reducing the incidence and mortality of ascites compared with conventional therapy.

However, due to the lack of clear clinical data and clinical efficiency evaluation, the role of albumin in some complications of liver cirrhosis has been controversial. For example, there is little evidence on the effect of albumin fold treatment in patients with non-SBP-related infections. A recent randomized study showed that treatment with albumin in combination with antibiotic improved the circulation and renal function in patients, but it was not observed between the two groups. It has a significant effect on the incidence of renal failure, and there is no difference in the 3-month cumulative survival rate. Therefore, further studies are needed to elucidate the therapeutic effect of albumin under this condition [26]. Although clinical studies have shown that transfusion of human albumin is beneficial in patients with severe HE, it is unclear whether cirrhosis complicated by hepatic encephalopathy is an indication for albumin due to the lack of clear clinical efficacy evaluation.

5.1.3. Amino Acid Supplementation. When hypoalbuminemia occurs in liver cirrhosis, the metabolism of amino acids and proteins in the body is mainly manifested as increased blood ammonia, decreased plasma albumin, and changes in the amino acid profile in the blood. Studies have shown that, in the amino acid metabolism disorder in the early stage of liver disease, the main reason is the reduction of branched chain amino acids (BCAA). Branched chain amino acids are essential raw materials for human protein synthesis and can be used as applied substances to provide the body with the necessary energy supply and reduce protein breakdown [27]. Clinically, compound amino acid injection has a wide variety of uses due to different uses. Amino acid injection has a high proportion of branched chain amino acids, which can help correct the imbalance of various amino acid ratios in patients with liver cirrhosis. It is often used for nutritional support treatment of patients with liver cirrhosis. Clinical studies have shown that the serum albumin concentration of patients with liver cirrhosis increases significantly after using branched chain amino acids, the incidence of ascites decreases, and the Child-Pugh score is reduced [28]. Ohno et al. confirmed through long-term clinical trials that supplemental therapy with branched chain amino acids can increase serum albumin levels in patients with liver cirrhosis [29] and reduce the risk of HCC and other complications [30].

5.1.4. Recombinant Human Growth Hormone. Growth hormone is a hormone secreted by the anterior pituitary gland, which can promote liver cell regeneration and albumin synthesis. It is difficult to obtain natural growth hormone. Artificially synthesized recombinant human growth hormone is commonly used in clinical practice, which has exactly the same structure and function as natural growth hormone. Recombinant human growth hormone can reverse the negative nitrogen balance and has an obvious "nitrogen storage" effect, thereby stimulating the expression of liver cell protein mRNA and increasing the body's protein level. Studies have shown [30, 31] that patients with liver cirrhosis have severe growth hormone resistance, and their serum GH levels are elevated, leading to reduction of the levels of IGF-1 and insulin-like growth factor binding protein-3 (IGFBP-3). Exogenous recombinant human growth hormone can overcome growth hormone resistance and increase the level of IGF-1 and IGFBP-3. IGF-1 can

inhibit protein breakdown and increase amino acid intake and cell proliferation, and IGFBP-3 can upregulate the biological activity of IGF-1 and further promote anabolism. Luo et al. [32] explored the effect of recombinant human growth hormone (rhGH) on the residual liver after hepatectomy in 24 patients with cancer and cirrhosis. The results showed that hepatic functional damage immediately after hepatectomy is a significant risk factor for early intrahepatic recurrence in cirrhotic HCC. The rhGH can promote the recovery of liver function by reducing the decline of cellular immune function in patients with liver cancer and liver cirrhosis and can also promote the body's protein synthesis and liver regeneration.

5.2. Traditional Medicine Treatment for LCH

5.2.1. Fubai Formula. Traditional Chinese medicine (TCM) believes that albumin belongs to the subtle category of qi and blood, while the spleen is the official source of qi and blood. Modern medicine shows that the drugs in Fubai prescription can not only directly supplement albumin but also reduce liver cell degeneration and necrosis, improve liver microcirculation, inhibit fibrous tissue proliferation, and significantly increase the infiltration of 3H-leucine into serum and liver to participate in protein synthesis, thereby improving the albumin level [33]. Shi et al. [34] analyzed the syndrome characteristics of patients with liver cirrhosis and hypoalbuminemia and the treatment effect of TCM, and the results showed that Fubai formula was significantly better than the control group in terms of TCM symptom improvement and serum albumin normalization rate. The long-term effect was more significant and no adverse reactions were seen. Serum cholinesterase (ChE) can sensitively and specifically reflect the anabolic function of the liver, and it is a sensitive indicator for evaluating the protein synthesis function of liver cells [35]. Xue [36] explored the effect of Fubai prescription on serum cholinesterase activity in patients with hepatitis and liver cirrhosis and found that the efficacy of Fubai prescription was significantly better than that of the control group. This is mainly related to the complex of Fubai Fang in promoting hepatocyte regeneration and eliminating immunity and increasing the activity of serum ChE.

5.2.2. Wuji Baifeng Pills. The prescription contains 30% black-bone chicken and is matched with Ginseng Radix et Rhizoma and Astragali Radix to invigorate *qi* and promote fluid. It is supplemented with Chuanxiong Rhizoma, Angelicae Sinensis Radix, Paeoniae Radix Alba, and Rehmanniae Radix Praeparata to nourish *qi* and blood, regulate menstruation, and relieve pain, and Cyperi Rhizoma, Dioscoreae Rhizoma, and Cervi Cornus Colla are added to regulate *qi* and invigorate the spleen and antler gum, as well as nourishing blood and *yang*. Hu et al. [37] showed that Wuji Baifeng Pill can protect liver cells from damage and regulate amino acid imbalance. It is also conducive to the synthesis of albumin and forms a virtuous circle. The study by Zhan et al. [38] and other studies have shown that the Wuji Baifeng Pill treatment group can improve the clinical symptoms, liver function, and blood coagulation function of patients more effectively than the control group and increase the serum total protein and albumin content of the patient. The total effective rate of the treatment group is 83.3%, was significantly higher than that of the control group (53.1%), and there were no adverse reactions during treatment. Therefore, Wuji Baifeng Pill is an ideal drug prescription for treating LCH. The main prescriptions of the TCM are listed in Table 1.

5.2.3. Shengbai Decoction. Ye and Wu [42] used liver hydrolyzed peptide intravenous infusion on the basis of routine liver protection, enzyme reduction, support, and diuresis, and the treatment group received Shengbai decoction with significantly better therapeutic effect than the control group. The treatment group was better than the control group in terms of restoring biochemical indicators, inhibiting HBV-DNA and HBeAg negative, and improving Child-Pugh score was also significantly higher than the control group. Zhu et al. [39] have shown that Shengbai decoction is better than the control group in improving the clinical symptoms of patients and improving the survival rate of patients. This may be related to the reduction of GH and LEP levels, improvement of insulin resistance, and adjustment of IGF-I and GH. The negative feedback is related to the increased albumin level.

5.2.4. Qijia Chaizhu Decoction. Kong et al. [40, 41] compared the efficacies of Qijia Chaizhu decoction and conventional liver-protecting therapy in 60 patients with clinical liver cirrhosis and hypoproteinemia. The results showed that Qijia Chaizhu decoction could significantly improve the symptoms of patients with liver cirrhosis and restore serum indicators, such as ALT, TBil, and DBil. Compared with the control group, the curative effect is significant, with an effective rate of 83.33%, which has a significant therapeutic effect on patients with liver cirrhosis and hypoproteinemia.

6. Discussion

Currently, modern medicine treatment of hepatitis B liver cirrhosis hypoalbuminemia is mainly to supplement exogenous albumin, amino acids, recombinant human growth hormone, and so forth, thereby enhancing the body's ability to synthesize albumin, and, to a certain extent, it can improve liver function and increase serum albumin levels, prolonging the survival of patients. However, this type of treatment is expensive and requires repeated treatment, which increases patient suffering and is prone to infusion reactions and infectious diseases.

TCM has a unique analysis of the etiology and pathogenesis of LCH. It is believed that insufficient liver blood is the basic pathogenesis, and the insufficiency of water and grain microbes is the main predisposing factor. The symptoms and signs of TCM in patients with LCH include hepatosplenomegaly, jaundice, swollen ascites, dull complexion, pain in the flanks, dark lips and tongue, damp-heat,

Table 1: The main prescriptions of the TCM.

Prescription name	Composition	Effects
Fubai formula [33, 36]	Poria, Atractylodis Macrocephalae Rhizoma, Astragali Radix, Angelicae Sinensis Radix, Bubali Cornu, Atractylodis Macrocephalae Rhizoma, Asini Corii Colla, Broussonetiae Fructus	Alleviating the symptoms of patients with liver cirrhosis and hypoalbuminemia, increasing the serum albumin content of patients, and improving the activity of serum cholinesterase in patients
Wuji Baifeng Pills [37]	Wuji, Cervi Cornus Colla, Trionycis Carapax, Ostreae Concha, Mantidis Ootheca, Ginseng Radix et Rhizoma, Astragali Radix, Angelicae Sinensis Radix, Paeoniae Radix Alba, Cyperi Rhizoma, Asparagi Radix, Glycyrrhizae Radix et Rhizoma, Rehmanniae Radix Praeparata, Rehmanniae Radix, Chuanxiong Rhizoma, Stellariae Radix, Salviae Miltiorrhizae Radix et Rhizoma, Dioscoreae Rhizoma, Euryales Semen, Cervi Cornu Degelatinatum	Protecting and improving liver cell function, reducing tyrosine production, promoting tyrosine degradation, and promoting albumin synthesis
Shengbai decoction [39]	Astragali Radix, Drynariae Rhizoma, Codonopsis Radix, Cuscutae Semen, Lycii Fructus, Spatholobi Caulis, Polygoni Multiflori Radix, Angelicae Sinensis Radix, Rehmanniae Radix Praeparata	Increasing the levels of albumin and insulin growth factor-1 in patients with liver cirrhosis and downregulating the serum levels of leptin and growth hormone
Qijia Chaizhu decoction [40, 41]	Astragali Radix, Rhizoma Atractylodis, Gizzard Pepsin, *Polygonum viviparum*, Turtle Shell, *Rehmannia muta*, *Angelica sinensis*, *Salvia miltiorrhiza*	Improving symptoms, signs, liver function, serum albumin, and ultrasonographic findings in patients with liver cirrhosis

blood stasis, phlegm and turbidity, as well as visceral *qi* and blood. A number of studies have shown that TCM therapy has a significant protective effect on damaged liver cells in liver cirrhosis. While promoting liver cell repair and regeneration, it can also reduce liver fibrosis, regulate the imbalance of amino acid levels, and form a virtuous cycle, which is beneficial to the synthesis of albumin in the body and has few adverse reactions. Therefore, the long-term efficacy of TCM in the treatment of LCH is more significant, and its related compatibility theory is worth exploring and learning. However, TCM has various types of syndrome differentiation for LCH and different criteria for determining efficacy. In addition, the long-term efficacy observation and evaluation of refractory LCH are less, which leads to certain limitations in the treatment of TCM.

It is well known that the growth hormone (GH)/IGF-I axis is important in growth [43, 44]. The presence of binding proteins, particularly IGFBP3, regulates the growth axis by controlling the levels of free IGF-I in circulation and prolonging the half-life of IGF-I [45]. In LCH patients admitted to hospital due to complications of the disease, IGF-I and IGFBP-3 serum levels were associated with variables related to liver dysfunction and with more advanced liver disease. The levels of these markers mainly reflect hepatic functional status and seem to undergo little influence from other clinical and laboratory variables [46, 47]. Therefore, serum IGF-I and IGFBP-3 can provide a new dimension for the evaluation of LCH. This study found that the regulations of IGF-I and IGFBP-3 simultaneously exist in a variety of sclerosing hypoproteinemia therapies, suggesting that IGF-I and IGFBP-3 are key targets for the treatment of cirrhotic LCH.

At present, modern medical treatment of hypoalbuminemia in liver cirrhosis is mainly to directly supplement exogenous albumin. Other treatment methods include eliminating incentives, increasing synthetic raw materials, and enhancing synthetic functions. These treatments can improve serum albumin levels to a certain extent, but the economic burden of patients is heavy, and the long-term efficacy is not as good as that of traditional Chinese medicine. A number of studies have shown that traditional Chinese medicine has obvious curative effect on the treatment of hypoalbuminemia, and the long-term curative effect is significant, but there are still many problems. ① The research design is not rigorous enough, and the curative effect is mostly limited to dozens of cases. In general, existing studies lack large-scale, multicenter evidence-based studies. ② Differential analysis of hypoalbuminemia in liver cirrhosis is inconsistent for each person, the medication lacks regularity, and there is also a lack of controlled studies between different syndrome differentiation treatments. ③ There is a lack of basic research on Chinese medicine treatment, and the mechanism of Chinese medicine to improve hypoalbuminemia is not clear. It is hoped that research in this area will be strengthened in the future to clarify the mechanism of TCM treatment and to screen out effective prescriptions. In recent years, integrating traditional Chinese and western medicine has had obvious curative effect in the treatment of hypoalbuminemia of liver cirrhosis, and it also shows certain advantages, which can be used as appropriate.

7. Conclusion

Hypoalbuminemia has been reported to be closely related to the occurrence and severity of a variety of malignant diseases, such as sepsis, bacteremia, community-acquired pneumonia, and catheter-related bloodstream infection [48]. In the global pandemic of coronavirus disease in 2019 (COVID-19), the liver damage analysis of 2623 hospitalized patients confirmed that hypoproteinemia is a significant risk factor for patients with severe COVID-19 and can

independently predict the progression and outcome of COVID-19 [49–51].

At present, hypoproteinemia is still a typical feature of the progression of LCH. It may appear in the early stages of the disease and may remain clinically silent for several years, eventually leading to a variety of complications. In order to improve the quality life of patients and prolong the life cycle, it is particularly important to find accurate and quantified disease severity and safe and effective treatment measures. However, the current clinical trials for the treatment of LCH still have limitations. Many interventions lack rigorous, multicenter, double-blind, and large-sample verification. The prognosis of patients also urgently requires further long-term follow-up trials. There is a lack of systematic medication rules for different syndromes in the treatment of LCH with TCM, and there is a lack of controlled studies between different syndromes. Therefore, in the future, attention should be paid to conducting large-scale, high-quality randomized controlled trials to verify the therapeutic effect of LCH. Simultaneously, researchers should strengthen the systematic study of TCM in the treatment of LCH and clarify the treatment mechanism of TCM, screen core drugs, and form a systematic medication rule to provide reference for clinical treatment of LCH.

Abbreviations

LCH: Liver cirrhosis with hypoproteinemia
CNKI: China National Knowledge Infrastructure
CBM: Chinese Biomedical Database
VMIS: VIP medicine information system
SBP: Spontaneous peritonitis
GH: Growth hormone
IGF-I: Insulin-like growth factor
IGFBP-3: Insulin-like growth factor binding protein-3
HCC: Hepatocellular carcinoma
HBV: Hepatitis B
BCAA: Branched chain amino acids
rhGH: Recombinant human growth hormone
TCM: Traditional Chinese medicine
ChE: Serum cholinesterase
COVID-19: Coronavirus disease 2019.

Data Availability

The data used to support the findings of this study are available from the corresponding author upon reasonable request.

Ethical Approval

Due to the fact that this study does not involve animal and patient experiments, the ethics approval and consent to participate are not applicable.

Disclosure

All data were generated in-house, and no paper mill was used.

Conflicts of Interest

The authors declare no conflicts of interest.

Authors' Contributions

Jianxia Wen and Xing Chen contributed equally to this study. Jianxia Wen provided important information for the completion and wrote and amended the manuscript. Xing Chen reviewed the drafts and searched the references. Shizhang Wei provided the methodological guidance and revised the manuscript. Xiao Ma carefully checked the references. Yanling Zhao conceived and designed the study. All authors agree to be accountable for all aspects of work ensuring integrity and accuracy.

Acknowledgments

This research was financially supported by the Project of Capital's Funds for Health Improvement and Research (no. 2018-2-5032), Science Foundation of Sichuan Education Department (18ZA0186), and Talent Introduction Project of Xihua University (Z211060).

References

[1] D. J. Nompleggi and H. L. Bonkovsky, "Nutritional supplementation in chronic liver disease: an analytical review," *Hepatology*, vol. 19, no. 2, pp. 518–533, 1994.

[2] Chinese Medical Association Intensive Medicine Branch, "Guidelines of nutritional support in critically ill patients (draft)," *Chinese Critical Care Medicine*, vol. 18, no. 10, pp. 582–590, 2006.

[3] L. Chen, *Systematic Review of Human Albumin in Patients with Liver Cirrhosis and Ascites*, Hunan Normal University, Changsha, China, 2014.

[4] J. González-González, G. Vázquez-Eylizondo, R. Monreal-Robles et al., "Hypoalbuminemia in the outcome of patients with non-variceal upper gastrointestinal bleeding," *Revista de Gastroenterología de México*, vol. 81, no. 4, pp. 183–189, 2016.

[5] C. F. Tung, W. K. Chow, C. S. Chang, Y. C. Peng, and W. H. Hu, "The prevalence and significance of hypoalbuminemia in non-variceal upper gastrointestinal bleeding," *Hepato-Gastroenterology*, vol. 54, no. 76, pp. 1153–1156, 2007.

[6] J. González-González, D. García-Compean, G. Vázquez-Elizondo, A. Garza-Galindo, J. O. Jáquez-Quintana, and H. Maldonado-Garza, "Nonvariceal upper gastrointestinal bleeding in patients with liver cirrhosis. Clinical features, outcomes and predictors of in-hospital mortality. A prospective study," *Annals of Hepatology*, vol. 10, no. 3, pp. 287–295, 2011.

[7] F. Karaahmet, S. Coban, and I. Yuksel, "Gastrointestinal bleeding and transfusion strategies in patients with hypoalbuminemia," *Digestive Diseases and Sciences*, vol. 59, no. 2, p. 493, 2014.

[8] C. Wang and H. Guo, "Analysis of the effect of hypoproteinemia on the diagnosis of cirrhotic spontaneous peritonitis by serum procalcitonin," *Medical Theory and Practice*, vol. 31, no. 2, pp. 260-261, 2018.

[9] A. Abdel-Razik, M. Abdelsalam, D. F. Gad et al., "Recurrence of spontaneous bacterial peritonitis in cirrhosis: novel predictors," *European Journal of Gastroenterology and Hepatology*, vol. 32, no. 6, pp. 718–726, 2020.

[10] A. Gatta, A. Verardo, and M. Bolognesi, "Hypoalbuminemia," *Internal and Emergency Medicine*, vol. 7, no. Suppl 3, pp. S193–S199, 2012.

[11] K. Fukazawa and H. T. Lee, "Updates on hepato-renal syndrome," *Journal of Anesthesia & Clinical Research*, vol. 4, no. 9, p. 352, 2013.

[12] J. A. Leithead, P. C. Hayes, and J. W. Ferguson, "Review article: advances in the management of patients with cirrhosis and portal hypertension-related renal dysfunction," *Alimentary Pharmacology & Therapeutics*, vol. 39, no. 7, pp. 699–711, 2014.

[13] X. Li and Q. Meng, "Malnutrition and nutritional support in patients with liver cirrhosis," *Parenteral and Enteral Nutrition*, vol. 13, no. 5, pp. 312–315, 2006.

[14] Z. Wu and H. Qin, "Progress of nutritional support in patients with liver cirrhosis," *Chinese Practical Surgery*, vol. 20, no. 6, pp. 337–339, 2000.

[15] H. Shen, F. Xi, C. Xu, and W. Zhang, "The change of protein malnutrition in patients with posthepatitic cirrhosis," *Journal of Clinical Internal Medicine*, vol. 23, no. 2, pp. 91-92, 2006.

[16] Y. Zhu and J. Fan, "The relationship between leptin and malnutrition in liver cirrhosis," *International Journal of Digestive Disease*, vol. 29, no. 2, pp. 92-93, 2009.

[17] H. Wang, X. Zhu, L. Wang et al., "Relationship between the levels of ghrelin and leptin and the hypoalbuminemia of advanced gastric carcinoma," *Chinese Journal of Clinical Pharmacology*, vol. 32, no. 2, pp. 180–182, 2016.

[18] B. Campillo, E. Sherman, J. Richardet, and P. Bories, "Serum leptin levels in alcoholic liver cirrhosis: relationship with gender, nutritional status, liver function and energy metabolism, liver function and energy metabolism," *European Journal of Clinical Nutrition*, vol. 55, no. 11, pp. 980–988, 2001.

[19] J. Feng, X. Fan, L. Ha, Z. Ren, L. Li, and F. He, "Correlation between serum leptin level and hepatocellular carcinoma (HCC) based on hepatitis B cirrhosis," *Electron Journal of Metabolism and Nutrition of Cancer*, vol. 6, no. 1, pp. 83–88, 2019.

[20] G. Wang, Z. Duan, Chinese Society of Infectious Diseases, Chinese Medical Association, and Chinese Society of Hepatology, "Guidelines for prevention and treatment of chronic hepatitis B," *Journal of Clinical and Translational Hepatology*, vol. 9, no. 5, pp. 769–791, 2021.

[21] H. Shang, "Lamivudine in the treatment of liver cirrhosis with hypoproteinemia," *Journal of Medical Forum*, vol. 28, no. 9, pp. 64-65, 2007.

[22] H. Li, J. Zhao, G. Luo, and X. Chen, "Comparison of entecavir and lamivudine antiviral therapy in treating severe hHepatitis B," *China Pharmaceutical*, vol. 25, no. 6, pp. 35–37, 2016.

[23] F. Salerno, R. J. Navickis, and M. M. Wilkes, "Albumin infusion improves outcomes of patients with spontaneous bacterial peritonitis: a meta-analysis of randomized trials," *Clinical Gastroenterology and Hepatology*, vol. 11, no. 2, pp. 123–130, 2013.

[24] S. Piano, H. H. Schmidt, X. Ariza et al., "Association between grade of acute on chronic liver failure and response to Terlipressin and albumin in patients with hepatorenal syndrome," *Clinical Gastroenterology and Hepatology*, vol. 16, no. 11, pp. 1792–1800, 2018.

[25] M. Bernardi, P. Caraceni, R. J. Navickis, and M. M. Wilkes, "Albumin infusion in patients undergoing large-volume paracentesis: a meta-analysis of randomized trials," *Hepatology*, vol. 55, no. 4, pp. 1172–1181, 2012.

[26] M. Guevara, C. Terra, A. Nazar et al., "Albumin for bacterial infections other than spontaneous bacterial peritonitis in cirrhosis. A randomized, controlled study," *Journal of Hepatology*, vol. 57, no. 4, pp. 759–765, 2012.

[27] H. Liu, J. Chen, P. Xu, L. Luo, L. Xia, and Q. Zhao, "The role of compound amino acid liquid rich in branched chain amino acids in parenteral nutrition of patients with liver cirrhosis," *Journal of Practical Medicine*, vol. 26, no. 3, pp. 454–456, 2010.

[28] H. Yatsuhashi, Y. Ohnishi, S. Nakayama, H. Iwase, T. Nakamura, and M. Imawari, "Anti-hypoalbuminemic effect of branched-chain amino acid granules in patients with liver cirrhosis is independent of dietary energy and protein intake," *Hepatology Research*, vol. 41, no. 11, pp. 1027–1035, 2011.

[29] Y. Yuan, L. Xia, D. Qiu et al., "The efficacy and safety of a branched-chain amino acid granules in the treatment of cirrhotic hypoproteinemia—a multicenter, randomized, control study," *Chinese Journal of Digestion*, vol. 21, no. 2, pp. 34–36, 2001.

[30] T. Ohno, Y. Tanaka, F. Sugauchi et al., "Suppressive effect of oral administration of branched-chain amino acid granules on oxidative stress and inflammation in HCV-positive patients with liver cirrhosis," *Hepatology Research*, vol. 38, no. 7, pp. 683–688, 2008.

[31] Y. Guo, C. Jiang, and W. Shu, "Meta-analysis of the efficacy of recombinant human growth hormone and human serum albumin in the treatment of liver cirrhosis with hypoproteinemia," *Chinese Journal of Primary Medicine and Pharmacy*, vol. 27, no. 23, pp. 2825–2829, 2020.

[32] S.-M. Luo, L.-J. Liang, and J.-M. Lai, "Effects of recombinant human growth hormone on remnant liver after hepatectomy in hepatocellular carcinoma with cirrhosis," *World Journal of Gastroenterology*, vol. 10, no. 9, pp. 1292–1296, 2004.

[33] W. Shi, X. Jin, and J. Ding, "Fubai formula for posthepatic cirrhosis with hypoproteinemia," *Infectious Disease Information*, vol. 22, no. 3, pp. 157–159, 2009.

[34] W. Shi, T. Zhang, and Y. Sun, "TCM syndrome characteristics of hypoproteinemia induced by hepatitis cirrhosis and curative effect of Chinese medicines," *Journal of Beijing University of Chinese Medicine (Clinical Chinese Medicine Edition)*, vol. 16, no. 6, pp. 7–10, 2009.

[35] F. Artru, M. Fraga, S. Godat, A. M. Schoepfer, and D. Moradpour, "Advances in gastroenterology and hepatology 2020," *Revue Médicale Suisse*, vol. 17, no. 720, pp. 29–32, 2021.

[36] A. Xue, "Effect of Fubai recipe on cholinesterase activity in patients with hepatitis and liver cirrhosis," *Chinese Clinical Practical Medicine*, vol. 4, no. 6, pp. 147-148, 2010.

[37] Y. Hu, X. Liang, and L. Xu, "The effect of Wuji Baifeng Pills against CCl_4 chronic liver injury," *Chinese Patent Medicine*, vol. 16, no. 1, pp. 33-34, 1994.

[38] G. Zhan, H. Tan, L. Zhu et al., "Treating cirrhotic hypoproteinemia by PHGF, wujibaifeng pill combined with salviate milttiorrhize," *Journal of Clinical Hepatobiliary Disease*, vol. 26, no. 1, pp. 39–41, 2010.

[39] X. Zhu, X. Du, and G. Li, "The influence of ruangan shengbai decoction to LEP, IGF-1, GH and Alb in patients with hepatitis cirrhosis," *Chinese Journal of Integrated Traditional and Western Medicine on Liver Diseases*, vol. 18, no. 3, pp. 134–136, 2008.

[40] Q. Kong, C. Liu, J. Zhang et al., *Clinical Study on the Treatment of Liver Cirrhosis Hypoproteinemia by Qigaichai Decoction*, Weihai Hospital of Traditional Chinese Medicine, Weihai, China, 2009.

[41] Q. Kong, C. Liu, B. Sun, Y. Sui, J. Zhang, and J. Gu, "Clinical study of qi jia chai shu yin in the treatment of liver cirrhosis hypoproteinemia," *Journal of Integrated Chinese and Western Medicine*, vol. 19, no. 4, pp. 200–202, 2009.

[42] W. Ye and W. Xu, "Sheng Bai Tang was mainly used to treat 44 cases of hepatic cirrhosis hypoproteinemia," *Zhejiang Journal of Traditional Chinese Medicine*, vol. 44, no. 5, pp. 324-325, 2009.

[43] S. Yakar, H. Werner, and C. Rosen, "Insulin-like growth factors: actions on the skeleton," *Journal of Molecular Endocrinology*, vol. 61, no. 1, pp. T115–T137, 2018.

[44] A. Grimberg and P. Cohen, "Role of insulin-like growth factors and their binding proteins in growth control and carcinogenesis," *Journal of Cellular Physiology*, vol. 183, no. 1, pp. 1–9, 2000.

[45] J. M. Castelino, M. N. Routledge, S. Wilson et al., "Aflatoxin exposure is inversely associated with IGF1 and IGFBP3 levels in vitro and in Kenyan schoolchildren," *Molecular Nutrition & Food Research*, vol. 59, no. 3, pp. 574–581, 2015.

[46] M. F. Ronsoni, C. Lazzarotto, L. Fayad et al., "IGF-I and IGFBP-3 serum levels in patients hospitalized for complications of liver cirrhosis," *Annals of Hepatology*, vol. 12, no. 3, pp. 456–463, 2013.

[47] S.-M. Luo, W. Tan, W. Deng, S. M. Zhuang, and J. W. Luo, "Expression of albumin, IGF-1, IGFBP-3 in tumor tissues and adjacent non-tumor tissues of hepatocellular carcinoma patients with cirrhosis," *World Journal of Gastroenterology*, vol. 11, no. 27, pp. 4272–4276, 2005.

[48] C. J. Wiedermann, "Hypoalbuminemia as surrogate and culprit of infections," *International Journal of Molecular Sciences*, vol. 22, no. 9, p. 4496, 2021.

[49] W. Huang, C. Li, Z. Wang et al., "Decreased serum albumin level indicates poor prognosis of COVID-19 patients: hepatic injury analysis from 2,623 hospitalized cases," *Science China Life Sciences*, vol. 63, no. 11, pp. 1678–1687, 2020.

[50] J. Huang, A. Cheng, R. Kumar et al., "Hypoalbuminemia predicts the outcome of COVID-19 independent of age and co-morbidity," *Journal of Medical Virology*, vol. 92, no. 10, pp. 2152–2158, 2020.

[51] L. Lin, K. Hu, S. Cai et al., "Hypoproteinemia is an independent risk factor for the prognosis of severe COVID-19 patients," *Journal of Clinical Biochemistry and Nutrition*, vol. 67, no. 2, pp. 126–130, 2020.

Hindawi
Evidence-Based Complementary and Alternative Medicine
Volume 2022, Article ID 7904845, 10 pages
https://doi.org/10.1155/2022/7904845

Research Article

The Potential Hepatoprotective Effect of Paeoniae Radix Alba in Thioacetamide-Induced Acute Liver Injury in Rats

Mi-Rae Shin, Se Hui Lee, and Seong-Soo Roh

Department of Herbology, College of Korean Medicine, Daegu Haany University, Daegu 42158, Republic of Korea

Correspondence should be addressed to Seong-Soo Roh; ddede@dhu.ac.kr

Received 14 October 2021; Revised 3 January 2022; Accepted 4 January 2022; Published 28 January 2022

Academic Editor: Chih-Yuan Ko

Aim. Acute liver injury (ALI) can occur for various reasons by induced inflammation and apoptosis of liver cells including hepatocytes, Kupffer cells, and hepatic stellate cells. Thioacetamide (TAA), which is a classic hepatotoxin, causes oxidative stress, membrane damage, and accumulation of lipid droplets and subsequently provokes consecutive liver injury. In the current study, we tested whether Paeoniae Radix Alba (PR) could alleviate TAA-induced ALI. *Methods*. Thirty-five male rats were equally separated into five groups. The first group was the normal group, which received distilled water only. The remaining four groups received intraperitoneal TAA (200 mg/kg) for 3 days to induce ALI. The four groups were divided into the control group (no treatment), silymarin-treated, 100 mg/kg PR-treated, and 200 mg/kg PR-treated. The efficacy of PR against hepatotoxicity was evaluated in terms of the serum biochemical index and protein expression associated with inflammation and apoptosis. Moreover, the dissected livers were analyzed by hematoxylin and eosin stain. *Results*. PR alleviated liver dysfunction as evidenced by decreased levels of aspartate aminotransferase, alanine aminotransferase, and ammonia. Phosphorylated AMP-activated protein kinase (AMPK) and Sirtuin 1 (Sirt1) levels were obviously decreased in the TAA control group, whereas PR reversed these changes. PR also prevented deteriorative effects through inhibition of inflammation and apoptosis via nuclear transcription factor-kappa Bp65 (NF-κBp65) inactivation. Moreover, we found that the hepatoprotective effect of PR pretreatment was mediated by restoration of histopathological changes. *Conclusion*. PR efficiently blocked both the inflammatory response and apoptosis through activating the AMPK/Sirt1/NF-κBp65 pathway. Therefore, PR is considered a potential therapeutic agent against ALI.

1. Introduction

Acute liver injury (ALI) is characterized by a rapid loss of liver function without preexisting liver disease and is frequently life-threatening. A variety of causes of ALI have been identified, including infections, neoplasms, toxic factors, and drugs [1]. Emerging evidence suggests that oxidative stress (OS) is involved in the development of liver injury [2]. Thioacetamide (TAA) converts into a highly toxic reactive intermediate, thioacetamide S-dioxide, by cytochromes P450 (CYP450) enzymes. CYP450 yields OS and participates in drug-induced liver damage. Accordingly, thioacetamide S-dioxide toxicity will be partially blocked by CYP450 inhibitors [3]. Bi et al. [4] reported that Paeoniae Radix Alba (PR; the root of the plant *Paeonia lactiflora Pallas*, Bai Shao) reduced toxicity via the degradation of toxic alkaloids and enhanced efficacy associated with CYP450. PR has been used as a medicinal herb in traditional Chinese medicine and is also named "White Paeony." Recently, PR has been used more widely than Radix Paeoniae Rubra (Red Paeony) [5]. The application of PR is widely reported to refresh blood circulation, regulate menstruation, alleviate pain, and nourish the liver [6, 7]. Moreover, recent studies demonstrated that the neuroprotective potential of PR against strychnine-induced neurotoxicity was related to the suppression of OS [8]. PR also effectively treated an experimental autoimmune hepatitis mouse model via inhibition of OS [9].

AMP-activated protein kinase (AMPK) is a major regulator of cellular energy balance. Once activated by an increase of the cellular AMP : ATP ratio [10], it suppresses the rate of anabolic ATP consumption and the synthesis of

proteins and/or lipids and increases the rate of catabolic ATP production and the oxidation of fatty acids and/or mitochondrial biogenesis to preserve ATP levels for intracellular energy homeostasis [11]. AMPK is composed of heterotrimeric complexes such as catalytic α-subunits and regulatory β- and γ-subunits. Under metabolic stress, catalytic α-subunits are phosphorylated, and then gene expressions and enzyme activities are altered to initiate corrective responses [12]. Specifically, AMPK controls gene expression by modulating Sirtuins in coordination with another metabolic sensor, the NAD^+-dependent deacetylase. Sirtuins control many biological processes, such as apoptosis, cellular senescence, endocrine signaling, glucose homeostasis, aging, longevity, and mitochondrial biogenesis [13]. In particular, Sirtuin 1 (Sirt1) regulates numerous activities including metabolism, mitochondrial function, inflammation, and apoptosis during OS [14]. Therefore, many scientists have been trying to find Sirt1 modulators that can activate Sirt1. In turn, decreased expression of Sirt1 exacerbates the loss of AMPK phosphorylation and triggers the overproduction of reactive oxygen species and inflammatory responses including NF-κBp65 transcription [15].

According to previous hepatoprotective studies using PR, Wang et al. [16] reported that it had a hepatoprotective effect by regulating the homeostasis of bile acids and homocysteine, and Lee et al. [17] reported that it exhibited a hepatoprotective effect through the inhibition of oxidative stress. However, the underlying mechanism of PR in rats with ALI has not been clearly established. Accordingly, we elucidated that the anti-inflammatory and antiapoptotic effects of PR via the regulation of the AMPK/Sirt1/NF-κBp65 pathway.

2. Materials and Methods

2.1. Materials. Silymarin, thioacetamide, and phenyl methyl sulfonyl fluoride were purchased from Sigma-Aldrich (St. Louis, MO, USA). The protease inhibitor solution and EDTA were purchased from Wako Pure Chemical Industries, Ltd. (Osaka, Japan). Sodium carbonate was purchased from Daejung Chemicals & Metals Co., Ltd. (Siheung, Korea). Sodium hydroxide was purchased from OCI Company Ltd. (Seoul, Korea). Phosphoric acid was purchased from Duksan Company (Ansan, Korea). The Pierce BCA Protein Assay kit was purchased from Thermo Fisher Scientific Inc. (Waltham, MA, USA). ECL Western Blotting Detection Reagents and pure nitrocellulose membranes were purchased from GE Healthcare (Chicago, IL, USA). The primary antibodies p-LKB1 (#3482), LKB1 (#3047), p-AMPK (#2531), AMPK (#2532), and Caspase-3 (#9662S) were purchased from Cell Signaling Technology (Danvers, MA, USA). The primary antibodies Sirt1 (SC-15404), NF-κBp65 (SC-372), Bax (SC-7480), Bcl2 (SC-7382), cytochrome C (SC-13156), survivin (SC-17779), MCP-1 (SC-28879), ICAM-1 (SC-1511-R), VCAM-1 (SC-13160), TNF-α (SC-1351), IL-6 (SC-57315), COX-2 (SC-19999), iNOS (SC-7271), histone (SC-8030), and β-actin (SC-4778) were purchased from Santa Cruz Biotechnology, Inc. (Dallas, TX, USA). Horseradish peroxidase-conjugated secondary antibodies were acquired from GeneTex, Inc. (Irvine, CA, USA). Isotroy was purchased from Troikaa Pharmaceuticals, Ltd. (Ahmedabad, GJ, India). All other chemicals and reagents were purchased from Sigma-Aldrich (St. Louis, MO, USA).

2.2. Plant Materials. Paeoniae Radix Alba (PR) was supplied by Bonchowon (Yeongcheon-si, Gyeongsangnam-do, Korea). PR (300 g) was extracted with 10 times the amount of water and boiled at 100°C for 2 h with distilled water (D.W.). After filtration, the water extracts were evaporated using a rotary evaporator at 50°C, and the solvent was evaporated *in vacuo* to give an extract with a yield of 9.3%. Then, the powder was kept at −80°C until animal experimentation.

2.3. Analysis of Paeoniflorin. Quantitative analysis was performed using Agilent 1290 Infinity II high-performance liquid chromatograph was equipped with Agilent 6470 triple-quadrupole mass spectrometer coupled with an Agilent Jet Stream source in electrospray ionization (ESI) mode (Agilent Technologies, CA, USA). The water extract of Paeoniae Radix Alba (1 mg) was dissolved in 1 mL of 100% ACN. 100 μL of the sample was mixed with an equal volume of internal standard (1 ng/mL Gliclazide in acetonitrile). Paeoniflorin separation solution (5 μL) was injected onto an Agilent Zorbax Eclipse Plus C18 column (2.1 mm × 50 mm id, 1.8 μm) and separated. The column and autosampler tray was kept at 40°C and 4°C, respectively. The mobile phase consisted of HPLC-grade water with 10 mM ammonium formate in distilled water as solvent A and acetonitrile as solvent B (A : B = 20 : 80 isocratic) with isocratic elution at a flow rate of 0.2 mL/min. The total run time was 2.5 min per sample. Quantification was performed with MS/MS detection set in the positive in multiple reaction monitoring modes for the analyte and IS. The amount of paeoniflorin (including 100 ng/mL) is analyzed to be 4.21 ± 0.40 ng/mL (Figure 1).

2.4. Experimental Animals and Induction of Acute Liver Injury. All animal experiments protocols were performed according to "The Guidelines for Animal Experiment" approved by the Ethics Committee of Daegu Haany University (Approval no. DHU2020-083). The 6-week-old male Sprague-Dawley rats (180–200 g) were purchased from DBL (Eumseong, Korea) and used for experiments after being adapted to the environment for 1 week. Environmental conditions were set to 12 h light/dark cycle, controlled humidity (50% ± 5%), and temperature (22 ± 2°C). After 1 week of adaptation, a total of thirty-five rats were randomly divided into 5 groups as follows ($n = 7$); we followed the methods of Shin et al. [18]. In addition, the concentrations of PR and silymarin were administered with reference to the doses used in the previously published acute liver injury paper [19].

(1) Normal group, received D.W. only

(2) Control group, TAA-induced ALI treated with D.W.

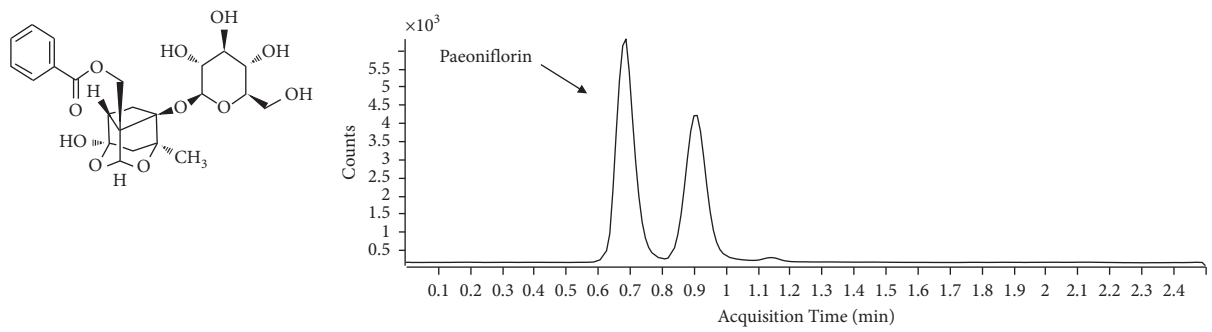

(a) (b)

Figure 1: Analysis of paeoniflorin in the extract of PR. (a) Chemical structure of paeoniflorin. (b) The chromatogram of the extract of PR. PR: Paeoniae Radix Alba.

(3) Silymarin group, TAA-induced ALI treated with silymarin (100 mg/kg)

(4) PR100 group, TAA-induced ALI treated with PR (100 mg/kg)

(5) PR200 group, TAA-induced ALI treated with PR (200 mg/kg)

All rats were weighed once a day at a certain time. Silymarin and PR were administered orally 90 min prior to TAA treatment. TAA (200 mg/kg dissolved in D.W.) was intraperitoneally administered to all groups except for the normal group every day for 3 d with drug treatment. No deaths were found in the TAA-injected group until the day of the autopsy. At the end of the experiment, rats were anesthetized by Isotroy inhalation anesthesia (induction, 4% isoflurane; maintenance, 2% isoflurane) for 5–7 min. Subsequently, blood was drawn from the abdominal vein and centrifuged at 4,800 × g for 20 min at 4°C. Next, the rats were euthanized by bleeding from the abdominal vein, and the death of the rats was confirmed through the absence of reflexes. The liver tissues were immediately stored at −80°C.

2.5. Measurement of Aspartate Aminotransferase (AST) and Alanine Aminotransferase (ALT) Levels. Hepatic functional parameters, such as AST and ALT, were measured using specific assay kits and a microplate fluorescence reader (Transaminase CII-Test; Wako Pure Chemical Industries, Ltd., Osaka, Japan).

2.6. Measurement of Ammonia Levels. Serum was collected from each group as above. Ammonia levels were measured by enzyme-linked immunosorbent assay (ELISA) kits (Abcam, Cambridge, UK) according to the manufacturer's instructions.

2.7. Hematoxylin and Eosin Staining of Liver Tissue. Microscopic examination was performed to evaluate the separated liver tissue. The separated liver tissue was fixed through a 10% neutral-buffered formalin and embedded in paraffin. It was cut into 2 μm sections and stained using hematoxylin and eosin for microscopic evaluation. The stained slides were observed under an optical microscope and then analyzed using the i-Solution Lite software program (InnerView Co., Korea). Also, quantitative analysis (%) for inflamed cells infiltrations on H&E stains was measured on randomly selected sections from at least three fields of each sample (at x200 magnification) using image analysis with the National Institutes of Health image program (ImageJ 1.52) following the user's guide (https://imagej.net/docs/guide).

2.8. Western Blotting. For cytosol samples, liver tissues were lysed with buffer A consisting of 0.1 mM EDTA, 10 mM HEPES (pH 7.8), 0.1 mM phenyl methyl sulfonyl fluoride, 10 mM KCl, 1 mM DTT, 2 mM $MgCl_2$, and 1,250 μL protease inhibitor solution (Wako). The homogenates were incubated at 4°C for 20 min and were mixed with 10% NP-40. After centrifugation (12,000 rpm at 4°C for 2 min) using an Eppendorf 5415R (Hamburg, Germany), the supernatant was collected as the cytosol sample. After that, the lysates were suspended with 20 mL ice-cold lysis buffer C consisting of 50 mM HEPES (pH 7.8), 50 mM KCl, 300 mM NaCl, 1 mM DTT, 0.1 mM EDTA, 1% (v/v) glycerol, 0.1 mM phenyl methyl sulfonyl fluoride, and 100 μL protease inhibitor solution and incubated at 4°C for 30 min. Samples were centrifuged at 12,000 rpm at 4°C for 10 min, and the supernatant collected was the nuclear sample. Both cytosol and nuclear samples were stored at −80°C before use. Samples containing 10 μg of protein were electrophoresed through 8–15% SDS-PAGE and transferred to a nitrocellulose membrane. Each membrane was blocked with 5% (w/v) skim milk solution for 1 h and visualized using ECL reagents. The bands were detected by Sensi-Q 2000 ChemiDoc (Lugen Sci Co., Ltd., Gyeonggi-do, Korea). We followed the methods of Shin et al. [20].

2.9. Statistical Analysis. The data were expressed as the mean ± standard error of the mean (SEM). Statistical analysis was analyzed using one-way analysis of variance (ANOVA) test followed by least-significant differences (LSD) test. All analyses were performed using SPSS version 26.0 software (SPSS Inc., Chicago, IL, USA). Statistical significance levels for each group were shown at $^{\#,*}$, $p < 0.05$, $^{\#\#,**}$, $p < 0.01$, and $^{\#\#\#,***}$, $p < 0.001$.

3. Results

3.1. PR Improved Body Weight Gain, Liver Weight, Relative Liver Weight, and Liver Function. As shown in Table 1, we first measured the effects of silymarin and PR on body weight gain and relative liver weight. TAA treatment significantly decreased body weight gain ($p < 0.001$) and significantly elevated relative liver weight ratio compared with that of the normal group ($p < 0.001$). Silymarin and PR treatment improved a relative liver weight ratio without a significant difference. To evaluate the effect of silymarin and PR on liver dysfunction, serum liver function biomarkers were measured (Table 2). TAA treatment led to significant elevations of both AST and ALT. The AST and ALT levels in the TAA control group significantly increased approximately 2.2-fold and 9.8-fold, respectively, whereas silymarin and PR administration significantly decreased these levels. Moreover, silymarin and PR treatment decreased serum ammonia levels ($p < 0.001$) (control: 19.18 ± 0.74 nmol/μL; silymarin: 14.73 ± 1.03 nmol/μL; PR100: 12.68 ± 0.46 nmol/μL; and PR200: 11.58 ± 0.73 nmol/μL).

3.2. PR Activated p-LKB1/AMPK/Sirt1 in ALI Rat Liver Tissue. Next, we investigated whether PR activates LKB1/AMPK/Sirt1 (Figure 2). Compared with the TAA control group, silymarin and PR treatment significantly increased the levels of p-LKB1, p-AMPK, and Sirt1 (silymarin, 21%, $p < 0.05$; 28%, $p < 0.01$; and 29%, $p < 0.01$; PR200, 43%, $p < 0.001$; 42%, $p < 0.001$; and 28%, $p < 0.01$, resp.). Silymarin exhibited similar efficacies of PR200 as compared with the control group in Sirt1 activation.

3.3. PR Suppressed the Release of NF-κBp65 and Proinflammatory Proteins in ALI Rat Liver Tissue. TAA injection upregulated the protein levels of NF-κBp65, COX-2, iNOS, TNF-α, and IL-6 by 1.49-, 1.67-, 1.14-, and 1.19-fold compared with the normal group. Moreover, silymarin and PR administration significantly suppressed proinflammatory targets including NF-κBp65, COX-2, iNOS, TNF-α, and IL-6 (Figure 3). Herein, the ameliorative effects of the higher dose of PR (200 mg/kg) were superior to those of the lower PR dose (100 mg/kg). Compared to the pharmacological properties between silymarin and PR200, there was a tendency that GF 200 seemed better in NF-κBp65 and IL-6 levels than silymarin, but other factors, such as iNOS, COX-2, and TNF-α, have shown similar effects.

3.4. PR Alleviated the Levels of MCP-1, ICAM-1, and VCAM-1 in ALI Rat Liver Tissue. The levels of MCP-1, ICAM-1, and VCAM-1 were evaluated by western blotting (Figure 4). The expression levels of MCP-1, ICAM-1, and VCAM-1 in the TAA control group were significantly higher than those in the normal group and increased by 1.40-, 1.32-, and 1.50-fold, respectively. In the silymarin and PR200 groups, the levels of MCP-1, ICAM-1, and VCAM-1 decreased significantly (silymarin: 35%, $p < 0.001$; 26% $p < 0.01$; and 29%, $p < 0.01$; PR200: 25.0%, $p < 0.001$; 15.2%, $p < 0.05$; and 16.4%, $p < 0.01$, resp.).

Table 1: Change of body weight, liver weight, and a relative liver weight.

Group	Liver weight (g)	Body weight (g)	LW/BW ratio (%)
Normal	8.3 ± 0.11	238.9 ± 2.08	3.5 ± 0.05
Control	$10.1 \pm 0.21^{\#\#\#}$	$202.9 \pm 3.48^{\#\#\#}$	$5.0 \pm 0.10^{\#\#\#}$
Silymarin	$9.8 \pm 0.13^{**}$	$202.5 \pm 2.53^{**}$	$4.8 \pm 0.06^{***}$
PR100	$9.8 \pm 0.17^{**}$	$200.2 \pm 3.06^{**}$	$4.9 \pm 0.08^{***}$
PR200	$9.5 \pm 0.24^{***}$	$197.4 \pm 4.09^{**}$	$4.8 \pm 0.11^{***}$

Data are represented as mean ± standard error of the mean ($n = 7$). $^{\#\#\#}p < 0.001$ versus the normal group and $^{**}p < 0.01$ and $^{***}p < 0.001$ versus the thioacetamide control group. LW: liver weight; BW: body weight; normal: received distilled water only; control: thioacetamide-induced acute liver injury treated with distilled water; (3) silymarin: thioacetamide-induced acute liver injury treated with silymarin (100 mg/kg); PR100: thioacetamide-induced acute liver injury treated with Paeoniae Radix Alba (100 mg/kg); and PR200: thioacetamide-induced acute liver injury treated with Paeoniae Radix Alba (200 mg/kg).

Table 2: Levels of AST, ALT, and ammonia in serum.

Group	AST (IU/L)	ALT (IU/L)	Ammonia (nmoL/μL)
Normal	26.67 ± 1.39	2.74 ± 0.54	11.62 ± 0.62
Control	$58.75 \pm 2.75^{\#\#\#}$	$26.48 \pm 2.37^{\#\#\#}$	$19.18 \pm 0.74^{\#\#\#}$
Silymarin	$50.06 \pm 1.98^{**}$	$17.07 \pm 2.13^{**}$	$14.73 \pm 1.03^{***}$
PR100	$49.01 \pm 2.34^{**}$	$14.99 \pm 3.65^{**}$	$12.68 \pm 0.46^{***}$
PR200	$44.73 \pm 2.09^{***}$	$14.50 \pm 3.54^{**}$	$11.58 \pm 0.73^{***}$

The higher dose of Paeoniae Radix Alba (200 mg/kg) significantly reduced the levels of AST, ALT, and ammonia. Data are mean ± standard error of the mean ($n = 7$). $^{\#\#\#}p < 0.001$ versus the normal group and $^{**}p < 0.01$ and $^{***}p < 0.001$ versus the thioacetamide control group. Normal: received distilled water only; control: thioacetamide-induced acute liver injury treated with distilled water; silymarin: thioacetamide-induced acute liver injury treated with silymarin (100 mg/kg); PR100: thioacetamide-induced acute liver injury treated with Paeoniae Radix Alba (100 mg/kg); and PR200: thioacetamide-induced acute liver injury treated with Paeoniae Radix Alba (200 mg/kg).

3.5. PR Abrogated Apoptosis in ALI Rat Liver Tissue. TAA induced apoptosis in liver tissues, as indicated by increases in Bax, cytochrome C, and cleaved caspase-3 activity ($p < 0.001$, $p < 0.001$, and $p < 0.01$, resp.) (Figure 5). In contrast, silymarin and the higher dose of PR (200 mg/kg) significantly downregulated the expression of these proteins (silymarin: $p < 0.01$, $p < 0.01$, and $p < 0.01$; PR200: $p < 0.01$, $p < 0.05$, and $p < 0.001$, resp.). PR effectively enhanced the expression of antiapoptotic proteins, such as Bcl2 and survivin (PR200: $p < 0.01$ and $p < 0.05$, resp.). These results indicated that PR inhibited hepatocyte apoptosis by suppressing the increased levels of Bax, cytochrome C, and cleaved caspase-3 and upregulating the levels of Bcl2 and survivin.

3.6. PR Improved Histological Alterations in ALI Rat Liver Tissue. Histological changes in the liver tissues of the rats were examined using hematoxylin and eosin staining.

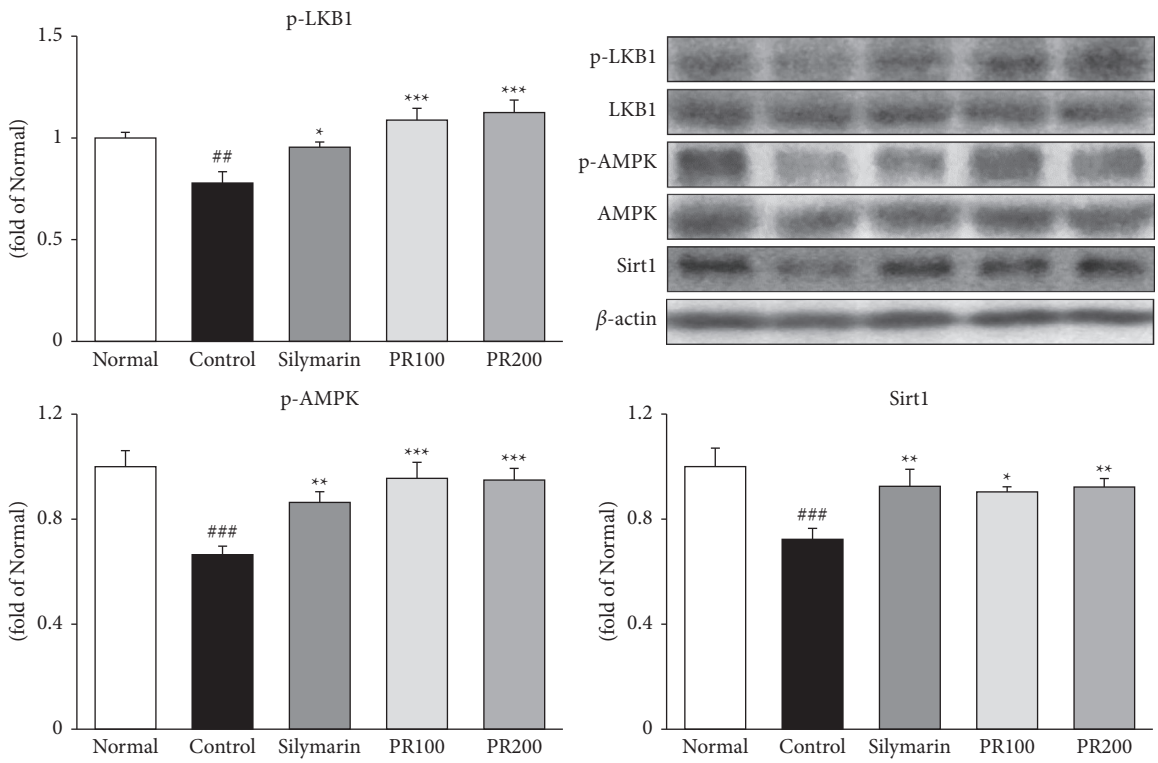

Figure 2: Paeoniae Radix Alba activated p-LKB1/AMP-activated protein kinase/Sirtuin 1. Paeoniae Radix Alba significantly elevated the protein expression of p-LKB1, p-AMP-activated protein kinase, and Sirtuin 1. Data are mean ± standard error of the mean ($n = 7$). $^{\#}p < 0.05$, $^{\#\#}p < 0.01$, and $^{\#\#\#}p < 0.001$ versus the normal group and $^{*}p < 0.05$, $^{**}p < 0.01$, and $^{***}p < 0.001$ versus the thioacetamide control group. AMPK: AMP-activated protein kinase; normal: received distilled water only; control: thioacetamide-induced acute liver injury treated with distilled water; silymarin: thioacetamide-induced acute liver injury treated with silymarin (100 mg/kg); PR100: thioacetamide-induced acute liver injury treated with Paeoniae Radix Alba (100 mg/kg); and PR200: thioacetamide-induced acute liver injury treated with Paeoniae Radix Alba (200 mg/kg).

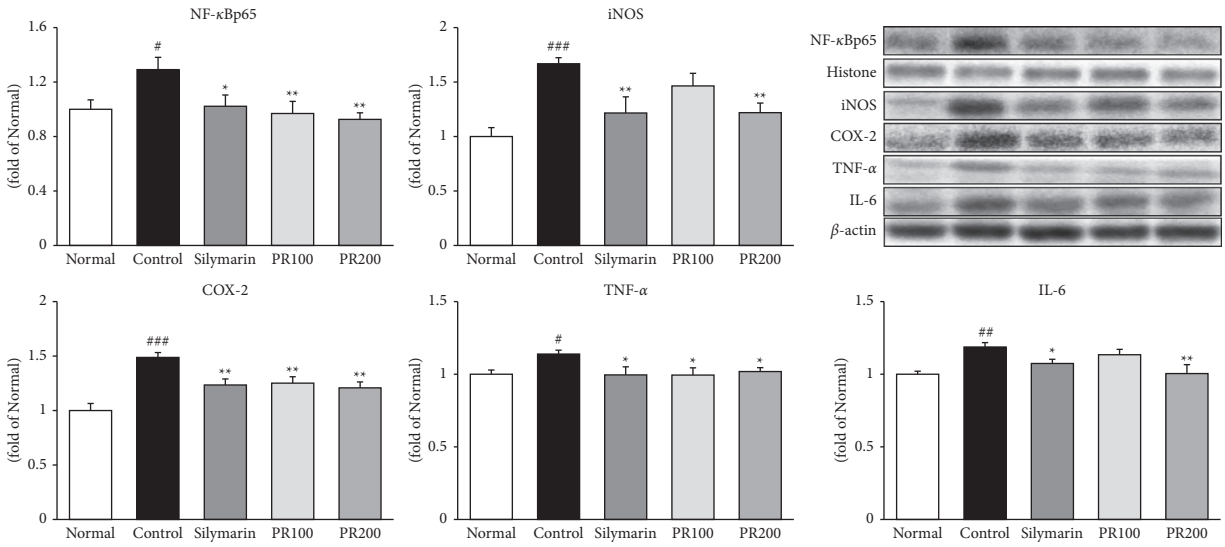

Figure 3: Paeoniae radix alba suppressed the release of NF-κBp65 and proinflammatory proteins. The higher dose of Paeoniae Radix Alba (200 mg/kg) significantly reduced the protein expression of NF-κBp65, iNOS, COX-2, TNF-α, and IL-6. Data are expressed as the mean ± standard error of the mean ($n = 7$). $^{\#}p < 0.05$, $^{\#\#}p < 0.01$, and $^{\#\#\#}p < 0.001$ versus the normal group and $^{*}p < 0.05$, $^{**}p < 0.01$ versus the thioacetamide control group. Normal: received distilled water only; control: thioacetamide-induced acute liver injury treated with distilled water; silymarin: thioacetamide-induced acute liver injury treated with silymarin (100 mg/kg); PR100: thioacetamide-induced acute liver injury treated with Paeoniae Radix Alba (100 mg/kg); and PR200: thioacetamide-induced acute liver injury treated with Paeoniae Radix Alba (200 mg/kg).

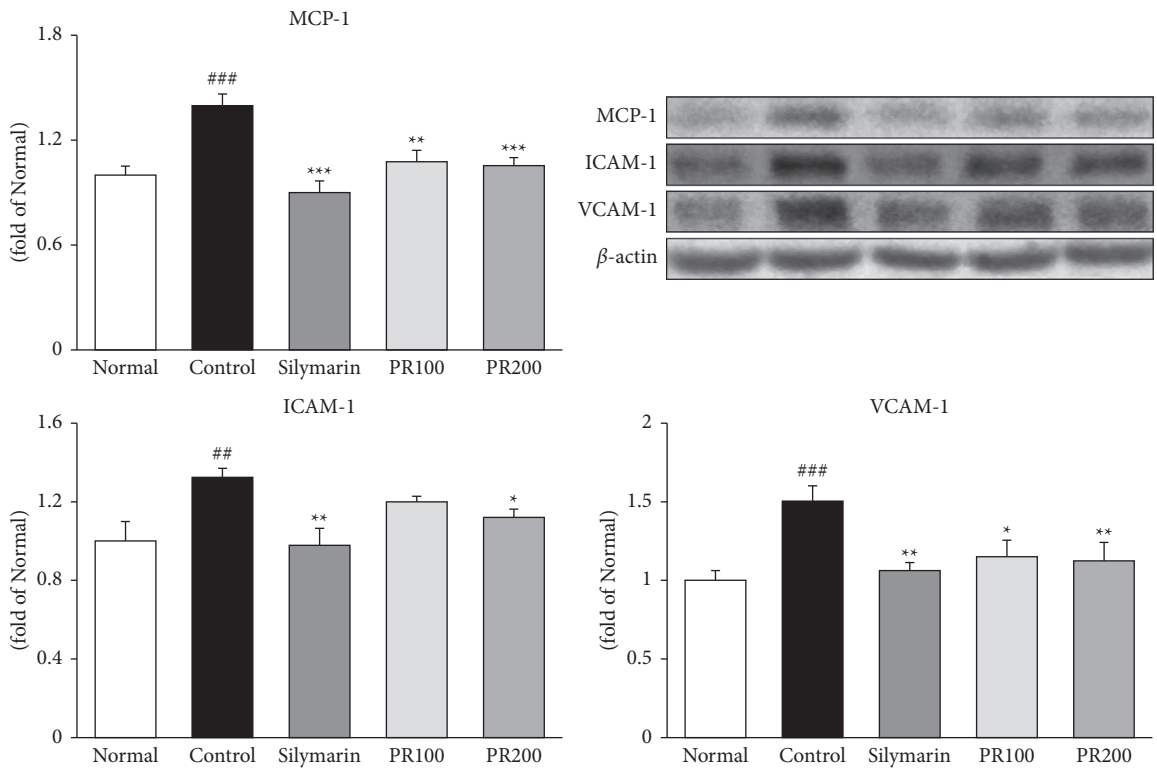

Figure 4: Paeoniae Radix Alba alleviated the levels of MCP-1, ICAM-1, and VCAM-1. The higher dose of Paeoniae Radix Alba (200 mg/kg) significantly reduced the protein expression of MCP-1, ICAM-1, and VCAM-1. Data are expressed as the mean ± standard error of the mean ($n = 7$). $^{\#\#}p < 0.01$ and $^{\#\#\#}p < 0.001$ versus the normal group and $^{*}p < 0.05$, $^{**}p < 0.01$, and $^{***}p < 0.001$ versus the thioacetamide control group. Normal: received distilled water only; control: thioacetamide-induced acute liver injury treated with distilled water; silymarin: thioacetamide-induced acute liver injury treated with silymarin (100 mg/kg); PR100: thioacetamide-induced acute liver injury treated with Paeoniae Radix Alba (100 mg/kg); and PR200: thioacetamide-induced acute liver injury treated with Paeoniae Radix Alba (200 mg/kg).

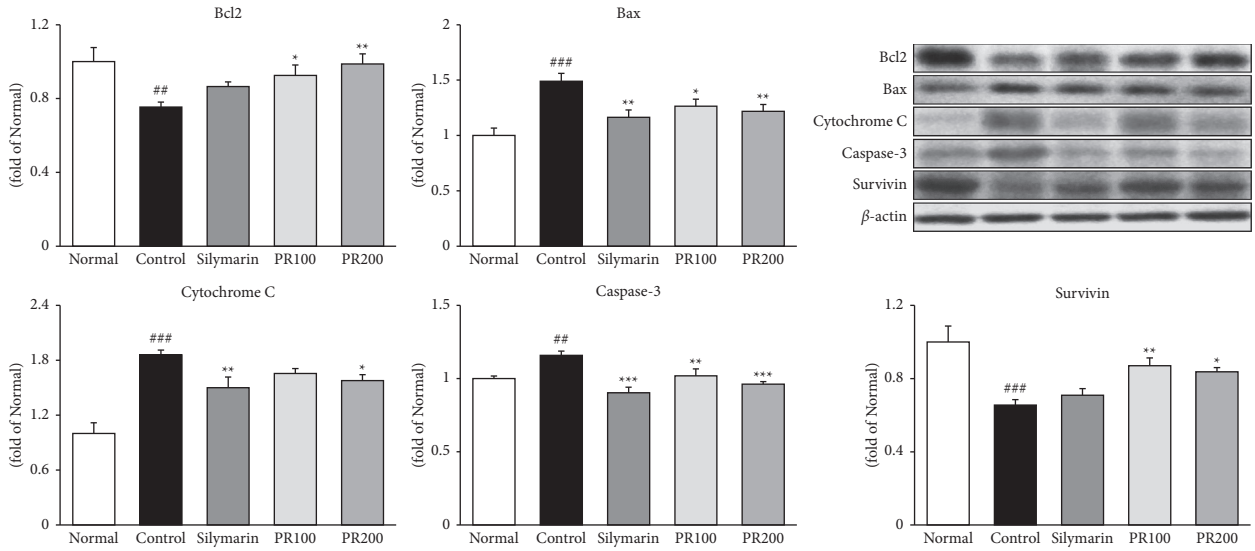

Figure 5: Paeoniae Radix Alba abrogated cell apoptosis. Expression of Bax, cytochrome C, and caspase-3 was significantly decreased after the administration of the higher dose of Paeoniae Radix Alba (200 mg/kg), whereas Bcl2 and survivin expression significantly increased. Data are expressed as the mean ± standard error of the mean ($n = 7$). $^{\#\#\#}p < 0.001$ versus the normal group and $^{*}p < 0.05$, $^{**}p < 0.01$, and $^{***}p < 0.001$ versus the thioacetamide control group. Normal: received distilled water only; control: thioacetamide-induced acute liver injury treated with distilled water; silymarin: thioacetamide-induced acute liver injury treated with silymarin (100 mg/kg); PR100: thioacetamide-induced acute liver injury treated with Paeoniae Radix Alba (100 mg/kg); and PR200: thioacetamide-induced acute liver injury treated with Paeoniae Radix Alba (200 mg/kg).

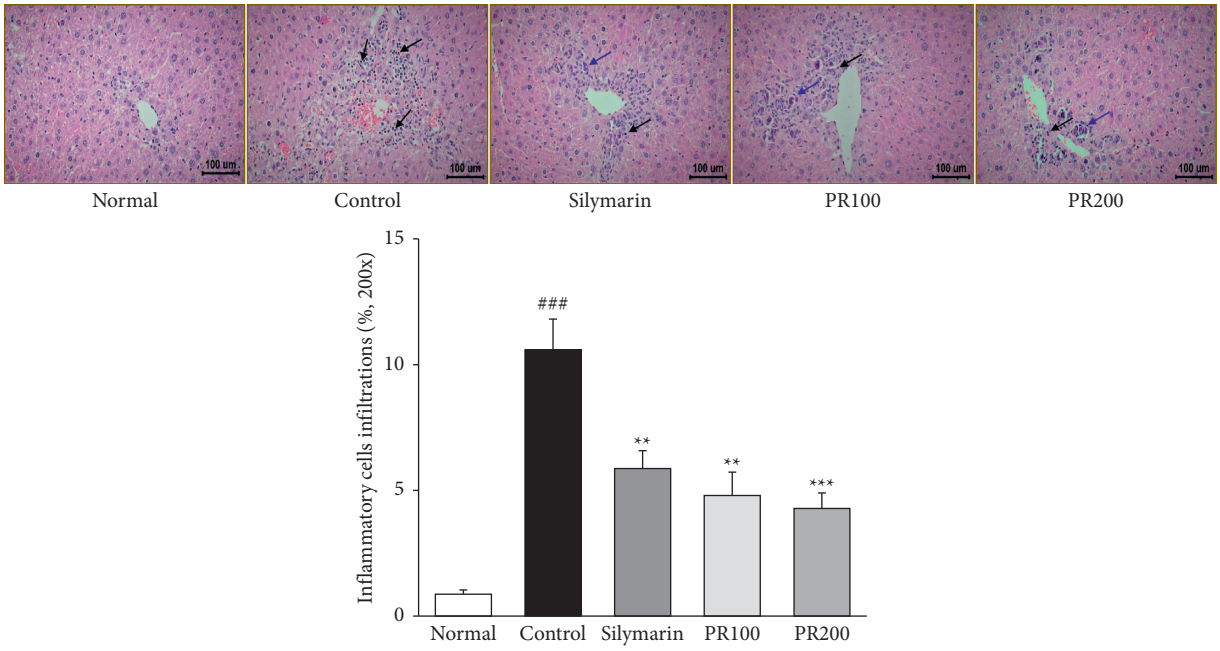

Figure 6: Paeoniae Radix Alba alleviated histological alterations in the liver. Representative hematoxylin and eosin staining of thioacetamide-induced acute liver injury. Injury was notably ameliorated by the administration of Paeoniae Radix Alba. Scale bar = 100 μm (magnification, ×200). Blue arrows indicate inflammatory cell infiltrations on H&E sections. Black arrows indicate apoptotic body. Histological analysis was measured using ImageJ (NIH). Data are expressed as the mean ± standard error of the mean ($n = 7$). $^{###}p < 0.001$ versus the normal group and $^{**}p < 0.01$ and $^{***}p < 0.001$ versus the thioacetamide control group. Normal: received distilled water only; control: thioacetamide-induced acute liver injury treated with distilled water; silymarin: thioacetamide-induced acute liver injury treated with silymarin (100 mg/kg); PR100: thioacetamide-induced acute liver injury treated with Paeoniae Radix Alba (100 mg/kg); and PR200: thioacetamide-induced acute liver injury treated with Paeoniae Radix Alba (200 mg/kg).

Representative images are shown in Figure 6. Treatment with TAA led to the elevation of liver volume and showed rough and granular apparatus of the liver surface. Silymarin and PR treatment relieved these liver lesions. The livers in the normal group did not present any structural changes. However, the livers in the TAA control group showed inflammatory cells infiltration (blue arrows) and necrosis of hepatocytes. Apoptotic cells show abnormal sizes, nuclear pyknosis, and karyorrhexis (black arrows). Herein, silymarin and PR treatment effectively recovered the injured livers (silymarin, $p < 0.01$; PR100, $p < 0.001$; and PR200, $p < 0.001$).

4. Discussion

ALI is defined as liver dysfunction and persistent liver injury that can lead to liver fibrosis and is a fundamental initiating factor in the outbreak of liver cirrhosis or hepatocellular carcinoma.

Although the etiological factor of ALI is not clear, it is known that it is caused by various causes, such as drug abuse, food additives, viral infection, alcohol, and radioactive damage [21]. It is known that ALI caused by these causes inflammation, hepatocellular necrosis, and oxidative stress [22]. However, there are no therapeutics for curative without side effects to cure liver injury globally till nowadays.

PR (white peony root) has been used in various prescriptions of traditional Chinese medicine. It is usually indicated for viral infections, menstrual disorders, and painful conditions [6]. In addition, PR is known for its functions of nourishing blood, preventing perspiration, astringing Yin, and eradicating liver wind caused by extreme Qi/Blood and Yin/Yang imbalance [23]. A recent study suggested that the bioactive component (polysaccharides) obtained from PR inhibited hepatic infiltration of inflammatory cells and overexpression of proinflammatory cytokines [9]. Moreover, paeoniflorin, a glucoside of PR, has been used to treat hepatic inflammatory disease including liver ischemia/reperfusion injury [24]. These studies indicate that PR possesses potent pharmacological activity associated with liver diseases. Therefore, using PR, a natural plant, we studied the mechanism of action of PR on liver damage that was different from studies reported so far, and we aimed to study the development of a natural therapeutic agent for liver damage based on PR.

A TAA-induced ALI model is a typical animal model that is commonly used to study the liver and its underlying mechanisms. The accumulating report indicates that TAA is a toxic substance that causes liver disease through abnormal detoxification that can cause liver tissue damage [25]. The highly toxic reactive intermediate (thioacetamide S-dioxide) of TAA damages the integrity and stability of biological membranes, which increases the permeability resulting in the outflow of enzymes, such as AST and ALT. Therefore, the determination of AST and ALT activities is a substantial index for judging liver injury [26]. Moreover, ammonia is

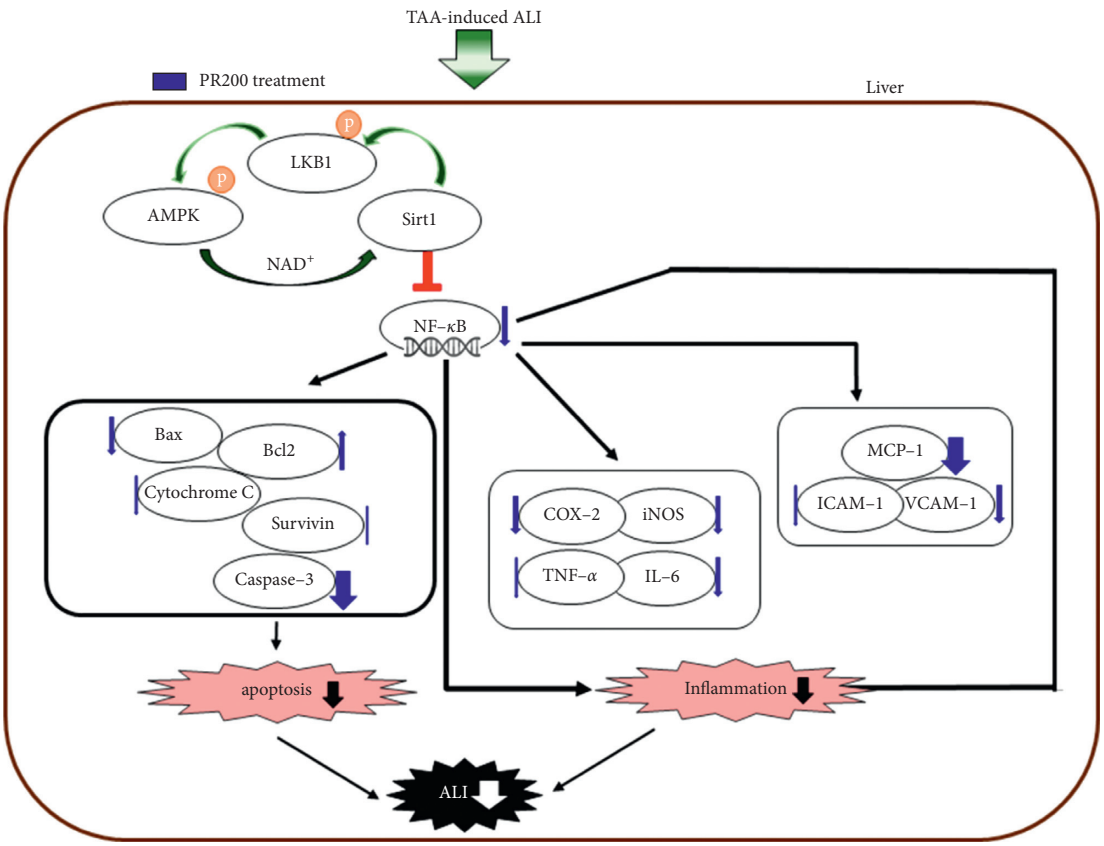

Figure 7: Possible mechanism of Paeoniae Radix Alba in thioacetamide-induced acute liver injury. TAA: thioacetamide; ALI: acute liver injury; PR200: thioacetamide-induced acute liver injury treated with Paeoniae Radix Alba (200 mg/kg); AMPK: AMP-activated protein kinase; and Sirt1: sirtuin 1.

the waste produced by nitrogen metabolism that is usually transported through the portal circulation to periportal hepatocytes. Hyperammonemia is a life-threatening metabolic syndrome characterized by elevated levels of toxic ammonia and can lead to a serious neurologic emergency that can induce liver cirrhosis, intracranial pressure crises, cerebral edema, hepatic encephalopathy, and seizures [27]. Thus, we addressed the effects of PR on TAA-induced liver injury. As expected, the serum AST, ALT, and ammonia levels of the PR-treated group were significantly lower than those of the TAA control group, indicating that it was more effective than the positive control group, silymarin. Therefore, this suggests that PR may exert a protective effect on TAA-induced ALI.

Sirt1 deacetylates LKB1 kinase, which is the upstream activator of AMPK and provides positive feedback between AMPK and Sirt1. LKB1 directly activates AMPK and has an established function in the control of OS and cell metabolism [28]. AMPK is involved in energy expenditure in specialized metabolic tissue including the liver by improving Sirt1 activity by increasing cellular NAD^+ level [29]. Sirt1 has been reported to modulate various activities through controlling oxidative stress response, inflammation, apoptosis, metabolism, and mitochondrial function [30]. For that reason, researchers have recently focused on the discovery of Sirt1 modulators that can lead to Sirt1 activity. The results of this present study indicated that the activities of both AMPK and Sirt1 were noticeably reduced in TAA-induced ALI rats. However, silymarin and PR treatment significantly increased the activities of both AMPK and Sirt1 via the deacetylation of LKB1. Apart from oxidative energy production, Sirt1 also inhibits NF-κB inflammatory signaling [31]. The activation of NF-κB is involved in the overproduction of inflammatory proteins including COX-2, iNOS, TNF-α, and IL-6 and chemokines including MCP-1. Meanwhile, cell adhesion molecules, such as ICAM-1 and VCAM-1, are elevated by macrophage activation [32, 33]. Namely, NF-κB acts as a common transcriptional regulator on the inflammatory response and exerts fundamental functions, such as cell survival and immune responses, in the liver. Notably, the expression of MCP-1, ICAM-1, and VCAM-1 was rapidly increased through stimulation with the toxic factor TAA. The high level of ICAM-1 improves the adhesion of monocytes to endothelial cells, VCAM-1 can promote monocyte adhesion to endothelial cells, and MCP-l can activate monocytes by binding with receptors [34]. In this study, we evaluated the inhibitory effect of PR on NF-κB activation in TAA-induced ALI rats. The increased NF-κB levels by TAA induction was remarkably suppressed in PR-treated groups. The silymarin and higher dose of PR (200 mg/kg) led to significant inhibition of proinflammatory proteins, chemokines, and cell adhesion molecules.

Excessive exposure to reactive oxygen species under inflammatory conditions increases the death of liver cells via the two standard mechanisms of apoptosis or necrosis. Apoptosis is the first response step of liver cells to diverse injury factors, and necrosis tends to occur following apoptosis. Accordingly, the apoptosis process takes charge of a key role in the formation of necrosis [35]. Many genes are involved in the apoptosis process, and of these, the activation of Bax has promoted mitochondrial membrane permeability and induces apoptosis and antagonizes the inhibitory action of Bcl-2 on apoptosis [36]. In addition, Bax forms a Bcl-2-Bax heterodimer to inhibit Bcl-2 function or induce apoptosis independently without Bcl-2 [37, 38]. Activation of caspase-3 also activates apoptosis by inducing leakage of cytochrome C, which triggers intrinsic apoptosis [39], whereas survivin in the cytoplasm inhibits caspase-3 activity or binds to the proapoptotic protein SMAC/DIABLO to inhibit apoptosis. Thus, the balance between these proteins is an important part of hepatocyte apoptosis [40–42]. Thus, further study on the mechanism of apoptosis is important to reveal the nature of ALI. Thus, we postulated that TAA injection is responsible for causing apoptotic signals through the regulation of apoptosis-related proteins including Bax, Bcl2, cytochrome C, caspase-3, and survivin. Treatment with the silymarin and higher dose of PR (200 mg/kg) showed a considerable decrease of proapoptotic genes, Bax, cytochrome C, and caspase-3. The higher dose of PR exhibited a significant increase of antiapoptotic genes, Bcl2, and survivin.

5. Conclusions

Taken together, the hepatoprotective effect of PR was revealed through the inhibition of TAA-induced inflammation via the AMPK/Sirt1/NF-κB pathway, as shown in Figure 7. This study demonstrated that PR could be developed as an effective therapeutic option for liver protection. Nevertheless, further research on PR is needed to increase both the safety and the therapeutic potential.

Data Availability

The data sets used and analyzed during this study are available from the corresponding author upon reasonable request.

Conflicts of Interest

The authors declare no conflicts of interest related to this study or its publication.

Authors' Contributions

Mi-Rae Shin and Se Hui Lee contributed equally to this work.

Acknowledgments

This work was supported by the National Research Foundation of Korea (NRF) grant funded by the Korean Government (MSIT) (no. 2018R1A5A2025272).

References

[1] V. Thawley, "Acute liver injury and failure," *Veterinary Clinics of North America: Small Animal Practice*, vol. 47, no. 3, pp. 617–630, 2017.

[2] X. Huo, C. Liu, L. Gao, X. Xu, N. Zhu, and L. Cao, "Hepatoprotective effect of aqueous extract from the seeds of orychophragmus violaceus against liver injury in mice and HepG2 cells," *International Journal of Molecular Sciences*, vol. 18, no. 6, Article ID 1197, 2017.

[3] J. S. Kang, H. Wanibuchi, K. Morimura et al., "Role of CYP2E1 in thioacetamide-induced mouse hepatotoxicity," *Toxicology and Applied Pharmacology*, vol. 228, no. 3, pp. 295–300, 2008.

[4] Y. F. Bi, Z. F. Pi, Z. Q. Liu, and F. R. Song, "Metabolic fingerprint of the compatibility of radix aconite and radix paeoniae alba and its effect on CYP450 enzymes," *Acta Pharmaceutica Sinica B*, vol. 49, pp. 1705–1710, 2014.

[5] W. Zhang and S.-M. Dai, "Mechanisms involved in the therapeutic effects of Paeonia lactiflora Pallas in rheumatoid arthritis," *International Immunopharmacology*, vol. 14, no. 1, pp. 27–31, 2012.

[6] B. Yan, M. Shen, J. Fang, D. Wei, and L. Qin, "Advancement in the chemical analysis of paeoniae radix (shaoyao)," *Journal of Pharmaceutical and Biomedical Analysis*, vol. 160, pp. 276–288, 2018.

[7] Z. A. Amin, M. Bilgen, M. A. Alshawsh, H. M. Ali, A. H. A. Hadi, and M. A. Abdulla, "Protective role of Phyllanthus niruriExtract against thioacetamide-induced liver cirrhosis in rat model," *Evidence-based Complementary and Alternative Medicine*, vol. 2012, Article ID 241583, 9 pages, 2012.

[8] S. Li, Y. Chu, R. Zhang, L. Sun, and X. Chen, "Prophylactic neuroprotection of total glucosides of paeoniae radix alba against semen strychni-induced neurotoxicity in rats: suppressing oxidative stress and reducing the absorption of toxic components," *Nutrients*, vol. 10, no. 4, Article ID 514, 2018.

[9] S. Wang, J. Xu, C. Wang et al., "Paeoniae radix alba polysaccharides obtained via optimized extraction treat experimental autoimmune hepatitis effectively," *International Journal of Biological Macromolecules*, vol. 164, pp. 1554–1564, 2020.

[10] F. Marín-Aguilar, L. Pavillard, F. Giampieri, P. Bullón, and M. Cordero, "Adenosine monophosphate (AMP)-Activated protein kinase: a new target for nutraceutical compounds," *International Journal of Molecular Sciences*, vol. 18, no. 2, Article ID 288, 2017.

[11] D. G. Hardie, "Sensing of energy and nutrients by AMP-activated protein kinase," *The American Journal of Clinical Nutrition*, vol. 93, no. 4, pp. 891S–896S, 2011.

[12] D. Stapleton, K. I. Mitchelhill, G. Gao et al., "Mammalian AMP-activated protein kinase subfamily," *Journal of Biological Chemistry*, vol. 271, no. 2, pp. 611–614, 1996.

[13] X. Bai, L. Yao, X. Ma, and X. Xu, "Small molecules as SIRT modulators," *Mini Reviews in Medicinal Chemistry*, vol. 18, no. 13, pp. 1151–1157, 2018.

[14] X. Ou, M. R. Lee, X. Huang, S. Messina-Graham, and H. E. Broxmeyer, "SIRT1 positively regulates autophagy and mitochondria function in embryonic stem cells under oxidative stress," *Stem Cells*, vol. 32, no. 5, pp. 1183–1194, 2014.

[15] H.-S. Zhang, T.-C. Wu, W.-W. Sang, and Z. Ruan, "MiR-217 is involved in Tat-induced HIV-1 long terminal repeat (LTR) transactivation by down-regulation of SIRT1," *Biochimica et*

Biophysica Acta (BBA)-Molecular Cell Research, vol. 1823, no. 5, pp. 1017–1023, 2012.

[16] R. Wang, A. Z. Xiong, Z. Q. Teng, Q. W. Yang, Y. H. Shi, and L. Yang, "Radix paeoniae rubra and radix paeoniae alba attenuate CCl_4-induced acute liver injury: an ultra-performance liquid chromatography-mass spectrometry (UPLC-MS) based metabolomic approach for the pharmacodynamic study of traditional Chinese medicines (TCMs)," *International Journal of Molecular Sciences*, vol. 13, no. 11, pp. 14634–14647, 2012.

[17] S. H. Lee, M.-R. Shin, J. H. Lee, and S.-S. Roh, "Effects of water extract of Paeoniae Radix Alba on a thioacetamide induced acute liver injury rat model," *Journal of Nutrition & Health*, vol. 54, no. 2, pp. 224–237, 2021.

[18] M. R. Shin, M. J. Kim, J. A. Lee, and S. S. Roh, "Effect of uncaria rhynchophylla against thioacetamide-induced acute liver injury in rat," *Chinese Journal of Gastroenterology and Hepatology*, vol. 2021, Article ID 5581816, 9 pages, 2021.

[19] F. Ahmad and N. Tabassum, "Preliminary phytochemical, acute oral toxicity and antihepatotoxic study of roots of Paeonia officinalis Linn," *Asian Pacific Journal of Tropical Biomedicine*, vol. 3, no. 1, pp. 64–68, 2013.

[20] M.-R. Shin, H.-J. Park, B.-I. Seo, and S.-S. Roh, "New approach of medicinal herbs and sulfasalazine mixture on ulcerative colitis induced by dextran sodium sulfate," *World Journal of Gastroenterology*, vol. 26, no. 35, pp. 5272–5286, 2020.

[21] J. Lambrecht, L. A. van Grunsven, and F. Tacke, "Current and emerging pharmacotherapeutic interventions for the treatment of liver fibrosis," *Expert Opinion on Pharmacotherapy*, vol. 21, no. 13, pp. 1637–1650, 2020.

[22] P. Muriel, "Cytokines in liver diseases," in *Hepatotoxicity: From Genomics to in Vitro and in Vivo Models*, S. Sahu, Ed., pp. 371–390, John Wiley & Sons, West Sussex, UK, 2008.

[23] X.-W. Ye, Y.-L. Deng, L.-T. Xia, H.-M. Ren, and J.-L. Zhang, "Uncovering the mechanism of the effects of Paeoniae Radix Alba on iron-deficiency anaemia through a network pharmacology-based strategy," *BMC Complementary Medicine and Therapies*, vol. 20, no. 1, Article ID 130, 2020.

[24] T. Xie, K. Li, X. Gong et al., "Paeoniflorin protects against liver ischemia/reperfusion injury in mice via inhibiting HMGB1-TLR4 signaling pathway," *Phytotherapy Research*, vol. 32, no. 11, pp. 2247–2255, 2018.

[25] T. Y. Low, C. K. Leow, M. Salto-Tellez, and M. C. Chung, "A proteomic analysis of thioacetamide-induced hepatotoxicity and cirrhosis in rat livers," *Proteomics*, vol. 4, no. 21, pp. 3960–3974, 2004.

[26] G. Xu, X. Han, G. Yuan, L. An, and P. Du, "Screening for the protective effect target of deproteinized extract of calf blood and its mechanisms in mice with CCl_4-induced acute liver injury," *PLoS One*, vol. 12, no. 7, Article ID e0180899, 2017.

[27] L. B. Vong, Y. Ibayashi, Y. Lee, D.-N. Ngo, Y. Nishikawa, and Y. Nagasaki, "Poly(ornithine)-based self-assembling drug for recovery of hyperammonemia and damage in acute liver injury," *Journal of Controlled Release*, vol. 310, pp. 74–81, 2019.

[28] D. B. Shackelford and R. J. Shaw, "The LKB1-AMPK pathway: metabolism and growth control in tumour suppression," *Nature Reviews Cancer*, vol. 9, no. 8, pp. 563–575, 2009.

[29] C. Cantó, Z. Gerhart-Hines, J. N. Feige et al., "AMPK regulates energy expenditure by modulating NAD^+ metabolism and SIRT1 activity," *Nature*, vol. 458, no. 7241, pp. 1056–1060, 2009.

[30] C. Iside, M. Scafuro, A. Nebbioso, and L. Altucci, "SIRT1 activation by natural phytochemicals: an overview," *Frontiers in Pharmacology*, vol. 11, Article ID 1225, 2020.

[31] A. Kauppinen, T. Suuronen, J. Ojala, K. Kaarniranta, and A. Salminen, "Antagonistic crosstalk between NF-κB and SIRT1 in the regulation of inflammation and metabolic disorders," *Cellular Signalling*, vol. 25, no. 10, pp. 1939–1948, 2013.

[32] X. Wang, L. Li, H. Wang, F. Xiao, and Q. Ning, "Epoxyeicosatrienoic acids alleviate methionine-choline-deficient diet-induced non-alcoholic steatohepatitis in mice," *Scandinavian Journal of Immunology*, vol. 90, no. 3, Article ID e12791, 2019.

[33] R. S. McCuskey, Y. Ito, G. R. Robertson, M. K. McCuskey, M. Perry, and G. C. Farrell, "Hepatic microvascular dysfunction during evolution of dietary steatohepatitis in mice," *Hepatology*, vol. 40, no. 2, pp. 386–393, 2004.

[34] X. Xu, B. Yang, D. Wang, Y. Zhu, X. Miao, and W. Yang, "The chemical composition of Brazilian green propolis and its protective effects on mouse aortic endothelial cells against inflammatory injury," *Molecules*, vol. 25, no. 20, Article ID 4612, 2020.

[35] R. Weiskirchen and F. Tacke, "Liver fibrosis: from pathogenesis to novel therapies," *Digestive Diseases*, vol. 34, no. 4, pp. 410–422, 2016.

[36] B.-X. Chu, R.-F. Fan, S.-Q. Lin, D.-B. Yang, Z.-Y. Wang, and L. Wang, "Interplay between autophagy and apoptosis in lead(II)-induced cytotoxicity of primary rat proximal tubular cells," *Journal of Inorganic Biochemistry*, vol. 182, pp. 184–193, 2018.

[37] I. Otter, S. Conus, U. Ravn et al., "The binding properties and biological activities of Bcl-2 and bax in cells exposed to apoptotic stimuli," *Journal of Biological Chemistry*, vol. 273, no. 11, pp. 6110–6120, 1998.

[38] C. M. Knudson and S. J. Korsmeyer, "Bcl-2 and Bax function independently to regulate cell death," *Nature Genetics*, vol. 16, no. 4, pp. 358–363, 1997.

[39] D. Gonzalez, I. Bejarano, C. Barriga, A. B. Rodriguez, and J. A. Pariente, "Oxidative stress-induced caspases are regulated in human myeloid HL-60 cells by calcium signal," *Current Signal Transduction Therapy*, vol. 5, no. 2, pp. 181–186, 2010.

[40] D. C. Altieri, "Survivin and IAP proteins in cell-death mechanisms," *Biochemical Journal*, vol. 430, no. 2, pp. 199–205, 2010.

[41] K. Wang, J. J. Brems, R. L. Gamelli, and A.-X. Holterman, "Survivin signaling is regulated through nuclear factor-kappa B pathway during glycochenodeoxycholate-induced hepatocyte apoptosis," *Biochimica et Biophysica Acta (BBA)-Molecular Cell Research*, vol. 1803, no. 12, pp. 1368–1375, 2010.

[42] S. Shin, B.-J. Sung, Y.-S. Cho et al., "An anti-apoptotic protein human survivin is a direct inhibitor of caspase-3 and -7," *Biochemistry*, vol. 40, no. 4, pp. 1117–1123, 2001.